NPS ARCHIVE
1963
MASTERSON, L.

DISSERTATION

PERTURBATION THEORY OF NUCLEAR MATTER AND FINITE NUCLEI

KLEBER SANLIN MASTERSON, JR.

LIBRARY
U.S. NAVAL POSTGRADUATE SCHOOL
MONTEREY, CALIFORNIA

Mont 56

UNIVERSITY OF CALIFORNIA
GRADUATE DIVISION, SAN DIEGO
ANNOUNCEMENT OF THE
FINAL EXAMINATION FOR THE DEGREE
OF DOCTOR OF PHILOSOPHY
OF
KLEBER SANLIN MASTERSON, JR.

B.S., 1954, U. S. Naval Academy, Annapolis, Maryland
M.S., 1961, U. S. Naval Postgraduate School, Monterey, California

PHYSICS
Friday, January 18, 1963, 9:00 A.M., Room 2202
Ritter Hall, San Diego Campus

Committee in Charge:
Professor Keith A. Brueckner, Chairman
Professor Walter Kohn
Professor Joseph E. Mayer
Professor Maria G. Mayer
Professor Clay L. Perry
Assistant Professor Manuel Rotenberg

VITA

September 26, 1932--Born, San Diego, California.

1954--B.S., U. S. Naval Academy,
Annapolis, Maryland.

1954--1963--U. S. Navy.

1961--M.S., U. S. Naval Postgraduate School,
Monterey, California

PUBLICATIONS

"Compilation for Two Computers with NELIAC," *Communications of the Association for Computing Machinery*, vol. 3 (1960), 607-611.

"The Influence of Diffusion Losses on the Probe Potential in a Dense Plasma" (with G. Ecker), *Bull. Am. Phys. Soc.*, vol. 6 (1961), 389.

"Probe Theory in a Dense Plasma" (with G. Ecker and J. J. McClure), University of California Radiation Laboratory Report 10128, 21 March 1962.

"Nuclear Matter Calculations and Phenomenological Potentials" (with K. A. Brueckner), *Phys. Rev.*, vol. 128 (1962), 2267-2276.

"Properties of Finite Nuclei" (with A. M. Lockett), *Phys. Rev.* (to be published).

ABSTRACT OF THE DISSERTATION

Perturbation Theory of Nuclear Matter and Finite Nuclei

This dissertation investigates several related topics in the theory and application of perturbation methods to nuclear matter and finite nuclei.

(1) Theoretical discussions include the concise rederivation of many basic equations describing the properties of many-fermion systems. The techniques thus developed are then employed, with a "change of parameter" procedure, to derive an approximate expansion for the energy of the "normal" state. In this expansion, the momentum density occurs in place of the Fermi functions and the "self-energy" terms are absent. Also discussed is a new method for including the "core volume energy" in the K-matrix approximation. A later discussion includes a study of other nuclear matter theories, and discloses a previously unreported second order difference between an expansion of the equations of the Puff theory and the Brueckner-Goldstone expansion.

(2) A simplified version of the Brueckner-Gammel K-matrix approximation is then presented, and employed to show that the variation of many-body properties with choice of phenomenological potentials is quite large: the saturation values for the ground state energy vary from -8.3 MeV at an equilibrium spacing of 1.28 Fermis for the Breit potential to -22.3 MeV at 0.9 Fermi for one Gammel-Thaler potential, a result that implies that comparison of results

with extrapolated experimental values is not at present an accurate test of a nuclear matter theory. The simplified approximation is also used to obtain estimates of the attractive contributions of many perturbation diagrams, leading to the conclusion that calculations with hard core potentials must be carried to the equivalent of the third Born approximation (on the attractive part of the potential) and that the self-consistent energy denominators must be computed with at least "first iteration" reaction matrices for quantitative (± 2 MeV) results.

(3) The approximation for finite nuclei is also extended with a semi-independent verification of previous calculations, an evaluation of a new rearrangement energy approximation (which gives a more accurate energy spectrum but only slightly better average properties than previous calculations), and the calculation of the properties of Pb^{208}. The latter yielded a mean energy of -6.86 MeV and mean rms proton radius of 4.63 Fermis, compared to experimental values of -7.87 MeV and (5.43 ± 0.07) Fermis. These results are slightly better than the results for the smaller nuclei, indicating that some of the errors in the theory arise from inadequacies in the treatment of the nuclear surface.

(4) In addition to the theoretical discussion of other nuclear matter approximations, this dissertation features quantitative analyses of the Moszkowski-Scott separation method and the Mohling and Puff approximations. In a computationally feasible form for hard core local potentials, the Puff and Mohling approximations

are the same, and are shown to give mean energy and equilibrium spacing which are 10% more negative and smaller respectively than more accurate K-matrix results. The Bethe reference spectrum method is briefly discussed, and a supplementary calculation presented.

(5) Finally, an approximation is developed which is computationally simpler than previous approximations for hard core potentials. For the potential employed in the calculation by Brueckner and Gammel, the mean energy with the new approximation is -14.0 MeV at 1.04 Fermis, compared to their -15.2 MeV at 1.02 Fermis.

FIELDS OF STUDY

Major Field: PHYSICS

FIELDS OF STUDY

Major Field: PHYSICS

UNIVERSITY OF CALIFORNIA, SAN DIEGO

Perturbation Theory of Nuclear Matter and Finite Nuclei

A dissertation submitted in partial satisfaction of the
requirements for the degree Doctor of Philosophy
in Physics

by

Kleber Sanlin Masterson, Jr.

January, 1963

NPS ARCHIVE
1963
MASTERSON, L.

~~Thesis~~
~~M368~~

Library
U. S. Naval Postgraduate School
Monterey, California

The dissertation of Kleber Sanlin Masterson, Jr., is approved:

University of California, San Diego

January, 1963

TABLE OF CONTENTS

I. INTRODUCTION 1

II. PERTURBATION THEORY OF THE ZERO-TEMPERATURE MANY-FERMION NORMAL SYSTEM 13

- A. THE BRUECKNER-GOLDSTONE LINKED-CLUSTER EXPANSION AND THE BRUECKNER K-MATRIX APPROXIMATION 14
- B. MANY-FERMION SYSTEM PROPERTIES 21
  - 1. True Momentum Density 21
  - 2. Single Particle Energy 24
- C. DISCONTINUITY IN MOMENTUM DENSITY AT THE FERMI SURFACE 27
- D. EFFECTIVE MASS EQUATION 31
- E. BETHE-HUGENHOLTZ-VAN HOVE SEPARATION ENERGY THEOREM 33
- F. THE "CHANGE OF PARAMETER" PROCEDURE--USE OF THE TRUE MOMENTUM DENSITY IN THE BRUECKNER-GOLDSTONE EXPANSION 36

III. INFINITE NUCLEAR MATTER AND PHENOMENOLOGICAL POTENTIALS 43

- A. NUCLEAR PARAMETERS 43
- B. PHENOMENOLOGICAL POTENTIALS 51

IV. NUCLEAR MATTER CALCULATIONS IN THE K-MATRIX APPROXIMATION 57

- A. SIMPLIFICATION OF THE K-MATRIX APPROXIMATION 57
- B. RESULTS 68

1. Variation of Predicted Nuclear Properties with Choice of Phenomenological Potential 68
2. Convergence Properties as a Measure of Higher Order Terms 73
3. Core Volume Energy 81

C. ERROR ANALYSIS 90
1. Contribution of Neglected Diagrams 91
2. Computational Approximations 93

V. FINITE NUCLEI 102
A. THEORY AND ERROR ANALYSIS 102
1. Theory 102
2. Error Analysis 110

B. RESULTS 114
1. Comparison with Previous Rearrangement Energy Approximation 114
2. General Properties of Pb^{208} 116
3. Energy Spectrum 117
4. Neutron-Proton Density Relations 119
5. Density-Potential Relations 120
6. Comparison with Surface Predictions of Other Theories 120
7. Summary of Results for the Four Nuclei Studied to Date 121

C. CONCLUSIONS 123

VI. OTHER NUCLEAR MATTER THEORIES 127
  A. MOSZKOWSKI-SCOTT SEPARATION METHOD 128
  B. REFERENCE SPECTRUM METHOD FOR NUCLEAR MATTER 139
  C. THE PUFF APPROXIMATION 144
  D. THE MOHLING APPROXIMATION 156
VII. AN EASY NUCLEAR MATTER CALCULATION 160
APPENDIX A. THE BRUECKNER-GOLDSTONE LINKED-CLUSTER EXPANSION 169
  A. RAYLEIGH-SCHROEDINGER PERTURBATION THEORY 172
  B. GOLDSTONE PROOF OF THE LINKED-CLUSTER EXPANSION 178
    1. The Development Operator 179
    2. Adiabatic Theorem 181
    3. Wick's Theorem 187
    4. The Graphical Procedure 191
    5. Proof of the Linked-Cluster Expansion 195
    6. Inclusion of Effective Single-Particle Potential 198
  C. COMMENTS ON THE BG EXPANSION 200
  D. THE ENERGY EXPANSION--GRAPHICAL EVALUATION 207
APPENDIX B. THE BRUECKNER K-MATRIX APPROXIMATION 212
  A. DERIVATION 212
  B. BRUECKNER-GAMMEL APPROXIMATION 224
    1. Reduction of the K-Matrix Equation 224
    2. Transformation to Coordinate Space 225
    3. Partial Wave Expansion 227

4. Treatment of the Hard Core 230

5. Determination of the K-Matrix Elements 232

6. Single Particle Energies 234

7. Computational Procedure 235

APPENDIX C. TRANSFORMED BRUECKNER-GOLDSTONE EXPANSION 238

APPENDIX D. COMPARISON OF PUFF EQUATIONS AND BG EXPANSION 243

APPENDIX E. EVALUATION OF MOMENTUM DENSITY WITH SEPARABLE POTENTIAL 247

APPENDIX F. GRAPHS OF BASIS FUNCTIONS AND WAVE FUNCTIONS FROM BRUECKNER-MASTERSON CALCULATION 262

APPENDIX G. "NUCLEAR MATTER CALCULATIONS AND PHENOMENOLOGICAL POTENTIALS" BY K. A. BRUECKNER AND K. S. MASTERSON, JR. 271

APPENDIX H. "PROPERTIES OF FINITE NUCLEI" BY K. S. MASTERSON, JR., AND A. M. LOCKETT 315

FOOTNOTES 361

TABLES

I. Predicted nuclear properties reported by Brueckner and Gammel. 59

II. Parameters of the Gammel-Christian-Thaler potential. 59

III. Variation of the contribution of the self-energy diagrams with the Fermi momentum and with potential. 80

IV. Mean energy per particle obtained with BBP reference spectrum. 83

V. Breakdown of single-particle energy. 108

VI. Summary of contributions to E_{Av} for the Brueckner-Gammel-Thaler potential (with Moszkowski-Scott separation method). 132

VII. Summary of contributions to E_{Av} for the MS "standard potential." 133

VIII. Analysis of the contributions to the binding energy as calculated in with K-matrix and as calculated by Moszkowski and Scott. 134

IX. Possible states of 2 nucleons and their contributions to the statistical weights. 233

FIGURES

1. Low-order diagrams of the BG expansion. 20
2. Low-order "rearrangement energy" diagrams. 20
3. Extrapolation of r_o and r_1 for infinite nuclear matter. 47
4. The three possible situations for the angular integration leading to Eq. (4.13) for V(p). 68
5. E_{Av} vs. r_o as computed with the t-matrix compared to the same quantity as computed with the K-matrix. 70
6. Diagrams contributing to successive Born approximations. 76
7. Leading self-energy diagrams contributing to the self-consistent propagator. 76
8. Lowest order diagrams in successive major iterations which were not included in previous iteration. 76
9. E_{Av} vs. r_o for the "simple approximation" using the BGT potential. 167
10. Momentum density using the Yamaguchi potential. 167
11. Typical graph contributing to the perturbation expansion of $\Psi_o = U(0,-\infty)\Phi_o$. 194
12. Graph used to illustrate the time integration. See Eq. (A.69) *et seq*. 194
13. "Ladder diagrams" contributing to the t-matrix. 215
14. "Self-energy diagrams" summed when propagator includes the "self-consistent" single-particle energies. 215

15. Typical diagrams which are summed when the propagator of Fig. 14 and Eq. (B.4) occurs between two v interactions. 215

16. Diagram used to illustrate the transformation (E.25). 255

17. Diagram used to obtain integration limits in Eq. (E.28). 255

18. Diagram used to obtain integration limits in Eq. (E.30). 255

19. Basis functions $s_\ell(kr)$, Eq. (4.8). 263

20. Radial wave functions $U_{\ell\ell'}^{Js}$, Eq. (4.10). 265

I.

INTRODUCTION

The calculation of the ground state properties of large nuclei by using only the nucleon-nucleon potential has been the subject of intensive investigation for several years. Because of the complexity of the problem, it is customary to concentrate first on "infinite nuclear matter" in which only nuclear forces act and in which the numbers of neutrons and protons are equal. If the theory yields results for this idealized medium which are consistent with the properties deduced by extrapolating the experimental data on large nuclei, then the extension to finite nuclei is attempted.

In recent years, the Brueckner-Goldstone linked-cluster expansion,[1,2] which is a basic perturbation-theoretic equation for the energy of the zero-temperature many-fermion system, has been applied with success to the calculation of nuclear properties. This application involves a partial summation of the Brueckner-Goldstone series, effected by the Brueckner K-matrix approximation.[1,3] The most accurate calculation performed to date, by Brueckner and Gammel,[3] yielded a mean binding energy of 15.2 MeV at an "equilibrium spacing" of 1.02 Fermis, in excellent agreement with the extrapolations then accepted, 15.5 MeV and 1.02 Fermis. An extension of the theory to finite nuclei was developed by Brueckner, Gammel and Weitzner,[5] and the properties of the closed-shell nuclei O^{16}, Ca^{40}, and Zr^{90} were computed by Brueckner, Lockett and Rotenberg.[6] The latter results were in "semi-quantitative" agreement with experiment,

the mean binding energies being about 3 MeV too small and the rms radii of the nuclear distributions being as much as 20% too small. Inadequacies in the treatment of the density dependence of the interactions in the nuclear surface and in the treatment of the "rearrangement energy" were evaluated as the principal sources of error.

Several problems remained to be investigated. During the past few years many different nucleon-nucleon potentials have been proposed, all of which give almost "equally good" agreement with the experimental data on nucleon-nucleon scattering: Do these potentials also yield equivalent many-body results? Another question, which has important consequences for the feasibility of various simpler approximations than the K-matrix approximation, involved the latter's convergence properties: At what order can the various perturbation sub-series be truncated without appreciable error when using realistic potentials? Going next to the application of the approximation to finite nuclei, an important task is the improvement of the treatment of the "rearrangement energy" in the hopes of obtaining substantially better agreement with experiment. These problems are essentially extensions of the original work of Brueckner and his collaborators. Recently there have also been several other efforts to develop approximate theories of nuclear matter. Unfortunately, they frequently employed nucleon-nucleon potentials differing from those used by Brueckner and Gammel, and quantitative comparisons between the theories were therefore difficult. Furthermore, although most of them are simpler computationally than the full

K-matrix approximation, they are still very difficult (often conceptually as well as computationally) for the full nucleon-nucleon potential, and an "easy" nuclear matter approximation which preserves the principal features of the problem is definitely needed.

This dissertation addresses all of these problems. The following paragraphs outline the general method of attack and the principal results.

Chapter II begins (Section A) with brief statements of the Brueckner-Goldstone linked-cluster expansion[1,2] (BG expansion) and of the Brueckner K-matrix approximation[3] for the energy of a many-fermion system. Comprehensive background material is relegated to Appendices A and B respectively, and the reader who is unfamiliar with this material is advised to begin with these Appendices. In particular, he should understand the interpretation of the basic equation of this theory, the BG expansion, as given schematically by (A.73) and explicitly through third order by (A.92). It is also desirable to read carefully the derivation of the K-matrix approximation (Section A of Appendix B) and to obtain at least a general concept of the K-matrix equations as they appear in coordinate space (Section B). With the BG expansion as a basis, Section B of Chapter II presents derivations and explicit perturbation series for many-fermion system properties. Though none of the equations are new, some of the derivations are, and taken together they form a brief and simple summary of many-fermion relations and a basis for further investigation of the BG expansion. The possible use of the true

momentum density instead of the unperturbed distribution (the Fermi step function) in the BG expansion and in the K-matrix approximation is then investigated, using a "change of parameter" method due to Sawada. The result is a simpler, approximate perturbation series for the interaction energy, whose accuracy for nuclear matter is estimated to be of the order of 2 MeV. The new approximation is exact to fourth order. Most of the material in Section B will appear in a paper to be submitted for publication by K. Sawada, L. Bruch and the author.

In Chapter III, the concept of "infinite nuclear matter" is discussed, and the two parameters which characterize it, the binding energy per particle ($-E_{Av}$) and the equilibrium spacing (r_o), are treated in some detail, with the conclusion that present evidence supports the following values: $E_{Av} = (-15.5 \pm 2.0)$ MeV and r_o(nuclear matter) = (1.07 ± 0.03) Fermis. Nucleon-nucleon potentials and the justification for their use in the computation of nuclear properties are then very briefly reviewed.

Chapter IV presents a revised K-matrix approximation suggested by Professor Brueckner. This approximation is a simplification of the treatment by Brueckner and Gammel, and is characterized by the neglect of the explicit dependence of the single-particle energies on the total momentum and by a single-particle excitation spectrum which is characterized by only one parameter, the relative momentum (as opposed to the Brueckner-Gammel spectrum[3] with its dependence on the particle momentum and on an energy parameter). The

new approximation yields a minimum mean energy vs. density of -16.9 MeV at a density corresponding to $r_o = 1.00$ Fermi using the slightly modified Gammel-Thaler[4] potential with which Brueckner and Gammel[3] obtained -15.2 MeV at 1.02 Fermis. Several different phenomenological nucleon-nucleon potentials which purportedly give almost "equally good" two-body scattering predictions were used in the calculation to see whether their many-body predictions were the same. They were not: the equilibrium energy and spacings varied from -8.3 MeV at 1.28 Fermis for the Breit potential[7] to -22.3 MeV at 0.90 Fermi for one of the Gammel-Thaler potentials.[4] Three possible sources of these differences were analyzed, with the conclusion that about one-third of the differences can be attributed to the Pauli exclusion principle together with differences in two-body scattering properties and that the remaining two-thirds is attributable to self-energy effects. The large variation in nuclear properties noted above implies that no really good test will exist for nuclear matter approximations until a nucleon-nucleon potential can be accurately and unambiguously described either theoretically or experimentally. Because the neglected terms in the K-matrix approximation cannot be calculated exactly (though most approximate calculations indicate they are small), the only tests available at present are relative comparisons between different approximations effected by using the same potential in all of them. The convergence rates of high order terms in the BG expansion are investigated quantitatively (after separate treatment of the infinite core repulsion), leading to

the conclusion that nuclear matter calculations with realistic hard core potentials must be carried to at least the equivalent of the third Born approximation and that the self-consistent energy denominators must be computed with at least "first iteration" K-matrices for quantitative (± 2 MeV) results. This study is more thorough and complete for hard core potentials than any reported to date, and includes estimates of the attractive contributions of many high order diagrams (or groups of diagrams), obtained by modifying the computational procedure in various ways. The "core volume energy," which had previously been considered negligible,[3,8] is examined following a suggestion by Bethe, Brandow and Petschek[9] (BBP). Their "reference spectrum" for particle energies (which includes the core volume effect) is used to check the effect of this core term on the binding energy (a calculation not performed by BBP), and to investigate the sensitivity of the calculations to the parameters of this reference spectrum. The binding energy was found to be of the order of 6 MeV less attractive with the BBP spectrum at normal density, but for reasons discussed in the text (including the sensitivity of the calculation to the BBP reference spectrum parameters), it is estimated that the net effect of the core volume term in a completely consistent calculation would be of the order of 2 MeV (repulsion). A procedure for including the core volume term approximately in the K-matrix approximations of Brueckner and Gammel or of this dissertation is derived and presented in detail. An approximate treatment of the three-body cluster term suggested by Rajaraman[10] is also investigated,

but without conclusive results. Some of the results mentioned above were reported in "Infinite Nuclear Matter Calculations and Phenomenological Potentials," Phys. Rev. 128, 2267 (1962) (with K. A. Brueckner), which is included as Appendix G of this dissertation. This paper is referred to as BM, and contains some material which is not repeated in the text.

Chapter V reports the semi-independent verification of the Brueckner, Lockett, Rotenberg[6] (BLR) calculation of the properties of Ca^{40}, the evaluation of a revised approximation for the rearrangement energy, and the extension of the Brueckner-Gammel-Weitzner[5] theory to the calculation of the properties of Pb^{208}. Most of the results have been reported in "Properties of Finite Nuclei," Phys. Rev. (to be published) (with A.M. Lockett), which is included with this dissertation as Appendix H. The revised rearrangement energy treatment referred to above is derived in more detail than in any of the papers, and is evaluated by computing the properties of Ca^{40} and comparing with the BLR results. The effect of the better approximation was to reduce the overall spread of eigenvalues from -70.1 through -4.9 MeV to -48.7 through -5.5 MeV. The effect on the binding energy per nucleon and the rms radii was much smaller, however, being to cause changes of -.43 MeV and +0.11 Fermi (about 3%) respectively. All of the properties affected were in better agreement with experiment. A slightly better approximation is developed for future calculations. However, it is concluded that the rearrangement energy is not the principal source of difficulty

with the finite nucleus calculations. In order to ascertain the importance of the errors in the treatment of the interactions in the nuclear surface (where the density changes rapidly), the properties of Pb^{208} (which has proportionally fewer nucleons in the surface region) were computed. The approximation yielded -6.86 MeV mean energy per nucleon (in fairly good agreement with the experimental -7.87 MeV) and 4.63 Fermis rms proton radius (about 15% smaller than the electron-scattering value, (5.42 ± 0.07) Fermis). For equivalent parameters, the BLR calculations for the smaller nuclei has yielded much poorer energies (by more than 3 MeV) and approximately 20% variance in rms radii. The considerable improvement in energy and the slight improvement in mean radius indicate that the surface treatment is responsible for part of the remaining discrepancy (recall, however, that much of the improvement in rms radius is due to the better rearrangement approximation). The fact that the nucleon-nucleon potential employed gave saturation at $r_o = 1.02$ Fermi vs. $r_o = 1.07$ as suggested by the arguments of Chapter III indicates that the phenomenological potential input is possibly responsible for much of the error. This is made more plausible by the fact that recent nucleon-nucleon potentials[7] have larger cores than the BGT potential used in these calculations.

In Chapter VI several other approximations which have recently been employed for nuclear matter calculations are investigated quantitatively and are compared with the calculations of Brueckner and Gammel (BG) and with BM. The approximations investi-

gated are those of Moszkowski and Scott,[11] Bethe, Brandow and Petschek,[9] Puff,[12,13,14] and Mohling.[15,16] The Moszkowski-Scott (MS) separation method is very good for central potentials, but as pointed out by Scott and Moszkowski,[17] it is only semi-quantitative for nucleons interacting via tensor forces. Our quantitative comparison of the contributions from various angular momentum states (based on a more accurate calculation of the individual contributions) shows that the MS calculation[18] underestimated the S-state attraction by about 5 MeV and differed in the P-state from the BM approximation by 2.3 MeV (repulsion). The D and higher states are within 0.5 MeV of the BM calculation. Thus the MS method is very good for states of high angular momentum, but is not sufficiently quantitative for S and P states. Improvements suggested by Köhler[18] and by BBP may improve the treatment considerably, but the slow convergence of the Born approximation noted previously probably puts an upper limit on the accuracy at about 2 MeV. The BBP reference spectrum method is briefly reviewed, and their treatment of the core analyzed. The Puff and Mohling approximations were evaluated in a computationally feasible form described by Bell.[19] This approximation is the lowest order Mohling approximation, but it is simpler than the Puff approximation (which involves additionally a self-consistent momentum density, and for a local interaction with hard core is more difficult to handle than the BM approximation). The approximation employed yields an equilibrium E_{Av} which is 10% more negative than the BM value at a spacing which is 10% smaller. It appears that the full

Puff approximation would give closer agreement, but as noted, only with considerably more difficulty. This section also points out a second order difference between an expansion of the Puff final equations for E_{Av} and the BG expansion which has not previously been noted. The Mohling equations, on the other hand, are formally in agreement with the BG expansion, but the second and higher order corrections would be very difficult to evaluate. Furthermore, these corrections would have to be evaluated very accurately because of a high degree of cancellation involved. Many of the results indicated above are reported in BM. It should be mentioned that this is the only reported employment of the Mohling-Puff approximation which has used a "realistic" hard core potential acting in states other than the S-state. The evaluations of the Moszkowski-Scott and Mohling-Puff approximations are thus the most quantitative reported to date.

Chapter VII presents a new nuclear matter approximation which is simpler than any of those previously discussed. In this approximation the free kinetic energies are used in the energy denominators of the reaction matrices, which are computed with the "average excitation energy" Δ (introduced in Chapters II and IV) equal to zero, even for particle energies. Thus the Green's functions, which are the most difficult and time-consuming part of the BG and BM calculations, are independent of the nucleon-nucleon potential (which previously appeared through self-consistent denominators) and can be calculated once and tabulated for all future nuclear matter calculations. A second order calculation of the true momentum

distribution is also used, in place of the Fermi step-function, as a weight function when calculating the potential energy. This density can be calculated with a separable potential or can be obtained indirectly by expanding the self-consistent denominators in the second iteration of the basic calculation. Both procedures have been employed in this dissertation. The latter yielded -15.0 MeV at 1.04 Fermis, in excellent (though fortuitous) agreement with BG's -15.2 MeV at 1.02 Fermis. For the former procedure, the Yamaguchi S-state potential without hard core was used, yielding very poor results (-32 MeV at normal density, the saturation properties not being determined). It is expected that a hard shell separable potential will give a density which will yield results comparable to the ones obtained using the expansion of the denominators: the hard shell has the effect of reducing the density by a very large amount below the Fermi sea. Some possible uses of this approximation are discussed and it is emphasized that although it greatly simplifies the computational problem (once the Green's functions and momentum density have been computed and tabulated), it maintains most of the features of the full calculation. Further, the approximation is simple enough to be easily included in graduate level courses.

ACKNOWLEDGMENTS

I wish to thank the many people who, through discussion and instruction, have contributed to these investigations. In particular, I am indebted to Professor Keith A. Brueckner for his counsel and guidance throughout these studies; to Dr. Katuro Sawada for many helpful discussions covering the analysis of the Puff approximation and the material in Chapters II and VII; to Dr. Andrew Lockett for his collaboration on the finite nucleus calculations (Chapter V) and Mr. Vemuri L. Narasimham, who collaborated in the calculations reported in Appendices D and E; to Professors Walter Kohn and Maria G. Mayer and Assistant Professor Manuel Rotenberg for invaluable assistance on various problems; and to Professor Clay Perry, the director of the Computation Facility, for the full cooperation of his organization.

II.

PERTURBATION THEORY OF THE ZERO-TEMPERATURE MANY-FERMION NORMAL SYSTEM

The theory of the many-fermion system has been the object of intense study for many years. This dissertation is limited to a small portion of the overall field, the study of the perturbation theory of the nuclear zero-temperature "normal" state -- that state in which there is no binding which would lead to a phenomenon such as superconductivity. The basic theory for the perturbation treatment has been developed, and is presented briefly in this chapter as the basic tool on which the remainder of this investigation depends. This basic tool is the Brueckner-Goldstone linked-cluster expansion (BG expansion), the perturbation theoretic expression for the ground state energy of the system described above. The Brueckner K-matrix approximation to this energy is also briefly presented. With the BG expansion as a basis, the properties of a many-fermion system are then analyzed and several general relations are developed. These have previously been derived within the framework of Green's function theory, but the equations developed here are expressed as explicit perturbation series in contrast to some of the original derivations. Following this, a new approximation for many-fermion systems is presented. This approximation is derived by using a "change of parameter" procedure which is described in the text.

A. THE BRUECKNER-GOLDSTONE LINKED-CLUSTER EXPANSION AND THE BRUECKNER K-MATRIX APPROXIMATION

The heart of the perturbation theory of the normal state of many-fermion systems is the Brueckner-Goldstone linked-cluster expansion (BG expansion).[1,2] Its derivation and its limitations are discussed in considerable detail in Appendix A as well as in texts on the many-body problem (e.g., Thouless[20]). Although there are many unanswered questions related to the applicability of this expansion to the atomic nucleus, it will be assumed (in the absence of a rigorous proof to the contrary) that the theory can be used to obtain a description of the properties of the "normal" state of large (and for simplicity, infinite) nuclei, and that this "normal" state is very close to the actual ground state -- much closer than the probable errors in our calculations.

The Schroedinger equation for the system is

$$(H_o + H_I)\Psi = E\Psi = (E_o + \Delta E)\Psi \tag{2.1}$$

with

$$H_o = \sum_k \frac{k^2}{2M} a_k{}^* a_k = \sum_k \epsilon_k \hat{n}_k \tag{2.2}$$

satisfying

$$H_o \, \Phi_o = E_o \, \Phi_o \tag{2.3}$$

and

$$H_I = \frac{1}{2} \sum_{k\ell;mn} v_{k\ell;mn}\, a_\ell^* a_k^* a_m a_n \tag{2.4}$$

satisfying

$$H_I \, \Psi = \Delta E \, \Psi \; . \tag{2.5}$$

The expectation value in the unperturbed ground state of the number operator $\hat{n}_k = a_k^* a_k$ is just

$$\begin{aligned} (\Phi_o, \hat{n}_k \, \Phi_o) \equiv n_k &= 1 \qquad |\underset{\sim}{k}| \le p_F \\ &= 0 \qquad |\underset{\sim}{k}| > p_F \; . \end{aligned} \tag{2.6}$$

The BG expansion for the interaction energy, $\Delta E(n,\epsilon)$, (Appendix A -- Eq. (A.73)) is just

$$\Delta E = \lim_{\alpha \to 0} \sum_c (\Phi_o, H_I \frac{1}{E_o - H_o + in\alpha} H_I \cdots H_I \frac{1}{E_o - H_o + i2\alpha} H_I \frac{1}{E_o - H_o + i\alpha} H_I \, \Phi_o) \tag{2.7}$$

where $\sum_c$ means summation over all connected graphs leading from Φ_o to Φ_o, i.e., over all linked graphs with no external lines. In terms of the two-body interaction, the BG expansion is given by

$$\begin{aligned} E &= \sum_k \epsilon_k n_k + \Delta E(n,\epsilon) \\ &= \sum_k \epsilon_k n_k + \frac{1}{2} \sum_{k\ell} v_{k\ell;(k\ell)}\, n_k n_\ell \\ &\quad + \lim_{\alpha \to 0} \frac{1}{4} \sum_{k\ell,mn} v_{k\ell;(mn)} \frac{(1-n_m)(1-n_n) n_k n_\ell}{(\epsilon_k + \epsilon_\ell - \epsilon_m - \epsilon_n + i\alpha)} v_{mn;(k\ell)} + O(v^3) \end{aligned} \tag{2.8}$$

(See (A.92) in Appendix A).

In Appendix A rules are given for expressing the terms of any order in the BG expansion (2.7) in terms of all possible connected graphs ("linked clusters") of that order. With two exceptions these rules are the same as those used by most authors.[20,2] These exceptions are: (1) indicate explicitly the creation and annihilation operators associated with each v-interaction, reduce them to expectation values of the number operator using the customary prescription

$$\begin{aligned} a_k^* a_k &= \hat{n}_k \\ a_k a_k^* &= (1 - a_k^* a_k) = (1 - \hat{n}_k) \ , \end{aligned} \tag{2.9}$$

and use the identities (for the expectation values)

$$n_k^n = n_k$$

and

$$(1 - n_k)^n = (1 - n_k) \tag{2.10}$$

to simplify the resulting expansion; and, (2) provide for the possibility of a non-spherical unperturbed Fermi sea by defining a state of momentum $\underset{\sim}{k}$ as a "particle" if $\epsilon_{\underset{\sim}{k}} > \epsilon_F$ and a "hole" if $\epsilon_{\underset{\sim}{k}} \leq \epsilon_F$, where $\epsilon_{\underset{\sim}{k}}$ is the unperturbed energy and ϵ_F is the Fermi energy. If the unperturbed Hamiltonian is just the sum of kinetic energies or if the potential term in the unperturbed Hamiltonian is spherically symmetric, then the above definition can be reduced to the often-used

definition of a "particle" as a state whose momentum is greater than the "Fermi momentum" and a "hole" as a state whose momentum is less than or equal to the "Fermi momentum." It is, of course, possible for the Fermi energy (or momentum) to depend on the spin (or isotopic spin) of the particles (e.g., as in a system with different neutron and proton densities).

A partial summation of the BG expansion is possible. This is effected by the Brueckner K-matrix approximation,[3] which is treated in detail in Appendix B. In this approximation, the energy is given by

$$E = \sum_k (\epsilon_k + \tfrac{1}{2} V_k) n_k = \sum_k \epsilon_k n_k + \sum_{k\ell} K(\Sigma, \delta E{=}0)_{k\ell;(k\ell)}\, n_k n_\ell + O(K^3) \,. \tag{2.11}$$

The K-matrix is, in turn, determined by the integral equation

$$K(\Sigma,\delta E)_{ij;k\ell} = v_{ij;k\ell} + \sum_{mn} v_{ij;mn} \frac{(1-n_m)(1-n_n)}{\Sigma - \omega_m(\Sigma) - \omega_n(\Sigma) - \delta E} K(\Sigma,\delta E)_{mn;k\ell} \,. \tag{2.12}$$

In this approximation, the energies of particles within the Fermi sea are computed "on the energy shell" with $\delta E = 0$, and with the "single-particle potential" given by

$$V_k = \sum_\ell K(\Sigma, \delta E{=}0)_{k\ell;(k\ell)}\, n_\ell \tag{2.13}$$

with

$$\Sigma = \omega_k + \omega_\ell \tag{2.14}$$

and

$$\omega_k = \epsilon_k + V_k \ . \tag{2.15}$$

The intermediate state energies $\omega_m(\Sigma)$, etc., are computed "off the energy shell," with

$$\delta E = \Delta \tag{2.16}$$

where Δ is a mean excitation energy, usually taken to be $\omega_{p_F} - \omega_{p=0}$. Thus the single-particle potential is given by

$$V_m(\Sigma) = \sum_j K(\Sigma,\Delta)_{jm;(jm)} \, n_j \tag{2.17}$$

and

$$\omega_m(\Sigma) = \epsilon_m + V_m(\Sigma) \ . \tag{2.18}$$

The details of the transformation of these equations to coordinate space are given by Brueckner and Gammel[3] (hereafter referred to as BG) and in Appendix B. Typical diagrams summed by this approximation are indicated in Fig. 1. Diagrams 3(c) (hole-hole scattering) and 3(d) (the so-called "three-body cluster diagram") are the only third-order diagrams not summed by the Brueckner approximation. Other low-order diagrams not summed include the "rearrangement diagrams" indicated in Fig. 2. Further discussion of these neglected terms can be found in Chapter IV.

Fig. 1. Low-order diagrams of the BG expansion. The diagrams are to be interpreted as including all possible exchanges (as explicitly indicated for diagrams 1(a) and 2(a)) and all possible positioning of various elements (e.g., 3(b) can be drawn in four different ways, with the self-energy insert on the lines k, m, ℓ, and n). The light horizontal lines in diagrams 4(d) through (f) indicate positions at which the energy denominators are investigated in the text.

Fig. 2. Low-order "rearrangement energy" diagrams calculated by Brueckner and Goldman[21] (diagrams (a) and (b)) and by Brueckner, Gammel and Kubis[22] (diagrams (a) and (c)) .

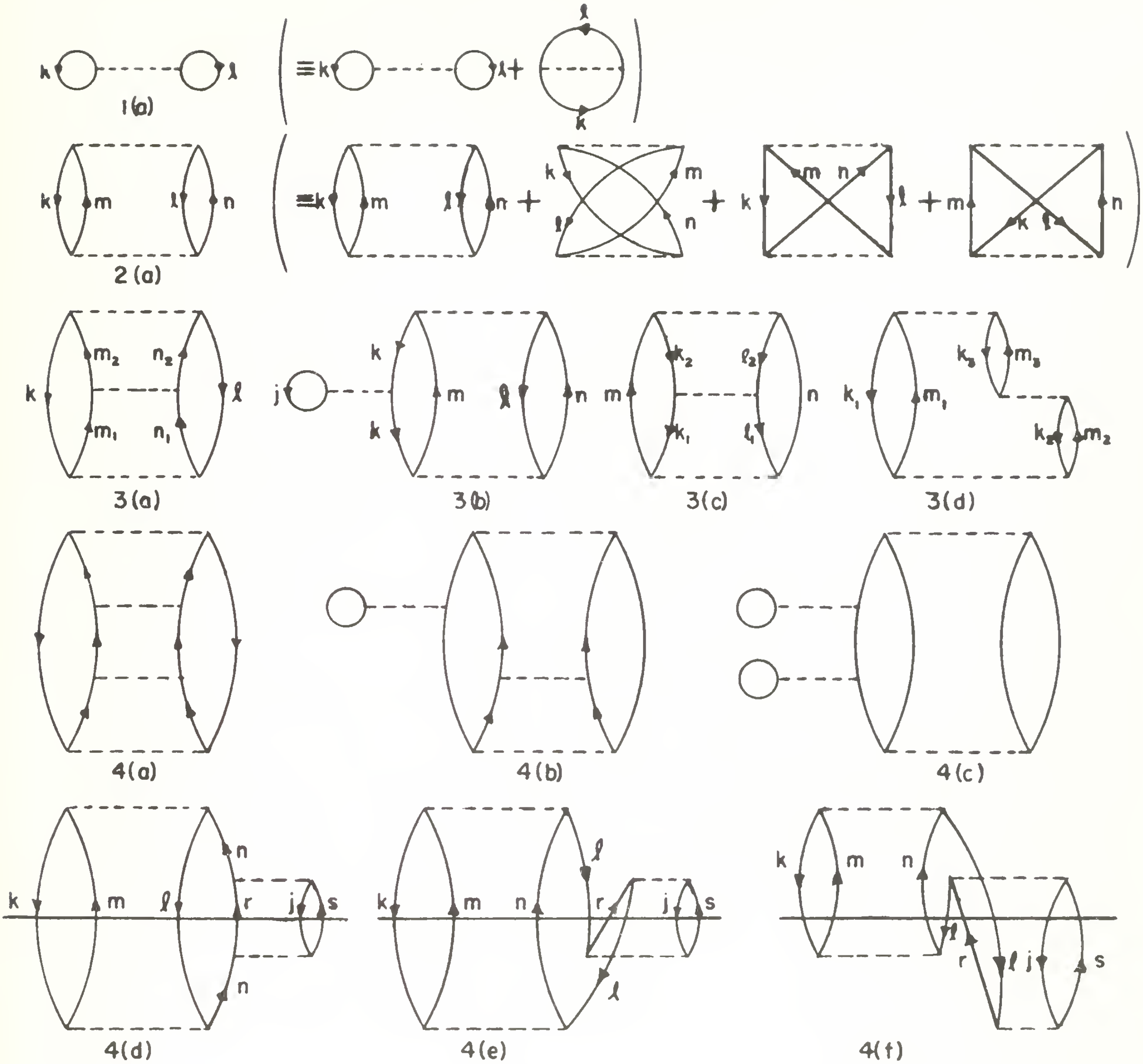

1

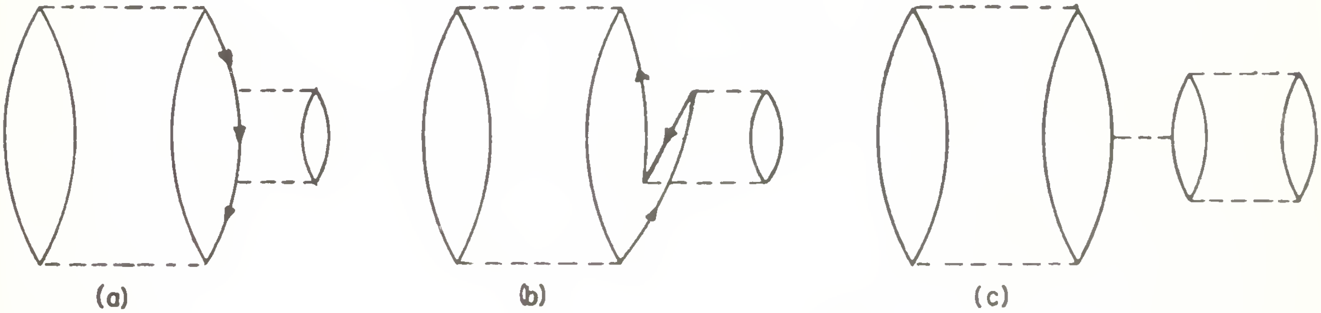

2

B. MANY-FERMION SYSTEM PROPERTIES

Following Sawada, Bruch and Masterson[23] (SBM), fundamental formulae for the true momentum density and the single-particle energy are developed from the Brueckner-Goldstone expansion. Explicit perturbation series are exhibited. In this and following sections several zero-temperature forms of the equations of the Landau theory are derived more concisely than by previous derivations using Green's function theory (e.g., Klein and Prange[24] and Noziéres and Luttinger[25]). Many of the relations so developed are then used in the development of a new approximation in Section F of this Chapter.

1. True Momentum Density

The expectation value of the number operator, $\hat{n}_p = a_p{}^* a_p$, is the Fermi step-function when evaluated between the unperturbed states, Φ_o. When evaluated between the states of the interacting system, Ψ, it yields the momentum density, ρ_p. From

$$E = [\Psi, (\sum_k \epsilon_k \hat{n}_k + v)\Psi]/(\Psi,\Psi) \ , \tag{2.19}$$

we then show that $\rho_p = (\Psi, \hat{n}_p \Psi)/(\Psi,\Psi)$ is

$$\frac{\delta}{\delta\epsilon_p} E = \frac{\delta}{\delta\epsilon_p} \{[\Psi(\epsilon_1\epsilon_2 \ldots),(\sum_k \epsilon_k \hat{n}_k + v)\Psi(\epsilon_1\epsilon_2\ldots)]/(\Psi,\Psi)\} \ . \tag{2.20}$$

The only dependence of the wave functions which is indicated above is their implicit dependence on the single-particle energies as, e.g., given by (A.72). To prove that (2.20) is $(\Psi, \hat{n}_p \Psi)/(\Psi,\Psi)$, we must show that the functional derivative on the wave functions vanishes. If we write that derivative as

$$\frac{\delta}{\delta \epsilon_{p'}} \Big[(\Psi(\ldots\epsilon_{p'}\ldots), (\sum_k \epsilon_k n_k + v)\Psi(\ldots\epsilon_{p'}\ldots)) / (\Psi(\ldots\epsilon_{p'}\ldots), \Psi(\ldots\epsilon_{p'}\ldots)) \Big]_{\epsilon_{p'}=\epsilon_p} \tag{2.21}$$

and, if $\epsilon_{p'}$ is regarded as a variational parameter, then the expectation value is stationary at the true wave function (where $\epsilon_{p'} = \epsilon_p$), and the above derivative vanishes for $\epsilon_{p'} = \epsilon_p$. Thus (2.20) reduces to $(\Psi, \hat{n}_p \Psi)/(\Psi, \Psi) = \rho_p$ (since v has no explicit dependence on the ϵ_k), and one obtains the well-known formula:[26]

$$\rho_p = \frac{\delta}{\delta \epsilon_p} E = n_p + \frac{\delta}{\delta \epsilon_p} \Delta E(n, \epsilon) \equiv n_p + \Delta n_p \ . \tag{2.22}$$

We remark here that the momentum indices are vector indices, and refer to both angle and magnitude of the momenta.

In (2.22) and throughout this discussion, the functional derivative is defined as operating on every ϵ_p which occurs in the expression which follows it, including those ϵ_p which occur under a summation (i.e., the single term in each sum for which the summation variable equals ϵ_p in the example above).

From the BG equation for E, (2.8), we obtain

$$\rho_p(n, \epsilon) = n_p \Big\{ 1 - \sum_{\ell mn} v_{p\ell;mn} \frac{n_\ell (1-n_m)(1-n_n)}{(\epsilon_p + \epsilon_\ell - \epsilon_m - \epsilon_n)^2} v_{mn;(p\ell)} + \ldots \Big\} +$$

$$+ (1-n_p) \Big\{ \sum_{k\ell n} v_{k\ell;pn} \frac{n_k n_\ell (1-n_n)}{(\epsilon_k + \epsilon_\ell - \epsilon_p - \epsilon_n)^2} v_{pn;k\ell} + \ldots \Big\} \ . \tag{2.23}$$

We have used a change of summation indices to combine terms with identical structure arising from (2.8), thus cancelling the factors

$\frac{1}{2}$ in that equation. For example,

$$\frac{1}{2}n_p \sum_{\ell mn} v_{p\ell;mn} \frac{n_\ell(1-n_m)(1-n_n)}{(\epsilon_p+\epsilon_\ell-\epsilon_m-\epsilon_n)^2} v_{mn;(p\ell)} + \frac{1}{2}n_p \sum_{kmn} v_{kp;mn} \frac{n_k(1-n_m)(1-n_n)}{(\epsilon_k+\epsilon_p-\epsilon_m-\epsilon_n)^2} v_{mn;(kp)} \tag{2.24}$$

$$= n_p \sum_{\ell mn} v_{p\ell;mn} \frac{n_\ell(1-n_m)(1-n_n)}{(\epsilon_p+\epsilon_\ell-\epsilon_m-\epsilon_n)^2} v_{mn;(p\ell)} .$$

Similar changes of summation indices to combine terms are employed throughout this dissertation without further comment.

The term not multiplied by n_p in (2.23) is the "tail" of the density distribution, extending beyond the Fermi sphere. It is readily verified that this equation for ρ_p can be truncated at any order in v and will still satisfy the identity[25a]

$$\sum_p \rho_p = \sum_p n_p = N \tag{2.25}$$

Eq. (2.23) can be inverted to yield an equation for n_p in terms of ρ_p:[25b]

$$n_p = \rho_p \left\{1 + \sum_{\substack{\ell \\ mn}} v_{p\ell;mn} \frac{\rho_\ell(1-\rho_m)(1-\rho_n)}{(\epsilon_p+\epsilon_\ell-\epsilon_m-\epsilon_n)^2} v_{mn;(p\ell)} + \cdots\right\}$$

$$- (1-\rho_p)\left\{ \sum_{\substack{k\ell \\ n}} v_{k\ell;pn} \frac{\rho_k\rho_\ell (1-\rho_n)}{(\epsilon_k+\epsilon_\ell-\epsilon_p-\epsilon_n)^2} v_{pn;(k\ell)} + \cdots\right\}. \tag{2.26}$$

2. Single-Particle Energy

The "single-particle" energy may be obtained from the perturbation expression for the total energy in a fashion analogous to that employed for the density. The energy of an added particle of momentum $\underset{\sim}{p}$ is the difference

$$\omega_p = E_p(n_p',\epsilon) - E(n,\epsilon) \tag{2.27}$$

where

$$n_{k,p}' = \begin{cases} 1 \quad \text{for} \quad \epsilon_k \le \epsilon_{k_F} \\ \begin{Bmatrix} 0 & \underset{\sim}{k} \ne \underset{\sim}{p} \\ 1 & \underset{\sim}{k} = \underset{\sim}{p} \end{Bmatrix} \quad \text{for } \epsilon_k > \epsilon_{k_F} \ . \end{cases} \tag{2.28}$$

Similarly, the energy of an additional hole is

$$\omega_p = E(n,\epsilon) - E_p(n_p'',\epsilon) \ , \tag{2.29}$$

with

$$n_{k,p}'' = \begin{cases} \begin{Bmatrix} 1 & \underset{\sim}{k} \ne \underset{\sim}{p} \\ 0 & \underset{\sim}{k} = \underset{\sim}{p} \end{Bmatrix} \quad |\underset{\sim}{k}| \le k_F \\ 0 \qquad |k| > k_F \ . \end{cases} \tag{2.30}$$

It is apparent from the above expressions that the single-particle energy can be written as

$$\omega_p = \pm(E_p - E) = \frac{\delta}{\delta n_p} E(n,\epsilon) = \epsilon_p + \frac{\delta}{\delta n_p} \Delta E(n,\epsilon) \tag{2.31}$$

$$= \epsilon_p + \Delta\epsilon_p ; \qquad \Delta\epsilon_p = \frac{\delta}{\delta n_p} \Delta E(n,\epsilon) \ .$$

The definition of $\delta/\delta n_p$ is similar to that of $\delta/\delta\epsilon_p$. It is shown in Appendix A that $E(n,\epsilon)$ is proportional to the total number, N; therefore, ω_p is of order unity compared to N because $\delta/\delta n_p$ removes one summation of $E(n,\epsilon)$. Rigorously, (2.31) should contain terms with the higher derivatives $\delta^2/\delta n_p^2$, $\delta^3/\delta n_p^3$, etc. However, each such derivative will remove one or more other summations and will thus introduce a factor of $1/N$ or smaller. Such terms may be discarded in the normal system (for which we take the limit $\Omega \to \infty$, with the ratio N/Ω remaining constant, Ω being the volume).[25c] From (2.8) we obtain the following expansion of (2.31).

$$\omega_p(\epsilon_p) = \epsilon_p + \sum_\ell v_{p\ell;(p\ell)}\, n_\ell + \lim_{\alpha \to 0} \sum_{\ell mn} v_{p\ell;mn} \frac{n_\ell(1-n_m)(1-n_n)}{\epsilon_p+\epsilon_\ell-\epsilon_m-\epsilon_n+i\alpha}\, v_{mn;(p\ell)} \tag{2.32}$$

$$- \lim_{\alpha \to 0} \sum_{k\ell n} v_{k\ell;pn} \frac{n_k n_\ell (1-n_n)}{\epsilon_k+\epsilon_\ell-\epsilon_p-\epsilon_n+ i\alpha}\, v_{pn;(k\ell)} + \cdots .$$

The imaginary terms from the Brueckner-Goldstone expansion, (2.7), are related to the lifetimes of the hole and particle states. In the subsequent discussions we shall not exhibit the imaginary terms explicitly. We should remember, however, that ω_{k_F} has no imaginary part. The original BG series for the ground state energy (of the normal system) contains no poles, and since (2.32) for $p = k_F$ is just the upper or lower limit of one summation in the equation for the ground state energy, it must also be real.

If we define an "effective interaction" matrix $U(k,\ell)$ such that

$$\Delta E(n,\epsilon) = \frac{1}{2}\sum_{k,\ell} U(k,\ell) n_k n_\ell \ , \tag{2.33}$$

then (2.31) becomes

$$\omega_p = \epsilon_p + \sum_\ell U(p,\ell) n_\ell + \frac{1}{2}\sum_{k\,\ell} n_k n_\ell \frac{\delta}{\delta n_p} U(k,\ell) \ , \tag{2.34}$$

which is a restricted form of the Landau equation, with all the quantities in (2.33) completely specified by the BG expansion (which is an equation for $U(k,\ell)$). For example, to second order in v,

$$U(k,\ell) = v_{k\ell;(k\ell)} + \sum_{m,n} v_{k\ell;mn} \frac{(1-n_m)(1-n_n)}{\epsilon_k+\epsilon_\ell-\epsilon_m-\epsilon_n} v_{mn;(k\ell)} \ , \tag{2.35}$$

and (2.32) is obviously obtained when this equation is substituted into (2.34). The third term in the equation for ω_p is the so-called "rearrangement energy."[21,27,28,29] It represents the difference in the energy to remove a particle to infinity "quickly" (with no change in the states of the rest of the system) and the energy required to remove the particle adiabatically (the rest of the system "rearranging" itself to the ground state of the N-1 particle system as the removed particle goes to infinity). As noted by Brueckner,[27] it is this term which is the obvious culprit in the failure of reaction-matrix calculations to satisfy the Bethe-Hugenholtz-Van Hove theorem[8,30] that the single-particle energy at the Fermi surface should equal the mean system energy: most reaction

matrix calculations use only the first two terms of (2.34) for the single-particle energy.[25a] If one identifies $U(k,\ell)$ with Brueckner's K-matrix, $K_{k\ell;(k\ell)}$, then (2.34) is identical to the equation derived by Brueckner and Goldman in their analysis of the rearrangement energy.[21]

C. DISCONTINUITY IN MOMENTUM DENSITY AT THE FERMI SURFACE

The possibility that a Fermi surface might exist for zero temperature interacting fermions was pointed out by Migdal,[31] who noticed that under some circumstances it could be so that the *mean* occupation number of different single-particle momentum states in the true ground state is discontinuous. Luttinger[32] has examined the conditions for its existence and rederived the equation for the discontinuity. A calculation for the electron gas has been reported by Daniel and Vosko.[26] We present here still another derivation, which is based on the assumption that a valid perturbation expansion for the system energy exists.

From expression (2.23) for the momentum density, ρ_p, it is evident that ρ_p can be separated into two parts, one multiplied by n_p and the other having no explicit dependence on n_p:

$$\begin{aligned}\rho_p &= \frac{\delta}{\delta\epsilon_p}\; E(n,\epsilon)\\ &= n_p + n_p \frac{\delta}{\delta\epsilon_p}\left(\frac{\delta}{\delta n_p}\,\Delta E(n,\epsilon)\right) + \frac{\delta'}{\delta\epsilon_p}\,\Delta E(n,\epsilon)\ . \qquad (2.36)\end{aligned}$$

Henceforth $\delta'/\delta\epsilon_p$ will indicate differentiation of those terms not

multiplied by n_p . Thus the leading terms of the last two elements on the right hand side of (2.36) are

$$n_p \frac{\delta}{\delta\epsilon_p}\left(\frac{\delta}{\delta n_p}\Delta E(n,\epsilon)\right) = -n_p\left\{\sum_{\ell mn} V_{p\ell;mn}\frac{n_\ell(1-n_m)(1-n_n)}{(\epsilon_p+\epsilon_\ell-\epsilon_m-\epsilon_n)^2}V_{mn;(p\ell)} - \right.$$

$$\left. - \sum_{k\ell n} V_{k\ell;pn}\frac{n_k n_\ell(1-n_n)}{(\epsilon_k+\epsilon_\ell-\epsilon_p-\epsilon_n)^2}V_{pn;(k\ell)} + \cdots\right\}, \tag{2.37}$$

and

$$\frac{\delta'}{\delta\epsilon_p}\Delta E(n,\epsilon) = -\sum_{k\ell n} V_{k\ell;pn}\frac{n_k n_\ell(1-n_n)}{(\epsilon_k+\epsilon_\ell-\epsilon_p-\epsilon_n)^2}V_{pn;(k\ell)} . \tag{2.38}$$

By using the definition of the single-particle energy change $\Delta\epsilon_p(n,\epsilon)$ from (2.31), we can write (2.36) as

$$\begin{aligned} \rho_p &= n_p\left(1+\frac{\delta}{\delta\epsilon_p}\Delta\epsilon_p\right) + \frac{\delta'}{\delta\epsilon_p}\Delta E(n,\epsilon) \\ &= n_p\frac{\delta}{\delta\epsilon_p}\omega_p(\epsilon_p) + \frac{\delta'}{\delta\epsilon_p}\Delta E(n,\epsilon) . \end{aligned} \tag{2.39}$$

It can be seen that $\delta/\delta\epsilon_p$ operates not only on the explicit ϵ_p in $\omega_p(\epsilon_p)$ but also on the single term in each sum for which the index of summation equals p. Because these latter operations yield terms of order $(1/N)$ (because of the removal of one sum), they may be neglected and the functional derivative may be replaced by the partial derivative, $\partial/\partial\epsilon_p$. The density is then given by

$$\rho_p = n_p \frac{\partial}{\partial\epsilon_p} \omega_p(\epsilon_p) + \frac{\delta'}{\delta\epsilon_p} \Delta E(n,\epsilon) \ . \qquad (2.40)$$

Usually $\delta/\delta\epsilon_p(\omega_p)$ is denoted as Z_p . Its physical meaning can be seen in the following way. For $\epsilon_p > \epsilon_F$, we have from the definition of ω_p and from (2.22)

$$Z_p = \frac{\delta}{\delta\epsilon_p} \omega_p = \frac{\delta}{\delta\epsilon_p} (\epsilon_p - \epsilon)$$

$$= (\Psi_p, \hat{n}_p \Psi_p) - (\Psi, \hat{n}_p \Psi) \ , \qquad (2.41)$$

where Ψ_p is the state with one extra particle of momentum $\underset{\sim}{p}$. If we introduce the creation and annihilation operators, a_p^* and a_p $(\hat{n}_p = a_p^* a_p)$, and the complete set of unperturbed states, Φ_ℓ , we obtain

$$Z_p = \sum_\ell |(a_p \Phi_\ell, \Psi_p)|^2 - \sum_\ell |(a_p \Phi_\ell, \Psi)|^2 \ . \qquad (2.42)$$

A similar equation is obtained for $\epsilon_p \leq \epsilon_F$. Thus Z_p is the difference between the total probabilities of finding in Ψ_p and Ψ unperturbed states which contain a particle in state $\underset{\sim}{p}$. If the state $\underset{\sim}{p}$ has a finite lifetime, Ψ_p must be replaced by an appropriate wave packet, and only the real part of Z_p can be interpreted in this manner. Because ω_{k_F} contains no imaginary part (see below (2.32)), the above formulation is exact at the Fermi surface.

From (2.39) it is apparent that the discontinuity across $\epsilon_p = \epsilon_F$ is given by

$$\frac{\delta}{\delta\epsilon_p}\,\omega_p\Big|_{\epsilon_p=\epsilon_F} = Z_p\Big|_{\epsilon_p=\epsilon_F} \underset{N\to\infty}{=} \frac{\partial}{\partial\epsilon_p}\,\omega_p\Big|_{\epsilon_p=\epsilon_F} . \qquad (2.43)$$

Using the formalism developed in this section, we are now able to cast (2.40) into a different form. If we solve (2.32) for ϵ_p as a function of ω_p, we can write $\Delta\epsilon_p$ of (2.31) in terms of ω_p and obtain a new function, $V(\omega_p)$, which is numerically equal to $\Delta\epsilon_p$. $V(\omega_p)$ is the "self-consistent" potential, since from (2.31):

$$\omega_p = \epsilon_p + V(\omega_p) . \qquad (2.44)$$

To obtain an expression for ρ_p, we operate on the above expression with $\partial/\partial\epsilon_p$, obtaining

$$\frac{\partial}{\partial\epsilon_p}\,\omega_p = 1 + \frac{\partial}{\partial\epsilon_p}\,\omega_p \cdot \frac{\partial}{\partial\omega_p}\,V(\omega_p) . \qquad (2.45)$$

This can be solved for $\partial/\partial\epsilon_p(\omega_p)$:

$$\frac{\partial}{\partial\epsilon_p}\,\omega_p = \frac{1}{1 - \frac{\partial}{\partial\omega_p}\,V(\omega_p)} . \qquad (2.46)$$

From (2.39) we then obtain

$$\rho_p = \frac{n_p}{1 - \frac{\partial}{\partial\omega_p}\,V(\omega_p)} + \frac{\delta'}{\delta\epsilon_p}\,\Delta E(n,\epsilon) . \qquad (2.47)$$

The first term on the right in (2.47) corresponds to the density obtained by Puff and Martin[13] (see also Falk and Wilets,[33] Eq. (21)). The smooth part in (2.47), which is neglected in their approximation,

can be seen from (2.23) to be of order v^2 .

D. EFFECTIVE MASS EQUATION

We shall now derive the effective mass equation which was first obtained semi-phenomenologically by Landau[34] and later from perturbation theory by Luttinger and Noziéres.[25]

By taking derivatives of ω_p (Eqs. (2.31) and (2.32)) with respect to p_x , we get:

$$\begin{aligned}
\frac{d}{dp_x}\omega_p &= \frac{p_x}{m} + \frac{d}{dp_x}\left(\frac{\delta}{\delta n_p}\Delta E(n,\epsilon)\right) \\
&= \frac{p_x}{m} + \frac{d}{dp_x}\left(\sum_{\ell} V_{p\ell;(p\ell)}\, n_\ell + \sum_{\ell mn} V_{p\ell;mn}\frac{n_\ell(1-n_m)(1-n_n)}{\epsilon_p+\epsilon_\ell-\epsilon_m-\epsilon_n} V_{mn;(p\ell)} + \cdots\right) \\
&= \frac{p_x}{m} + \lim_{\Delta p_x\to 0}\left\{\left(\sum_{\ell} V_{p+\Delta p_x,\ell;(p+\Delta p_x,\ell)}\, n_\ell + \right.\right. \\
&\quad \left.\left. + \sum_{\ell mn} V_{p+\Delta p_x,\ell;mn}\frac{n_\ell(1-n_m)(1-n_n)}{\epsilon_{p+\Delta p_x}+\epsilon_\ell-\epsilon_m-\epsilon_n} V_{mn;(p+\Delta p_x,\ell)}+\cdots\right) - \right. \\
&\quad \left. - (\Delta p_x=0)\right\}\frac{1}{\Delta p_x} \; .
\end{aligned} \tag{2.48}$$

We next change all the momentum variables under the summations by an amount Δp_x, and observe that in a Galilean invariant system

$$V_{p+\Delta p_x,\ell+\Delta p_x;m+\Delta p_x,n+\Delta p_x} = V_{p\ell;mn}$$

and due to conservation of total momentum

$$\epsilon_{p+\Delta p_x} + \epsilon_{\ell+\Delta p_x} - \epsilon_{m+\Delta p_x} - \epsilon_{n+\Delta p_x} =$$

$$= \epsilon_p + \epsilon_\ell - \epsilon_m - \epsilon_n + O\left((\Delta p_x)^2\right) . \qquad (2.49)$$

The result is

$$\frac{d}{dp_x}\omega_p = \frac{p_x}{m} + \lim_{\Delta p_x \to 0} \Bigg\{\Bigg(\sum_\ell V_{p\ell;(p\ell)}\, n_{\ell+\Delta p_x} + \sum_{\ell mn} V_{p\ell;mn} \frac{n_{\ell+\Delta p_x}(1-n_{m+\Delta p_x})(1-n_{n+\Delta p_x})}{\epsilon_p+\epsilon_\ell-\epsilon_m-\epsilon_n} V_{mn;(p\ell)} + \cdots\Bigg) - (\Delta p_x = 0)\Bigg\} \frac{1}{\Delta p_x} . \qquad (2.50)$$

The second term on the right can be identified with

$$\sum_{\ell'} \frac{dn_{\ell'}}{d\ell'_x} \frac{\delta}{\delta n_{\ell'}} \left(\sum_\ell V_{p\ell;(p\ell)}\, n_\ell + \sum_{\ell mn} V_{p\ell;mn} \frac{n_\ell(1-n_m)(1-n_n)}{\epsilon_p+\epsilon_\ell-\epsilon_m-\epsilon_n} V_{mn;(p\ell)} + \cdots \right)$$

$$= \sum_\ell \frac{dn_\ell}{d\ell_x} \frac{\delta}{\delta n_\ell} \left(\frac{\delta}{\delta n_p} \Delta E(n,\epsilon) \right) . \qquad (2.51)$$

Since n_ℓ is a step-function, $dn_\ell / d\ell_x$ is zero except at the Fermi surface, where its magnitude is $-\ell_x/\ell$. Thus,

$$\frac{d}{dp_x}\omega_p = \frac{p_x}{m} - \sum \frac{\ell_x}{\ell}\, \delta(\ell - k_F) \frac{\delta^2}{\delta n_\ell \delta n_p} \Delta E(n,\epsilon) . \qquad (2.52)$$

This equation is identical to that obtained by Landau, except now, by virtue of the BG expansion for $\Delta E(n,\epsilon)$, we have an explicit expression for every term in it.

If we take $\omega_p \Big| |\underset{\sim}{p}| \approx k_F = p^2/2m^*$ and operate with $1/p^2 \sum_{xyz} p_x\, d/dp_x$ on ω_p , we obtain

$$\begin{aligned} \frac{1}{m^*} &= \frac{1}{m} - \frac{1}{k_F} \sum_{\ell} \cos(\underset{\sim}{p},\underset{\sim}{\ell})\,\delta(\ell-k_F)\, \frac{\delta^2}{\delta n_\ell \delta n_p} \Delta E(n,\epsilon)\Big|_{p=k_F} \\ &= \frac{1}{m} + \frac{\Omega}{(2\pi)^3} k_F \int d\Omega_\ell \cos(\underset{\sim}{p},\underset{\sim}{\ell})(-) \frac{\delta^2}{\delta n_\ell \delta n_p} \Delta E(n,\epsilon)\Big|_{p=k_F} . \end{aligned} \tag{2.53}$$

The quantity $(-)\delta^2 E(n,\epsilon)/\delta n_\ell \delta n_p = f_{\ell;p}$ was interpreted by Landau[34] as (minus) the forward scattering amplitude of two particles, $\underset{\sim}{\ell}$ and $\underset{\sim}{p}$, in the system. We reach the same identification by following the procedure by which we derived Eq. (2.31) for ω_p .

E. BETHE-HUGENHOLTZ-VAN HOVE SEPARATION ENERGY THEOREM

With our formalism we can easily derive the Bethe-Hugenholtz-Van Hove[8,30] theorem which states that the energy of a particle on the Fermi surface is the negative of the energy required to remove the particle adiabatically to infinity (the separation energy) and equals the average energy of all the particles in the system. Alternately, the separation energy is the negative of the energy the system acquires when one particle is added at constant volume whereas the average energy is the energy acquired when a

single particle is added at constant density. A somewhat more involved derivation has also been given by Brueckner.[27]

The proof begins with the observation that the total energy E is a function of two parameters, N and ρ, where the density ρ is related to the total number of particles, N, and to the volume, Ω, by the following equation (neglecting spin which gives a constant):

$$\rho = \frac{N}{\Omega} = \frac{1}{\Omega} \sum_k \hat{n}_k = \frac{1}{(2\pi)^3} \int_0^{p_F} d\underset{\sim}{k} = p_F{}^3/6\pi^2 \ . \qquad (2.54)$$

Further, since E is proportional to N, it may be written as $E = Nf(\rho)$ where $f(\rho)$ denotes the (unknown) functional dependence on the density. From the definition of the average energy, it is easily seen that $E_{Av} = E/N$. For a free system, the pressure, P, must be zero, and therefore at zero temperature

$$P \sim \frac{\partial}{\partial \rho} (E/N)_\Omega = 0 \qquad (2.55)$$

(since the average energy, E/N, is a function of density alone). We can then expand the derivative of $E = Nf(\rho)$ to obtain

$$\frac{\partial}{\partial N} (E)_\Omega = f(\rho) + N \frac{\partial f(\rho)}{\partial \rho} \frac{\partial \rho}{\partial N} \ , \qquad (2.56)$$

to show that the separation energy equals the negative of the average energy, viz.:

$$E_s = - \frac{\partial}{\partial N} (E)_\Omega = - \frac{E}{N} - \rho \frac{\partial}{\partial \rho} (\frac{E}{N})_\Omega = - \frac{E}{N} \ . \qquad (2.57)$$

We can now apply the techniques of previous sections to obtain another equality involving E/N. Expanding (2.55), we obtain

$$-\frac{E}{N^2}\frac{\partial}{\partial\rho}(N)_\Omega + \frac{1}{N}\frac{\partial}{\partial\rho}(E)_\Omega = -\frac{E}{N^2}\Omega + \frac{1}{N}\frac{\partial}{\partial\rho}(E)_\Omega = 0 \; . \qquad (2.58)$$

Thus

$$\frac{E}{N} = \frac{1}{\Omega}\frac{\partial}{\partial\rho}(E)_\Omega \; . \qquad (2.59)$$

Using (2.54), we can rewrite (2.59) as

$$\frac{E}{N} = \frac{1}{\Omega}\frac{2\pi^2}{{p_F}^2}\frac{\partial}{\partial p_F}(E) = \frac{2\pi^2}{\Omega {p_F}^2}\sum_k \left\{ \frac{\partial n_k}{\partial p_F}\frac{\delta}{\delta n_k} E + \frac{\partial \epsilon_k}{\partial p_F}\frac{\delta}{\delta \epsilon_k} E \right\} \; . \qquad (2.60)$$

The kinetic energy, ϵ_k, is unchanged by an infinitesimal increase, η, in the magnitude of the Fermi momentum, but n_k will increase by unity for $k = p_F + \eta$ if p_F increases by η. Therefore, $\partial\epsilon_k/\partial p_F = 0$ and $\partial n_k/\partial p_F = \delta(k-p_F)$. Using

$$\sum_k \rightarrow \frac{\Omega}{(2\pi)^3}\int d\underset{\sim}{k} \; , \qquad (2.61)$$

and identifying $\delta/\delta n_k(E)$ with ω_k (2.24), we obtain

$$\frac{E}{N} = \frac{1}{4\pi {p_F}^2}\int d\underset{\sim}{k}\; \delta(k-p_F)\, \omega_k = \omega_{p_F} \; . \qquad (2.62)$$

From (2.57) and (2.62),

$$\frac{E}{N} = \omega_{p_F} = -E_s \; , \qquad (2.63)$$

which proves the theorem. It should be noted that this derivation is strictly valid only if the single-particle energy, ϵ_k, is continuous at the Fermi surface, since otherwise its derivative with

respect to p_F does not vanish.

F. THE "CHANGE OF PARAMETER" PROCEDURE--USE OF THE TRUE MOMENTUM DENSITY IN THE BRUECKNER-GOLDSTONE EXPANSION

The Brueckner-Goldstone expansion for the interaction energy, $\Delta E(n,\epsilon)$, is a function of the unperturbed distribution of particles in momentum space, n_k, and the free kinetic energies, ϵ_k. Because of the intimate relation between ω_p and ρ_p as given in (2.22) and (2.31), it is interesting to investigate the possibility of using the true distribution ρ_p instead of the "mathematical" n_p in this expansion. This substitution will force us to change free-kinetic energies, ϵ_p, to some other energies, w_p. In the following we give an explicit derivation of the energy w_p.

First, we note the invariance of the interaction energy $\Delta E(n,\epsilon)$ under the following infinitesimal displacements of n_k and ϵ_k:

$$\Delta E\left(n_k+\lambda_k \frac{\delta}{\delta\epsilon_k} \Delta E(n,\epsilon);\ \epsilon_k-\lambda_k \frac{\delta}{\delta n_k} \Delta E(n,\epsilon)\right) . \tag{2.64}$$

This can be expanded in a Taylor series about $\Delta E(\underset{\sim}{n_k},\underset{\sim}{\epsilon_k})$ to yield

$$\Delta E(n_k,\epsilon_k) + O(\lambda^2) . \tag{2.65}$$

We know from (2.22) and (2.31) that $\delta\Delta E(n,\epsilon)/\delta\epsilon_k = \Delta n_k$ and $\delta\Delta E(n,\epsilon)/\delta n_k = \Delta\epsilon_k$. Therefore, the above relation shows that if we change n_k by $\lambda_k\,\Delta\, n_k$ (λ_k a small quantity) and simultaneously change ϵ_k by $-\lambda_k\,\Delta\epsilon_k$, the BG expansion remains unchanged up to

order $(\lambda_k)^2$.

The above invariance indicates that if we make the replacement of n_k by ρ_k (given by (2.22)) by adding up infinitesimal changes, the kinetic energy ϵ_k in the denominators should be reduced by a quantity which is roughly equal to $\Delta\epsilon_k$ in order to keep the numerical values of $\Delta E(n,\epsilon)$ and $\Delta E(\rho,w)$ equal. The change in the kinetic energy ϵ_k will not be exactly $\Delta\epsilon_k$, of course, because the above identity holds only for infinitesimal λ_k. To determine exactly the modified free-energy, w_k, we proceed as follows: For a given function of n's and ϵ's, $f(n,\epsilon)$, we assume we know the dependence on n and ϵ (for instance, for $\Delta E(n,\epsilon)$ we have the explicit series (2.8)). Then we try to find the quantities ρ_k and w_k which satisfy[34a]

$$f(n,\epsilon) = f(\rho,w) \ . \tag{2.66}$$

To find w let us first introduce intermediate quantities $\rho_k(\lambda)$ and $w_k(\lambda)$ which satisfy

$$\rho_k(0) = n_k \ , \qquad w_k(0) = \epsilon_k \ , \tag{2.67}$$

and require the following relation to be true for arbitrary λ :

$$f(n,\epsilon) = f\Big(\rho(\lambda), w(\lambda)\Big) \ . \tag{2.68}$$

In other words,

$$\frac{d}{d\lambda} f\Big(\rho(\lambda), w(\lambda)\Big) = 0 \tag{2.69}$$

or, using the chain rule,

$$\sum_k \left(\frac{d\rho_k(\lambda)}{d\lambda} \frac{\delta f\left(\rho(\lambda),w(\lambda)\right)}{\delta\rho_k(\lambda)} + \frac{dw_k(\lambda)}{d\lambda} \frac{\delta f\left(\rho(\lambda),w(\lambda)\right)}{\delta w_k(\lambda)} \right) = 0 \ . \qquad (2.70)$$

Integration gives (taking (2.67) for $w_k(0)$ into account)

$$w_k(\lambda) = \epsilon_k - \int_0^\lambda d\lambda' \frac{\dfrac{\delta f\left(\rho(\lambda'),w(\lambda')\right)}{\delta\rho_k(\lambda')}}{\dfrac{\delta f\left(\rho(\lambda'),w(\lambda')\right)}{\delta w_k(\lambda')}} \frac{d}{d\lambda'}\rho_k(\lambda') \ . \qquad (2.71)$$

Now, let us give $\rho_k(\lambda)$ at $\lambda = 1$ the value ρ_k' and try to find $w_k(1)$. A form of $\rho_k(\lambda)$ which satisfies both $\rho_k(0) = n_k$ and $\rho_k(1) = \rho_k'$ can be written as

$$\rho_k(\lambda) = n_k + \lambda(\rho_k' - n_k) \qquad (2.72)$$

with this definition of $\rho_k(\lambda)$, (2.71) becomes

$$w_k(\lambda) = \epsilon_k - (\rho_k' - n_k) \int_0^\lambda d\lambda' \frac{\dfrac{\delta f\left(\rho(\lambda'),w(\lambda')\right)}{\delta\rho_k(\lambda')}}{\dfrac{\delta f\left(\rho(\lambda'),w(\lambda')\right)}{\delta w_k(\lambda')}} \ . \qquad (2.73)$$

This is the desired formula for $w_k(\lambda)$ in terms of $\rho_k(\lambda)$; if $w_k(1) = w_k'$ is found for given ρ_k' ,

$$f(n,\epsilon) = f(\rho',w') \ . \qquad (2.74)$$

Now, we can apply (2.73) and (2.74) to $\Delta E(n,\epsilon)$. We identify ρ_k' with the true density, ρ_k , and w_k' with the desired energy, w_k , and use (2.22) and (2.31) to obtain the following set of equations:

$$\Delta E(n,\epsilon) = \Delta E(\rho,w)$$

$$\rho_k(\lambda) = n_k + \lambda(\rho_k - n_k)$$

$$w_k(\lambda) = \epsilon_k - \frac{\delta\Delta E(n,\epsilon)}{\delta\epsilon_k}\int_0^\lambda d\lambda' \frac{\dfrac{\delta\Delta E\left(\rho(\lambda'),w(\lambda')\right)}{\delta\rho_k(\lambda')}}{\dfrac{\delta\Delta E\left(\rho(\lambda'),w(\lambda')\right)}{\delta w_k(\lambda')}} \qquad (2.75)$$

$$w_k = w_k(1) = \epsilon_k - \Delta\epsilon_k - \Delta n_k \int_0^1 d\lambda' \left[\frac{\dfrac{\delta\Delta E\left(\rho(\lambda'),w(\lambda')\right)}{\delta\rho_k(\lambda')}}{\dfrac{\delta\Delta E\left(\rho(\lambda'),\ w(\lambda')\right)}{\delta w_k(\lambda')}} - \frac{\Delta\epsilon_k}{\Delta n_k}\right] .$$

The equation for w_k is obtained from that of $w_k(\lambda)$ after a minor rearrangement of terms by setting $\lambda = 1$. In the last term of the w_k equation, $\delta\Delta E(\rho,w)/\delta\rho_k$ and $\delta\Delta E(\rho,w)/\delta w_k$ have the same structure as $\Delta\epsilon_k = \delta\Delta E(n,\epsilon)/\delta n_k$ and $\Delta n_k = \delta\Delta E(n,\epsilon)/\delta\epsilon_k$ respectively; the only differences are that n and ϵ are replaced by ρ and w.

Strictly speaking, even if we know ρ_k, we should solve the complicated integral equation (2.75) to find $w_k(\lambda)$. However, if we utilize $\Delta E(\rho,w)$, we find the following situation. Since the

last term of w_k, Eq. (2.75), is the difference between quantities with the same structure, it is not unreasonable to suppose it to be small (it turns out to be second order in v as we show in Appendix C, leading to a fourth order error in ΔE). Then $w_k \approx \epsilon_k - \Delta\epsilon_k$. From the analysis of Brueckner (Eq. (2.11) et seq. and Appendix B) we know that a large class of the terms in the BG expansion can be summed if the energy is determined by a K-matrix defined by the integral equation

$$K_{ij;k\ell} = v_{ij;k\ell} + \sum_{mn} v_{ij;mn} \frac{(1-n_m)(1-n_n)}{\omega_k+\omega_\ell-\omega_m-\omega_n} v_{mn;k\ell} \,. \qquad (2.76)$$

The interaction energy is then approximated by

$$\Delta E(n,\epsilon) = \frac{1}{2} \sum_{k\ell} K_{k\ell;(k\ell)} n_k n_\ell \,. \qquad (2.77)$$

The self-consistent single-particle energies in the denominator are a consequence of the "self-energy" terms in the BG expansion and are approximately $\epsilon_k + \Delta\epsilon_k$. Hence, w_k + (self-energy correction) will very nearly equal the "free" ϵ_k. Thus $\Delta E(n,\epsilon)$ can be approximated by replacing n_k with the true ρ_k and simultaneously omitting the single-particle self-energy correction. I.e., $E(\rho,\epsilon)$ with no single-particle self-energy processes is roughly equal to $E(n,\epsilon)_{BG}$ (the BG meaning that the term is to be evaluated with the full BG expansion, including the self-energy terms). Brueckner[35] has suggested the possibility of such a substitution; Eq. (2.75) indicates exactly what the situation is. In Appendix C it is shown that the

error in the energy resulting from this substitution is fourth order in t (or equivalently, in K). Brueckner and Masterson[36] (BM) have found that the fourth order scattering terms are of the order of half a MeV for nuclear matter, and that higher order terms are successively smaller by a factor of about ten (see Table IV of BM). Therefore, reasonably small errors would result from this substitution.

One should remark at this point that such a simplification can only occur in the evaluation of the interaction energy, $\Delta E(n,\epsilon)$; it cannot apply to $E(n,\epsilon)$ itself. The total energy is approximated by

$$E = \sum_k \epsilon_k n_k + [\Delta E(\rho,w)]_{\substack{\text{no self-energy}\\ \text{processes}}} \quad . \tag{2.78}$$

Of course, one could apply (2.73) and (2.74) to $E(n,\epsilon)$, but the physical insight in $E(\rho,w)$ is not as clear as in $\Delta E(\rho,w)$, and the defining equation of w, Eq. (2.73), behaves differently. Balian, Bloch and DeDominicis[37] have examined a many-body perturbation theory in which $n \rightarrow \rho$ throughout. Suhl and Werthamer[38] have also reported an analogous effect to that represented by Eq. (2.78) occurring in the renormalization of the momentum space distribution function in their "second random phase approximation." We shall not pursue either of these alternate approaches, however.

By virtue of the close relationships between the parameters of the theory, it is possible to obtain alternate expressions for

$$\Delta E(n,\epsilon) = \Delta E(\rho',w') \ . \tag{2.79}$$

For instance, if we concentrate only on the single-particle self-energy compensation after the transformation, it seems better to take

$$w_k(\lambda) = \epsilon_k + \lambda(w'_k - \epsilon_k)$$
$$w'_k = \epsilon_k + \frac{\delta\Delta E(\rho',w')}{\delta\rho'_k} \quad . \tag{2.80}$$

Then

$$\rho_k(\lambda) = n_k - (w'_k - \epsilon_k) \int_0^\lambda \frac{\dfrac{\delta E\big(\rho(\lambda'),w(\lambda')\big)}{\delta w_k(\lambda')}}{\dfrac{\delta E\big(\rho(\lambda'),w(\lambda')\big)}{\delta\rho_k(\lambda')}} \quad . \tag{2.81}$$

Rearranging terms, the latter equation becomes

$$\rho'_k = n_k + \frac{\delta\Delta E(\rho',w')}{\delta w'_k} + \frac{\delta E(\rho',w')}{\delta\rho'_k} \int_0^1 d\lambda' \frac{\dfrac{\delta\Delta E\big(\rho(\lambda'),w(\lambda')\big)}{\delta w_k(\lambda')}}{\dfrac{\delta\Delta E\big(\rho(\lambda'),w(\lambda')\big)}{\delta\rho_k(\lambda')}} - \frac{\dfrac{\delta\Delta E(\rho',w')}{\delta w'_k}}{\dfrac{\delta\Delta E(\rho',w')}{\delta\rho'_k}} \quad . \tag{2.82}$$

The integral in (2.82) can be expected to be small for the same reasons that the integral in (2.75) is small. Unfortunately, (2.82) does not correspond to the real density and it loses physical meaning.

III.

INFINITE NUCLEAR MATTER AND PHENOMENOLOGICAL POTENTIALS

A. NUCLEAR PARAMETERS

There are two experimentally observed phenomena in nuclear physics which any theory must explain. One of these is the constancy of the binding energy per nucleon (about -8 MeV) throughout most of the periodic table. Further information on the binding energy of nuclei can be deduced from the success of the Bethe-Weizsäcker semi-empirical mass formula. A general form of the formula (as given by Falk and Wilets^{33}) is:

$$\text{Binding energy} = \left[C_v + C_{sy} \frac{(N-Z)^2}{A^2} \right] A + \left[C_{surf} + C_{surf,sy} \frac{(N-Z)^2}{A^2} \right] A^{2/3}$$
$$+ \text{ Coulomb Energy} + O(A^{1/3}) + \text{Pairing and Shell Corrections} \quad (3.1)$$

Because one set of constants can be chosen to fit almost the full range of nuclei, it is reasonable to speculate about the properties of a large system of nucleons in which the charge and surface effects are missing: "infinite nuclear matter." The mass formula indicates that the energy per particle of an "infinite" system in which the number of neutrons and protons were equal and in which the coulomb forces were absent would be given by a single constant, $C_v = E_{Av}$. Unfortunately, this semi-empirical binding energy for an infinite system has not been unambiguously determined. Two recent values are those of Green^{39} (-15.83 MeV) and of Cameron^{40} (-17.04 MeV). Green

fits a formula without explicit $A^{1/3}$ terms, whereas Cameron's formula has such a term. Green also fits Cameron's formula (by least squares) to a formula without $A^{1/3}$ terms and obtains -16.34 MeV. A more recent semi-empirical mass formula has been reported by Ayres, Hornyak, Chan and Fann,[41] resembling the Bethe-Weizsäcker formula but having coefficients which vary slightly with A. The extrapolation of the volume coefficient to an infinitely large nucleus is ambiguous, but two logical extrapolations are -14.75 MeV and -13.81 MeV. The authors warn against taking such extrapolations too seriously.

The second phenomenon which a quantitative theory must explain is the ample experimental evidence that the nucleon densities of intermediate and heavy nuclei are nearly uniform and are also nearly independent of nuclear size. A recent general discussion of the experimental evidence on nuclear size is given by Preston,[42] Chapter 3. The most accurate determinations of nuclear size and density seem to be those from electron-nucleus scattering.[43] The procedure used in these experiments is to assume a density distribution, which for heavy nuclei is usually

$$\rho = \frac{\rho_o}{1+\exp\frac{(r-c)}{a}} \qquad (3.2)$$

and then to vary the parameters so that the scattering properties predicted from the above distribution match those experimentally observed. Thus the half-density radius, c, is determined (with an accuracy of $\pm 2\%$). In terms of the half-density radius, another radial parameter, r_1, is defined such that

$$c = r_1 A^{1/3} . \tag{3.3}$$

The experimental values of r_1 are plotted in Fig. 3. For intermediate and heavy nuclei its variation is very slight, and it can be represented as

$$r_1 = (1.07 \pm 0.02)\text{F} . \tag{3.4}$$

The parameter z_1 is also determined, and in terms of these parameters one can calculate from (3.2) another characteristic of the distribution, its surface thickness, t, defined as the distance in which the density decreases from 90% to 10% of its central value. The rms radius, a, can also be calculated, and from this the radius of the "equivalent uniform nucleus" is determined:

$$R = (5/3)^{1/2} a \tag{3.5}$$

A final radial parameter, r_o, is then defined in terms of R and A:

$$R = r_o A^{1/3} . \tag{3.6}$$

The variation of r_o with mass number is indicated in Fig. 3. Its variation is much greater than that of r_1, but for heavy nuclei it, too, is nearly constant:

$$r_o = (1.19 \pm 0.01) \text{ F} \qquad \text{(heavy nuclei)} . \tag{3.7}$$

In terms of r_o the density of the uniform model is obviously

$$\rho = \left(\frac{4\pi}{3} r_o^3 \right)^{-1} . \tag{3.8}$$

Fig. 3. Extrapolation of r_o and r_1 for infinite nuclear matter $(A \rightarrow \infty)$.

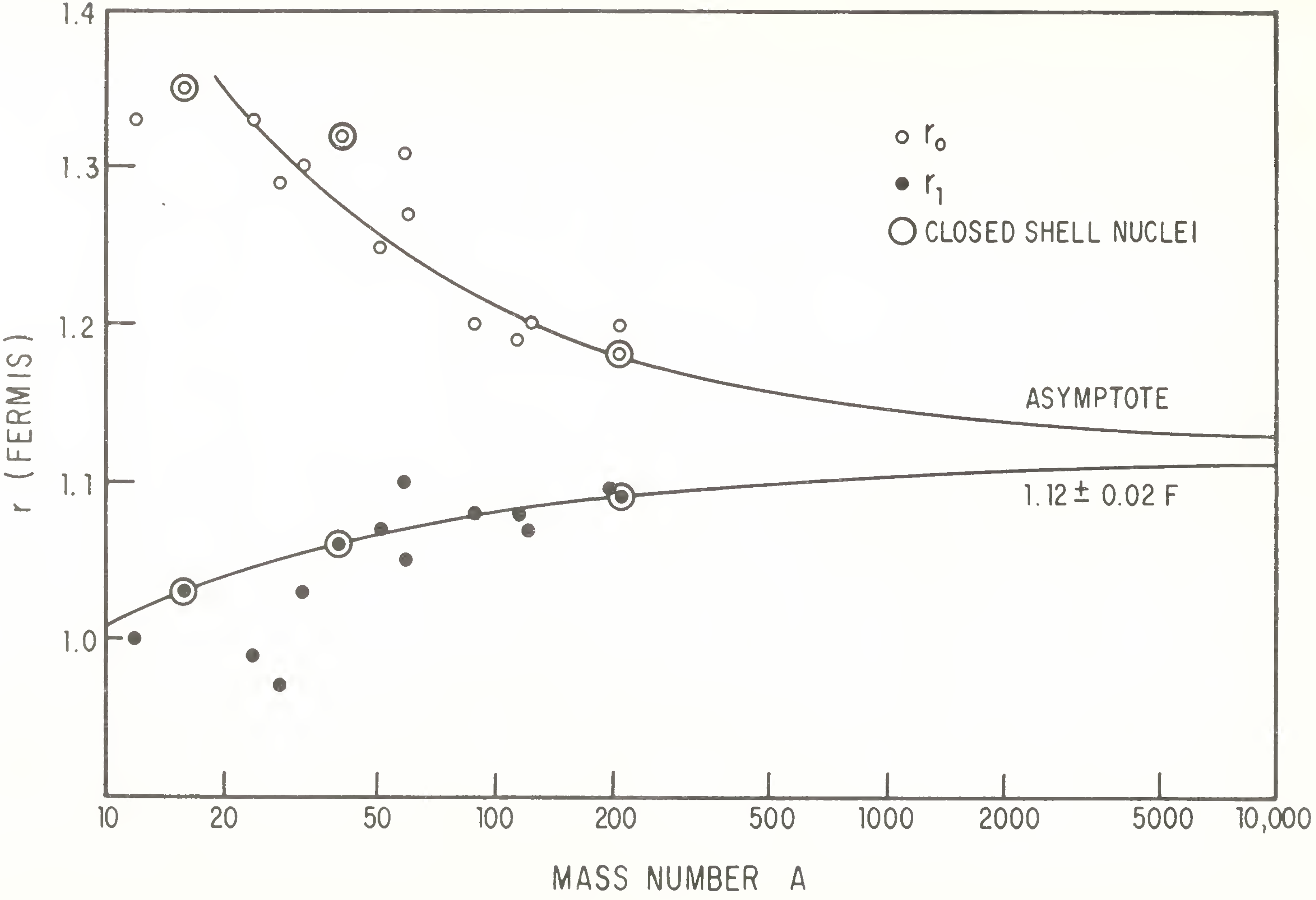
1.4
1.3
1.2
1.1
1.0
r (FERMIS)
10
20
50
100
200
500
1000
2000
5000
10,000
MASS NUMBER A
○ r_o
● r_1
◯ CLOSED SHELL NUCLEI
ASYMPTOTE
1.12 ± 0.02 F

3

The asymptotic value (as $A \to \infty$) of the parameter r_o can be related to the Fermi momentum appearing in the BG expansion through the total density. From (2.25) we have (inserting the internal variables spin and isotopic spin):

$$N = \sum_s \sum_T \sum_p n_p = 4 \cdot \frac{\Omega}{(2\pi)^3} \cdot 4\pi \int_0^{p_F} k^2 dk \, . \tag{3.9}$$

The sums over spin, s, and isotopic spin, T, each give a factor two. We have assumed a spherically symmetric unperturbed Fermi surface so that

$$\sum_p n_p \to \frac{\Omega}{(2\pi)^3} \int_0^{p_F} d\underset{\sim}{k} \, . \tag{3.10}$$

Dividing both sides of (3.10) by Ω leads to

$$\rho = \frac{N}{\Omega} = \frac{2p_F^{\,3}}{3\pi^2} \, . \tag{3.11}$$

Thus, (3.8) combines with the above relation to yield the following equation for the Fermi momentum in terms of the parameter r_o (in units where $\hbar = 1$):

$$p_F = \left(\frac{9\pi}{8} \right)^{1/3} \frac{1}{r_o} = \frac{1.524}{r_o} \, . \tag{3.12}$$

Unfortunately the determination of the asymptotic value of r_o requires extrapolation from $A \approx 210$ to $A = \infty$! The procedure for doing this makes use of the fact that the surface thickness, t, (which is known to about ±10%) is observed to be nearly constant for all nuclei:

$$t = (2.40 \pm 0.20)\ F. \tag{3.13}$$

Thus, if we assume t to remain constant as the system becomes infinitely large, then r_1 and r_o should approach each other in the limit of infinitely large mass number, A. Most of the nuclear matter calculations to date have been compared with the value 1.07 F taken from (3.2) (and corrected to 1.02 F as we show later) on the basis that this is more nearly constant than r_o; and, indeed, its variation over much of the range of A is less than the ±2% error assignment. However, as we indicate in Fig. 3, we believe that a better extrapolation for this value is

$$r_o = (1.12 \pm 0.02)\ F \quad (= r_1) \quad (A = \infty)\ . \tag{3.14}$$

Clearly this extrapolation is not rigorous, and much more accurate determinations of nuclear size are necessary before we can put any reliance on such a quantity. However, the above value is certainly plausible. Furthermore, the calculations for finite nuclei described in Chapter V of this dissertation, which are based on a calculation which yields $r_o = 1.07$ F (when coulomb effects are accounted for), have yielded radii which are 12% to 15% too small. It seems quite probable that a portion of this error is due to an underestimate of the parameter r_o in the infinite calculation. This latter possibility is not, in itself, sufficient justification for saying that r_o is greater than 1.07 F, but it does lend support to the other arguments.

There are two additional factors which must be taken into

account when extrapolating the results for finite nuclei to infinite nuclear matter. These are the repulsive effects of the symmetry energy $(C_{sy}(N-Z)^2/A)$ and the coulomb repulsion (since the electron scattering experiments measure only the charge distribution). Falk and Wilets[33] have estimated that the repulsive effects would cause an increase of r_o of about 0.05_5 F for the finite nucleus compared to the infinite nucleus. Brueckner and Gammel[3] obtained a shift of 0.05 F for the coulomb effect alone, and consider the symmetry effect to be negligible in large nuclei.

The net conclusion from the above considerations is that it is evidently valid to consider an idealized "infinite nuclear matter" in which the number of neutrons and protons are equal and in which the only interaction is the specifically nuclear interaction. Our theory should then hope to predict a binding energy per particle somewhere in the range

$$E_{Av} = (-15.5 \pm 2.0) \text{ MeV} \tag{3.15}$$

and an "equilibrium spacing" in the neighborhood of

$$r_o = (1.07 \pm 0.03) \text{ F} . \tag{3.16}$$

The estimated uncertainties in the above quantities are a direct consequence of the difficulty in extrapolating to infinity from the properties of finite nuclei.

B. PHENOMENOLOGICAL POTENTIALS

Although it appears that we are justified in considering the hypothetical infinite nuclear matter, we may well question whether we are justified in using an ordinary two-body potential in a non-relativistic Schroedinger equation to describe the nuclear problem.

One question, for instance, is that of relativistic effects. These are not expected to be more than a few percent. The maximum relative momentum of two nucleons in the Fermi sea corresponds to a lab energy for a scattering experiment of less than 200 MeV. Since the nucleonic rest mass is about 938 MeV, we expect the relativistic effect to be small so far as it affects the mean binding energy. However, excitation energies which are much greater than the Fermi momentum may well be influenced by relativistic effects.

A second question is the probable existence of specifically many-body forces. That they should exist can be deduced easily from the picture of inter-nucleon forces arising from the exchange of pi-mesons. It is probable that the resultant force on a nucleon in the presence of two others is not exactly that resulting from superposition of the forces between it and each of the other two separately. Such specifically many-body forces have not been experimentally observed or quantitatively predicted theoretically to our knowledge, and we do not believe that their effect is appreciable in the nuclear case. One argument for their insignificance is the fact that the two-body correlation distance in nuclear matter appears to be less than

the mean separation distance so that three-body (and higher) encounters are relatively insignificant.

We conclude that we can treat the nuclear many-body problem with a two-body, non-relativistic potential. What, then, should this potential be? We shall not go into the details of the determination of the inter-nucleon potential, but shall indicate briefly the current progress in its determination. The long-range part of the potential (due to exchange of a single pion) is now known theoretically and apparently confirmed experimentally (principally through the work of Breit and his co-workers[5]). However, the short-range part of the potential is imperfectly known, and there are a large variety of phenomenological potentials (various static potentials with Yukawa shapes, velocity dependent potentials, and potentials which are separable in momentum space) which give very nearly equally good fit to the two-body scattering data. The existence of such a large number of different potentials is a consequence of the fact that the scattering matrix has not yet been fully determined from experiment; hopefully, as the experimental evidence improves further it will lead to an unambiguous potential. Reviews of nucleon-nucleon potential determinations can be found in Chapter 5 of Preston[42] and in the references cited in footnotes 4 and 44. The potential which currently appears to give the best fit to the phase-shifts deduced from nucleon-nucleon scattering is that of Breit and his co-workers,[5] but there are still several arbitrary features about even this potential. The potentials of Gammel and Thaler,[4] which predate

the Breit potential, have many fewer parameters and yet most of the apparently essential components (central, tensor and spin-orbit forces in odd and even states); they also give quite good fit to the phase-shift analyses. Both the Gammel-Thaler and the Breit potentials are characterized by infinite repulsive cores (r_o = 0.3, 0.4 or 0.5 F for the GT potentials, and ~ 0.5 F in the Breit potential). The Breit potential is of the form

$$V_{LL'}{}^{Js}(r) = V^{(2)}(r) + V_c(r)\delta_{LL'} + V_T(r)S_{12} + V_{LS}(r)(\underset{\sim}{L}\cdot\underset{\sim}{S})\delta_{LL'} + \\ + V_q(Q_{12} - (\underset{\sim}{L}\cdot\underset{\sim}{S})^2) \ . \qquad (3.17)$$

The operator $Q_{12} - (\underset{\sim}{L}\cdot\underset{\sim}{S})^2$ has the value $-L(L+1)$ for uncoupled states, $J = L$, and is zero otherwise. $V^{(2)}$ is the one-pion exchange potential

$$V^{(2)} = \frac{1}{3}\,\mu_\pi \underset{\sim}{\tau}^{(1)}\cdot\underset{\sim}{\tau}^{(2)} \frac{f^2}{4\pi}\left\{\left[\underset{\sim}{\sigma}^{(1)}\cdot\underset{\sim}{\sigma}^{(2)} + S_{12}\left(1 + \frac{3}{x} + \frac{3}{x^2}\right)\right]\frac{e^{-x}}{x} + \right. \\ \left. + \underset{\sim}{\sigma}^{(1)}\cdot\underset{\sim}{\sigma}^{(2)}\delta(x)\right\} \qquad (3.18)$$

where μ_π is the pion mass, and where $x = \mu_\pi r$ (in units where $c = \hbar = 1$). The delta-function term can be neglected in actual computations. The other potentials in (3.15) have the form

$$V = \sum_n a_n e^{-2x}/x^n \ . \qquad (3.19)$$

The values of a_n and of the coupling constant in (3.16), f^2, are given in BM. All potentials have a hard core, specified by x_c=0.35. Because weighted means of neutral and pion masses are used in some

states and for other states the neutral pion mass is used, the core differs between these two groups of states. Complete details are given in BM. The usual tensor operator is S_{12}. The Gammel-Thaler potentials are simpler in form. They have no $V^{(2)}$ and V_q components, and are of the form

$$V e^{-\mu r}/\mu r \, . \qquad (3.10)$$

The parameters of each component of these potentials are thus a strength parameter, V, and a range parameter, μ. Full details can be found in reference 4, and the details on the potentials we have employed are in BM.

On the theoretical side, Chew and Frautschi[45] have defined a relativistic generalized potential within the framework of S-matrix theory and have shown that it plays a role in dynamics analogous to that of the ordinary non-relativistic potential in a Schroedinger equation. Below the threshold for inelastic processes (the region in which we are interested), the generalized potential is real and its energy dependence is expected to be weak for the nucleon-nucleon combination. Charap, Fubini and Tausner[46] have shown that at least to moderate energies, S-matrix theory leads to an unambiguous definition of a static potential which can be calculated in terms of the exchange of one, two, etc., pions.

The above argument apparently rules against the velocity-dependent potentials of Levinger, Peierls and collaborators.[47] However, Bell[48] and Baker[49] have shown that it is possible to transform canonically from a local hard core potential to a velocity-dependent

potential or vice versa, and that the two will be indistinguishable from the viewpoint of two-body scattering though they will involve different many-body properties whose importance is not yet known. It would not be too difficult to check the importance of the many-body effects of the above transformation by using both a velocity-dependent potential and its canonically related hard-core static potential in the same many-body calculation, and we suggest this calculation as one which should be done. One preliminary calculation[50] with velocity-dependent potentials seems to indicate that they do not predict the many-body saturation properties as well as similar hard-core potentials. A major advantage of a velocity-dependent non-singular potential is that it can be treated by ordinary perturbation theory whereas the static potential with hard core requires special treatment.

Another class of potential which has received considerable attention is the non-local potential of the separable type. This potential has the advantage that the interaction can be completely separated into partial waves (e.g., the spin and isotopic spin states can be separated), and also the momentum space representation of the interaction is particularly simple. Mitra[51] has shown that a separable potential is also "compatible" with dispersion relations, and has undertaken several investigations in the low-energy region with such potentials.[52,53] However, there is no reason to believe that the "unique" description of the nucleon-nucleon interaction should be a non-local potential, although it appears that at least a

portion of it may be. Gammel and Thaler[4] had concluded that the proton-proton scattering data require that the singlet-even nucleon-nucleon interaction be non-local, a result which comes from the energy dependence of the $^1S_0$ and $^1D_2$ phase shifts, and Giltinan and Thaler[54] have recently reported a non-local potential with hard core which apparently has the proper energy dependence. Whether their potential fits this dependence better than, for example, the Breit potential we do not know; Breit does not report requiring a non-local interaction.

The question of "uniqueness" for the nucleon-nucleon potential is a non-trivial one because the detailed structure of the potential (particularly the strength of the tensor force) has a considerable influence on the many-body problem even though the predictions for the two-body problem may be indistinguishable. The variation between several apparently equivalent two-body potentials in their effects on the nuclear matter problem is examined quantitatively in the next Chapter and in BM.

IV.

NUCLEAR MATTER CALCULATIONS IN THE K-MATRIX APPROXIMATION

This Chapter discusses an approximation to the K-matrix equations which is considerably simpler computationally than the Brueckner-Gammel[3] approximation (see Appendix B). This approximation has been used to study the nuclear properties predicted by the theory for several different phenomenological potentials and to compare several recent nuclear matter approximations with the K-matrix approximation (see Chapter VI and BM (Appendix G of this dissertation)). This Chapter begins with a description of the approximation. Following that, the results are discussed. Included in this discussion are the properties predicted for several different phenomenological potentials and an analysis of the causes of the differences in these predicted properties. Also included is a report of several calculations which shed further light on the convergence properties of the BG expansion, and on the previously neglected core volume energy. The Chapter ends with a discussion of various sources of error in the approximations and suggests calculations which would yield further insight into the effect of several of them.

A. SIMPLIFICATION OF THE K-MATRIX APPROXIMATION

Brueckner and Gammel[3] (BG) solved the K-matrix equations (2.11) and following with only the two further approximations discussed in BG (and in Appendix B) as being necessary to remove the dependence of the energy denominators in the K-matrix equation (2.12)

and of the Pauli exclusion principle operator (which restricts the momentum integrals to intermediate states outside the Fermi sea) on the angle between the total and relative momenta. The approximations consisted of using appropriate angular averages of the terms involved. The BG results are summarized in Table I.

In this section, further simplifications of the K-matrix equations are discussed, leading to the approximation used by BM. The principal additional assumption is that the single-particle energy differences in the denominator of the K-matrix equations are independent of the total momentum, $\underset{\sim}{P}$. The approximation is accurate if the single-particle energies have a quadratic dependence on the momenta or if the relative momentum is large compared to the total momentum. Even though these conditions are not always met, the dependence on the total momentum has been found to be slight[3,5] and the approximation is good. As a further approximation, in the case of two holes with relative momentum $\underset{\sim}{k}$, the energy denominators of the K-matrix (2.12) are modified as follows:

$$\Sigma(P,k) - \omega_m(\Sigma) - \omega_n(\Sigma) \rightarrow 2[\omega_k - \omega_{k^*}(\bar{\Sigma})] \qquad (4.1)$$

with k and k^* being the initial and intermediate relative momenta. The particle energy, $\omega_{k^*}(\bar{\Sigma})$, is defined in terms of the most probable (or average) energy, $\bar{\Sigma}$, of the holes with which two particles of momentum k^* interact. Thus the particle energies are uniquely defined in terms of the momentum k^* alone (instead of being a function of an energy parameter, Σ, (2.18) in addition to

Potential	GCT	BGT
Binding energy ($-E_{Av}$) (in MeV)	18.5	15.2
Equilibrium spacing, r_o (in F)	0.95	1.02
Effective Mass at Fermi surface	0.72M	0.73M

Table I. Predicted nuclear properties reported by Brueckner and Gammel[3] for the Gammel-Christian-Thaler potential of Table II and for a slightly modified Gammel-Thaler potential. (Table I of BM). These potentials are referred to respectively as the GCT and the BGT potentials.

State	$-V_c$ (MeV)	N_c (F^{-1})	$-V_T$ (MeV)	N_T (F^{-1})
triplet even	6395	2.936	45	0.73421
singlet even	905.6	1.7	...	...
triplet odd	150	1.5	-57.5	1.12
singlet odd	-113	1.0	...	...

Table II. Parameters of the Gammel-Christian-Thaler potential.[54a]

$r_c = 0.5$ F

the momentum). For particles of relative momentum $\underset{\sim}{k}'$ outside the Fermi sea, the energy denominator is

$$2\,[\omega_{k'} - \omega_{k''}(\overline{\Sigma})] - \Delta \qquad\qquad k' \le p_F$$

or

$$2\,[\omega_{p_F} - \omega_{k''}(\overline{\Sigma})] - \Delta \qquad\qquad k' > p_F \quad . \qquad (4.2)$$

The "mean excitation energy" Δ was set equal to $\omega_{p_F} - \omega_{p=0}$.

Another way to view the above approximation is to recognize that it is equivalent to the assumption that the potential energy of two particles of relative momentum $\underset{\sim}{k}$ is independent of the angle between their individual momenta and independent of their total momentum. Therefore, their momenta can be taken to be equal and the angle between them to be 180°, and it is apparent that their potential energy is just twice the potential energy of a single particle of momentum $\underset{\sim}{k}$. Similarly their kinetic energy is just twice the kinetic energy of a single particle of momentum $\underset{\sim}{k}$, and therefore

$$\omega\left(\underset{\sim}{k} = \frac{1}{2}\,(\underset{\sim}{p}_k - \underset{\sim}{p}_\ell)\right) = \omega_{p_k} + \omega_{p_\ell} = 2\omega_k = 2\left[k^2/2M + V(k)\right] . \qquad (4.3)$$

Consistent with the accuracy of this approximation, the total momentum $\underset{\sim}{P}$, which enters into the treatment of the exclusion principle (see (B.33)) is replaced by its average value $\overline{P}$, (as a function of the relative momentum, $\underset{\sim}{k}$). This can be calculated in a straightforward manner, and is obtained from

$$\frac{\overline{P^2}}{4} = \frac{3}{5} p_F^{\,2} \left(1 - \frac{k}{p_F}\right) \frac{\left(1 + \frac{1}{2}\frac{k}{p_F} + \frac{1}{6}\frac{k^2}{p_F^{\,2}}\right)}{\left(1 + \frac{1}{2}\frac{k}{p_F}\right)} \qquad k \leq p_F \, . \qquad (4.4)$$

For $k > p_F$, $\overline{P}$ is assumed to be zero.

It is apparent that the resulting computational simplification is considerable. In the first place, this approximation yields a single excitation spectrum which depends only in an average way on the particular unexcited states from which the excited particles come. Further, the angular integrations which occur in the computation of the single particle energy (2.13) or (2.17) can now be done explicitly, whereas in BG it was necessary to do one of them numerically.

The equations to be solved are quoted below, with a note on the method of solution used by BM. They are listed in the order of solution; the full system is solved self-consistently by iterating the series of equations until the new E_{Av} agrees with the previous energy to within desired limits. See Table V of BM for a sample iteration sequence. Three iterations generally sufficed to obtain agreement to within 0.1 MeV if the initial energy spectrum was approximated by the kinetic energies alone. The meshes used are described in detail in BM. The transformation to coordinate space of equations (2.11) through (2.18) is treated in detail in BG and in Appendix B. The equations below are obtained from the transformed equations of BG in a direct manner.

The equations to be solved are:

1) Green's functions, solved by numerical integration to an intermediate value of k'', with a Padé approximant[55] used for the remaining integral:

$$G_k^\ell(r,r') = \frac{1}{2\pi^2}\int_0^{10p_F} \frac{k''^2dk''\; j_\ell(k''r)j_\ell(k''r')f(\overline{P},k'')}{2[\omega_k - \omega_{k''}]} -$$

$$- \frac{M}{2\pi^2}\int_{10p_F}^{\infty} j_\ell(k''r)j_\ell(k''r')dk'' \qquad (4.5)$$

for on-energy shell propagation (holes), and with the denominator defined by (4.2) for off-energy shell propagation. The Pauli step-function, $f(\overline{P},k'')$, is given by

$$\begin{aligned} f(\overline{P},k'') &= 0 & & k''^2 + \tfrac{1}{4}\overline{P}^2 \le p_F^{\,2} \\ &= 1 & & k'' - \tfrac{1}{2}\overline{P} \ge p_F \qquad (4.6) \\ &= \frac{k''^2 + \frac{1}{4}\overline{P}^2 - p_F^{\,2}}{k''\,\overline{P}} & & \text{otherwise} \end{aligned}$$

with $\overline{P}$ given by (4.4). Note that for the integral from $10p_F$ to infinity it is assumed that

$$2\,[\omega_k - \omega_{k''}]_{k'' \ge 10p_F} \qquad - k''^2/M \;. \qquad (4.7)$$

The energies used in (4.5) are those calculated on the previous

iteration (and on the first iteration are just the kinetic energies).

2) Plane wave basis functions and Green's functions modified to vanish at the hard-core radius, r_c :

$$s_\ell(kr) = j_\ell(kr) - j_\ell(kr_c)G_k^\ell(r,r_c)/G_k^\ell(r_c,r_c) \qquad (4.8)$$

$$F_k^\ell(r,r') = G_k^\ell(r,r') - G_k^\ell(r,r_c)G_k^\ell(r_c,r')/G_k^\ell(r_c,r_c) \ . \qquad (4.9)$$

3) Radial wave functions, solved by iteration with $s_\ell(kr)\delta_{\ell\ell'}$ as the first guess:

$$U_{\ell\ell'}{}^{Js}(k,r) = s_\ell(kr)\delta_{\ell\ell'} + 4\pi \sum_{\ell''} \int_{r_c}^{\infty} r'^2 dr' F_k^{\ell'}(r,r') \, V_{\ell'\ell''}{}^{Js}(r')U_{\ell\ell''}{}^{Js}(k,r') \ . \qquad (4.10)$$

The $V_{\ell'\ell''}{}^{Js}(r')$ are the appropriate phenomenological two-body potentials defined in Chapter III.

4) K-matrices, computed by numerical integration:

$$K_{k;k} = K(k) = \sum_{Js} \sum_{\ell=J-1}^{J+1} C_{J\ell s} \{ - j_\ell{}^2(kr_c)/G_k^\ell(r_c,r_c) + 4\pi \int_{r_c}^{\infty} r^2 dr \, s_\ell(kr) \sum_{\ell'=J-1}^{J+1} V_{\ell\ell'}{}^{Js}(r)U_{\ell\ell'}{}^{Js}(k,r) . \qquad (4.11)$$

The statistical weights, $C_{J\ell s}$, are given by (B.48) in Appendix B.

5) Single-particle potential, also computed by numerical integration:

$$V(p) = \frac{4}{\pi^2} \int_0^{\frac{p_F - p}{2}} k'^2 dk' \, K_{k';k'} + \frac{2}{\pi^2} \int_{\frac{|p_F - p|}{2}}^{\frac{p_F + p}{2}} k'^2 dk' \, K_{k';k'} \times$$

$$\times \quad \left(1 + \frac{p_F^{\,2} - p^2 - 4k'^2}{4pk'}\right) . \tag{4.12}$$

For $p \geq p_F$ the first integral vanishes.

6) Mean energy per particle (see (2.11)):

$$E_{Av} = \frac{3}{5} \frac{p_F^{\,2}}{2M} + \frac{3}{2p_F^{\,2}} \int_0^{p_F} p^2 dp \, V(p) . \tag{4.13}$$

Graphs of $s_\ell(kr)$ and $U_{\ell\ell'}^{Js}(k,r)$ are included in Appendix F. Figures of the other quantities may be found in BM.

The equation for the single-particle potential, (4.12), is not explicitly derived in BM. It can be obtained from (2.13) (for holes) or (2.17) (for excitations) as follows. The sum over states in the Fermi sea is converted into an integral, viz.:

$$\sum_\ell n_\ell \rightarrow \frac{1}{(2\pi)^3} \int_{|p_\ell| \leq p_F} d^3 p_\ell \quad . \tag{4.14}$$

To convert this into an integral over the relative momentum

$$\underset{\sim}{k} = \frac{1}{2} (\underset{\sim}{p} - \underset{\sim}{p}_\ell) \tag{4.15}$$

where $\underset{\sim}{p}$ is the momentum of the particle whose potential energy is being computed, one uses the fact that $d\underset{\sim}{k} = -1/8\, d\underset{\sim}{p}_\ell$ so that

$$\omega_p = \frac{p^2}{2M} - \frac{1}{(2\pi)^3} \underset{|p_\ell| = |\underset{\sim}{p}-2\underset{\sim}{k}| \le p_F}{\int_0^{2\pi} dp \int k^2 dk \int d(\cos\theta) K_{k;k}} \quad . \tag{4.16}$$

In order to determine the limits of integration, one must consider three different cases. For $p \le p_F$, if $|\underset{\sim}{p} + 2\underset{\sim}{k}| \le p_F$ it is apparent from Fig. 4(a) that the limits on the $\cos\theta$ integration are 1 to -1, and the integration over $\cos\theta$ gives a factor -2. The k limits are obviously 0 to $(p_F - p)/2$. If $|\underset{\sim}{p} + 2\underset{\sim}{k}| > p_F$ (i.e., k lies between $(p_F - p)/2$ and its maximum value, $(p_F + p)/2$), the upper limit of the $\cos\theta$ integral becomes $-(p_F^2 - p^2 - (2k)^2)/4kp$ (see Fig. 4(b)). For $p > p_F$, there is only one possibility, Fig. 4(c), with $\cos\theta$ going from 1 to $-(p_F^2 - p^2 - 4k^2)/4kp$. The k limits are $(p - p_F)/2$ to $(p - p_F)/2$. Putting these limits into (4.16) and doing the $\cos\theta$ integration leads to (4.12). Eq. (2.8) of BM differs from (4.12) by a constant factor, 3/2: the $C_{J\ell s}$ defined in that paper are modified accordingly.

Fig. 4. The three possible situations for the angular integration leading to Eq. (4.13) for V(p):

(a) $p \leq p_F$, $|\underset{\sim}{p} + 2\underset{\sim}{k}| \leq p_F$;

(b) $p \leq p_F$, $|\underset{\sim}{p} + 2\underset{\sim}{k}| > p_F$;

(c) $p > p_F$.

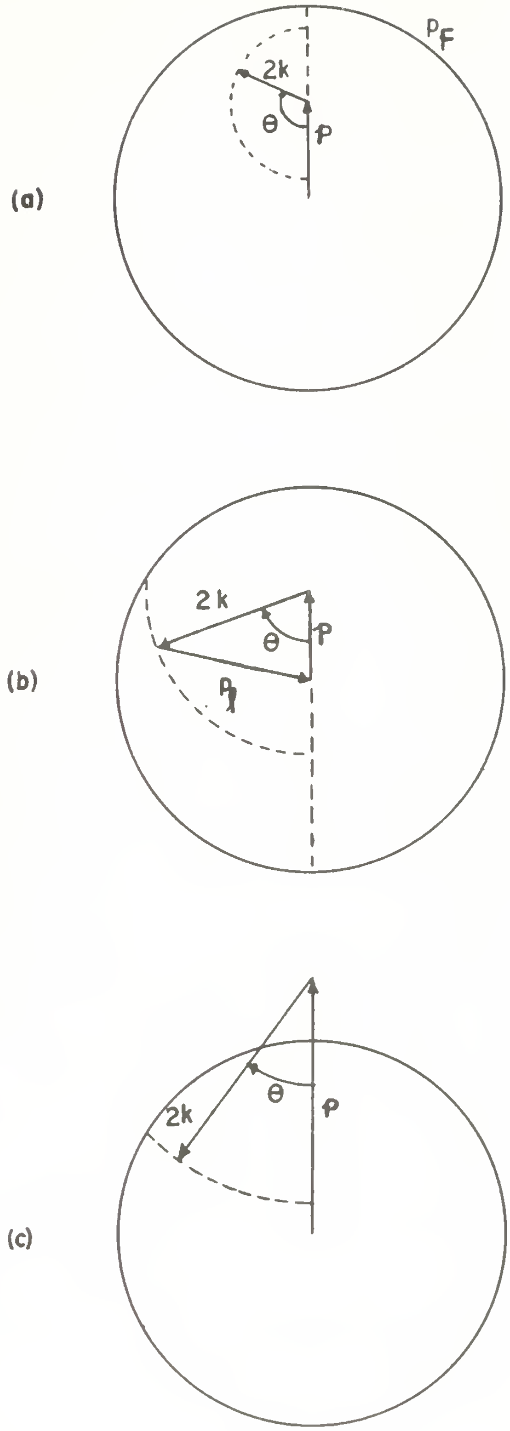

4

B. RESULTS

1. Variation of Predicted Nuclear Properties with Choice of Phenomenological Potential

Table I of BM lists the parameters of several Gammel-Thaler potentials[4] and Table II the parameters of the Breit potential.[5] A full discussion of these potentials is included in Section IV of that paper. In Fig. 5 and Table III of BM the variation of the E_{Av} vs. r_o curves predicted by the simplified K-matrix approximation for each of these potentials is clearly indicated. For the several Gammel-Thaler potentials with 0.4 F cores, the minimum E_{Av} varies from -14.1 MeV at 1.08 F to -22.3 MeV at 0.90 F. It should be noted that the potential which yielded the least binding had the strongest tensor force (and the weakest triplet-central force) of the various potentials and that the downward shift of the curves for the various GT potentials corresponds to steadily increasing triplet-central forces and weaker tensor forces (these being the two parameters which Gammel and Thaler could not uniquely determine). The Breit potential, one of the most recent and most carefully determined potentials, yielded -8.3 MeV at 1.28 F. This is to be compared with the BG result for the 0.5 F core GCT potential, -18.5 MeV at 0.95 F. Since the Breit potential has a very strong tensor force and correspondingly weak triplet-central force, and the GCT potential has an extremely strong central force and a tensor force which is proportionately much weaker, this very small value for the binding

Fig. 5. E_{Av} vs. r_o as computed with the t-matrix (defined with kinetic energies in propogators but obeying Pauli principle) compared to the same quantity as computed with the K-matrix (defined with self-consistent energies in the propogators - i.e., accounting for the "self-energy" terms in the BG expansion) .

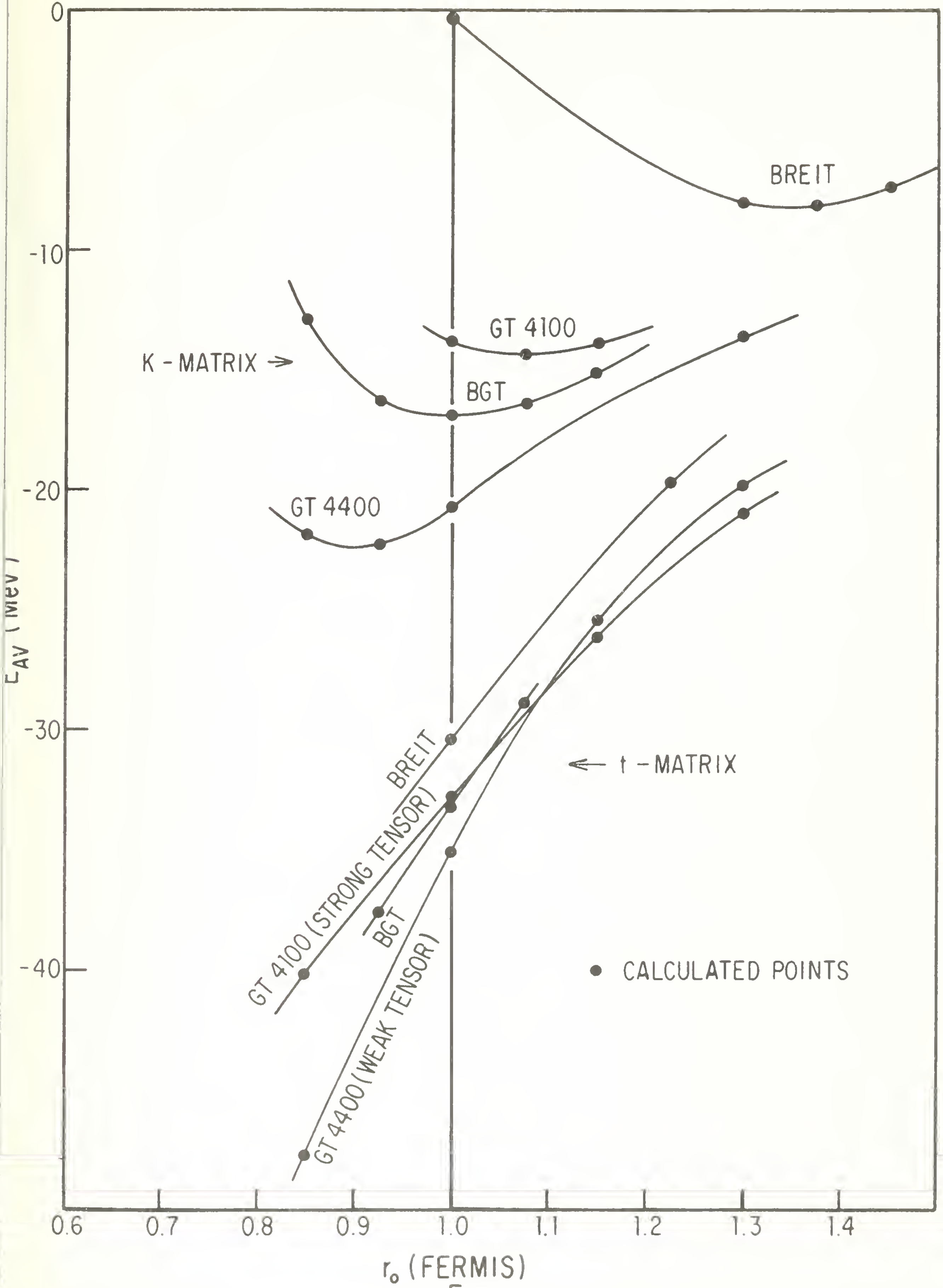
0
-10
-20
-30
-40
E_AV (MeV)
0.6
0.7
0.8
0.9
1.0
1.1
1.2
1.3
1.4
r_o (FERMIS)
BREIT
GT 4100
K - MATRIX →
BGT
GT 4400
← t - MATRIX
BREIT
GT 4100 (STRONG TENSOR)
BGT
GT 4400 (WEAK TENSOR)
● CALCULATED POINTS

energy with the Breit potential, and the large value of r_o, are quite consistent with the general trend observed for the GT potentials.

This pronounced variation of the many-body properties of these several potentials is a direct consequence of (1) the Pauli exclusion principle, (2) the self-energy effects, and (3) differences in free-particle scattering properties. In the absence of either of the first two effects, we would expect that all the potentials, insofar as they identically duplicated the two-body scattering results, should give equivalent results in the many-body calculation. Of course, there is some variance in the way these potentials fit the two-body data; however, the several GT potentials were indistinguishable in the sense that the two-body data was "equally well fitted" by all of them. The Breit potential is believed to give a better fit to the two-body data than the GT potentials, but it is by no means unique.[5]

In order to obtain a measure of the relative importance of the Pauli principle and the self-energy effects on the differences between these potentials, we have indicated in Fig. 5 the first iteration results for several potentials, as well as the final, self-consistent results. The first iteration is performed with the kinetic energies in the denominators of the K-matrix equations (i.e., the reaction matrix is just the t-matrix, Eq. (B.1) of Appendix B). The various potentials should (if they are truly equivalent from the two-body scattering standpoint) yield identical free-particle scattering

matrices. The slight variation between the various t-matrix curves in Fig. 5 is therefore partially due to different exclusion principle effects between the various potentials, and partially due to minor differences in their two-body scattering properties. The relative importance of these differences is not known.

The differences between the t-matrix lines and the K-matrix lines in Fig. 5 are due almost completely to self-energy processes -- i.e., averaged interactions between any two particles and the rest of the system. There is a small (essentially negligible) variation caused by the fact that Δ varies between iterations because it is defined in terms of the energy spectrum from the previous iteration.

The results shown in Fig. 5 indicate that about one third of the difference in the saturation properties of the various potentials is due to the exclusion principle and to the differences in the free-particle scattering properties, and that the remaining two-thirds of the differences can be attributed to self-energy effects.

There is another manifestation of the effect of the self-energy terms: the importance of the single-particle potential energy, defined by (4.12), in these calculations. In Figures 6(a) and 6(b) of BM this single-particle potential is given as a function of the phenomenological potentials and as a function of p_F. The important thing to note about the variation is that energy differences calculated from the various curves will differ (as well as the energies themselves). This is important because only differences in energy appear in the K-matrix denominators. Fig. 7 of BM indicates

the results of a computation in which V(k) was not allowed to vary with the Fermi momentum. The saturation is not properly predicted at all.

2. Convergence Properties as a Measure of Higher Order Terms

A considerable amount of data was obtained relative to the convergence of the perturbation calculation, and much of it is directly interpretable in terms of high order diagrams.

Fig. 6 of this dissertation and Table IV of BM indicate the contributions from various orders of the "Born approximation" (see BM for a full discussion of how the Born approximation was computed). The term "Born approximation" is used here to refer to the effects of successive orders of that part of the potential which is outside the core since the core is treated (almost) exactly by the Brueckner approximation and does not enter into the iteration sequence. This comment is applicable to all the perturbation sequences discussed in this dissertation: the core has been treated independently of the rest of the potential, and the perturbation sequences are a function of the remainder of the potential. It is quite apparent from the data obtained on the Born approximation that the modified Born sequence converges rapidly for nuclear matter, but not so rapidly that it can be truncated without appreciable error before third order. This is primarily a consequence of the strong tensor forces which have no effect in first order.

The contribution of the self-energy diagrams could also be

obtained directly. To see how this is possible, let us look at the expression for the four possible variants of the first diagram in Fig. 7(a):

$$-\sum_{\substack{k\ell\\mn}} v_{k\ell;mn} \frac{n_k n_\ell(1-n_m)(1-n_n)}{(\epsilon_k+\epsilon_\ell-\epsilon_m-\epsilon_n)^2} v_{mn;(k\ell)} \left[\sum_j (v_{jk;(jk)}-v_{j\ell;(j\ell)}-v_{jm;(jm)}-v_{jn;(jn)})n_j\right] . \tag{4.17}$$

The four terms in the square brackets come from the four possible lines on which the bubble self-energy insert can be placed. Now look at the following term extracted from the K-matrix expression for the energy

$$\sum_{k\ell mn} v_{k\ell;mn} \frac{n_k n_\ell(1-n_m)(1-n_n)}{\omega_k+\omega_\ell-\omega_m-\omega_n} v_{mn;(k\ell)} \tag{4.18}$$

with

$$\omega_k = \epsilon_k + V_k = \epsilon_k + \sum_\ell K_{k\ell;(k\ell)} n_\ell . \tag{4.19}$$

If we expand the denominator as $(1 + x)^{-1} = 1 - x + x^2 - \ldots,$ we obtain the following term (among others):

$$v_{k\ell;mn} \frac{n_k n_\ell(1-n_m)(1-n_n)}{\epsilon_k+\epsilon_\ell- \epsilon_m-\epsilon_n} v_{mn;k\ell} \left[-\sum_j \frac{(v_{jk;(jk)}+v_{j\ell;(j\ell)}-v_{jm;(jm)}-v_{jn;(jn)})n_j}{(\epsilon_k+\epsilon_\ell-\epsilon_m-\epsilon_n)}\right] . \tag{4.20}$$

Fig. 6. Diagrams contributing to successive Born approximations. Energy below each diagram is a representative contribution for that diagram to the mean energy per particle: (a) with free kinetic energy propogator; (b) with self-consistent propogator. The contributions indicated do not include the core repulsion.

Fig. 7. Leading self-energy diagrams contributing to the self-consistent propogator:

(a) $1/\omega \rightarrow 1/e - (V - V')/e^2$;

(b) $1/\omega \rightarrow 1/e - (V - V')/e^2 + (V - V')^2/e^3$.

See Table III for typical contributions to the mean energy per particle.

Fig. 8. Lowest order diagrams in successive major iterations which were not included in previous iteration. Representative contributions to the mean energy per particle are indicated below each diagram; the figures represent the contribution of all new diagrams involved in the given iteration. Core repulsion is not included.

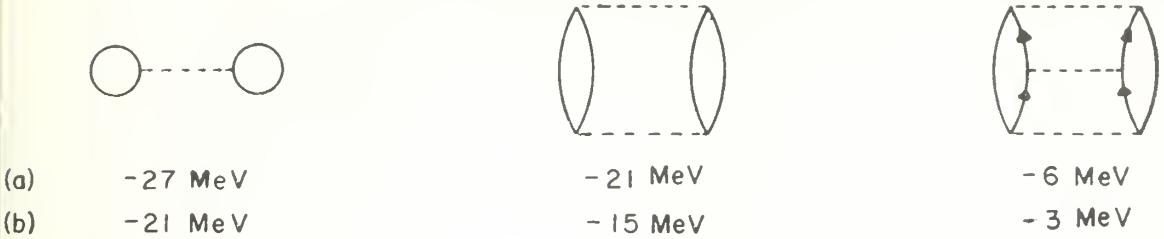

6

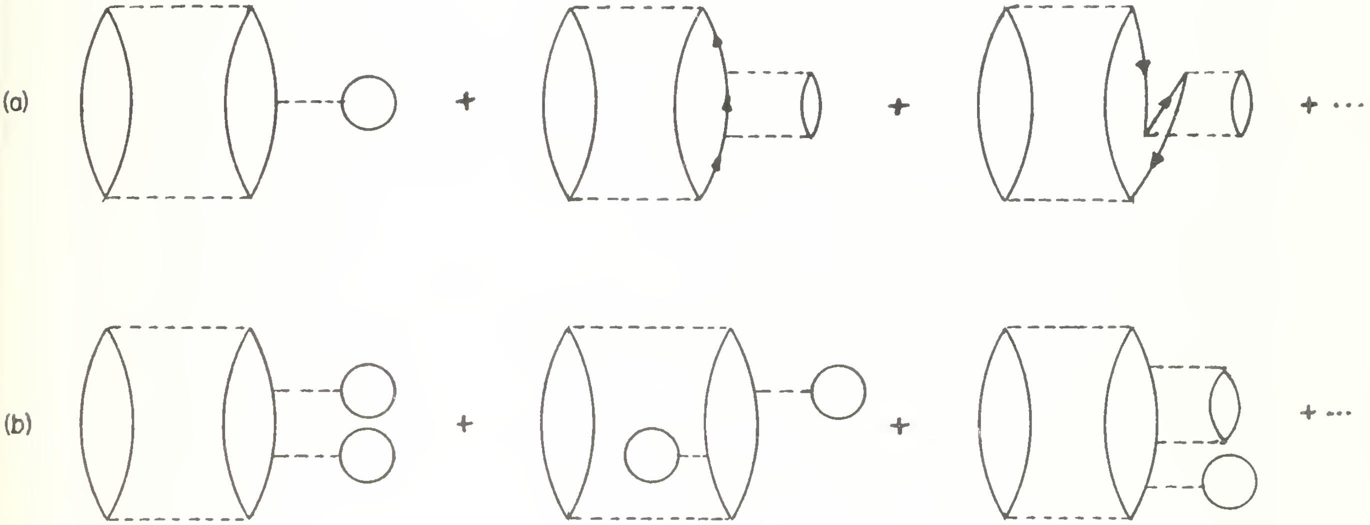

7

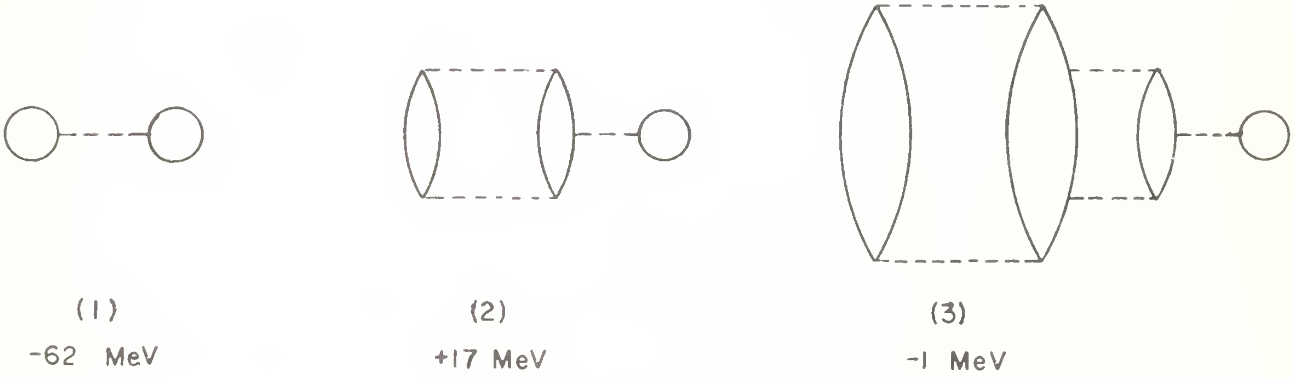

8

This is identical to (4.17). In order to calculate the self-energy terms represented in Fig. 7, then, one simply expands the self-consistent denominator in a power series, and truncates the series at various orders. Using just the first term of the series,

$$\frac{1}{\epsilon_k+\epsilon_\ell-\epsilon_m-\epsilon_n} \equiv \frac{1}{e} \qquad (4.21)$$

in the equation for the K-matrices yields the t-matrix defined by (B.1). The results of this approximation are the sum of all the direct Born terms (Fig. 6); these results are graphed in Fig. 5. Using two terms of the series,

$$\frac{1}{\epsilon_k+\epsilon_\ell-\epsilon_m-\epsilon_n} - \sum_j \frac{(V_{jk;(jk)}+V_{j\ell;(j\ell)}-V_{jm;(jm)}-V_{jn;(jn)})}{(\epsilon_k+\epsilon_\ell-\epsilon_m-\epsilon_n)^2} \equiv$$

$$\equiv \frac{1}{e} - \frac{V-V'}{e^2} \qquad (4.22)$$

where the V's are defined by (4.19), but with t-matrices instead of K-matrices, yields the sum of all the terms in Fig. 7(a). The first three terms,

$$\frac{1}{e} - \frac{V-V'}{e^2} + \frac{(V-V')^2}{e^3} \qquad (4.23)$$

yields the sum of all terms in Fig. 7(b), etc.

Only one other minor item needed to be determined -- what value of Δ (the "mean excitation energy") should be used in the t-matrix equations for computing the particle energies? In the

normal calculation, the Δ used for any given iteration is simply the difference between the single-particle energy at the Fermi surface and at the bottom of the Fermi sea. This means that Δ varies from iteration to iteration, and this variation actually tends to improve the iteration sequence. For this calculation, however, we used

$$\Delta = 0.75\ p_F^{\,2}/M \tag{4.24}$$

which is equivalent to an effective mass approximation with $M^* = 0.667\ M$, a value which is consistent with the mean effective mass calculated by Brueckner and Gammel and also consistent with the final results obtained in this calculation. The following iteration sequence was obtained with this approximation, compared to the sequence in BM (Table V):

major iteration	$\Delta = \omega_{p_F} - \omega_o$ from previous iteration	$\Delta = 0.75\ p_F^{\,2}/M$	
1	-32.963	-33.166	
2	-15.720	-14.311	(4.25)
3	-16.936	-17.084	
4	-16.887	-16.943	

The above data is for the BGT potential with $k_F = 1.52\ F^{-1}$. The value chosen for Δ has no effect on the first iteration value: the difference above is due to the fact that the wave functions were iterated only three times for the first value in the left column and were iterated seven times for all others (with the iteration

procedure being to use the same table of U(r) for both sides of (4.10)). The close agreement of the two figures indicates the rapidity of convergence of the wave function iteration scheme employed in these calculations.

In Table III are the results of this calculation for various potentials and various values of the Fermi momentum (recall Eq. (3.12) relating p_F to r_o). The results for the BGT potential at $p_F = 1.52\ F^{-1}$ indicate the slow convergence of the sequence of diagrams in Fig. 7, or, equivalently, their importance in the calculation of the system energy. It is interesting to note that the weaker the tensor force the smaller the contribution of this type of diagram (and the more rapid the convergence of this expansion). This supports quantitatively our assertion that the principal difference between these potentials is in their effect on the self-energy diagrams. The results tabulated in Table III also indicate that the self-energy diagrams become less important as the density decreases--indeed, their dependence on the density is very pronounced. The absolute values of the energies indicated in Table III are fairly sensitive to the choice of Δ and therefore only the relative rates of convergence can be considered significant.

The final class of diagrams we are able to compare are those indicated in Fig. 8. The contributions indicated in that figure are taken from Table V of BM. This sequence is also rapidly convergent. It is interesting to note, however, that the convergence of this sequence is considerably better at low densities than at high

Potential	GT 4100	BGT	GT 4400
$p_F = 1.32\ F^{-1}$			
$1/e$	-26.1		-25.4
$1/e - (V-V')/e^2$	- 3.8		-11.9
$p_F = 1.42\ F^{-1}$			
$1/e$		-29.4	
$1/e - (V-V')/e^2$		- 6.3	
$1/e - (V-V')/e^2 + (V-V')^2/e^3$		-18.9	
$p_F = 1.52\ F^{-1}$			
$1/e$	-32.9	-33.2	-34.2
$1/e - (V-V')/e^2$	+ 5.7	- 2.9	-11.7
$1/e - (V-V')/e^2 + (V-V')^2/e^3$		-21.2	
$1/e - (V-V')/e^2 + (V-V')^2/e^3 - (V-V')^3/e^4$		- 7.64	
$p_F = 1.64\ F^{-1}$			
$1/e$		-37.7	
$1/e - (V-V')/e^2$		+ 4.9	
$1/e - (V-V')/e^2 + (V-V')^2/e^3$		-24.1	
$p_F = 1.79\ F^{-1}$			
$1/e$	-40.2		-47.7
$1/e - (V-V')/e^2$	+48.3		+ 4.2

Table III. Variation of the contributions of the self-energy diagrams (Fig. 7) with the Fermi momentum and with potential. GT 4100 has the strongest tensor and weakest triplet-central force of the three potentials. GT 4400 has the weakest tensor force.

density; e.g., for the BGT potential we obtained the following sequences:

$p_F =$	$1.79\ F^{-1}$	$1.52\ F^{-1}$
	-42.703	-32.963
	-11.507	-15.720
	-12.746	-16.936
	-12.913	-16.887 .

(4.26)

3. Core Volume Energy

In Fig. 3(a) of BM it will be noted that the K-matrix reaches a maximum at about $k = 1.7\ p_F$ and then begins to become less repulsive. This behavior is clearly not correct because at high momentum the interaction is essentially due to the hard core alone and should increase with increasing momentum. The main reason for this behavior of our K-matrix is the neglect of the core volume energy, recently shown by Bethe, Brandow and Petschek[9] to be more important in the off-the-energy-shell calculation of particle energies than had previously been supposed. In particular, these authors claim that the momentum range between $2p_F$ and $4p_F$ is very important in the overall calculation (c.f. the BG and BM range lying below $2.6p_F$) and that in this range the core volume term is sufficiently strong that the potential energy becomes positive and is proportional to k^2. They have calculated the energy spectrum at $p_F = 1.5\ F^{-1}$ with the BGT potential, using their "reference spectrum" method (see

Chapter VI), but have not performed a quantitative calculation of the mean binding energy. We have used their energy spectrum, both with and without a suggested modification to account for the three-body cluster term, and have obtained the results tabulated in Table IV. The expression for the excitation spectrum in the BBP approximation is

$$\omega_m = A_2 + \frac{p_m^2}{2M^*} \tag{4.27}$$

where A_2 is given as -5.5 MeV and -10 MeV in different parts of their paper, and with $M^* = 0.77M$ without the three-body correction and $M^* = 0.88M$ with it. They have also estimated the hole energies, and when combined with the above spectrum, they obtain the following expression for the energy differences in the denominator of the on-energy-shell K-matrix equations:

$$2(\omega_k - \omega_{k'}) \rightarrow \frac{k^2}{M^*} - \frac{k'^2}{M^*} - .75 \frac{p_F^2}{M^*} \quad . \tag{4.28}$$

The results, indicated in Table IV, are rather large. The "core volume" effect appears to be about +8 MeV if the three-body term is allowed for in the manner suggested by Rajaraman, and the three-body term appears to yield something between 6 and 9 MeV attraction. However, we note the sensitivity to the exact value of A_2 (a 4.5 MeV change yielding a change of 0.5 MeV in the binding energy), which indicates that the detailed structure of the excitation spectrum in low momentum states is not entirely negligible: the

	E_{Av} in MeV	
	with 3- body correction $M^* = .88M$	without 3-body correction $M^* = .77M$
BBP hole and particle spectrum	-7.13	+ 1.94
BBP particle spectrum; self-consistent hole spectrum		
$A_2 = -5.5$	-8.2	
$A_2 = -10$	-8.9	- 3.0
BM		-16.9
BG		-15.2

Table IV. Mean energy per particle obtained with BBP reference spectrum (see text) for $p_F = 1.5\ F^{-1}$.

reference spectrum is defined to give agreement at $2.6\ p_F$. Secondly, the fact that the three-particle contribution differs so much in the two approximations indicates that it is still not well understood, and for the reasons indicated below, these figures should not be considered correct. Finally, the sensitivity of the calculation to the value of the parameter M^* (the change from .77M to .88M increasing the attraction 6 MeV) indicates the importance of determining this parameter precisely, and also suggests that the effective mass approximation may not be sufficiently quantitative.

There are several corrections which must be made to the results obtained with the BBP reference spectrum. One of these is the so-called "dispersion correction," a correction for the difference in the reaction matrices as computed with the reference spectrum and with the true energy spectrum. It appears from BBP's estimates that this may be about -3 MeV. Another problem comes from the fact that the above spectrum takes the core into account in all angular momentum states. They also include the attractive effects of the outside potential, but in our calculations we include neither core nor attraction for states with $\ell > 2$. To be consistent, we should do so and would thus obtain an undetermined amount of further attraction. Finally, it is probable that the BBP method for computing "off-the-energy-shell" may be enhancing the repulsive effect in the excitation spectrum, whereas the BG and BM procedure inhibits this effect. To see this, let us look at the manner in which BG and BBP treat the energy denominator for the K-matrix used to calculate the energy of the particle n, in, for example, diagram 4(d) of Fig. 1. The BG prescription is to use (at the horizontal line in the diagram):

$$\omega_k+\omega_\ell-\omega_r-\omega_s-\Delta \tag{4.29}$$

where

$$\Delta = \omega_{p_F} - \omega_o \simeq \overline{\omega_m-\omega_j} \tag{4.30}$$

whereas the BBP prescription is

$$\omega_j + 2\omega_{Av} - \omega_r - \omega_s - \omega_m \simeq \omega_j + 2\omega_{Av} - \omega_r - \omega_s - \omega_n \quad (4.31)$$

where $2\omega_{Av} \simeq \overline{\omega_k + \omega_\ell}$ (ω_{Av} is the average energy of a particle in the Fermi sea). The last equality in (4.31) is a consequence of momentum conservation, since for $\underset{\sim}{p}_n$ very large, $\underset{\sim}{p}_m \simeq - \underset{\sim}{p}_n$. Clearly the BG and BM treatment neglects the fact that one should compute farther and farther off the energy shell with increasing momentum. However, (4.31) may not be sufficiently accurate in the intermediate region below $4p_F$.

Because of the uncertainties indicated above, a reliable estimate of the effect of the core volume term on the mean energy is not at present possible. We believe the properly computed effect will be less than 2 MeV, but suggest that a computation should be attempted with the energy denominators properly accounted for (as in the procedure suggested in the Appendix to the Brueckner-Gammel paper^3) and with the core volume term included. The method for doing the latter is indicated below.

The problem of the core volume energy comes from the fact that although the wave function vanishes within the core, the potential there is infinite and the product $v\Psi$ may therefore be finite and non-zero. In the two-body scattering case this product vanishes everywhere but at the core boundary, and the equations of this section (e.g., (4.10) for the radial wave function) are exact. Let us now rederive the wave function and K-matrix equations in the presence of the hard core, keeping all terms.

We will drop all indices at first, and treat S-waves only, for simplicity. The extension to all ℓ values is quite obvious. The integral equation for the radial part of the wave function is (see Eq. (51) of BG or (B.38) of Appendix B):

$$U(r) = U_o(r) + 4\pi \int_0^\infty G(r,r')V(r')U(r')r'^2dr'. \qquad (4.32)$$

We now assume that

$$V(r')U(r') = \lambda\delta(r'-r_c) + \omega(r') \qquad r' \leq r_c \qquad (4.33)$$

where $\omega(r')$ is the core volume term which has previously been considered negligible. Substituting (4.33) into (4.32) leads to

$$U(r) = U_o(r) + 4\pi r_c^2 \lambda G(r,r_c) + 4\pi \int_0^{r_c} G(r,r')\omega(r')r'^2dr'$$

$$+ 4\pi \int_{r_c}^\infty G(r,r')V(r')U(r')r'^2dr'. \qquad (4.34)$$

Letting $r = r_c$ then yields the following equation for λ:

$$U(r_c) = 0 = U_o(r_c) + 4\pi r_c^2 \lambda G(r_c,r_c)V(r_c)U(r_c) +$$

$$+ 4\pi \int_0^{r_c} G(r_c,r')\omega(r')r'^2dr' +$$

$$+ 4\pi \int_{r_c}^\infty G(r_c,r')V(r')U(r')r'^2dr' . \qquad (4.35)$$

This equation can be solved, and

$$\lambda = - \frac{U_o(r_c)+4\pi\int_0^{r_c}G(r_c,r')\omega(r')r'^2dr'+4\pi\int_{r_c}^\infty G(r_c,r')V(r')U(r')r'^2dr'}{4\pi r_c^2 G(r_c,r_c)} . \qquad (4.36)$$

Eq. (4.36) for λ is then substituted into (4.32). The resulting equation can be simplified by using the defining equations for $s(kr)$ and $F(r,r')$, (4.8) and (4.9):

$$U(r) = s(kr) + 4\pi \int_0^\infty F(r,r')V(r')U(r')r'^2dr'$$

$$+ 4\pi \int_0^{r_c} F(r,r')\omega(r')r'^2dr' \ . \qquad (4.37)$$

The last term is neglected in the BG and BM calculations; its neglect probably has a negligible effect on the energy.

However, continuing to the K-matrix equation, one obtains a term which apparently is not negligible. In configuration space, the K-matrix equation is (schematically)

$$K = \int \Phi \, V \, \Psi \ , \qquad (4.38)$$

a familiar equation. In terms of the radial wave functions, this is

$$K = 4\pi \int_0^\infty U_o(r)V(r)U(r)r^2dr = 4\pi r_c{}^2U_o(r)\lambda + 4\pi \int_0^{r_c} U_o(r)\omega(r)r^2dr \ +$$

$$+ 4\pi \int_{r_c}^\infty U_o(r)V(r)U(r)r^2dr = \qquad (4.39)$$

$$= - \frac{U_o{}^2(r_c)}{G_\ell(r_c,r_c)} + 4\pi \int_{r_c}^\infty s(r)V(r)U(r)r^2dr + 4\pi \int_0^{r_c} s(r)\omega(r)r^2dr \ .$$

It is now necessary to obtain an equation for $\omega(r)$. To do this, we operate with $[E(P,k,\Delta) - H(P,k')]$ on (4.37). First we restore the indices, write out the definitions of $s(kr)$ and $F(r,r')$ in (4.37) and use

$$\sum_{\ell''} V_{\ell'\ell''}{}^{Js}(r')U_{\ell\ell''}{}^{Js}(r') = \lambda\delta(r'-r_c) + \omega_{\ell\ell'}(r') \qquad (4.40)$$

to obtain (eliminating λ as before)

$$U_{\ell\ell'}{}^{Js}(r) = j_\ell(kr)\delta_{\ell\ell'} + j_\ell(kr_c)\frac{G_\ell(r,r_c)}{G_\ell(r_c,r_c)}\delta_{\ell\ell'} + $$

$$+ \sum_{\ell''} \int_{<r_c} \left[G_{\ell'}(r,r') - \frac{G_{\ell'}(r,r_c)G_{\ell'}(r_c,r')}{G_{\ell'}(r_c,r_c)} \right] \omega_{\ell'\ell''}(r')d\tau \ . \qquad (4.41)$$

Then, assuming that

$$[E(P,k,\Delta) - H(P,k')]\, G_\ell(r,r') = \frac{1}{4\pi r^2}\,\delta(r-r') \qquad (4.42)$$

which is strictly valid only in the absence of the exclusion principle, we obtain, for $r < r_c$:

$$0 = (E-H)j_\ell(kr)\delta_{\ell\ell'} - j_\ell \frac{(kr_c)\delta(r-r_c)}{G_\ell(r_c,r_c)4\pi r_c{}^2}\,\delta_{\ell\ell'}$$

$$+ \omega_{\ell\ell'}(r) - \frac{\delta(r-r_c)}{G_{\ell'}(r_c,r_c)} \int_{<r_c} \frac{G_\ell(r_c,r')}{4\pi r_c{}^2}\,\omega_{\ell\ell'}(r')d\tau \ . \qquad (4.43)$$

It is apparent that

$$\omega_{\ell\ell'}(r) = (E-H)j_\ell(kr)\delta_{\ell\ell'} \qquad (4.44)$$

must be the solution if the first and third terms are to be equal. Then, looking at the last term, we see that

$$\int G_\ell(r_c,r')(E-H)j_\ell(kr')d\tau = \int \frac{\delta(r'-r_c)}{4\pi r_c^{\,2}}\, j_\ell(kr')d\tau$$

$$= j_\ell(kr_c) \qquad (4.45)$$

so that (4.44) satisfies the full equation (4.43). Writing out the equation for $\omega(r)$ in terms of the energy eigenvalues, we have

$$\omega_{\ell\ell'}(r) = \left[\Sigma - \omega\,(k+\tfrac{1}{2}\,P,\Sigma) - \omega(k-\tfrac{1}{2}\,P,\Sigma)-\Delta\right] j_\ell(kr)\delta_{\ell\ell'}\ . \qquad (4.46)$$

This equation vanishes identically for the on-energy shell calculation of hole energies because $\omega(k + \frac{1}{2}\,P) + \omega(k - \frac{1}{2}\,P) = \Sigma$ and $\Delta = 0$. However, for the off-energy shell calculations, where Σ is just a parameter and $\Delta \neq 0$, the contribution from this term is not negligible. It would be easy to include in the full calculation, however, just by adding such a term to the wave function and the K-matrix equations.

The error in the above treatment of the core is essentially that due to the neglect of the exclusion principle in (4.42). In BG this is shown to be less than 0.1% of the K-matrix in the case of hole energies (where the exclusion principle is the only reason the core volume contribution is not identically zero as in the approximation above). For particle energies the exclusion principle should have even less effect (particularly as the particle momentum becomes very much greater than the Fermi momentum), and consequently we conclude that the neglect of the exclusion principle will cause only negligible error.

C. ERROR ANALYSIS

The analysis of the errors in the nuclear matter calculation just described is extremely difficult for several reasons. In the first place, the basis for the entire calculation -- the inter-nucleon potential -- is imperfectly known. Secondly, the "experimental" results with which an infinite nuclear matter calculation should be compared are obtained by a drastic extrapolation, and are consequently imperfectly known. Finally, the large (infinite) number of "diagrams" which the theory does not account for have an effect on the calculation which is virtually impossible to estimate -- no satisfactory calculation having been attempted to date -- even though (as discussed later) it appears "reasonable" to expect their cumulative effect to be small. We are therefore in the position that a quantitative comparison of the theory with "experiment" is, at present, quite unsatisfying. Whatever "error" appears to exist cannot be pinned down specifically to any one of the possible sources. That the extrapolated "experimental" mean energy and equilibrium spacing appear to be within the limits of the variation in these properties predicted for the various phenomenological potentials (which are known to be non-unique) is an argument for believing the theory of infinite nuclear matter is quantitatively correct (see Fig. 5 of BM). A study of the possible sources of error in the theory and in the calculations appears below, and supports the above conclusion insofar as one is able to estimate the effects involved.

1. Contribution of Neglected Diagrams

There are several classes of diagrams which are not summed in the K-matrix formalism. The first of these is the group of so-called rearrangement energy diagrams. These are the diagrams corresponding to the derivative term in (2.34). Several of the lowest-order diagrams are indicated in Fig. 2. As indicated, the lowest-order rearrangement diagram is fourth order in the interaction, v. The contributions from the diagrams in Fig. 2 have been calculated and their effect on both the single-particle potential and on the binding energy of nuclear matter have been determined.[22] The energy spectrum for holes was shifted as much as +35 MeV (for zero momentum), and the energy at the Fermi surface (where the shift was about +12 MeV) was then about three MeV more negative than the mean binding energy, in good agreement with the Bethe-Hugenholtz-Van Hove theorem (and considerably improved over the approximately 15 MeV rearrangement energy obtained without consideration of the diagrams of Fig. 2). The effect on the mean binding energy was repulsive, and was about 1.5 MeV.[55a] The rearrangement corrections are discussed further in the next Chapter in connection with the treatment of finite nuclei.

Two other classes of omitted diagrams are indicated in Fig. 1. The first of these is the "hole-hole scattering" diagram, 3(c) and the other is the "three-body cluster," 3(d). The hole-hole contribution has been estimated by Moszkowski and Sessler,[56] and has been found to contribute about +0.5 MeV to the mean binding energy.

Brueckner[1] has called the terms involving three or more

quasi-particles (other than two-particle terms with self-energy corrections) "cluster corrections." The validity of K-matrix theory rests on the fact that these terms appear to be quite small for nuclear matter. Brueckner[1,57,58] and Bethe[6] have evaluated the first of these corrections, that due to the three-body terms indicated in diagram 3(d) of Fig. 1, and found that the correction to E_{Av} at normal density is about -0.12 MeV. They used, as an approximation to the K-matrix interaction, a Serber exchange-Yukawa interaction. Kohler[59] has evaluated this contribution with an interaction of the Serber type with a hard core, using the Moszkowski-Scott separation method (Chapter VI). Kohler's calculation yields -0.1 MeV, being a combination of 0.17 MeV repulsion from the direct interaction and -0.27 MeV from the exchange interaction. Rajaraman[8] recently re-examined the three-body terms in the light of the Bethe-Brandow-Petschek "reference spectrum method"[7] (Chapter VI), and has developed an approximation in which the three-body terms are included as self-energy inserts in the reaction matrix calculation. Bethe et al[7] have estimated the effect on the binding energy to be as much as several MeV in this approximation, the increased contribution over previous estimates being a consequence of a better accounting for all of the effects of the hard core. Their estimate has been checked in this dissertation by using their spectrum of particle energies, both with and without the effects of the three-body term included, in the BM code and calculating the energy for $k_F = 1.5\ F^{-1}$ (the value for which they had computed the single-particle energy spectrum -- they

did not do the full calculation to obtain mean energies). The difference is quite large (see Table IV). However, this cannot be considered a rigorous evaluation, and further investigation is indicated.

In this regard, one aspect of the estimation of the higher order many-body clusters which must be considered is the definite possibility that if the higher order diagrams are "properly summed" there will result a considerable reduction in the overall contribution over that of the lowest order diagram(s) alone brought about by an effect similar to the "screening effects" in the coulomb case.

In addition to the above problems, there is still the question of the convergence of the BG expansion itself. A very brief outline of the current status of the investigation into this problem is given in Section C of Appendix A.

It is apparent that more detailed investigation is definitely needed. However, even though interesting cooperative phenomena are no doubt being lost when the cluster terms are neglected, it is probable (as indicated in Section C of Appendix A) that the effects of cooperative phenomena (over and above those accounted for by the K-matrix approximation) will have only a minute effect on gross nuclear properties.

2. Computational Approximations

Brueckner - Gammel

The solution of the K-matrix equations with a hard core inter-nucleon potential is a large problem, even for modern high-

speed computers. In order to reduce the problem to one of reasonable size, several further approximations are generally employed. Those adopted by Brueckner and Gammel[3] are analyzed first. The additional simplifications of the BM calculation are then examined.

One of the major approximations is the use of an average value of the excitation energy, $\Delta \simeq \overline{\delta E}$, when computing the off-energy shell particle energies (see Eq. (B.16) and preceding discussion). There is undoubtedly some value of Δ such that the system energy computed with it will equal the energy computed with δE treated exactly, but that value of Δ is not known at present. There is, therefore, only the slightest possibility that the value chosen for this parameter $(\omega_{p_F} - \omega_{k=0})$ is the "correct" one, even though it appears to be a reasonable choice. Brueckner and Gammel obtained a measure of its importance by evaluating the energy for $\Delta = 0$ as well as for the choice indicated above. The effect of reducing Δ by this amount was to shift the energy minimum down about 1 MeV and to reduce the equilibrium spacing r_0 about 0.04 F. Thus it appears reasonable to assume that the use of delta equal to the difference in a single particle's energy between the top and bottom of the Fermi sea causes an error which is less than 0.5 MeV and 0.02 F. We should mention that it is computationally feasible to remove this approximation. Brueckner and Gammel show that one can use instead a parameter with infinite range which is determined by an extra pair of simultaneous equations. This calculation should be performed to ascertain more precisely the error from

the Δ approximation, and to determine the optimum Δ to use in the regular calculation.

A second approximation, which is discussed in Appendix B, Eq. (B.33) and (B.34), is to use angular averages so as to uncouple the dependence of the Pauli operator and the energy denominators on the angle between the total and relative momenta in the intermediate states. There is no easy way to measure the errors introduced by this approximation, but they are expected to be small. One possible indirect test of the approximation can be suggested. If one assumes that the total momentum, $\underset{\sim}{P}$, is zero in all states, then the angle between $\underset{\sim}{P}$ and the relative momentum, $\underset{\sim}{k}'$, can be treated analytically without further approximation. The $P = 0$ approximation is a more drastic one, and the difference in the results with the two approximations should be considerably more than the effect of the average treatment alone, and thus would provide an indirect estimate of the overall error.

Another approximation, the neglect of the core volume energy, has already been discussed. Although it is not possible to ascertain definitely from the calculations to date what the true contribution of the core volume energy is, it does appear possible that it could be of the order of two MeV (repulsion).

The contribution of the states with $\ell > 2$ (in particular the F and G states) is not entirely negligible. Moszkowski and Scott[10] have calculated these with their separation method (which is accurate for states of such high angular momentum), and their effect

can be seen in Fig. 8 of BM. These additional states would lower the minimum energy about 0.5 MeV and decrease the corresponding r_0 about 0.02 F. If a full calculation is performed again, it is recommended that these states be included. Since Moszkowski and Scott have computed at many values of p_F the contributions from the individual states with the BGT potential,[18] it would probably be sufficient (as we indicate in Chapter VI) to use their results for $\ell \geq 3$. However, slightly better accuracy would be obtained if these states were treated completely (i.e., if the appropriate K-matrices were calculated, etc.) so that the calculation would be fully self-consistent.

The final general source of error in the Brueckner-Gammel calculation is in the numerical procedures. In this category we lump such things as the choice of meshes for numerical integrals, the matrix-inversion process used to calculate the wave functions from (B.43), and the analytical approximation used to extend the Green's function evaluation to infinity from the large value of k" to which the integral was performed numerically. The matrix inversion process undoubtedly provided precision well within the accuracy of the overall calculation. The correction to the Green's function can be presumed to have similarly negligible error, and the meshes were all checked by using finer meshes. Consequently, it is reasonable to conclude that numerical procedures led to negligible errors.

In summary, the errors in the Brueckner-Gammel calculation cannot all be evaluated explicitly. However, it appears at present that of all of the sources of error which we have discussed, the

uncertainty in the potentials is probably the greatest. BM have pointed to the need for further investigation in phenomenological potentials with the aim of obtaining some experimental or theoretical measure of the agreement between the phenomenological and the "true" nucleon-nucleon potential, and ultimately obtaining the "true" potential itself.

Brueckner - Masterson

The following additional approximations are made by Brueckner and Masterson: redefinition of particle energies (see (4.1) and (4.2)), and neglect of the dependence of the energy denominators on the total momentum. In addition, we should re-examine the possible sources of computational error since the computational procedure was slightly different.

The definition of the particle energies leading to a single spectrum of off-energy shell energies was probably the most severe departure from the Brueckner-Gammel calculation. Coupled with the removal of the dependence of the energy denominators on the total momentum (an approximation which is accurate in the limits of zero total momentum, high relative momentum or quadratic dependence of the energies on total momentum), this average treatment of off-energy shell propagation had as one of its effects the fact that the Green's function (4.5) for particles whose relative momentum was greater than p_F was independent of their relative momentum (and consequently of their individual momenta since the total momentum had already been factored out). This is clearly incorrect, and the energy spectrum for

$k \geq p_F$ must therefore have a small but increasing error as k increases (it appears to differ from that calculated by Brueckner and Gammel (Reference 3, Fig. 4) by about 20-30 MeV at $k = 2.4\ p_F$, which can be compared to the kinetic energy which is more than 300 MeV). Most of the difference between the BG and BM results (1.7 MeV and 0.02 F, the BM values being more negative and smaller respectively) can be attributed to these effects. These errors are well within the uncertainties presented by the imperfect knowledge of the nucleon-nucleon interaction. Nevertheless, it appears possible to improve this approximation without re-introducing the P-dependence. This procedure would be to calculate the off-energy shell spectrum as a function of the variable Σ instead of the average Σ, and thus to reobtain a system of equations similar to the BG system. We are not able to give a quantitative estimate of the effect of this revised approximation on the calculation, but believe that it would probably remove between half and three-quarters of the 2 MeV discrepancy between the BM and BG approximations.

The numerical methods employed by BM differed from those of the earlier calculation in several respects. The Green's function correction (for the interval from the end of the numerical integration to infinity) was approximated by a Padé approximant.[15] The approximation was checked by extending the numerical integral to $20p_F$ and $40p_F$ and by varying the numerical meshes. The error in the mean energy due to mesh spacing (0.2 F^{-1} for the k" integration) and to the Padé approximant is estimated from the above checks to be less

than 0.2 MeV. In a future calculation we would not employ the Padé approximant and so will not describe it in further detail. We would instead compute the correction numerically with great accuracy and tabulate it, and then use the tables in the actual calculations. This computation could be done once and for all, to arbitrary accuracy. The individual computations would then be considerably faster since the Padé approximant would not have to be computed with each iteration. We did not employ this procedure in our calculations (in BM) because the recoding and "debugging" effort required were not justified by the resulting small improvement to the code.

There were two other computational differences between the calculations of BM and those of Brueckner and Gammel. Both involved negligible differences so far as the final results were concerned. One involved a finer mesh of r and r' near the core. BM used a spacing of 0.05 F for the first seven points compared to BG's 0.1 F. The effect on the final answer (as tested with BM's code) was about 0.1 MeV, the coarser mesh giving the lower energy. The other computational difference was the method of solving the wave equations, (4.10). We used successive iteration, and found that excellent agreement could be obtained with six iterations. The coupled equations $U_{00}^{00}(r)$ and $U_{02}^{11}(r)$ converged most slowly. One method of iteration employed two tables of wave functions: a table of "old" wave functions, from the previous iteration, for input to the numerical integrals (4.10), and a table of "new" wave functions generated in the given iteration by the numerical integration of (4.10). The

least convergent iteration sequence (for $k = 0.1p_F$ and $r = 0.6$ F) was:

iteration	$U_{00}^{00}(r)$	$U_{02}^{11}(r)$
0 $s_\ell(kr)\delta_{\ell\ell'}$	0.587318	0
1	0.705780	0.0843447
2	0.729165	0.121214
3	0.733508	0.137015
4	0.734293	0.143678
5	0.734434	0.146461
6	0.734459	0.147618
7	0.734463	0.148098

When the mean energy was computed after each iteration, we obtained the successive "Born approximations" -- although the term is not strictly correct since the core is treated exactly from the beginning. The other method of iteration, used for the majority of the calculations reported in BM, was to use the same table of wave functions on both sides of (4.10). Thus only the first point is actually computed with all terms in the table equal to those of the last iteration -- successive terms (for successively larger values of the radius) are computed with the new terms whose radii are less than the radius in question and the previous iteration values for terms whose radii are still greater. The iteration sequence was then greatly improved, an illustrative example (for $k = 0.1p_F$ and $r = 0.6$ F)

being:

iteration	$U_{00}^{00}(r)$	$U_{02}^{11}(r)$
0	0.542841	0
1	0.690567	0.215530
2	0.723036	0.174754
3	0.728496	0.206215
4	0.729264	0.202705
5	0.729364	0.204112
6	0.729376	0.204206
7	0.729378	0.204194

The potentials used in the two sets of computations were not the same so the final wave functions are not, of course, identical. The errors in the wave function from this iteration procedure were reduced to complete insignificance by using on major iterations other than the first the wave functions from previous iterations and then iterating the wave functions four or more times in order to improve them. Fewer wave function iterations were required on the first major iteration because its purpose was to provide a rough estimate of the single-particle energies, and minor inaccuracies did not impair the overall convergence of the calculation.

V.

FINITE NUCLEI

A. THEORY AND ERROR ANALYSIS

1. Theory

The extension of the K-matrix approximation to finite nuclei is a reasonably straightforward problem in principle but is very difficult in practice. Brueckner, Gammel and Weitzner[4] (BGW) and Brueckner, Lockett and Rotenberg[5] (BLR) have discussed clearly and completely a computationally feasible procedure for extending the theory to finite nuclei, and have discussed the approximations involved, explicit equations which must be solved, and the results obtained therefrom for the closed-shell nuclei O^{16}, Ca^{40} and Zr^{90} (using the Gammel-Thaler potential used in the Brueckner-Gammel nuclear matter calculation[3] as the nucleon-nucleon potential). This is now textbook material (Preston,[42] Chapter 9), and consequently we present only a very general discussion of the procedure with such elaboration necessary to present hitherto unpublished material. Masterson and Lockett (hereafter called ML, and included in this dissertation as Appendix H) have explicitly stated the equations actually solved and have extended the results by calculating the properties of Pb^{208}, using an improved approximation to the rearrangement energy. This chapter discusses this calculation, and treats the rearrangement energy approximation in more detail than any of the papers do.

The principal problem with finite nucleus calculations is the fact that the Hartree-Fock calculation with the pure internucleon potential is unsatisfactory. As is well known this calculation gives the best energy that is possible with a product wave function, so that, e.g., the interaction energy defined by (2.5) is given by

$$\Delta E \leq (\Phi, v\Phi) \tag{5.1}$$

where Φ is the product wave function so determined that the expectation value of the energy is stationary with respect to variation in the wave function. For nuclear matter, however, we have already found that (5.1) is too simple an approximation and that

$$\Delta E = (\Phi, v\Psi) \simeq (\Phi, K\Phi) \tag{5.2}$$

(where Ψ is the true wave function) is the most elementary approximation which gives accurate results. However, the variational calculation involved for even the last quantity is too complicated for finite nuclei. For infinite nuclear matter, we know the best form of the wave function (plane waves), and only the K-matrices need to be determined (self-consistently). For finite nuclei, both K and Φ must in principle be computed self-consistently. This is too difficult at present, and the assumption is made that the K-matrix for nuclear matter at the density corresponding to the local density of the nucleus is the appropriate K-matrix for (5.2). Thus, only the wave function Φ needs to be determined with the Hartree-Fock variational procedure, with the K-matrix as the "known" effective interaction.

This approximation is equivalent to the assumption that the correlation length (related to the "healing distance" of the two-particle wave function) is sufficiently short that at any point in the nucleus the interaction is the K-matrix interaction for infinite nuclear matter whose density is the same as the local density. The approximation is accurate in the center of the nucleus, where the density is nearly constant over distances of many Fermis (the healing distance is of the order of one Fermi).

The actual procedure in the calculation was the calculation (by BGW) of the coordinate space transformation of the K-matrix using the wave function Ψ calculated in the course of the infinite nuclear matter calculation of BG:[3]

$$(r_{12}|K|r'_{12}) = (2\pi)^{-3}\int d\underset{\sim}{k}\ \Phi^*_k(r_{12})v(r)\Psi_k(r'_{12}). \qquad (5.3)$$

(An angular momentum decomposition is made just as in the infinite nuclear matter problem, and the $U_{\ell\ell'}{}^{Js}(r)$ of (B.37) are used for the components of Ψ above.)

One then conjectures, without proof, that the coordinate space operator (5.3) is the appropriate interaction energy operator for the product wave function. The equation for the system energy is then

$$E = \sum_i \int \varphi^*_i(r)\, \frac{p^2}{2m}\, \varphi_i(r)d\underset{\sim}{r} + \frac{1}{2}\sum_{ij} \varphi^*_i(\underset{\sim}{r}_1)\varphi^*_j(\underset{\sim}{r}_2)(r_{12}|K(\rho)|r'_{12}) \times$$

$$\times\ \varphi_i(\underset{\sim}{r}'_1)\varphi_j(\underset{\sim}{r}'_2)d\underset{\sim}{r}'_1\, d\underset{\sim}{r}'_2\, d\underset{\sim}{r}_1\, d\underset{\sim}{r}_2 \qquad (5.4)$$

(the exchange term is not indicated explicitly). It is further

conjectured that a "Hartree-Fock" variation with respect to $\varphi_i^*(r)$

$$\frac{\delta E}{\delta\varphi_i^*(r)} = 0 \quad \text{for all } i \tag{5.5}$$

will lead to optimum wave functions. From this variation, we obtain the system of equations

$$E_i\varphi_i(\underset{\sim}{r}) = \frac{p^2}{2m}\,\varphi_i(\underset{\sim}{r}) + \int V_{HF}(\underset{\sim}{r},\underset{\sim}{r}')\varphi_i(\underset{\sim}{r}')d\underset{\sim}{r}' + V_R(r)\varphi_i(\underset{\sim}{r})\ . \tag{5.6}$$

The two interaction terms V_{HF} and V_R are the "Hartree-Fock" and the "rearrangement" potentials. The former is given by

$$V_{HF}(\underset{\sim}{r},\underset{\sim}{r}') = \sum_i \int d\underset{\sim}{r}_1\ d\underset{\sim}{r}_1'\ \varphi_i^*(\underset{\sim}{r}_1)(\underset{\sim}{r},\underset{\sim}{r}_1|K(\rho)|\underset{\sim}{r}',\underset{\sim}{r}_1')\ \varphi_i(\underset{\sim}{r}_1')\ . \tag{5.7}$$

In the treatment of the K-matrix above, it was necessary to treat the singular core separately from the rest of the potential. We mention the treatment of the core because the results reported in BLR and ML involve a variation of the core parameters to partially compensate for other errors in the approximation. The core is treated in a manner very similar to the nuclear matter procedure (B.38) et seq. Further, its contribution was found to be strongly density dependent, and the assumption is made that its dependence on the density is of the form given by the theory of core repulsion alone

$$K_{core} \sim (1 + b/r_o)^{-1}\ . \tag{5.8}$$

These considerations lead to (2.15) of ML,

$$\begin{aligned}(r_c|K|r_c) &= C\ \frac{\delta(r_{12}-r_c)\delta(r_{12}'-r_c)}{4\pi r_c^{\ 2}}\ \frac{(1 - b/1.07)}{(1 - b/r_o)} \\ &= A(\rho)(4\pi r_c^{\ 2})^{-1}\ \delta(r_{12}-r_c)\delta(r_{12'}-r_c)\end{aligned} \tag{5.9}$$

with the actual parameters being $C = 215$ or 257 MeV-Fermi and $b = 0.488$ or 0.459 Fermi for singlet or triplet states respectively. The attractive part of the K-matrix has a very small dependence on the density, on the other hand, and this dependence is neglected in the computations.

The rearrangement potential V_R in (5.7) results from the dependence of the K-matrix on the density. The density is related to the single-particle functions by

$$\rho(R) = \sum_i \varphi_i^*(R)\varphi_i(R) \tag{5.10}$$

so that

$$\frac{\delta\rho(R)}{\delta\varphi_i{}^*(r)} = \varphi_i(r)\delta(r-R) \ . \tag{5.11}$$

The density as it appears in the K-matrix is evaluated at the center-of-gravity of the interacting nucleons, so that $R = \frac{1}{2}(r_1 + r_2)$. Then, assuming that the range of interaction in the density-dependent part of the K-matrix is sufficiently short so that we can set $r_1 = r_2$ above, we obtain

$$V_R(r) = \frac{1}{2}\sum_{ij}\int dr_2 dr_1' dr_2' \ \varphi_i^*(r)\varphi_j^*(r_2)\frac{\partial}{\partial\rho}(r_1 r_2|K(\rho)|r_1' r_2')\varphi_i(r_1')\varphi_j(r_2') \ . \tag{5.12}$$

Eq. (5.12) is just (2.1) of ML (Appendix H of this dissertation). The procedure for solving this equation is given in detail in the equations following (2.1) in ML and will not be repeated here, with one exception: the detailed procedure for obtaining the equation for $V_R(r)$, (2.21) of ML, has not previously been reported.

Brueckner and Goldman[28] calculated the density dependence of V_R by using the fact that the dependence of $K(\rho)$ on ρ is almost entirely in the core term given by (5.9). The core term can be related to the density through

$$\rho^{-1} = \frac{4\pi}{3} r_o^{\,3} \,. \tag{5.13}$$

V_R is obtained from substituting (5.9) into (5.12), and then using the three delta functions to obtain, in good approximation

$$\begin{aligned} \underset{\sim}{r}_1' &= \underset{\sim}{r}_2' = \underset{\sim}{r}_3 \\ \tfrac{1}{2}(r_1 + r_2) &= \underset{\sim}{R} = r_3 \\ \underset{\sim}{r}_1 &= \underset{\sim}{r}_2 = \underset{\sim}{r}_3 \,. \end{aligned} \tag{5.14}$$

The above approximations (which are exact in the limit $r_c = 0$) lead to the following expression for $V_R(\underset{\sim}{r}_3)$ if spin or isotopic spin polarization are neglected:

$$V_R(\underset{\sim}{r}_3) = \frac{3}{16} \frac{\partial}{\partial\rho} [A_s(\rho) + A_t(\rho)] 4\pi r_c^{\,2} \rho^2(r_3) \,. \tag{5.15}$$

Then, using (5.17), we obtain

$$V_R = \frac{3}{16} \frac{r_c^{\,2}}{r_o^{\,3}} \left[\frac{C_s b_s (1-b_s/1.07)}{r_o\,(1-b_s/r_o)^2} + \frac{C_t b_t (1-b_t/1.07)}{r_o\,(1-b_t/r_o)^2} \right] \text{MeV} \,. \tag{5.16}$$

The variation of the function V_R/r^2 is very slow in the vicinity of normal density and to a good (±5%) approximation in the region $0.8\ \text{F} < r_o < 1.15\ \text{F}$

$$V_R = (240\text{ MeV})\ \rho^2 \times F^6$$

$$\simeq (9.6\text{ MeV})\ \rho^2(r_o)/\rho^2(r_o = 1.07\text{ F}) \qquad (5.17)$$

since $\rho(r_o = 1.07) = 0.19488$ particles/F^3. The latter form, in which V_R is given as a function of the density relative to its value at normal density, will be used later when we point out that the magnitude of V_R is actually larger at $r_o = 1.07$ F than indicated above. However, it is expected that its variation with density will still be of this form in the region near normal density, at least within the accuracy of the overall approximation.

In a subsequent paper, Brueckner, Gammel and Kubis[22] evaluated the rearrangement energy corrections to the single-particle energies using the K-matrix procedure. They evaluated the second and third order terms of Fig. 2, with the results as given in Table V.

Momentum	Potential Energy (MeV)			Single Particle Energy (MeV)
	K Matrix	second order	third order	
$0.1\ p_F$	-112.0	+ 26.8	+ 9.4	-75.6
$0.9\ p_F$		6.9	6.4	
p_F	- 70.3	4.4[a]	6.1[a]	-17.8

[a] Extrapolated from computed values at $p = 0.1\ p_F$ and $p = 0.9\ p_F$

Table V. Breakdown of single-particle energy. The density corresponds to $r_o = 1.07$ F and an average binding energy per particle of 15.5 MeV.

The above corrections correspond to the definition of "rearrangement energy" represented by the last term of (2.34) (i.e., variation of ΔE by n). Consequently, they are not exactly the V_R of (5.12), which is obtained by differentiation with respect to ρ. However, since ρ and n are equal to second order, the two can be equated within the limits of the accuracy of the overall approximation.

The approximation to the rearrangement energy used by ML is a simple approximation to the above dependence on both the energy and the momentum. Based on an estimate of the momentum of the lowest and top states of Ca^{40} (which can be obtained from their kinetic energies -- the differences between their energy eigenvalues and their potential energy expectation values), the rearrangement energy was estimated at 12 MeV for the top state and 26 MeV for the deepest state. Eq. (2.21) of ML is the simplest means of interpolating between these two values in order to obtain the rearrangement potential appropriate to the other states. Its accuracy was expected to be commensurate with the degree of approximation, and since its effect is primarily on the wave functions (and only indirectly on the energy), the crude interpolation was expected to generate negligible error. The dependence of (2.21) on the density is a direct consequence of the argument following (5.17).

In a future calculation, we recommend the use of one further improvement in the treatment of V_R -- namely, the use of the following interpolation formula:

$$(V_R)_2 = \left[12.5 + 26.2\,\frac{p_i - p_F}{p_F}\right] \frac{\rho^2(r_o)}{\rho^2(r_o = 1.07)} \text{ MeV}, \quad (5.18)$$

where p_F is the Fermi momentum corresponding to the nuclei's rms radius. This would be a slightly better approximation than those which have been utilized to date, and it probably represents the farthest one should go in utilizing the approximation that the rearrangement effects can be accounted for as in Eq. (5.6). The momentum dependence in (5.18) is a linear interpolation between the rearrangement correction at 0.1 p_F in Table V and the value found at the Fermi surface by Brueckner, Gammel and Kubis,[22] 12.5 MeV. The momenta of each state, p_i, can easily be estimated from the previous iteration's kinetic energy. This approximation is not expected to result in significant improvement in average properties (see discussion in Section B, "Results"), but it might lead to some improvement in the level spectra.

2. Error Analysis

At this point it is necessary to make a few comments about the possible errors. The approximations necessary to transform the K-matrix to coordinate space are treated in detail in BGW. Those involved in the solution of the modified Hartree-Fock problem are treated in BLR and summarized in ML. There are a lot of them, and for many no precise estimate is possible. Their justification was invariably twofold: (1) they were necessary in order to simplify the problem to manageable proportions; and, (2) their effect,

estimated as rigorously as possible, was considered to be negligible. For some of the approximations, little more can be said. Furthermore, in view of the present uncertainty in phenomenological potentials (see previous Chapter and BM), it is doubtful if much more can be learned about the theory until a potential is obtained which is known to be significantly "more correct" than the present ones. However, we can suggest one further check of the calculation. In equation (2.4) of ML we evaluate $(r_1|V|r_1')$ by using the first two terms of an expansion in Legendre polynomials so that, for a given difference x between r_1 and r_1', only explicit evaluation at two points is necessary to obtain the estimated value of this function for any angle between the two. Because the evaluation of this matrix elements occurs in the innermost "loop" of the longest calculation (about $3\frac{1}{2}$ hours per iteration for lead), it is necessary to keep the number of elements which must be evaluated for any given separation, x, to a minimum. The first two terms of the expansion in Legendre polynomials is known to be a good approximation, but its effect could be explicitly obtained by one iteration (say for Ca^{40}) in which the first three or four terms of the expansion were obtained. On the present generation computers (where, for Ca^{40} the CDC-1604 takes about 30 minutes for this particular iteration), the cost would not be justified. However, in the next generation of computers, which will be much faster, this check should be economical.

Further, when there is available a phenomenological potential whose experimental and theoretical justification are greater

than for current potentials, the properties of infinite nuclear matter should again be calculated, preferably in the manner suggested in the Appendix to the Brueckner-Gammel paper (e.g., without using a mean excitation energy in the denominators for off-energy shell propagation but using the exact formulation and solving the extra pair of equations involved). If the results of this are in good agreement with the semi-empirical values, then the transformation of the K-matrix to coordinate space should again be performed, for approximately twice as many values of the arguments as reported by BGW. If this is done, a further check on the meshes used in the BLR and ML calculations will be possible (again assuming that a "next-generation" computer is utilized). But more important, if the new potential and nuclear matter calculation gives a better agreement than the mean energy of -15.2 MeV (cf. -13.5 to -17.5 MeV semi-empirical range) and the equilibrium spacing 1.02 F (5% less than the extrapolated and corrected 1.07 F), then it is reasonable to expect the results summarized later and in ML would be considerably improved (since the mean energy per particle and rms radii of the nuclei treated are invariably too small).

There is also a finite possibility of error in the computer program itself for such large problems: e.g., the finite nucleus code must be run in three "shifts" on the CDC-1604 computer in order to accommodate the large number of states involved in the lead calculation. This last source of error can now be considered negligible for both nuclear matter and finite nuclei, however: the former

calculation (reported in BM and in Chapter IV) was completely independent, and the differences between it and BG can be attributed entirely to the additional approximations; and, the latter calculation can be considered to be semi-independent. In the case of the finite nucleus calculation, the computer program for the BLR calculations was extensively reorganized for the ML computation, and furthermore the code was, over a period of about a year, almost completely rewritten by this author to improve its speed and operating characteristics (i.e., to make it "more automatic" in operation). During this rewriting, the program was extensively checked for minor errors, such as integration limits, coding errors, etc., and after correcting the few that were found, the properties of Ca^{40} were calculated and compared with those calculated at Los Alamos with the new rearrangement approximation but otherwise unmodified original code. The agreement between the two codes was good: -6.78 vs. -6.55 MeV mean energy per particle, 3.00 vs. 2.99 Fermi rms radii, and 0.7 or less difference in the eigenvalues. The minor differences are entirely attributable to the corrections which were made in the ML code.

In addition to errors due to numerical procedures or to the input (the phenomenological potentials), there are also some shortcomings in the theory itself. The most obvious of these is the neglect of correlations other than two-body correlations. These will have a negligible effect everywhere except possibly in the surface region where nucleon clusters (akin to alpha particles, etc.) may

form and where superfluidity might exist. These effects are not expected to have much influence on gross properties such as binding energies, nuclear radii, and surface depth, however. Nevertheless, the improvement of the computed binding energy with increasing nuclear size (discussed in the next section) strongly suggests that the principle source of error is in the treatment of the "surface" energy, which is considerably too large. This "surface" energy arises not only from the classical effect -- variation of density in the surface -- but also from the rearrangement energy which is important only for the calculation of the wave function and therefore has little effect in the infinite nuclear matter problem but does influence considerably the finite nucleus calculation. Its effect is thus in fact a "surface" effect, and the method outlined here for treating it is at best a treatment based on plausibility since it has not been rigorously proved (and, indeed, in higher order it is incorrect). Further investigations of this many-body problem peculiar to the finite system are clearly needed.

B. RESULTS

Throughout this section frequent references are made (with no further comment) to tables and figures in ML, Appendix H of this dissertation.

1. Comparison with Previous Rearrangement Energy Approximation

In order to ascertain the effects of the new treatment of

the rearrangement energy, Eq. (2.21) of ML, the properties of Ca^{40} were compared with those without the new energy treatment. We note that V_R as determined by Eq. (2.21) of ML is, on the average, almost twice as strong as the V_R used by BLR, our Eq. (5.17). Table II compares the new results with those reported in BLR. The net effect of the improved approximation is slightly better agreement with experiment for almost every property tabulated: separation energies, total energy per particle, and rms radii. In addition, the spin-orbit splittings are more nearly porportional to the $(2\ell + 1)$ separations generally expected. However, the magnitude of the total energy per particle is still not large enough (-6.55 MeV *vs.* the experimental -8.55 MeV),[60] the proton rms radius is too small (although increased by 3% to a new value which is 83% of the experimental value),[61] and there is slightly too much difference between the separation energy of the last particle and the total energy per particle (1.1 MeV compared to the previous 1.2 MeV and the experimental 0.2 MeV). Comparative potential energies and eigenvalues are given in Table III for every state of Ca^{40} with the old and new approximations. The range of eigenvalues has been reduced from -70.1 through -4.9 MeV to -48.7 through -5.5 MeV. This reduction in spread of energies indicates that the previous approximation reproduced the absolute magnitudes of the energy spectrum quite poorly except near the top levels; the otherwise close agreement between the two calculations indicates that the approximation employed in BLR was adequate for the computation of the average properties of the nuclei (such as

mean energies, rms radii, etc.), and that further improvement in this direction would change such properties only slightly. Nevertheless, this conclusion should be checked by performing a calculation with V_R as given by (5.18).

2. General Properties of Pb^{208}

In Table IV are the principal properties of Pb^{208} as calculated by the theory for hard core strengths equal to 90% and 100% of the normal strength. The 100% core data is the result of a single full iteration from the 90% data. Experience with the rapid convergence of these computations indicates that the properties tabulated are very near the values one would obtain with further iteration (e.g., probably within 0.1 MeV for the mean energy and 0.01 Fermi for the rms radii). Since the individual energy level predictions (next section) are subject to slight fluctuations on the first iterations, they are not quoted for the full core. The 90% core was chosen to permit comparison with the calculations in BLR. In those calculations, the reduced core contributions were arbitrarily employed as a means of improving the binding energies. As seen in Table V, too little binding was obtained for the smaller nuclei even with the reduced core strength. However, for lead with the 90% core the binding energies of the last particles are a fraction of an MeV too great (-8.8 vs. -8.4 MeV for the top neutron and -8.9 vs. -8.0 MeV for the proton), and the magnitude of the total energy per particle (10.0 MeV) is 2.1 MeV greater than that calculated from the

masses. The energy of the top nucleon differs by [illegible] MeV from the total energy per particle, compared with the experimental value of 0.5 MeV. For the 100% core, the magnitude of the total energy per particle is several MeV less than the energy with the 90% core, and is one MeV less than the experimental value.

The rms proton radii are 16% and 15% too small (for the 90% and 100% cores respectively). Similar errors were reported for Ca^{40} and Zr^{90}. The surface depths are 1.8 and 1.9 Fermis for the proton distributions and 1.9 and 2.1 Fermis for the total distributions. (We have taken the surface depth to be the distance over which the density falls from 90% to 10% of its maximum value in the vicinity of the center of the nucleus.) The computed depths are slightly smaller than the experimentally deduced (2.2 ± 0.3) Fermis for the charge distribution[61] and $(2.45 \begin{smallmatrix} +\ 0.45 \\ -\ 0.15 \end{smallmatrix})$ Fermis for the nuclear distribution.[62] The small discrepancies might vanish with the correction of the error in the rms radii.

3. Energy Spectrum

Table VI gives the energy spectrum for the reduced (90%) hard core strength. The ordering of states is generally in accord with that deduced from experiment for the shell model.[63] Up through the [illegible] state, the Pb^{208} level assignment is the same as that calculated for Zr^{90} (and differs from the Ca^{40} order in the [illegible] and $2s_{1/2}$ states). With the new rearrangement energy treatment, the spread in energy levels and the coarse level spacing are

probably the most accurate calculated to date. Thus we compare our spread in eigenvalues of about 70 MeV with those determined in the shell-model calculations with central potentials and spin-orbit coupling of (for example) Malenka[64] (about 50 MeV) and of Ross, Mark and Lawson[65] (less than 40 MeV). In general, their relative spacing of low-lying levels is in good agreement with ours. However, both authors obtain a level sequence at the surface which differs from ours: for instance, for neutrons, Ross et al have $3p_{1/2}$, $3p_{3/2}$, $2f_{5/2}$, $1i_{13/2}$,... compared to our $3p_{1/2}$, $1i_{13/2}$, $2f_{5/2}$, $3p_{3/2}$,... and the Mottelson and Nilsson[66] $3p_{1/2}$, $2f_{5/2}$, $3p_{3/2}$, $1i_{13/2}$,...; and, for protons, they have $3s_{1/2}$, $2d_{3/2}$, $1h_{11/2}$,... in agreement with Mottelson and Nilsson and compared to our $1h_{11/2}$, $3s_{1/2}$, $2d_{3/2}$,... . In both cases, the spread of energies is less than 2 MeV. Most of the above differences can be traced to the spin-orbit potential, which is imperfectly known and which is treated as a parameter in the shell-model calculations to improve agreement with experiment. Better treatment of V_R with (5.18) might also help.

The spin-orbit splittings for the various states are tabulated in Table VII. They are of the right order of magnitude and follow in a reasonable manner the expected $(2\ell + 1)$ graduation in magnitude. In Fig. 2(g) and 2(h) the dependence of the local equivalent potential, $F(r)$, and of the wave functions on this splitting is indicated. In particular, there is an appreciable spatial splitting of levels with the same orbital angular momentum but with opposite spin.

4. Neutron-Proton Density Relations

The neutron, proton and total density distributions are indicated in Fig. 3 for the two core strengths. There is a remarkably uniform total density, but moderate non-uniformity of the neutron and proton contributions. Further, the neutron and proton wave functions (Fig. 2(d) and 2(f)) are almost identical for corresponding states, with the exception of a very slight shift towards the center of the nucleus in the low angular momentum states. Thus, much of the difference in the density distributions is due to the "extra" neutrons in the outer energy shell (which are distributed throughout the nucleus as well as at the surface). The neutron-proton radii differ by about 0.2 Fermi, extending to the larger nuclei the tendency noted in BLR for the proton and neutron distributions to have nearly equal radii. The origin of this effect lies in the symmetry energy and in the insensitivity of the wave functions to differences in potential. The absence of an appreciable neutron-proton difference for the light nuclei (BLR) and the slight difference noted for lead are compatible with experimental results.[67] Quantitatively, for lead we conclude from pion and nucleon scattering calculations[62] that $R_N - R_p = (0.2 \pm 0.2)$ Fermi, where R is the half-density radius, in agreement with our calculation. This figure does not include that part of the difference which results from the finite extension of the nuclear potential beyond the matter distribution when the radii are determined from separate nuclear and charge-dependent interactions. This difference is discussed next.

5. Density-Potential Relations

In Fig. 4 are plotted the potential function F(r) for the two top neutron states against the density distribution. The top proton potential is not shown because it lies inside the neutron potentials, a consequence of the smaller proton distribution. The separation between total density and potential (0.5 Fermi) is slightly less than that of Ca^{40} and Zr^{90} (0.75 Fermi); the difference between the proton half-density point and the nuclear potential half-maximum is 0.7 Fermi. These results agree within the limits of experimental error with the differences between $R_p = (1.18 \pm 0.02) A^{1/3} = (7.00 \pm 0.14)$ Fermis from electron scattering[62,68] and from μ mesonic atoms,[69] and $R_V = (1.25 \pm 0.05) A^{1/3} = (7.41 \pm 0.30)$ Fermis from low and high energy neutron scattering.[70] Wilets[71] has concluded from neutron and proton scattering that the difference between the nuclear potential radius and the matter radius is independent of A and is (1.0 ± 0.3) Fermi. This difference in radii is largely due to three effects previously discussed,[72] namely: (a) finite range of interaction; (b) nonlinear variation of potential energy with density (Wilets effect);[73] and (c) nonlocality of the effective interaction.

6. Comparison with Surface Predictions of Other Theories

It is interesting to compare the character of the nuclear surface as predicted by previous semi-empirical theories with our results (which are essentially from "first principles" if the concept

of a two-body nuclear potential is valid). Two previous calculations are mentioned to indicate the degree of precision obtainable. One is the pure Hartree-Fock calculation by Rotenberg[74] with $N = Z = 92$. It yielded surface thicknesses of 2.7 and 3.1 Fermis for Gaussian and Yukawa wells respectively, and predicted a marked dip in the proton distribution near the origin (which is absent in our more exact calculation). The calculated separation between the rms radii of the particle density and of the self-consistent collective potential in this model was less than 0.2 Fermi. An intermediate step between the pure Hartree-Fock calculation and the BGW theory is the semi-empirical model of Berg and Wilets.[71,73] This model yields $R_N - R_P = 0.2$ Fermi (in agreement with our result) and R(potential) - R(nucleon) = 0.7 Fermi (compared to our 0.5 Fermi).

7. Summary of Results for the Four Nuclei Studied to Date

The following is a summary of the general features of the results for full-shell nuclei (O^{16}, Ca^{40}, Zr^{90} and Pb^{208}) studied in ML and in BLR.

1. The magnitudes of the total energy per particle and of the separation energies are smaller than their experimental counterparts.

2. The difference between observed and calculated energies decreases with increasing nuclear size.

3. The energy spectrum is in general agreement with experiment, and the computation of the coarse spacing, with the new

rearrangement energy approximation, is probably the most accurate to date. However, the detailed spacing between close levels, particularly when widely different angular momenta are involved, is not correct in every instance.

4. The energy spectrum is quite sensitive to any changes in the calculation (as, for example, the changes in the treatment of the rearrangement energy and in the core strength). This is to be expected, because the single particle energies are to be compared with potential wells of the order of 70 MeV. Thus an MeV change in particle energy is less than a 2% change in potential energy.

5. The radii of the nucleon distributions are in good agreement with experiment for O^{16}, with full core, but are about 15% too small for the other nuclei studied.

6. These radii are relatively insensitive to changes in the calculation, a "stiffness" which has been observed in the calculations of BLR and of this paper.

7. The theory predicts the details of the internal density distribution, and the calculations have brought out a remarkably uniform ratio of neutron and proton densities in the lighter nuclei, with only minor variance in Pb^{208}. To date it has not been possible to verify the detailed internal distributions of these nuclei experimentally, although the analysis of Ford and Hill[68] indicates that the charge distribution for lead is probably reasonably uniform (and especially that there is no dip in the center as deduced for gold),[61] in agreement with our results.

8. The calculated surface properties are compatible with present experimental evidence. In particular, the surface depth, neutron-proton radius differences, and the matter-potential relations at the surface are quantitatively predicted.

C. CONCLUSIONS

The surface depth of the nucleus is now known experimentally to within about 10%.[60] Our results are compatible with experiment and form a theoretical explanation of its shape from first principles. Indeed, there is a need for further refinement of the experiment to verify the internal structure of each nucleus and to ascertain the surface shape consistent with it. There is also a need for further refinement of the BGW theory to obtain better rms radii, with the result that the surface depths predicted might be more accurate. In addition, our theoretical knowledge of the neutron and proton density ratios and of the potential-density relation at the surface is compatible with, and at present more definitive than, experiment. A feature of the surface which this theory does not describe is possible existence (discussed by Wilkinson)[74a] of nucleon clusters, possibly "alpha" particles, in the nuclear surface. Superfluidity in the low density region, if present, is also not treated, but it is believed to have negligible effect on a gross property such as surface depth.

For the remaining properties (binding energy, mean proton and neutron radii, separation energies, and spin-orbit splittings),

the theory is in semiquantitative agreement with experiment, the maximum errors being of the order of 15%. The sources of these errors can be grouped into three categories: 1) the numerical procedures, 2) the input (i.e., the phenomenological potentials), and 3) the theory itself (both the Brueckner theory of infinite nuclear matter and the BGW theory of finite nuclei). The first of these (the numerical procedures) is rejected as a source of major error on the basis of the thorough tests by BLR of the meshes employed and the improvement of the results with nuclear size in spite of the fact that any errors from the numerical procedures probably increased also.

However, some of the error may arise in the choice of the phenomenological two-body nuclear potential, as indicated by the calculations in Chapter IV. It is possible that a better potential would resolve some of the discrepancies between our calculations and experiment. It should be noted that of the seven potentials employed in the calculations of Chapter IV, the potential used for the finite nucleus calculations (the BGT potential) gives the best agreement between the calculated and semi-empirical properties of infinite nuclear matter. This, however, does not mean that this potential is the "correct" one, and more work in phenomenological potentials is indicated. Further, in the more accurate calculations of Brueckner and Gammel[1] this potential yielded for nuclear matter a slightly smaller binding energy (-15.2 MeV) than the semi-empirical value (-15.5 ± 2.0) MeV and an equilibrium spacing that was 5% too small (1.02 *vs.* 1.07 F). These effects undoubtedly influence the computa-

tions of BLR and of this dissertation. In addition, there is some question whether the hard core should be nearer 0.4 F (as in the Gammel-Thaler potential we use) or 0.5 F (as suggested by more recent determinations of phenomenological potentials).[7] A potential with a larger core might give lower density saturation and larger nuclear radii.

The improvement with increasing mass number of the computed binding energy strongly suggests that the principal source of error is in the treatment of the "surface" energy, which is considerably too large. It should be emphasized that the "surface" energy, which is essential in the finite system in the determination of the wave function and density, and hence indirectly in the determination of the total energy, does not appear in the uniform system. Thus its effect in the finite nucleus is in fact a "surface" effect. The methods of BLR and of this paper are at best a treatment of the rearrangement problem based on plausibility; they are not rigorously proved. Further investigations of this many-body problem peculiar to the finite system are clearly needed.

In conclusion, we have ascertained that the BGW theory of finite nuclei is in semiquantitative agreement with experiment, the agreement improving with nuclear size. Further, we have seen that our state-dependent approximation to the rearrangement energy correction gives appreciably better results than those obtained in the previous calculations. Finally, it appears probable that much of the residual error in the results can be removed by improvements in

the phenomenological two-body potential upon which the calculations are based, and by improvement of the "surface" energy.

VI.

OTHER NUCLEAR MATTER THEORIES

In this chapter several representative approximations for nuclear matter calculations are studied briefly. Brueckner and Masterson (BM) have made quantitative comparisons with some of these approximations which are elaborated on here.

Before discussing the approximations, one further point should be noted about the potentials used to test them. Two large, and apparently unavoidable, components of static nucleon-nucleon potentials are the hard cores and the tensor forces. However, this does not imply extensive mixing of states, especially at lower energies, and one can employ an equivalent central force in each state in some problems. This has led to the use of simplified potentials as tests for nuclear matter theories, and several authors have used for this purpose S-state interactions. One of the principal tests of a nuclear matter theory is whether it yields the proper saturation; i.e., whether the minimum of the E_{Av} vs. ρ curve occurs at the "correct" density. Bethe[8] has shown that any S-state force saturates, even if it has no repulsive core, whereas for realistic static forces the core seems to be required for proper saturation. For nuclear matter, this means that at least S and D state contributions should be included in a quantitative test of an approximation.

As an illustration of the importance of employing realistic potentials, let us look at the second Born approximation for the S-state Yamaguchi separable potential[75] without hard core and for the

BGT potential (the modified Gammel-Thaler potential[4] employed by Brueckner and Gammel[3] (BG)). For the BGT potential, the core must be treated separately, and the term "second Born approximation" refers to the perturbation calculation of the long-range part of the potential (see Chapter IV). The corresponding values (with free kinetic energy propagators) are -8 MeV and -21 MeV. The third Born approximation for the BGT potential yields -6 MeV! Thus a theory which is powerful enough to obtain good results with the rapidly converging S-state potential without hard core may not necessarily be able to yield good results with a realistic potential. Further, as will be shown later, the fact that the tensor force gives no contribution in first order but is responsible for a large contribution in higher orders also mitigates against the use of purely central interactions as tests of nuclear matter theories.

Finally, in line with the above remarks, one should note the danger inherent in using a simple potential to estimate the error terms for any given approximation: this could yield results in error by a factor of two or three -- and perhaps more -- quite easily.

A. MOSZKOWSKI - SCOTT SEPARATION METHOD

The first approximation we discuss is the Moszkowski-Scott separation method[11,17,18,76] (henceforth referred to as MS). MS separate the interaction into a short- and a long-ranged part, $v = v_s + v_\ell$. The separation distance, d, is chosen so that the short-range part, v_s, gives zero phase shift for free particle

scattering. Thus most of the attraction is in v_s (as well as all of the hard core repulsion for hard core potentials), and the effect of the long-range potential is quite small (and is calculated in second Born approximation). A detailed discussion of the method and the physical significance of the approximation is given in Reference 11 for central forces; the extension to tensor forces is discussed in Reference 17.

With the separation of v defined above, the many-body wave function Ψ is approximated for $r < d$ by Ψ^F, the free-particle wave function (with interactions between the two particles but no effect of any other particles) and at larger distances by Φ_o, the unperturbed wave function. The condition for determining d guarantees that

$$\Psi^F(d) = \Phi(d) \quad \text{and} \quad \nabla\Psi^F(d) = \nabla\Phi_o(d) \ . \tag{6.1}$$

This definition of the separation distance gives a quantitative definition to the term "healing distance" originally introduced by Gomes, Walecka and Weisskopf.[77]

The two-potential problem has been previously treated for the scattering matrix by Watson[78] and by Gell-Mann and Goldberger.[79] The derivation for the reaction matrix is similar in many respects. We present here a brief sketch of the MS separation method, and indicate the improvements in the approximation suggested by Köhler.[18] Other improvements have also been suggested by Becker,[80] but they are necessary only if the detailed calculations are extended to third order, and we will not discuss them here. We shall use the matrix

notation of MS except that the nuclear reaction matrix will be designated by K instead of G^N.

Equation (2.12) for the K-matrix can be written in matrix form as

$$K = v + v \frac{Q}{e} K \tag{6.2}$$

where Q is the Pauli exclusion operator (restricting intermediate states to momenta greater than k_F) and e is the self-consistent denominator. We shall use relative momentum states, as in the approximation of Brueckner and Masterson,[36] so that $e = k^2/M + V(k) - (k'^2/M + V(k'))$, where k' is the relative momentum of the intermediate state. We will express K in terms of v_ℓ and t_s, where t_s is the reaction matrix for free particles under the influence of v_s alone. I.e., if v_s is Hermitian

$$t_s = v_s + v_s \frac{1}{e_o} t_s = v_s + t_s \frac{1}{e_o} v_s \tag{6.3}$$

where $e_o(k,k') = (k^2 - k'^2)/M$. Solving (6.3) for v_s (formally), we obtain

$$v_s = (1 - t_s \frac{1}{e_o})^{-1} t_s . \tag{6.4}$$

Substituting this into (6.2) and multiplying by $1 + t_s(1/e_o)$ on the left yields

$$K = t_s + t_s \left(\frac{Q}{e} - \frac{1}{e_o} \right) K + (1 + t_s \frac{1}{e_o}) v_\ell \left(1 + \frac{Q}{e} K\right) . \tag{6.5}$$

Therefore, to first order in t_s and v_ℓ

$$K^{(1)} = t_s + v_\ell \ . \tag{6.6}$$

Substituting this in the right hand side of (6.5) leads to the Moszkowski-Scott approximation:

$$K^{(2)} = t_s + v_1 + v_\ell \frac{Q}{e} v_\ell + t_s \frac{Q-1}{e} t_s + t_s(\frac{1}{e} - \frac{1}{e_o})t_s +$$

$$+ v_\ell \frac{Q}{e} t_s + t_s \frac{Q}{e} v_\ell$$

$$= t_s + v_\ell + v_\ell \frac{Q}{e} v_\ell + \Delta K(P) + \Delta K(D) + \Delta K(I) \tag{6.7}$$

or, in terms of $K^{(1)}$:

$$K^{(2)} = K^{(1)} + K^{(1)} \frac{Q}{e} K^{(1)} - t_s \frac{1}{e_o} t_s \ . \tag{6.8}$$

The physical interpretation of the terms on the right hand side of (6.7) is as follows:

1. As already noted, t_s is the reaction matrix for free particles acting under the potential v_s only.

2. v_ℓ and $v_\ell(Q/e)v_\ell$ are the first and second Born approximations for the long-range part of the potential.

3. The Pauli correction is:

$$\Delta K(P) = t_s \frac{Q-1}{e} t_s \ . \tag{6.9}$$

4. The so-called "dispersion" correction is:

$$\Delta K(D) = t_s (\frac{1}{e} - \frac{1}{e_o})t_s \ . \tag{6.10}$$

5. The second-order interference or cross term is:

$$\Delta K(I) = v_\ell \frac{Q}{e} t_s + t_s \frac{Q}{e} v_\ell = 2v_\ell \frac{Q}{e} t_s \, . \qquad (6.11)$$

The contributions of all terms in (6.7) for $p_F = 1.5\ F^{-1}$ is indicated in Table VI, when the potential used is the Brueckner-Gammel-Thaler potential discussed in the previous section. The data are taken from Reference 17. For this potential, the MS approximation predicted a minimum average energy of -14.2 MeV at $r_o = 1.02$ F compared to BG's -15.2 MeV at 1.02 F and BM's -16.9 MeV at 1.00 F. With only S, P and D waves (the only ones used by BG and BM), the MS energy was -13.6 MeV. Table VII shows the much more rapid convergence with a purely central potential, a feature which is discussed in more detail later.

	$K^{(1)}$	$v_\ell(Q/e)v_\ell$	ΔK(P)	ΔK(D)	ΔK(I)	Total
S-wave	-27.9	-6.2	0.5	6.2	-6.0	-33.3
P-wave	- 2.2	-1.8	1.2	1.1	0.0	- 1.7
D-wave	- 6.6					- 6.6
F-wave	- 0.1					- 0.1
G-wave	- 0.5					- 0.5
All states	-37.3	-8.0	1.7	7.3	-6.0	-42.2

Table VI. Summary of contributions to E_{Av} (in MeV) for the Brueckner-Gammel-Thaler potential,[a] $p_F = 1.5\ F^{-1}$. The kinetic energy is 28.0 MeV, so that $E_{Av} = 14.2$ MeV.

a This is the Gammel-Thaler potential quoted in Reference 3, as modified by Brueckner and Gammel (same reference).

	$K^{(1)}$ [a]	$v_\ell(Q/e)v_\ell$	$\Delta K(P)$	$\Delta K(D)$	$\Delta K(I)$	Total
S-wave	-42.5	-0.8	0.2	5.4	-1.9	-39.5
D-wave	- 9.6	-0.3				- 9.9
G-wave	- 0.6					- 0.6
All states	-52.7	-1.1	0.2	5.4	-1.9	-50.0

Table VII. Summary of contributions to E_{Av} (in MeV) for the MS standard potential,[b] $p_F = 1.5\ F^{-1}$. The kinetic energy is 28.0 MeV; therefore E_{Av} = 022.0 MeV. Contributions not indicated are all less than 0.01 MeV.

a The separation distance, d, between v_s and v_ℓ was chosen so that the first order contribution of t_s vanished.

b See Eq. (6.13) of text.

In Table VIII we indicate the contributions from various states using the BM approximation (Chapter IV). As indicated in that chapter, this calculation yielded an average energy about 1.7 MeV more negative than Brueckner and Gammel's calculation. However, because the MS calculation also uses relative-momentum two-particle states (instead of single-particle states) as does the BM method, it is appropriate to compare it to the -16.9 MeV of the BM calculation.

	Brueckner Method (this paper)	Moszkowski-Scott Method		
		1st order	2nd order	Total
S states	-38.7	-28.6	-4.9	-33.5
P states	+ 0.6	- 2.3	+0.6	- 1.7
D states	- 7.5	- 7.1	---	- 7.1
Total	-45.6	-38.0	-4.3	-42.3
Binding Energy	-16.9			-13.6
Tensor Contribution*				
a) self-consistent	-14.1			- 9.0
b) with V(k) above	-16.7			

Table VIII. Analyses of contributions to binding energy as calculated in this paper and by Moszkowski and Scott.[10] The tensor contribution was calculated by setting ${}^3V_T^{+} = 0$ and computing the binding energy (a) with a single-particle potential V(k) that is self-consistent with respect to the modified phenomenological potential, and (b) with the single-particle potential V(k) with which the S, P, and D state contributions were computed. Moszkowski and Scott used a first-order approximation to a self-consistent V(k) to compute the tensor contribution.

We note that the largest error is in S-states, where MS underestimate the potential energy by about 5 MeV. In P-states, whose energy consists of large contributions of opposite signs (as much as 14 MeV), the MS method predicts -1.7 MeV compared to 0.6 MeV, a difference of -2.3 MeV. The D-state contribution is underestimated by 0.4 MeV. The tensor force is a principal source of the S-state error. With the MS method, its contribution is -9 MeV; with the BM approximation it contributes -16 MeV.

Evaluation of the error in the Moszkowski-Scott method is not simple. In principle we can generate the third order approximation, $K^{(3)}$, by substituting the second order approximation, $K^{(2)}$, in the right hand side of (6.5). The approximation can be extended formally to higher and higher orders in this fashion. Unfortunately, the third order terms are extremely difficult to calculate, and one of the essential features of the approximation -- its computational simplicity -- is lost. Köhler[18] has investigated the higher order terms and has concluded that the following equations are better approximations than the second order terms in (6.7):

$$\begin{aligned} \Delta K(P) &= t_s \frac{(Q-1)e}{e_o^2} t_s \\ \Delta K(D) &= t_s \frac{1}{e_o} (e_o - e) \frac{1}{e_o} t_s \qquad (6.12) \\ \Delta K(I) &= 2v_\ell \frac{Q}{e_o} t_s \quad . \end{aligned}$$

He estimates (crudely) that the MS approximation underestimates $\Delta K(P)$ by a factor of 4, $\Delta K(I)$ by a factor of 2, and $\Delta K(D)$ by

about 37%. He predicts that with the corrections suggested above $\Delta K(D)$ will be overestimated by 10%, and the other terms will be approximately correct. The major error should then be due to neglecting the third and higher Born approximations for the contribution of v_ℓ .

Unfortunately, this is not the full story. Indeed if we apply Köhler's error estimates to the quantities listed in Table VI, the S-state contribution becomes about -35.8 MeV, which differs from the BM result by about 3 MeV. Much of this remaining difference would probably be obtained from the higher Born approximation terms. A similar analysis for the P-state also points to some improvement. The corrections to the second-order terms would lead to about 2 MeV repulsion in P-states, a part of which would be cancelled by the third order Born approximation, $v_\ell(Q/e)v_\ell(Q/e)v_\ell$. The calculation with the modified correction terms has been done for a central potential which MS calls the "standard potential."[11] It is defined by the equations

$$\begin{aligned} v(r) &= +\,0 \qquad r < r_c && \text{where} \quad \mu = \frac{3.5412}{r_b - r_c} \\ &= -s\, v_o\, e^{-\mu(r-r_c)} \quad r_c < r && v_o = \frac{\hbar^2}{m}\mu^2\, 1.4458 \end{aligned} \tag{6.13}$$

and the parameters were: $r_c = 0.4$ F, $r_b = 2.5$ F, and $s = 1$. Table VII gives the results for this potential using the MS equations. Köhler's error predictions applied to the second order terms suggest that the corrected mean energy would be about 1 MeV less attractive,

a prediction that a later calculation by Scott and Moszkowski[76] verified. However, because of the complicated effects of the tensor force, we cannot expect the analysis to carry over rigorously to the calculation with the more realistic BGT potential.

Comparison of the rates of convergence with the central interaction (Table VII) and with the full interaction (Table VI) indicates that the strong tensor potential definitely worsens the convergence of the approximation. Scott and Moszkowski[17] predict that higher order terms might contribute several MeV. This poorer rate of convergence is a direct consequence of the fact that the tensor force contributes nothing in first order, and thus all its contributions must come in second and higher orders. Furthermore, the tensor force makes the selection of the separation distance between the short- and long-ranged interaction very difficult, and it is no longer possible to obtain zero-phase shift. That most of the error in the MS calculation[17] is due to high order tensor force effects is also borne out by the calculations done by both MS and BM without the tensor force. As indicated in Table VIII, the BM calculation showed a contribution of -16.7 MeV, or -14.1 MeV if $V(k)$ is computed self-consistently with respect to the tensor-less potential, compared to MS's estimate of -9.0 MeV with an approximately self-consistent $V(k)$.

The error in the MS approximation (6.7) with Köhler's revised second order corrections (6.12) would probably come from the following sources: (1) neglect of higher order Born approximations

involving v_ℓ and higher order corrections; (2) errors due to the inability to choose the separation distance, d, so that the phase shift vanishes for v_s when the tensor force is included (this is discussed in Reference 17); (3) errors in approximating the higher order terms contributing to the Pauli, dispersion and interference corrections with second order terms; (4) errors arising from the approximations used for computational simplicity in the evaluation of the various second order contributions (see Reference 11 for a detailed description of these approximations); and (5) higher order corrections in (6.3) and (6.5) coming from the fact that v_s is not Hermitian (due to the slight momentum dependence of the separation distance, d -- see Table III of Reference 11). The above errors are listed in the probable order of decreasing magnitude: the first listed is probably a two or three MeV error, the last less than half an MeV. Our analysis has also shown that most of the error will be in the contributions from low angular momentum states. For $\ell \geq 2$, the error is less than 0.5 MeV. This improvement is to be expected since the Born approximation is adequate in very high angular momentum states. It must be emphasized that these error estimates are with respect to the Brueckner approximation. Any errors inherent in that approximation will also be inherent in the MS approximation.

Some cancellation of errors undoubtedly does occur, but we must agree with Scott and Moszkowski[17] that the separation method is probably not an adequate quantitative tool for use with tensor interactions. However, it does appear to predict the qualitative effects

properly, and because of its conceptual and computational simplicity, it has considerable merit as an analytical tool. In particular, it has been used to obtain an estimate of the size of the three-body cluster term using a potential with a hard core,[59] to study the effects of the repulsive core,[11] and to evaluate the use of various potentials for approximate many-body calculations.[17] Recently Bethe, Brandow and Petschek[9] have used the MS separation method in conjunction with a "reference spectrum" approximation to obtain a powerful variant of the approximation which may be capable of greater accuracy. This new approximation is discussed in the next section.

B. REFERENCE SPECTRUM METHOD FOR NUCLEAR MATTER

This section reviews the "reference spectrum" method proposed by Bethe, Brandow and Petschek (Reference 9, hereafter referred to as BBP). The two principal techniques employed are (1) to replace the spectrum of intermediate states with a "reference spectrum" of the form $A + Bk^2$ (enabling the reference K-matrix, K^R, with energies so defined to be calculated easily), and (2) to employ the MS separation method, but with the separation distance so defined that the reference wave function for $r > d_R$ goes over exactly into the free particle function (whereas MS put this requirement on the wave function of two nucleons interacting outside of nuclear matter). Complete calculations have not yet been made with this method, but the authors estimate the error for central potentials to be about 0.1 MeV for the diagrams usually included (i.e., not including the error from fourth and higher order "cluster terms").

The error for tensor potentials will be greater, for the same reasons that the MS separation method was not fully quantitative for tensor potentials. The details of their calculation are quite involved and only certain key features will be discussed here.

In (6.7) we have indicated the terms through third order which one must calculate in the MS separation method. The leading terms are

$$K = K_s + v_\ell + v_\ell \frac{Q}{e} v_\ell + O(v^2) \ . \tag{6.14}$$

The Born approximation terms (the second two) can be calculated through second order because the wave function for the long-range part of the interaction is just the unperturbed basis function. The third order Born approximation is too complicated for direct computation at present, and unfortunately is not negligible for tensor forces. However, it is probably smaller than the apparent error in the MS calculations because the separation distance will be larger by virtue of its definition (see preceding paragraph). From (6.14) it is apparent that it is important to calculate K_s precisely. BBP have found that this can be done in a relatively simple approximation. MS point out that K_s has matrix elements mostly to intermediate states of high momentum (of order $3p_F$). Consequently the Pauli principle (the operator Q) does not have much influence on K_s but the energy spectrum "e" of the intermediate states does. This suggests the use of a "reference matrix"

$$K_s^R = v_s + v_s \frac{1}{e_R} K_s^R \tag{6.15}$$

with the "reference energy" of the excited particles defined by

$$\omega_R(p_n) \simeq A_2 + p_n{}^2/2M^* \tag{6.16}$$

where M^* is an effective mass. Thus, the energy denominator becomes

$$e = \Sigma - k'^2/M^* - 2A_2 - P^2/4M^* \tag{6.17}$$

with

$$\Sigma = \omega(\underset{\sim}{k} - \frac{1}{2}\underset{\sim}{P}) + \omega(\underset{\sim}{k} + \frac{1}{2}\underset{\sim}{P}) \; .$$

The coefficients A and M^* are chosen to give the best average fit to the actual energy spectrum $E(k')$ in the region of k' which matters most for the solution of (6.15), $2p_F$ to $4p_F$. Once K^R is obtained, the actual nuclear reaction matrix should be calculated from the exact integral equation

$$K = K^R + K^{R\dagger}(\frac{1}{e_R} - \frac{Q}{e})\, K \; . \tag{6.18}$$

Since e_R is chosen to be a good approximation to e in the region of k' important for the short-range forces, the second term in the above equation should be small. Therefore, it is a good approximation to replace K on the right above with K^R; the approximate equation for K is then

$$\langle k|K|k\rangle \simeq \langle \underset{\sim}{k}|K|\underset{\sim}{k}\rangle + (2\pi)^{-3}\int d\underset{\sim}{k}'\,|\langle k'|K^R|k\rangle|^2 \left(\frac{1}{e_R(k')} - \frac{Q(k')}{e(k')}\right) . \tag{6.19}$$

K^R is Hermitian when defined as in BBP.

The importance of the "reference spectrum" method is the

fact that it permits the extension of the MS calculations to the full nuclear potential inasmuch as it makes it possible to obtain with reasonable effort the energy spectrum (recall that MS had used the BG self-consistent potential for their calculations with the BGT potential[17]). Furthermore, by using the reference spectrum, BBP have been able to treat the effect of the hard core on the energies of particles with high momentum more accurately than previously done because they have picked up the core volume term neglected in previous calculations. A more exact method for incorporating this term in reaction matrix calculations is discussed in Chapter IV (Section B.3), and we will not treat it further here. However, it should be noted that it was the BBP calculations which pointed to the importance of this term in the off-energy shell calculations of particle energies. The fact that the particle energies should be computed farther and farther off the energy shell for higher particle momenta (see the above referenced discussion in Chapter IV) also increases the effect of the core terms, and the potential energy for particles of high momentum becomes large and positive instead of going to zero as in the calculations of BG and BM. The effect of this change in energy spectrum on the self-consistent calculation of the mean energy was not calculated by BBP, but it has been estimated (in Chapter IV) to reduce the calculated mean energy a fairly large amount, perhaps two MeV or more.

Rajaraman[10] has investigated the effect of the core volume term on the three-body cluster's contribution to the energy of the

system, and concludes that it is comparable to the other third order terms for high momenta. He suggests a procedure for treating the three-body cluster as self-energy inserts for the calculation of the particle energies. The effect of this term is to reduce the core contribution to the single particle energies in the region around $3\ p_F$ about half. However, he accounted for the effects of the tensor potential very crudely. Further, even though BBP estimate the effect of the three-body cluster may be two or three MeV on the binding energy per nucleon, we do not believe that it is consistent to take it into account without some effort to sum the higher order diagrams which can be related to it. Self-energy and ladder-diagrams related to the basic three-body cluster will cause its contribution to be considerably reduced. A calculation with reaction matrix interaction and self-consistent energy denominators would help to clarify the picture considerably. The calculation referred to in Chapter IV (see Table IV), which yielded about 6 MeV for the contribution of the three-body term as obtained from the BBP spectra with and without the estimated three-body correction, should not be considered quantitative because, as indicated in Chapter IV, the remainder of our calculation using their spectrum is subject to several large corrections.

One further comment should be made about the BBP calculation. They treat the core separately and in good approximation for all angular momentum states. BG, and also BM, treated the core only for those states for which they also treated the attraction since

there is considerable cancellation between the two interactions for the other states. Thus, to be consistent, the treatment of the attractive interaction must be extended to many of the higher states, including the appropriate tensor couplings. Further, as BBP point out, the treatment of the core in all states involves the assumption that the core is present in all states, and is the same for all of them. This assumption has not been verified either experimentally or theoretically.

C. THE PUFF APPROXIMATION

The Puff approximation[13,14] is based on the Green's function formalism of Martin and Schwinger.[12] The derivation is quite lengthy, and we shall merely sketch it here and then discuss the final system of equations. A thorough discussion can be found in the papers by Martin and Schwinger[12] and Puff,[14] and a heuristic derivation and another summary in a paper by Falk and Wilets.[33] Bell[19] has also briefly reviewed the theory, though not in detail.

Consider the Hamiltonian

$$\mathcal{H} = H - \mu N \tag{6.20}$$

where H is the usual Hamiltonian

$$H = \int d\underset{\sim}{r}_1 \, \Psi^\dagger(\underset{\sim}{r}_1 t_1)(-\nabla_1{}^2/2m)\, \Psi(\underset{\sim}{r}_1 t_1) + \frac{1}{2}\int d\underset{\sim}{r}_1 d\underset{\sim}{r}_2 d\underset{\sim}{r}_3 d\underset{\sim}{r}_4$$

$$\times\, \Psi^\dagger(\underset{\sim}{r}_1 t_1)\Psi^\dagger(\underset{\sim}{r}_2 t_2) v(\underset{\sim}{r}_1\underset{\sim}{r}_2;\underset{\sim}{r}_3\underset{\sim}{r}_4)\Psi(\underset{\sim}{r}_3 t_1)\Psi(\underset{\sim}{r}_4 t_1) \tag{6.21}$$

(with $\hbar = 1$). The total number of particles operator, N, is

given by

$$N = \int d\underset{\sim}{r}_1 \; \Psi^\dagger(\underset{\sim}{r}_1 t_1)\; \Psi(\underset{\sim}{r}_1 t_1) \tag{6.22}$$

and μ is a Lagrange multiplier (which, of course, turns out to be the chemical potential). For fermions the n-particle Green's operators are defined by

$$\overline{G}_n(1\ldots n;1'\ldots n') \equiv (-i)^n \epsilon(t_1\ldots t_n t_1'\ldots t_n')T$$
$$[\Psi(1)\ldots\Psi(n);\Psi^\dagger(n')\ldots\Psi^\dagger(1')] \tag{6.23}$$

where $T[\quad]$ is the time-ordered product, and ϵ is $(-1)^p$ where p is the number of permutations to go from the time-ordered sequence to the "standard" sequence, $t_1 \ldots t_n t_n' \ldots t_1'$, and $1, \ldots,$ n mean $r_1 t_1, \ldots, r_n t_n$. Averaged Green's functions are defined by

$$G_n = [NE|\overline{G}_n|NE] = \frac{\sum_\xi (NE\xi|\overline{G}_N|NE\xi)}{\sum_\xi (NE\xi|NE\xi)} \tag{6.24}$$

where $|NE\xi)$ is a state of given N, E (eigenvalues of the operators N and E) and any other quantum numbers ξ. For simplicity, we will not indicate the latter quantum numbers in our equations, but they are there, of course, and must be summed over in actual calculations.

The G_n obey a set of linked equations:

$$G_n(1\ldots n;1'\ldots n') = G_1^o(1\ n{+}1)V(n{+}1\ n{+}2)G_{n+1}(2\ 3\ldots n{+}1;n{+}2;(n{+}2)^+$$
$$1'\ldots n') + \sum_{j=1'}^{n'} (-1)^{j'+1}\, G_1^o(1\ j')G_{n-1}(2\ 3\ldots n;1'\ldots \text{omit } j'\ldots n') \tag{6.25}$$

where $V(12) = i\, v(r_1 - r_2)\delta(t_1 - t_2)$ for a local potential and $(n + 2)^+$ involves a time infinitesimally larger than that of $(n + 2)$. G_1^o is defined to be G_1 for no interaction, and the equation for it can be easily solved (so that G_1^o is a known quantity).

Finally, it can be shown that the total energy per unit volume of the system is given by

$$\frac{E}{\Omega} = \frac{\langle H \rangle}{\Omega} = \pm \frac{i}{(2\pi)^3} \int d\, \underset{\sim}{k}_1 \lim_{t_1' \to t_1^+} \frac{1}{2}\left(i \frac{\partial}{\partial t_1} + \frac{k_1^{\;2}}{2m} + \mu\right) G_1(k_1, t_1 - t_1') \tag{6.26}$$

where $G_1(k_1, t_1 - t_1')$ is the Fourier transform of $G_1(r_1 t_1; r_1' t_1')$.

With these definitions and equations in mind, we proceed to develop the approximation. The equations for G_1 and G_2 can be written

$$G_1(1,1') = G_1^o(1,1') + G_1^o(1,2)V(23;45)G_2(45;3^+1') \tag{6.27}$$

and (with considerable rearrangement of terms from (6.25)),

$$\begin{aligned} G_2(12,1'2') = {} & [G_1(1,1')G_1(2,2') - G_1(1,2')G_1(2,1')] \\ & + G_1^o(1,3)G_1^o(2,4)V(34;56)G_2(56,1'2') \\ & + (\text{terms of order } V^2 \text{ involving } G_4 \text{ and } G_2G_2) . \end{aligned} \tag{6.28}$$

It is in this equation that the approximation is made. The terms of order V^2 are dropped. An S-matrix is then defined (schematically) by

$$VG_2 = S(G_1G_1 - G_1G_1) . \tag{6.29}$$

For zero temperature nuclear matter, S is determined by

$$S(\omega)_{ij;k\ell} = v_{ij;k\ell} + \sum_{\text{all } m,n} v_{ij;mn} \frac{1}{\omega-\epsilon_m-\epsilon_n} S(\omega)_{mn;k\ell} \qquad (6.30)$$

where the ϵ are the kinetic energies and ω is an energy parameter. This equation, identical in form to the free two-body scattering equation, is obtained only after considerable manipulation, and depends on the analytic properties of the approximate Green's function arising from a further approximation: that the chemical potential μ is independent of the interaction and is less than one half the binding energy of the deuteron (since the deuteron binding energy determines the location of the pole in the two-body scattering matrix). This assumption that μ is fixed, negative and independent of v removes the Puff approximation from the realm of pure perturbation theory. If $G_1(rt,r't')$ is expressed as a double Fourier transform of a spectral function, $A(k,\omega)$, then it can be shown that, subject to the above approximations,

$$A(k,\omega) = 2\pi\rho_k\delta(\omega-\omega_k) \qquad (6.31)$$

for two particles in the Fermi sea, where

$$\omega_k = \epsilon_k + V_k(\omega_k) \qquad (6.32)$$

$$\rho_k = \left[1- \left.\frac{\partial V_k(\omega)}{\partial\omega}\right|_{\omega=\omega_k}\right]^{-1} \qquad (6.33)$$

and

$$V_k(\omega) = \sum_{\ell\leq p_F^P} S_{k\ell;(k\ell)}\rho_\ell \ . \qquad (6.34)$$

p_F^P is a modified Fermi momentum which is determined by requiring

the sum of the ρ_k to equal the particle density (or, equivalently, the integral over the approximate one-particle Green's function to equal the total number, N). Thus, the density is given by

$$\rho = 4 \sum_{k \leq p_F} P \rho_k \tag{6.35}$$

where the factor 4 accounts for the spin and isotopic spin degeneracy. Finally, the energy per particle is

$$\frac{E}{N} = \frac{4}{\rho} \sum_{k \leq p_F} P[\epsilon_k + \frac{1}{2} V_k(\omega_k)]\rho_k \ . \tag{6.36}$$

In this approximation, the center-of-mass and relative motions separate, and the T-matrix can be solved in terms of the relative momenta alone (as in the Brueckner-Masterson approximation). This leads to considerable simplification of the actual calculations.

If we had solved G_1 exactly, instead of approximately through (6.27) and the first two terms of (6.28), then the energy expression we would have obtained would have been exact, and we would have

$$E_B = \mu \tag{6.37}$$

and, at the equilibrium density (where the pressure of the system vanishes,

$$E/N = \mu \ . \tag{6.38}$$

(6.37) and (6.38) are just the equations of the Bethe-Hugenholtz-Van Hove theorem.[8,30] Puff uses (6.38) as the condition for the proper value of E/N. However, as Falk and Wiletshas pointed out,[33]

the use of an approximate equation for G_1, as well as the presence of the "rearrangement energy," make (6.38) invalid and we must instead use the relation

$$\frac{\partial}{\partial\rho}\left(\frac{E}{N}\right)_\Omega = 0 \tag{6.39}$$

as the condition for determining E/N.

Therefore, the proper prescription for calculating E/N in the Puff-Martin approximation is the following: (1) calculate the scattering matrix, $S(\omega)$, as a function of the energy parameter, ω; (2) solve the simultaneous equations for ω_k (6.32), ρ_k (6.33), and $V_k(\omega)$ (6.34) for a given value of $p_F{}^P$; (3) calculate the density, ρ (6.35), and the mean energy, E/N (6.36); and (4) repeat the process for a sufficient number of values of $p_F{}^P$ to determine the minimum of E/N as a function of the density, ρ.

This set of equations is actually more difficult to solve for a local, hard core potential than the equations in ML, because the T-matrix must be computed for sufficient many values of the parameter ω to make an accurate evaluation of ρ_k (6.33) possible. However, for a separable potential it is possible to obtain an analytic solution for $S(\omega)$, and the remainder of the problem is then fairly simple. Puff[14] and Falk and Wilets[33] have obtained solutions for an S-state Yamaguchi separable potential with a hard shell (with $r_c = 0.4$ F). Puff, using the condition $E/N = \mu$, obtained $E/N = -14.7$ MeV at 0.92 F. Falk and Wilets found the minimum of E/N to occur at 1.01 F, with E/N equal to -17.6 MeV. In both calculations, $p_F{}^P$ was about 5% greater than the Fermi

momentum of the non-interacting gas (i.e., the perturbation theory Fermi momentum).

In evaluating their error, Puff and Falk and Wilets estimate the contribution to E/N resulting from the terms neglected in G_2 by dropping the last term of (6.28). They obtain several contributions of order S^3 (or v^3), which are estimated to cause an error in E/N of "less than about 2 MeV" and an error in r_o of "less than about 10%."[33] This error estimate is borne out by the calculations of BM (Fig. 9) in which, with a simpler version of the approximation (described below) an error of 10% in these quantities resulted for two different Gammel-Thaler potentials (-18.9 MeV at 0.90 F vs. -16.9 MeV at 1.00 F for the BGT potential). The BM version of the calculation, based on a description by Bell,[19] uses the S-matrix as defined by (6.30) but uses the Fermi distribution, n_k, in place of ρ_k and the unperturbed Fermi momentum, p_F, in place of p_F^P. This approximation was no easier computationally than the full BM approximation for the local, hard core potentials, and the use of the full Puff approximation would have been an order of magnitude more difficult because of the extra simultaneous equation, (6.33) for ρ_k, which requires knowing the S-matrix as a function of ω sufficiently well to take accurate derivatives of it. In terms of the computation itself, this would require calculating $S(\omega)$ for many values of ω for every value of the momentum instead of using the "best available value" (i.e., the value ω_k computed on the previous iteration) in an iteration scheme. The use of the full

Puff approximation would undoubtedly shift the result in the direction of the BM result, but how much is not known. The full calculation was not attempted because of its additional complexity and because, as discussed below, there exists a second order discrepancy between an expansion of the Puff equations and the BG expansion. This difference between the two approximations is a direct consequence of the assumption that μ is fixed and independent and negative, said approximation removing (as noted before) the Puff approximation from the status of a pure perturbation expansion.

The Puff-Martin approximation is easily compared to the BG expansion if we expand in powers of the two-body potential, v. Equation (6.33) for the momentum density then becomes

$$\rho_k = \left[1 - \frac{\partial}{\partial\omega'} \sum_{\ell\le p_F^P} S(\omega=\omega'+\omega_\ell)_{k\ell;(k\ell)}\Big|_{\omega'=\omega_k}\right]^{-1}$$

$$= 1 + \frac{\partial}{\partial\omega'} \sum_{\ell\le p_F^P} S(\omega'+\omega_\ell)_{k\ell;(k\ell)}\Big|_{\omega'=\omega_k} + \ldots$$

$$= 1 + \frac{\partial}{\partial\omega'} \Bigg[\sum_{\ell\le p_F^P} v_{k\ell;(k\ell)} + \sum_{\substack{\ell\le p_F^P \\ \text{all } m,n}} v_{k\ell;mn} \frac{1}{\omega'+\omega_\ell-\epsilon_m-\epsilon_n} v_{mn;(k\ell)} \Bigg]_{\omega'=\omega_k} + O(v^3). \quad (6.40)$$

An equation similar to this is used as the starting point of a heuristic derivation of (6.33) for ρ_k by Falk and Wilets. Next the Puff equations are expanded in terms of the unperturbed Fermi momentum, p_F, instead of p_F^P. To do this, we note that

$$\rho = 4 \sum_{k\le p_F} 1 = 4 \sum_{k\le p_F} \rho_k \, . \tag{6.41}$$

Thus, using (6.40)

$$\sum_{k\le p_F} 1 = \sum_{k\le p_F} 1 + \sum_{k=p_F}^{p_F^P} + \sum_{k\le p_F} \left[\frac{\partial}{\partial\omega'} \sum_{\substack{\ell\le p_F \\ \text{all } m,n}} v_{k\ell;mn} \frac{1}{\omega'+\omega_\ell-\epsilon_m-\epsilon_n} v_{mn;(k\ell)} \right]_{\omega'=\omega_k} + O(v^3). \tag{6.42}$$

From this we obtain

$$\sum_{k=p_F}^{p_F^P} 1 = - \sum_{k\le p_F} \left[\frac{\partial}{\partial\omega'} \sum_{\substack{\ell\le p_F \\ \text{all } m,n}} v_{k\ell;mn} \frac{1}{\omega'+\omega_\ell-\epsilon_m-\epsilon_n} v_{mn;(k\ell)} \right]_{\omega'=\omega_k} + O(v^3) \tag{6.43}$$

and, consequently, using a Taylor expansion of the sums from k_F to p_F^P about p_F and expanding ρ_k:

$$\sum_{k\le p_F^P} \epsilon_k \rho_k = \sum_{k\le p_F} \epsilon_k - \epsilon_{p_F} \sum_{k\le p_F} \left[\frac{\partial}{\partial\omega'} \sum_{\substack{\ell\le p_F \\ \text{all } m,n}} v_{k\ell;mn} \frac{1}{\omega'+\omega_\ell-\epsilon_m-\epsilon_n} v_{mn;(k\ell)} \right]_{\omega'=\omega_k} +$$

$$+ \sum_{k\le p_F^P} \left[\frac{\partial}{\partial\omega'} \sum_{\substack{\ell\le p_F \\ \text{all } m,n}} v_{k\ell;mn} \frac{\epsilon_k}{\omega'+\omega_\ell-\epsilon_m-\epsilon_n} v_{mn;(k\ell)} \right]_{\omega'=\omega_k} + O(v^3). \tag{6.44}$$

Then the Puff-Martin expression (6.36) for E/N is, through second

$$\frac{E}{N} = 4\rho^{-1}\Bigg\{ \sum_{k\le p_F} \epsilon_k + \frac{1}{2}\sum_{k,\ell\le p_F} v_{k\ell;(k\ell)} - \sum_{k\le p_F} \Bigg[\frac{\partial}{\partial\omega'} \sum_{\substack{\ell\le p_F \\ \text{all } m,n}} v_{k\ell;mn} \frac{\epsilon_{p_F}-\epsilon_k}{\omega'+\omega_\ell-\epsilon_m-\epsilon_n} v_{mn;(k\ell)}\Bigg]_{\omega'=\omega_k} + \frac{1}{2}\sum_{\substack{k,\ell\le p_F \\ \text{all } m,n}} v_{k\ell;mn} \frac{1}{\omega_k+\omega_\ell-\epsilon_m-\epsilon_n} v_{mn;(k\ell)} + O(v^3)\Bigg\} . \qquad (6.45)$$

Here we have used (6.43) to resolve the second term of (6.44). The BG expansion, on the other hand, yields

$$\frac{E}{N} = 4\rho^{-1}\Bigg\{ \sum_{k\le p_F} \epsilon_k + \frac{1}{2}\sum_{k\ell\le p_F} v_{k\ell;(k\ell)} + \frac{1}{2}\sum_{\substack{k\ell\le p_F \\ mn>p_F}} v_{k\ell;mn} \frac{1}{\omega_k+\omega_\ell-\epsilon_m-\epsilon_n} v_{mn;(k\ell)} + O(v^3)\Bigg\} . \qquad (6.46)$$

The higher order terms include terms arising from the expansion of V_m and V_n out of the propagator. By symmetrizing the second term on the right in (6.45), and by combining the last two terms of that equation and then subtracting (6.46), we find the difference in the two expressions to be

$$\delta\left(\frac{E}{N}\right)^{(2)} = -4\rho^{-1}\Bigg\{\frac{1}{2} \sum_{k\le p_F} \Bigg[\frac{\partial}{\partial\omega'} \sum_{\substack{k\ell\le p_F \\ \text{all } m\ n}} v_{k\ell;mn} \frac{2\epsilon_{k_F}-\epsilon_m-\epsilon_k}{\omega'+\omega_\ell-\epsilon_m-\epsilon_n} v_{mn;k\ell}\Bigg]_{\omega'=\omega_k} +$$

$$+ \frac{1}{2} \sum_{\substack{k\ell \leq p_F \\ mn > p_F}} v_{k\ell;mn} \frac{1}{\omega_k + \omega_\ell - \epsilon_m - \epsilon_n} v_{mn;(k\ell)} \Big\} \; . \tag{6.47}$$

This second order discrepancy has been evaluated for the S-state Yamaguchi separable potential[75] with the same parameters used by Puff for $r_c = 0$. The details of the reduction are given in Appendix C, and the result indicates that these terms neither cancel each other nor vanish identically. It is emphasized that this calculation does not provide a real measure of the Puff-Martin approximation; however, it does indicate the existence of a non-vanishing second-order term which has not been previously noted.

We should also append a comment about the density, ρ_k, as given by (6.33). As we have shown in Section I, the true density is given by

$$\rho_{\underset{\sim}{k}} = \frac{n_k}{1 - \frac{\partial}{\partial \omega_k} V(\omega_k)} + \frac{\delta'}{\delta \epsilon_k} \Delta E(n, \epsilon) \; . \tag{6.48}$$

The second, continuous term, which is missing from (6.33), was shown to be of order v^2. Therefore, (6.33) is an approximation to the true ρ_k in which the effect of the continuous portion is approximated by allowing p_F to increase to p_F^P. That p_F^P is about 5% greater than p_F is indicative of the importance of this continuous portion.

There is one other comment about the reaction matrix, (6.30), which should be mentioned in conjunction with its similarity

to the free two-body scattering matrix. There is a major distinction between the two. For the free scattering matrix, the energy parameter is identified as

$$\omega_k = \epsilon_k + \Delta E \tag{6.49}$$

where ΔE is the energy shift of a single particle due to the interaction with one other particle, and is therefore of order $(1/\Omega)$. In the many-body case, where ω_k is given by (6.32), the energy shift V_k is due to the interaction with all the other particles and is therefore of order $N/\Omega = \rho$. In the former case it has been shown[82] that

$$\lim_{\Omega \to \infty} \Delta E = - \lim_{\Omega \to \infty} \frac{1}{\Omega} \left(\frac{2E}{k}\right) \delta_\ell(E) \tag{6.50}$$

where the $\delta_\ell(E)$ are the free-scattering phase shifts. The binding energy computed in this approximation is much too attractive (-52 MeV at normal density, with no sign of saturation for $r_0 \geq 0.8F$).[3]

In the many-body case, the $O(1/\Omega)$ term, which leads to the direct dependence on δ_ℓ, is "washed out" by the many-body effects, and the energy is proportional to $\tan \delta_\ell$. Furthermore, the δ_ℓ should be the phase shifts appropriate to a many-body medium, not the free-scattering phase shifts. It is clear, furthermore, that the region of $\omega(k)$ for which the S-matrix is required for the many-body problem is far removed from the region determined from two-body scattering experiments.

D. MOHLING APPROXIMATION

The central element of the Mohling approximation[15,16] is the free-scattering matrix, just as in the Puff approximation. The derivation, and the approximation itself, differ from Puff's, however. Bell[19] has summarized the approximation as follows:

> Mohling uses a variation of the 'binary collision' expansion of Lee and Yang. The essential ideas are conveniently explained in terms of the diagrams of Montroll and Ward[81] (see also Bloch and de Dominicis[92]). They represent the perturbation development of the grand partition function
>
> $$Z = \text{Trace } [\exp - \beta(H - \mu N)] \text{ .}$$
>
> The solid lines [see the typical diagram below] represent the propagation of any number of particles from 'time' 0 to 'time' β. Because of the trace operation the particles must end in their initial positions or (because of antisymmetrization) in a permutation thereof. The pairing of initial and final states is indicated by dotted lines;

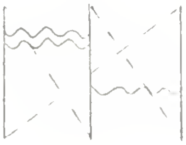

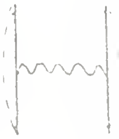

> these may be thought of as continuing the solid lines on the far side of a cylindrical surface. The siggly lines represent interactions between particles. Each such graph contributes a term to Z by rules that we need not set out here.
>
> Now by a number of partial summations smaller sets of diagrams, with modified rules of calculation, can be made to suffice. In the Lee-Yang-Mohling development the following types of diagrams are eliminated in the following order:
>
> (A) 'Unlinked diagrams,' containing parts not connected to the remainder by either dotted or wiggly lines. Z is the exponential of the sum of the linked diagrams only.

> (B) Diagrams containing 'ladders' in which two particles interact repeatedly, without interacting with a third. In calculating with the remaining diagrams a wiggly line represents a matrix element of a scattering operator rather than a potential.
>
> (C) Diagrams with 'self-energy parts' connected to the remainder only by two solid lines. Each solid line is given a modified propagation factor to allow for the possible insertions.
>
> Because (B) is performed before (C), the intermediate states of the ladders propagate in an unperturbed way. This results in unperturbed kinetic energies appearing in (1). But the subsequent insertion (C) of self-energy parts in the external lines of ladders modifies the initial and final energies, and hence the appearance in (1) [the scattering matrix equation] of W' [the self-consistent single particle energy for holes].

The Brueckner reaction matrix is obtained by doing (C) before (B) and by eliminating, between (C) and (B), the "spirals" -- lines which completely loop the cylinder one or more times without interaction.

Mohling's expansion matrix is the same as Puff's, (6.30). However, Mohling's equations are correct to a higher order because his energy expansion contains second-order terms (in the reaction matrix) which explicitly cancel the second-order terms arising from the differences between his expansion matrix and the Brueckner K-matrix. The calculation in BM is exactly the first-order Mohling approximation and indicates that the BM approximation will yield approximately 10% errors in r_o and E_{Av}. In Mohling's own calculations, however, he further reduces the problem so that he can

isolate a part which depends only on scattering phase shifts. His initial results,[16] in which he uses an S-state square well with repulsive core to calculate the other parts of the approximation, yielded a disappointing -36 MeV at $r_o = 0.75$ F (c.f., Gomes, Walecka and Weisskopf[77] with -6.9 MeV at $r_o = 1.13$ F for the same potential with a very simple K-matrix approximation). Mohling estimates that the use of a better potential and more accurate accounting for correction terms would improve these results considerably. However, some error is undoubtedly generated by his use of the free-scattering phase shifts: the phase shifts appropriate to this type of calculation should be the phase shifts for scattering of two particles in the nuclear medium. Although the BM calculations indicate that the version of the approximation employed by them gives reasonably good results, they also indicate that the approximation in this form is no simpler with local, hard core potentials than the BM approximation -- and is less accurate.

Finally, there exists a high degree of cancellation in the second-order terms occurring in this approximation and also between the second-order terms (due to the exclusion principle) and the third-order terms (due to neglect of particle self-energy in propagators). Because of this cancellation, these terms must be calculated quite accurately and with realistic potentials to be meaningful. In particular, the use of a different potential from the one used for the first-order terms could lead to appreciable error (as it does in the approximation described in Chapter VII) because of the

different high order behavior of the potentials employed. However, for calculations in which a simple formulation is desired, and 10% accuracy is sufficient, the first-order theory described in ML (and by Bell[19]) is very simple to use with separable potentials. It is much simpler to employ than the Puff approximation because the self-consistent equations for the momentum density do not appear.

VII.

AN EASY NUCLEAR MATTER APPROXIMATION

In this chapter a relatively easy nuclear matter approximation is suggested and evaluated. Motivated by a result derived in Chapter II, it features a release from the "self-consistency" requirement which complicates other nuclear matter calculations. There are only two computationally difficult quantities required, the Green's functions and the momentum density (through second order). The former, being independent of the nucleon-nucleon potential in this approximation, can be computed once (on a computer) and tabulated for all future use of the approximation. The momentum densities, on the other hand, can be calculated with a separable potential and likewise tabulated. The remaining equations are all easily handled: a desk calculator would suffice, though a small computer would be desirable.

The approximation to be employed is motivated by the derivation of (2.78) in Chapter II:

$$E = \sum_k \epsilon_k n_k + [\ \Delta E(\rho,\epsilon)\ ]_{\substack{\text{no self-energy}\\ \text{processes}}} \tag{7.1}$$

which would lead to an expansion matrix

$$t'_{ij;k\ell} = \Sigma\, v_{ij;k\ell} + \Sigma\, v_{ij;mn} \frac{(1-\rho_m)(1-\rho_n)}{\epsilon_k+\epsilon_\ell-\epsilon_m-\epsilon_n} t'_{mn;k\ell} \tag{7.2}$$

so that

$$E = \sum_k \epsilon_k n_k + \sum_{k\ell} t_{k\ell;k\ell}\, \rho_k \rho_\ell \quad . \tag{7.3}$$

In the absence of an experimental ρ_k the above calculation would be very difficult. However, we may approximate the above reaction matrix with the t-matrix derived in Appendix B (B.1)

$$t_{ij;k\ell} = v_{ij;k\ell} + \sum_{mn} v_{ij;mn} \frac{(1-n_m)(1-n_n)}{\epsilon_k+\epsilon_\ell-\epsilon_m-\epsilon_n} t_{mn;k\ell} \tag{7.4}$$

and use a second-order (in t) calculation of the density, defined in Chapter II (2.23):

$$\rho_q = n_q \left\{ 1 - \sum_{\substack{\ell \\ mn}} t_{mn;q\ell} \frac{(1-n_m)(1-n_n)}{(\epsilon_q+\epsilon_\ell-\epsilon_m-\epsilon_n)^2} t_{mn;(q\ell)} n_\ell + \cdots \right\}$$

$$+ (1-n_q) \left\{ \sum_{k\ell n} t_{qn;k\ell} \frac{(1-n_n)}{(\epsilon_k+\epsilon_\ell-\epsilon_q-\epsilon_n)^2} t_{qn;(k\ell)} n_k n_\ell + \cdots \right\} . \tag{7.5}$$

To verify this solution, we substitute (7.5) in (7.3)

$$\Delta E = \frac{1}{2} \Sigma t_{k\ell;(k\ell)} n_k n_\ell - \frac{1}{2} \sum_{k\ell} t_{k\ell;(k\ell)} \left\{ 2 \sum_{\substack{j \\ mn}} t_{mn;j\ell} \frac{(1-n_m)(1-n_n)}{(\epsilon_q+\epsilon_\ell-\epsilon_m-\epsilon_n)^2} \right.$$

$$\left. t_{mn;(j\ell)} n_j \right\} n_k n_\ell \tag{7.6}$$

$$+ \frac{1}{2} \sum_{km} t_{km;(km)} \left\{ 2 \sum_{j\ell n} t_{mn;j\ell} \frac{(1-n_n)(1-n_m)}{(\epsilon_j+\epsilon_\ell-\epsilon_m-\epsilon_n)^2} t_{mn;j\ell}\, n_j \right\} n_k n_\ell + O(t^4).$$

Or, changing indices

$$\Delta E = \frac{1}{2} \Sigma\, t_{k\ell;(k\ell)} n_k n_\ell - \frac{1}{2} \sum_{\substack{k\ell \\ mn}} t_{k\ell;mn} \frac{(1-n_m)(1-n_n)}{(\epsilon_k+\epsilon_\ell-\epsilon_m-\epsilon_n)^2} t_{mn;(k\ell)} \times$$

$$\times \left\{ \sum_j \left(t_{jk;(jk)} + t_{j\ell;(j\ell)} - t_{jm;(jm)} - t_{jn;(jn)} \right) n_j \right\} . \tag{7.7}$$

On comparison with (B.2), it is apparent that this approximation is exact to fourth order. Further, the terms in the brackets in (7.7) are just the single-particle potential energies in the t-matrix approximation, with $\Delta = 0$ (in the t-matrix denominator) for all momenta.

For those t-matrices computed with hard core separable potentials, the further approximation of Chapter IV was employed: namely, the "realtive momentum approximation" with the t-matrix defined by

$$t_{k';k} = v_{k';k} + \sum_{k''} v_{k';k''} \frac{f(\overline{P},k'')}{\Sigma - \frac{k''^2}{M}} t_{k'';k} \tag{7.8}$$

with

$$\begin{aligned} \Sigma &= k'^2/M & &\text{holes} \\ &= \left\{ \begin{array}{ll} = k'^2/M & ;\ k' < p_F \\ = p_F^2/M & ;\ k' \geq p_F \end{array} \right\} & &\text{particles .} \end{aligned} \tag{7.9}$$

The above approximation leads to considerable computational simplicity. Furthermore, the neglect of the P-dependence of the energy denominators of BM is exact. The calculation consists of the following:

(1) The Green's functions (4.5) are independent of the nucleon-nucleon potential because the energy denominator consists of kinetic energies alone. Therefore, the Green's functions can be computed very accurately just once and tabulated. Because they need to be computed only once, they can be treated in a straightforward manner, by numerical integration to an extremely large momentum so that

the correction to the integral is either negligible or very trivial. Once tabulated and reported, they need never be computed again.

(2) The density (7.5) can also be calculated once and similarly tabulated. For this purpose a separable potential with hard core or hard shell could be used.

(3) Then with the Green's functions and densities as "known" quantities, the full system of equations to be solved for any given local potential with hard core consists of

(a) Eq. (4.8) for the modified basis functions, $s_\ell(kr)$;

(b) Eq. (4.9) for the modified Green's function, $F_\ell^k(r,r')$;

(c) Eq. (4.10) for the radial wave functions, $U_{\ell\ell'}^{Js}(k,r)$;

(d) Eq. (4.11) for $t_{k;k}$;

(e) Eq. (4.12) modified as follows for V_k:

$$V(p) = \frac{2}{\pi^2}\Bigg[\int_0^{\frac{1}{2}(p_F-p)} k^2dk \int_{-1}^{1} t_{k;k}\,\rho\left(\sqrt{4k^2+p^2-4pk\mu}\right)d\mu \; + \tag{7.10}$$
$$+ \int_{\frac{1}{2}(p_F-p)}^{\frac{1}{2}(p_F+p)} k^2dk \int_{-\left(\frac{p_F{}^2-p^2-4k^2}{4kp}\right)}^{1} t_{k;k}\,\rho\left(\sqrt{4k^2+p^2-4pk\mu}\right)d\mu\Bigg] \quad p \le p_F .$$

For $p > p_F$ the first integral vanishes.

(f) Eq. (4.13) modified as follows for E_{Av}

$$E_{Av} = \frac{3}{5}\frac{p_F^2}{2M} + \frac{3}{2p_F^2}\int_0^\infty p^2 dp V(p)\rho(p) . \qquad (7.11)$$

The equations of (3) above are all independent, and most are trivial. Only the equation for the radial wave functions, (4.10), presents any difficulty at all. However, it can be solved by iteration, and if iterated as indicated in BM, three iterations should suffice for accuracy commensurate with the overall approximation (within 0.2 MeV). The numerical integral in (7.11) cuts off quite rapidly.

Equations (a) through (f) above can be solved on a desk calculator even for a fairly complicated nucleon-nucleon potential.

This approximation has been evaluated in two different cases. The first evaluation, used to test its feasibility, was to use the approximation indicated by (4.22) with V' computed with $\Delta = 0$; i.e., using (7.7) above. To calculate $V - V'$ $(\Delta = 0)$ we actually used $V(\Delta) - V'(\Delta)$. This is a good approximation because the curves of V and $V(\Delta)$ are nearly parallel (see Fig. 4 of BM). The other calculation, involving $V(\Delta = 0)$, would have required modification of the code to perform a principle value integral in (4.5). This could have been achieved computationally with the replacement

$$\frac{1}{\omega_k - \omega_{k''}} \rightarrow \frac{\omega_k - \omega_{k''}}{(\omega_k - \omega_{k''})^2 + \delta^2} \qquad (7.12)$$

where δ^2 is chosen small enough ($\sim$ 5 to 10 MeV) that the two sides of (7.12) are essentially equal except very near $\omega_k = \omega_{k''} = \omega_{p_F}$.

The calculation yielded the curve of E_{Av} vs. r_o shown in Fig. 9. The values obtained differ considerably from those indicated in Table IV, an indication of the importance of taking $\Delta = 0$ for this approximation. The minimum of the above curve is $E_{Av} = -14.0$ MeV at $r_o = 1.04$ F, in good agreement with the BG and BM results (-15.2 MeV at 1.02 F and -16.9 MeV at 1.00 F, respectively). This result indicates that the approximation can be expected to be semi-quantitative.

An attempt was also made to calculate ρ_k with a separable potential. The Yamaguchi potential without hard core[75] was used. The calculation of the density is described in detail in Appendix E. The resulting density is indicated in Fig. 10. Brueckner[83] has obtained a similar density from an approximate calculation with a non-local interaction. When used in (7.10) and (7.11) with the same t-matrices as used in the previous calculation, the density of Fig. 10 gives 32.1 MeV at $p_F = 1.52$ F^{-1} (no attempt being made to find the minimum). The reason for this result is obvious. Without the core, the Born approximation converges rapidly, and therefore the high order terms are small. Alternately, a hard core would deplete to a much greater extent the states below the Fermi sea (the average density being about 0.87[33] vs. 0.98 without the core). Therefore, it is exceedingly important to use a separable potential which includes the hard shell or hard core interaction. It may also be important that the potential include a reasonable tensor-central force ratio. However, since ρ_k represents an average over the

Fig. 9. E_{Av} vs. r_o for the "simple approximation" using the BGT potential.

Fig. 10. Momentum density using the Yamaguchi potential. The potential does not have a hard core.

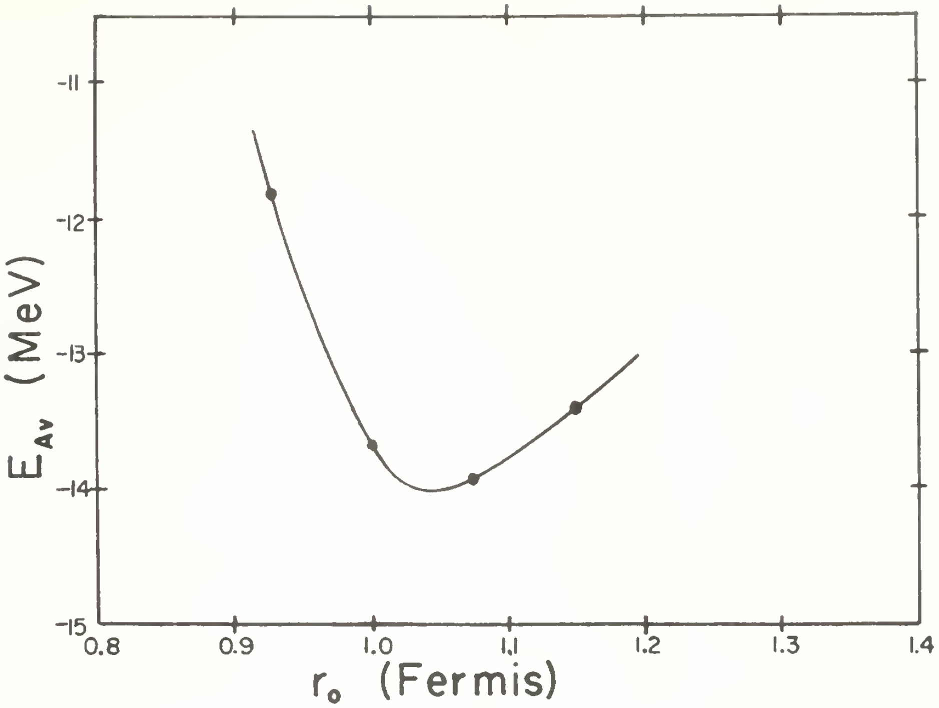
-11
-12
-13
-14
-15
E_{Av} (MeV)
0.8
0.9
1.0
1.1
1.2
1.3
1.4
r_o (Fermis)

9

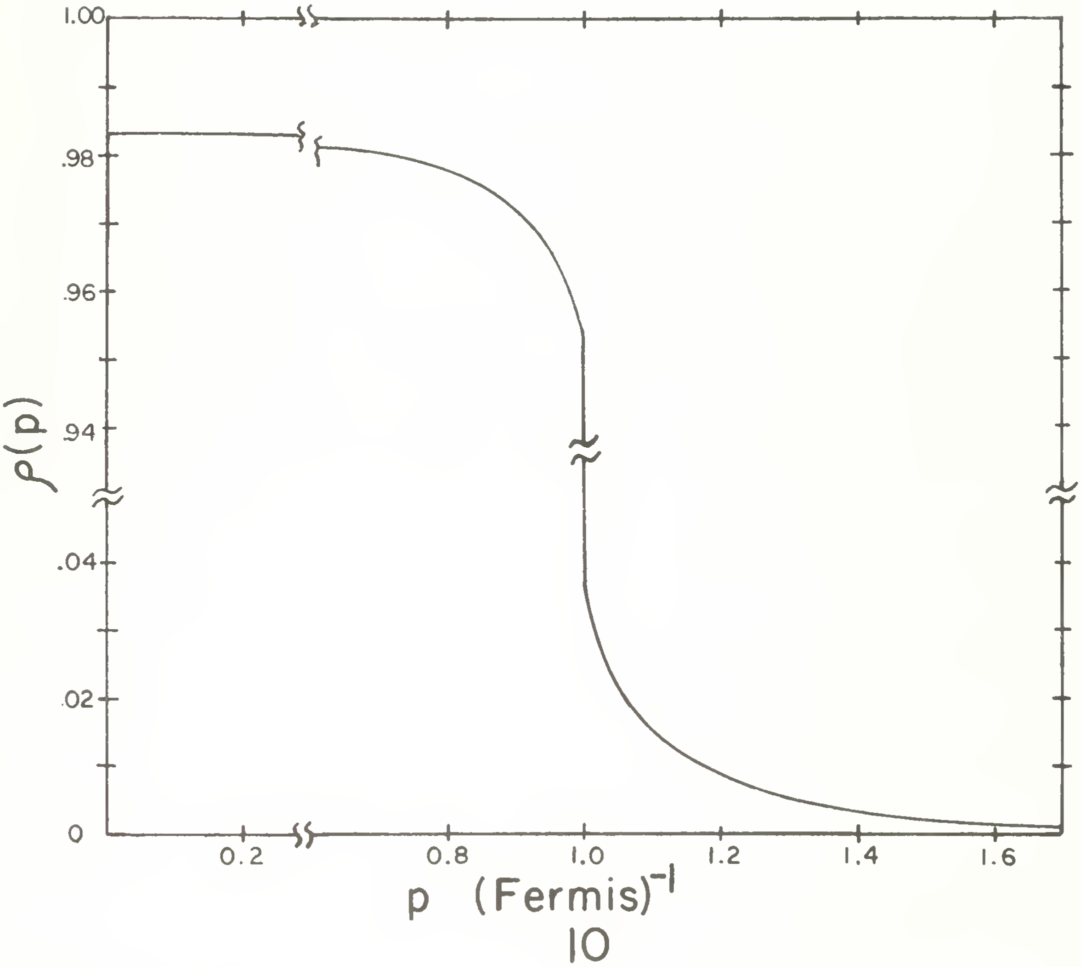
1.00
.98
.96
.94
.04
.02
0
$\rho(p)$
0.2
0.8
1.0
1.2
1.4
1.6
p (Fermis)$^{-1}$

10

t-matrix elements and since the third-order term in (7.6) will include one power of t computed with the full potential, it is probable that just including the core effects will be sufficient for the type of investigations for which this approximation will be useful. A program in now underway to use an S-state potential with hard shell (the same as that used by Puff[14] and by Falk and Wilets[33] since it is known to give reasonable saturation properties).

Once the density and Green's functions have been calculated and reported, this approximation should be quite useful for a large variety of investigations. As emphasized earlier, it can even be completed on a desk calculator, though a computer (even of very limited capabilities) would be desirable. Among the possible uses one can envision are the evaluation of the effects of various phenomenological potentials, further investigation into the influence of various terms in the potentials and in the expansion, and any other investigations into the nuclear matter problem where relative comparisons would be informative. The approximation might even be simple enough to use as a problem in graduate courses. It would be simple to teach and its solution should prove quite instructive.

APPENDIX A

THE BRUECKNER-GOLDSTONE LINKED CLUSTER EXPANSION

This appendix discusses several derivations of the Brueckner-Goldstone linked-cluster expansion[1,2] (BG expansion) for the energy of the "normal" many-particle Fermion system interacting via two-body isotropic forces under conditions such that the unperturbed ground state is characterized by a spherical Fermi surface. Two of these derivations are reviewed in detail. The first derivation, by Rayleigh-Schroedinger perturbation theory, is conceptually simpler but cannot be easily extended to all orders. The second derivation, due to Goldstone,[2] is rigorously correct to all orders of perturbation theory for the type of system being considered. Extension of the BG expansion to systems for which the unperturbed ground state is not spherical and some topics related to the general validity of the expansion are discussed.

The Schroedinger equation for the system is

$$(H_o + H_I)\Psi = E\Psi = (E_o + \Delta E)\Psi \ . \tag{A.1}$$

The unperturbed Hamiltonian

$$H_o = \sum_k \epsilon_k a_k^* a_k = \sum_k \epsilon_k \hat{n}_k \tag{A.2}$$

satisfies

$$H_o \Phi_o = E_o \Phi_o \ . \tag{A.3}$$

Φ_o is the unperturbed many-particle wave function; it describes a filled Fermi sea -- a state with no "particles" (a "particle" being a quasi-particle with momenta greater than the Fermi momentum, p_F) and no "holes" (a "hole" denoting the absence of a quasi-particle with momentum less than p_F). The term "quasi-particle" is used to denote the fact that the independent "particle" of the model need not be a real nucleon, but it may be a nucleon surrounded by some distortion of the neighboring nuclear matter. The interaction Hamiltonian

$$H_I = \frac{1}{2} \sum_{k\ell;mn} v_{k\ell;mn}\, a_\ell^* a_k^* a_m a_n \tag{A.4}$$

satisfies

$$H_I \Psi = \Delta E \Psi \tag{A.5}$$

where Ψ is the true wave function of the interacting system. Units are chosen such that $\hbar$ is equal to unity. For the present, H_o, the unperturbed Hamiltonian, is simply the sum of the single-particle kinetic energies, so that

$$\epsilon_k = k^2/2M \ .$$

The quasi-particle creation operator a_k^* is, in the "particle-hole" framework, the creation operator for a "particle" $(|\underset{\sim}{k}| > p_F)$ or annihilation operator for a "hole" $(|\underset{\sim}{k}| \leq p_F)$. The corresponding annihilation/creation operator is a_k . The expectation value in the unperturbed ground state of the number operator, $\hat{n}_k = a_k^* a_k$, is

just

$$(\Phi_o, \hat{n}_k \Phi_o) = n_k = 1 \qquad |\underset{\sim}{k}| \leq p_F$$
$$= 0 \qquad |\underset{\sim}{k}| > p_F \ . \tag{A.6}$$

The two-body interaction, $v_{k\ell;mn}$, is the momentum space transform of the actual spatial two-body potential (whose existence we postulate). Throughout this section momentum indices are vector quantities.

Before discussing the "successful" many-body perturbation theories, it is instructive to review the reason for the failure of the well-known Brillouin-Wigner perturbation theory. The prescription for obtaining a perturbation expansion in this theory is to expand the wave function, Ψ, in terms of the unperturbed wave function, Φ_o. Substitution into the Hamiltonian (A.1) then leads to the following expansion for the interaction energy (indicated in operator notation):

$$\Delta E = (\Phi_o, (H_I + H_I \frac{Q}{E_o + \Delta E - H_o} H_I + \ldots) \Phi_o) \ . \tag{A.7}$$

Q is an operator which projects out the unperturbed ground state (i.e., equals zero when operating on Φ_o). An analysis of the N-dependence of the terms in this series[6,57] shows that the first order term is proportional to the total number of particles, N, and that all higher order terms are of order unity compared to N. This looks, at first sight, like an ideal expansion for an infinite (or very large) system. Unfortunately, however, the higher order terms

are all about the same size, and their sum is of order N. Terms of every order must therefore be considered in computing ΔE . For this reason, Brillouin-Wigner theory is not suitable for many-particle systems.

A. Rayleigh-Schroedinger Perturbation Theory

An early successful method of obtaining a perturbation expansion valid for many-body systems was Rayleigh-Schroedinger perturbation theory. It has the advantage of conceptual simplicity, and the disadvantages that one can work with it effectively only in the first few (up to about six) orders, and that extrapolation to all orders of any results obtained therefrom cannot always be rigorously proven.

We write the Schroedinger equation as

$$(H_o + \lambda H_I)\Psi_o = E\Psi_o \qquad (A.8)$$

and where λ is an expansion parameter (which is assumed to be small but which is set to unity in the final results). The true (interaction) wave function, Ψ , is written in terms of the non-interaction wave function, Φ_o , as

$$\bar{\Phi}_o = S\Phi_o \ . \qquad (A.9)$$

Then both S and E are expanded in power series in the expansion parameter

$$S = 1 + \lambda S_1 + \lambda^2 S_2 + \ldots \qquad (A.10)$$

$$E = \epsilon_o + \lambda \epsilon_1 + \lambda^2 \epsilon_2 + \ldots . \qquad (A.11)$$

We then substitute (A.9), (A.10) and (A.11) into the Schroedinger equation (A.8) and equate equal powers of λ. One can show, after some algebra, that

$$\epsilon_n = (\Phi_o, H_I S_{n-1} \Phi_o) \qquad n \geq 1 , \qquad (A.12)$$

and

$$S_n = \frac{1}{e} H_I S_{n-1} - \frac{1}{e} \sum_{m=1}^{n-1} \epsilon_m S_{n-m} \qquad (A.13)$$

where $S_o = 1$ and the propagator is defined as

$$\frac{1}{e} = \frac{Q}{E_o - H_o} \qquad (A.14)$$

with Q being a projection operator which projects out the unperturbed state Φ_o ,

$$Q = 1 - |\Phi_o)(\Phi_o| \quad . \qquad (A.15)$$

Brueckner[1] gives this expansion explicitly through fourth order.

At this point it is instructive to examine the N-dependence of various terms in the energy expansion. Brueckner[57] analyzes this dependence quite thoroughly, and we shall merely indicate the method and the results. The first term, $\epsilon_o = (\Phi_o, H_o \Phi_o) = E_o$, is clearly proportional to N: the total kinetic energy is the total number of particles times the average kinetic energy per particle. The first order energy, $\epsilon_1 = (\Phi_o, H_I \Phi_o)$, is proportional to $N\rho$

(where the density, ρ , is kept constant as the volume, Ω , and N become infinite). To see this, we will write out the matrix element explicitly:

$$\epsilon_1 = \frac{1}{2}\sum_{ij} v_{ij;(ij)} = \frac{1}{2}\sum_{ij}(v_{ij;ij}-v_{ij;ji}) =$$

$$= \frac{1}{2}\sum_{ij}\int d\underset{\sim}{r}_1\, d\underset{\sim}{r}_2\, \varphi_i^*(r_1)\varphi_j^*(r_2)v(r_{12})\varphi_i(r_1)\varphi_j(r_2)n_in_j \ . \qquad (A.16)$$

In the last equality we neglected the exchange term, which merely contributes a constant factor. Transforming to center-of-mass and relative coordinates, and using the explicit representation of the non-interacting wave function

$$\varphi_{\underset{\sim}{k}}(r) = \frac{1}{\Omega^{1/2}}\, e^{i\underset{\sim}{k}\cdot\underset{\sim}{r}}$$

we obtain

$$\epsilon_1 = \frac{1}{2\Omega}\sum_{ij}\int d\underset{\sim}{r}\ v(\underset{\sim}{r})\ n_in_j \ . \qquad (A.17)$$

In a large system, the integral over $\underset{\sim}{r}$ is independent of Ω if v(r) has a finite range. The sum over i and j gives a number of order N^2, so that the total dependence is $N^2/\Omega = N\rho$. For

$$\epsilon_2 = (\Phi_o, H_I \frac{1}{e} H_I\Phi_o) = \frac{1}{4}\sum_{ijmn} v_{ij;(mn)} \frac{(1-n_m)(1-n_n)n_in_j}{\epsilon_i+\epsilon_j-\epsilon_m-\epsilon_n} v_{mn;(ij)} \qquad (A.18)$$

there is a factor N^2 from the i,j sum, a factor Ω from the single independent sum over intermediate momentum states from the well-known relation

$$\Sigma_k \rightarrow \frac{\Omega}{(2\pi)^3} \int d\underset{\sim}{k} , \qquad (A.19)$$

and a factor $1/\Omega^2$ from the normalization of the single-particle wave functions appearing in the two matrix elements. The propagator, being a difference of free kinetic energies, is a local property of order unity compared to N. Thus ϵ_2 is also proportional to N. Similarly, it can be shown that the energy contribution in every order will have a term proportional to N, such a term including all possible "linked clusters" and associated renormalization terms. A "linked cluster" is a multiple interaction in which the separate two-body interactions are so linked through their momentum indices that the interaction cannot be described in terms of two or more mutually independent parts of the original interaction. An example of an "unlinked" term occurs in third order, below.

In third order, with

$$\epsilon_3 = (\Phi_o, H_I \frac{1}{e} [H_I - (\Phi_o, H_I \Phi_o)] \frac{1}{e} H_I \Phi_o$$

$$= (\Phi_o, H_I \frac{1}{e} H_I \frac{1}{e} H_I \Phi_o) - \epsilon_1 (\Phi_o H_I \frac{1}{e^2} H_I \Phi_o) \qquad (A.20)$$

one finds an "unlinked" term in $(\Phi_o, H_I \frac{1}{e} H_I \frac{1}{e} H_I \Phi_o)$,

$$\frac{1}{\delta} \sum_{\substack{ij \neq k\ell \\ mn}} v_{k\ell;(mn)} \frac{(1-n_m)(1-n_n)}{(\epsilon_k+\epsilon_\ell-\epsilon_m-\epsilon_n)} v_{ij;(ij)} \frac{(1-n_m)(1-n_n)}{(\epsilon_k+\epsilon_\ell-\epsilon_m-\epsilon_n)} v_{mn;(k\ell)} n_k n_\ell \qquad (A.21)$$

which can be shown to be of order $(N\rho)^2$ as follows. Since $v_{ij;ij}$

is independent of the $k\ell,mn$ sum, we may write (A.21) as

$$\frac{1}{4}\sum_{k\ell mn} v_{k\ell;mn}\,\frac{(1-n_m)(1-n_n)n_k n_\ell}{(\epsilon_k+\epsilon_\ell-\epsilon_m-\epsilon_n)^2}\,v_{mn;(k\ell)} \times \frac{1}{2}\sum v_{ij;(ij)}n_i n_j \qquad (A.22)$$

by using the fact that $(1-n_m)^2 = (1-n_m)$ and by separating the sums. Each term in (A.22) is separately proportional to $N\rho$; therefore, the full unlinked term is proportional to $(N\rho)^2$. However, the renormalization term (the second term on the right hand side of (A.20)) can be written

$$-\left(\frac{1}{2}\sum_{k\ell} v_{k\ell;(k\ell)}n_k n_\ell\right)\left(\frac{1}{4}\sum_{ijmn} v_{ij;(mn)}\,\frac{(1-n_m)(1-n_n)n_i n_j}{(\epsilon_i+\epsilon_j-\epsilon_m-\epsilon_n)^2}\,v_{mn;(ij)}\right)$$

$$-\frac{1}{4}\sum_{k\ell mn} v_{ij;(mn)}\,\frac{(1-n_m)(1-n_n)n_k n_\ell}{(\epsilon_k+\epsilon_\ell-\epsilon_m-\epsilon_n)^2}\,v_{mn;(ij)}\left[\sum_j\left(v_{jk;(jk)} + v_{j\ell;(j\ell)}\right)n_j\right] \qquad (A.23)$$

$$-\frac{1}{4}\sum_{k\ell mn} v_{ij;(mn)}\,\frac{(1-n_m)(1-n_n)n_k n_\ell}{(\epsilon_k+\epsilon_\ell-\epsilon_m-\epsilon_n)^2}\,v_{mn;(k\ell)}\;v_{k\ell;(k\ell)}n_k n_\ell$$

The first term on the right is identical to (A.22) except for sign, and thus cancels it. The second term, of order $N\rho^2$, may be combined with the "linked" portion of $(\Phi_o, H_I\,\frac{1}{e}\,H_I\,\frac{1}{e}\,H_I\Phi_o)$. The last term is of order ρ^2 and vanishes compared to N as N becomes infinite. The term in square brackets has no factor $\frac{1}{2}$ because we have included in it the (equal) term with the index j interchanged with k or ℓ as appropriate.

Similarly, in every order one obtains unlinked parts, all of which are cancelled exactly by the appropriate terms from the renormalization corrections of the same order. Brueckner[1,57] shows this explicitly through fourth order and reports carrying the proof out through sixth order.

The conclusion that only "linked clusters" contribute to the energy of the quantum many-particle system is not surprising -- the corresponding theorem in statistical mechanics is well-known. It is of fundamental importance to quantum many-body perturbation theory because it ensures that the energy series has a normal behavior: for large N the energy per particle is independent of the size of the system.

Unfortunately, the Rayleigh-Schroedinger theory still fails to supply a criterion for setting up a meaningful first order trial function of the form

$$\tilde{\Psi}_o^{(1)} = \Phi_o + \frac{Q}{E_o - H_o} H_I \Phi_o . \qquad \text{(A.24)}$$

The Ritz variational principle

$$E \leq \frac{(\tilde{\Psi}_o^{(1)}, H \tilde{\Psi}_o^{(1)})}{(\tilde{\Psi}_o^{(1)}, \tilde{\Psi}_o^{(1)})} \qquad \text{(A.25)}$$

then yields

$$E \leq \epsilon_o + \epsilon_1 + \frac{(\epsilon_2 + \epsilon_3)}{1 + \Delta^{(2)}} \qquad \text{(A.26)}$$

where

$$\Delta^{(2)} = (\Phi_o, H_I \frac{Q}{(E_o - H_o)^2} H_I \Phi_o) \ . \tag{A.27}$$

Since $\Delta^{(2)}$ is proportional to $N\rho$ for large N, the last term vanishes in the limit $N \to \infty$, and we have

$$E \leq \epsilon_o + \epsilon_1$$

which is the result we would have obtained using Φ_o alone as a trial function. Since this trial function produces no improvement in the energy of the many-body system, we conclude that it has no physical meaning for our problem. Brueckner[57] analyzes the apparent inconsistency in the fact that we can have a rapidly convergent energy expansion while having at the same time an exceedingly poorly converging wave function expansion. The heart of the argument is the fact that the energy is determined by the local properties of the wave function (which the perturbation series can predict quite accurately) whereas the wave function for the entire system requires a description of the full system which is equally precise at every locality in the system. The energy of the system is independent of the normalization because the normalization factor is cancelled in numerator and denominator whereas the total wave function is, of course, normalization dependent.

B. Goldstone Proof of the Linked-Cluster Expansion

Goldstone[2] was the first one to prove the linked-cluster

expansion to all orders of perturbation theory. His proof leans heavily on four quantum-mechanical "tools" which are briefly discussed first: the development operator, the adiabatic theorem, Wick's theorem, and graphical representation of perturbation terms. Although these topics can be found in textbooks on quantum field theory (e.g., Schweber[84]), they are reviewed here in order to make the discussion complete and to fill in a few of the intermediate steps that are frequently omitted.

1. The Development Operator

The development operator

$$U(t_2,t_1) = \exp(-iH(t_2-t_1)) \tag{A.28}$$

has a simple physical interpretation as the time-translation operator for the wave function, $\varphi(t)$, of the system described by the Hamiltonian H:

$$\varphi(t_2) = U(t_2,t_1)\varphi(t_1) \quad . \tag{A.29}$$

(A.29) can be verified by operating with $\partial/\partial t_2$ to recover the time-dependent Schroedinger equation. We now go into the interaction representation, with $H = H_o + H_I$, by defining a new wave function Ψ by

$$\varphi = \exp(-iH_o t)\Psi \quad . \tag{A.30}$$

We find that Ψ satisfies

$$i\Psi = H_I(t)\Psi \qquad (A.31)$$

where

$$H_I(t) = \exp(iH_o t)\ H_I\ \exp(-iH_o t)\ . \qquad (A.32)$$

In the interaction representation, the development operator

$$U(t_2,t_1) = e^{iH_o t_2}\ e^{-iH(t_2-t_1)}\ e^{-iH_o t_1} \qquad (A.33)$$

satisfies the differential equation

$$\partial U(t_2,t_1)/\partial t_2 = -iH(t_2)U(t_2,t_1) \qquad (A.34)$$

with the boundary condition $U(t,t) = 1$. Equivalently, it satisfies the integral equation

$$U(t_2,t_1) = 1 - i \int_{t_1}^{t_2} H_I(t)U(t,t_1)dt\ . \qquad (A.35)$$

Iterating this equation leads to the expression given by Dyson[85] :

$$U(t,t_o) = \sum_{n=o}^{\infty} (-i)^n \int_{t_o}^{t} dt_1 \int_{t_o}^{t_1} dt_2 \cdots \int_{t_o}^{t_{n-1}} dt_n H_I(t_1)H_I(t_2) \cdots H_I(t_n)$$

$$= \sum_{n=o}^{\infty} \frac{(-i)^n}{n!} \int_{t_o}^{t} dt_1 \int_{t_o}^{t} dt_2 \cdots \int_{t_o}^{t} dt_n\ T\left[H_I(t_1)H_I(t_2) \cdots H_I(t_n)\right] . \qquad (A.36)$$

T is the chronological (time-ordering) operator: it orders the terms in the brackets in order of increasing time from right to left. The factor 1/n! in the last line corrects for the over-counting of equivalent terms introduced by using the T operator and extending all integrations over the full time range.

2. Adiabatic Theorem

The form of the adiabatic theorem we are interested in was proved for scattering theory by Gell-Mann and Low.[86]

If the interaction Hamiltonian depends linearly on a coupling constant, g, so that $H = H_o + gH_I$, then the adiabatic theorem asserts that the true eigenfunction of the interacting system, Ψ, can be obtained from the unperturbed wave function, Φ, by starting at $t = \pm\infty$ with the interaction "off" and turning it on gradually until at time zero it is up to full strength, and further asserts that the prescription for describing this process is as follows. We use the "adiabatic" U matrix which satisfies the differential equation

$$\partial/\partial t\, U_\alpha(t,t_o) = -ig \exp(-\alpha|t|)H_I(t)\, U_\alpha(t,t_o) , \qquad \alpha > 0 . \qquad (A.37)$$

$U_\alpha(0,-\infty)$ thus describes the process of gradually turning the interaction on from zero to full strength between $t = -\infty$ and $t = 0$. $U_\alpha(0,+\infty)$ has a similar interpretation. We shall prove that

$$\Psi = \lim_{\alpha \to 0} \frac{U_\alpha(0,\pm\infty)\, \Phi}{(\Phi, U_\alpha(0,\pm\infty)\Phi)} . \qquad (A.38)$$

The expression for the energy is then

$$E = \frac{(\Phi, H\Psi)}{(\Phi, \Psi)} = \frac{(\Phi, (H_0 + gH_I)\Psi)}{1} = E_0 + \Delta E \,, \tag{A.39}$$

with

$$\Delta E = \lim_{\alpha \to 0} \frac{(\Phi, gH_I U_\alpha(0, \pm\infty)\Phi)}{(\Phi, U_\alpha(0, \pm\infty)\Phi)} \,. \tag{A.40}$$

The fact that $(\Phi, \Psi) = 1$ is a consequence of the normalization of Ψ in (A.38). The assumptions needed to obtain the above results are: 1) the state in question is non-degenerate; 2) the states are discrete (which is true for the finite system and which we assume to be true for the limit $\Omega \to \infty$; and, finally, 3) the desired state Ψ of the interacting system is continuously derivable from the chosen unperturbed state Φ -- i.e.,

$$\lim_{g \to 0} \Psi = \Phi \,, \tag{A.41}$$

and

$$\lim_{g \to 0} E = E_0 \,. \tag{A.42}$$

In terms of the coupling constant, g, we will also prove that

$$(\Psi, gH_I\Psi) = \Delta E' = \lim_{\alpha \to 0} \frac{1}{2}\, i\alpha g \, \frac{\frac{\partial}{\partial g}(\Phi, U_\alpha(\infty, -\infty)\Phi)}{(\Phi, U_\alpha(\infty, -\infty)\Phi)} \,. \tag{A.43}$$

For the two-body problem, $U_\alpha(\infty, -\infty)$ is the conventional scattering matrix.

To begin our proof, let us define a state $\Psi(\alpha)$ by

$$\Psi(\alpha) = U_\alpha(0,-\infty)\Phi \ . \tag{A.44}$$

We will prove that $\lim_{\alpha \to 0} \Psi(\alpha)$ is (except for normalization) the true state of the interacting system, Ψ. Now, by virtue of our definitions of E_o (eigenvalue of H_o) and of $U_\alpha\Phi$, we have

$$[H_o, U_\alpha(0,-\infty)]\Phi = H_o\Psi(\alpha) - E_o\Psi(\alpha) \ . \tag{A.45}$$

But,

$$[H_o, U_\alpha(0,-\infty)] = [H_o, \sum_n \int_{-\infty}^{o} dt_1 \ldots \int_{-\infty}^{o} dt_n \frac{(-i)^n}{n!} g^n e^{\alpha(t_1+t_2+\ldots t_n)}$$

$$T[H_I(t_1)\ldots H_I(t_n)]] \tag{A.46}$$

$$= -i \sum_{n=o}^{\infty} \frac{(-i)^n}{n!} \int_{-\infty}^{o} dt_1 \ldots \int_{-\infty}^{o} dt_n \, g^n e^{\alpha(t_1+t_2+\ldots t_n)}$$

$$\sum_{\ell=1}^{n} \frac{\partial}{\partial t_\ell} T[H_I(t_1)\ldots H_I(t_n)] \ .$$

The last line is a consequence of the fact that in the interaction representation H_o is the time translation operator; i.e., for any operator $F(t)$,

$$i[H_o, F(t)] = \partial F(t)/\partial t \ . \tag{A.47}$$

The integrand in (A.46) is symmetric, so that $\sum_{\ell=1}^{n} \partial/\partial t_\ell = n \, \partial/\partial t_1$, and (A.46) is equal to the following when operating on Φ

$$(H_0-E_0)\Psi(\alpha)=\Big\{-\sum_{n=1}^{\infty}\frac{(-i)^{n-1}}{(n-1)!}\,g^n\int_{-\infty}^{0}dt_1\cdots\int_{-\infty}^{0}dt_n\,e^{\alpha(t_1+t_2+\ldots+t_n)}$$

$$\frac{\partial}{\partial t_1}\,T\,[H_I(t_1)\ldots H_I(t_n)]\Big\}\,\Phi$$

$$=\Big\{-\sum_{n=1}^{\infty}\frac{(-i)^{n-1}}{(n-1)!}\,g^n\int_{-\infty}^{0}dt_1\cdots\int_{-\infty}^{0}dt_n \qquad (A.48)$$

$$\frac{\partial}{\partial t_1}\Big(e^{\alpha(t_1+t_2+\ldots+t_n)}\,T\,[H_I(t_1)\ldots H_I(t_n)]\Big)$$

$$-\,\alpha e^{\alpha(t_1+t_2+\ldots+t_n)}\,T[H_I(t_1)\ldots H_I(t_n)]\Big\}\,\Phi\,.$$

The second equality reduces to the first if the partial derivative with respect to t_1 is performed. Now

$$\int_{-\infty}^{0}dt_1\,\frac{\partial}{\partial t_1}\,[e^{\alpha t_1}\,H_I(t_1)] = e^{\alpha t_1}\,H_I(t_1)\Big|_{t_1=-\infty}^{t_1=0} = H_I(0)\,. \qquad (A.49)$$

Therefore, by changing indices of summation in the first sum of (A.48) so that this sum again runs from zero to infinity, by assuming that the dependence of $H(0)$ on g is linear, $(H(0) = H_0+gH_I(0))$, and by using (A.47) and

$$g^n = \frac{1}{n}\,g\,\frac{\partial}{\partial g}\,g^n\,, \qquad (A.50)$$

we find

$$(H_o-E_o)\Psi(\alpha) = (-gH_I(0)+i\alpha g\,\frac{\partial}{\partial g})\left\{\sum_{p=o}^{\infty}\frac{(-i)^p}{p!}\,g^p\int_{-\infty}^{0}dt_1\ldots\int_{-\infty}^{0}dt_p\right.$$

$$\left. e^{\alpha(t_1+t_2+\ldots+t_p)}\,T\,[H_I(t_1)\ldots H_I(t_p)]\right\}\Phi$$

$$= -gH_I(0)U_\alpha(0,-\infty)\Phi + i\alpha g\,\frac{\partial}{\partial g}\,U_\alpha(0,-\infty)\Phi\ . \qquad (A.51)$$

The last equality follows directly from (A.36). We have therefore shown that

$$(H_o + gH_I(0) - E_o)\Psi(\alpha) = (H-E_o)\Psi(\alpha) = i\alpha g\,\frac{\partial}{\partial g}\,\Psi(\alpha)\ . \qquad (A.52)$$

Similarly, one can show that

$$(H_o-E_o)U_\alpha(0,+\infty)\Phi = -\,i\alpha g\,\frac{\partial}{\partial g}\,U_\alpha(0,+\infty)\Phi. \qquad (A.53)$$

Taking the scalar product of (A.52) with Ψ and using the fact that $(\Psi|H = E(\Psi|$, we obtain

$$\Delta E = E-E_o = \frac{i\alpha g(\Psi,\frac{\partial}{\partial g}\,U_\alpha(0,-\infty)\Phi)}{(\Psi,U_\alpha(0,-\infty)\Phi)}\ . \qquad (A.54)$$

On the other hand, using (A.52), we note that

$$\frac{(H_o-E_o-i\alpha g\,\frac{\partial}{\partial g})\Psi(\alpha)}{(\Phi,\Psi(\alpha))} = i\alpha g\left[\frac{\partial}{\partial g}\,\ell n(\Phi,\Psi(\alpha))\right]\frac{\Psi(\alpha)}{(\Phi,\Psi(\alpha))}\ , \qquad (A.55)$$

so that if we call

$$\Psi'(\alpha) = \frac{U_\alpha(0,-\infty)\Phi}{(\Phi,U_\alpha(0,-\infty)\Phi)} = \frac{\Psi(\alpha)}{(\Phi,\Psi(\alpha))} \quad , \tag{A.56}$$

then

$$(\Phi,(H-E_o)\Psi'(\alpha)) = i\alpha g \frac{\partial}{\partial g}\left[\log(\Phi,U_\alpha(0,-\infty)\Phi)\right] . \tag{A.57}$$

Thus, if the $\lim_{\alpha\to 0} \Psi'(\alpha)$ exists and is well-defined, we have from (A.55) and (A.53):

$$(H-E_o)\Psi'(0) = \lim_{\alpha\to 0}\left[i\alpha g \frac{\partial}{\partial g}\log(\Phi,U_\alpha(0,-\infty)\Phi)\right]\Psi'(0)$$

$$= (\Phi,(H-E_o)\Psi'(0))\Psi'(0) \quad , \tag{A.58}$$

and $\Psi'(0)$ is an eigenfunction of H which goes over into Φ as $g \to 0$. Therefore, $\Psi'(0) = \Psi$. A similar calculation for $U(0,+\infty)\Phi$ leads to (A.38). It must be stressed that $U(0,-\infty)\Phi$ and $U(0,+\infty)\Phi$ converge to the same state only for the discrete spectrum. For the continuous spectrum, $U(0,\pm\infty)\Phi$ converge to the in- and out-solutions, $\Psi^{\pm}$, respectively, which are different eigenstates of the total Hamiltonian.

Combining (A.38) for Ψ and (A.54) for the level shift, we have

$$(\Psi,gH_I\Psi)=\Delta E'= \lim_{\alpha\to 0} i\alpha g \frac{(\Phi,U_\alpha^{-1}(0,+\infty)\frac{\partial}{\partial g}U_\alpha(0,-\infty)\Phi)}{(\Phi,U_\alpha(\infty,-\infty)\Phi)} .$$

$$= \lim_{\alpha\to 0} i\alpha g \frac{(\Phi,\frac{\partial}{\partial g}U_\alpha(\infty,0)\,U_\alpha(0,-\infty)\Phi)}{(\Phi,U(\infty,-\infty)\Phi)}$$

$$= \lim_{\alpha \to 0} \frac{1}{2} i\alpha g \frac{\frac{\partial}{\partial g}(\bar{\varphi}, U_{\alpha}(\infty,-\infty)\bar{\varphi})}{(\bar{\varphi}, U(\infty,-\infty)\bar{\varphi})} \quad . \tag{A.59}$$

The perturbation formulae for Ψ and ΔE are now obtained by carrying out the time integrations in the expressions for the limits in equations (A.38) and (A.40) (we will use the latter expression for ΔE rather than (A.59) at this time). In order to do this explicitly, we obtain $gH_I(t)$ from

$$gH_I = \frac{1}{2} \Sigma\, v_{ij;k\ell}\, a_{\ell}{}^{*} a_{k}{}^{*} a_{i}\, a_{j} \tag{A.60}$$

by substituting

$$a_k(t) = a_k \exp(-i\epsilon_k t)$$

for a_k and then multiplying by $\exp(-\alpha|t|)$. The ϵ_k are the eigenvalues of the unperturbed Hamiltonian. Wick's theorem, which is discussed next, is then used in order to simplify the resulting expressions.

3. Wick's Theorem

As can be seen from (A.36), the equation for $U(0,-\infty)$ will involve an extremely large number of terms with even less apparent order than the Rayleigh-Schroedinger perturbation theory result. However, with the help of a theorem due to Wick,[87] the expressions for the true eigenfunction and the interaction energy can be considerably simplified.

In order to discuss this theorem, we must temporarily break our operators a_k and a_k^* down into hole operators, h_k^* and h_k, and particle operators, p_k and p_k^*. The creation operators are h_k^* and p_k^*. The unperturbed ground state wave function, Φ_o, is then defined as the "vacuum" state with no holes and no particles, so that

$$h_k\,\Phi_o = 0 \qquad \text{and} \qquad p_k\,\Phi_o = 0\ . \tag{A.61}$$

We will also need two further definitions. The first is the normal product, $N[AB\ldots]$, which is defined as a rearrangement of the operators $AB\ldots$ (with an appropriate sign change if an odd number of permutations are required) such that the creation operators are to the left of the annihilation operators. For example, $N[h_k h_k^* p_m^* p_m] = -\,h_\ell^* p_m^* p_n\, h_k = +\,h_\ell^* p_m^* h_k\, p_n$. The order of creation operators or of annihilation operators among themselves is not important since they anticommute. From the definition of the normal product and from (A.61),

$$N\,[AB\ldots]\,\Phi_o = 0 \tag{A.62}$$

for any operators $A, B, \ldots$ which are composed of creation and annihilation operators. The other new term is the contraction:

$$A^{\cdot}B^{\cdot} = T\,[AB] - N\,[AB] \tag{A.63}$$

where T is the time-ordering operator previously introduced. Note that a contraction is clearly a c-number, either zero or plus or

minus the anticommutator of the operators A and B. The only non-zero contractions are

$$h_k(t_2)^{\cdot} h_{\ell}^{*}(t_1)^{\cdot} = -\delta_{\ell k} \exp\left[-i\epsilon_k(t_1-t_2)\right] \quad \text{for} \quad t_2 \leq t_1 \qquad (A.64)$$

and

$$p_m(t_2)^{\cdot} p_n^{*}(t_1)^{\cdot} = +\delta_{mn} \exp\left[i\epsilon_m(t_1-t_2)\right] \quad \text{for} \quad t_2 > t_1 \ . \qquad (A.65)$$

These contractions are also called the unperturbed propagators.

In terms of these definitions, Wick's theorem states:

$$\begin{aligned} T[ABC \cdots Y] = {} & N[ABC \cdots Y] \pm N[A^{\cdot}B^{\cdot}C \cdots Y] \pm N[A^{\cdot}BC^{\cdot} \cdots Y] \pm \cdots \\ & \pm N[A^{\cdot}B^{\cdot}C^{\cdot\cdot}D^{\cdot\cdot} \cdots Y] \pm \cdot \cdot \cdot \pm N[A^{\cdot}B^{\cdot}C^{\cdot\cdot} \cdots Y^{\cdot\cdot}] \\ & \pm \cdot \cdot \cdot \pm A^{\cdot}B^{\cdot}C^{\cdot\cdot}D^{\cdot\cdot}E^{\cdot\cdot\cdot} \cdots Y^{n\cdot} \pm \cdot \cdot \cdot \pm \\ & \pm A^{\cdot}B^{\cdot\cdot}C^{\cdot\cdot} \cdots Y^{\cdot} \ . \end{aligned} \qquad (A.66)$$

The rules for forming the terms on the right hand side of (A.66) are:

1) Form as many terms as required for all possible contractions.

2) Contractions may be factored outside normal products (they are c-numbers).

3) The sign of each term is determined by the number of permutations to bring each contracted pair together from the original order. It is negative if an odd number of permutations is required.

The theorem is proved by induction. It obviously holds when there are only two operators, since (A.63) and (A.66) are then equivalent. We can also prove that if it is true for a produce of n

operators it must be true for a product of $n + 1$ operators. Suppose the operator with the earliest time coordinate is Z. Then

$$T[ABC \cdots YZ] = T[ABC \cdots Y]Z \ . \qquad (A.67)$$

If Z is an annihilation operator, the theorem holds for the $n + 1$ operators, since Z can be immediately included in the normal products of (A.66) and its contraction with all the other operators is zero. If Z is a creation operator, it can be commuted through to the left of all the products on the right of (A.66) and then put inside the normal product signs. The anticommutator of Z with any operator is just the contraction, and the theorem again holds. If Z is a sum of a creation and an annihilation operator, the distributive law (which holds for time-ordered products, normal products and contractions) ensures that the theorem again holds. Thus the theorem is valid for any product of $n + 1$ operators if it holds for n operators. Since it is true for $n = 2$, it must be true for all higher n.

The simplification brought about by Wick's theorem is apparent if we consider the effect of a time-ordered product operating on the ground state. Only the sum of all possible contractions (the last line of (A.66)) can contribute; all other terms will vanish identically because the annihilation operators on the right of each normal product will give zero when operating on the ground ("vacuum") state.

4. The Graphical Procedure

Application of Wick's theorem to the problem of evaluating U leads to an expansion which is exactly equivalent to the following prescription in terms of graphs.

The "graphs" represent specific interactions between a given number of "particles" (particle-like excitations of the system whose energy is greater than the Fermi energy) and "holes" (excitations of the system whose energy is less than the Fermi energy). All other momentum states are filled or empty depending on whether they lie inside or outside the Fermi sea. The only interactions which are considered are those explicitly indicated by a graph. The complete description of the full interaction of the "particles" of the system is then given by the sum of all the possible graphs which can be drawn, each graph describing one particular combination of interactions. Unless explicitly stated, we are describing a zero-temperature system.

We use a vertical time scale. For every "particle" we draw an ascending line (in the positive sense of time) labelled with the particle's momentum and spin. For every "hole," we have a descending line. For each interaction we wish to describe we draw a horizontal line at a height corresponding to the appropriate time. This interaction can be either the simple two-body interaction, v, or it may (if so specified) be some "effective" interaction (such as the scattering matrix, t, which represents the sum of all possible two-body particle-particle interactions, v).

The prescription for $U(0,-\infty)\Phi_o$ is then quite simple. Draw all distinct graphs starting with no free lines at the bottom, that is, with Φ_o. Note that there can be free (external) lines at the top. For each graph form the product of the v matrix elements, the $\exp(i\epsilon t)$ and $\exp(\alpha t)$ factors (the time "t" will be negative), and a factor $(-1)^{L+H}$ where H is the number of internal hole lines and L the number of closed loops. Then attach the appropriate creation and annihilation operators at each vertex, with the hole operators to the right of other terms from the same time and with terms arranged from right to left in order of increasing time. For example, Fig. 11 contributes

$$(-1)^{5+2} v_{ij;kn} e^{i(\epsilon_i+\epsilon_j-\epsilon_n-\epsilon_k)t_3} e^{\alpha t_3} v_{j\ell;j\ell} e^{i(\epsilon_j+\epsilon_{\ } -\epsilon_j-\epsilon_{\ })t_2} e^{\alpha t_2} \times$$

$$\times v_{mn;ij} e^{i(\epsilon_m+\epsilon_n-\epsilon_i-\epsilon_j)t_1} e^{\alpha t_1} n_i n_j n_\ell (1-n_n) a_m^* a_k \quad . \qquad (A.68)$$

We have used the relations $a_i^* a_i = n_i$ (the number operator) and $a_n a_n^* = (1 - n_n)$, and the fact that $n_j n_j = n_j$. Now carry out the time integrations. $\Phi_o = U_\alpha(0,-\infty)\Phi_o$ is the sum of all the resulting terms acting on Φ_o. It is important to note that the exclusion principle is ignored in labelling the graphs. The next result depends on this. At this point, those graphs which violate the exclusion principle are exactly cancelled by the corresponding exchange graphs, and there is no error or approximation in our expression for $U_\alpha\Phi_o$.

Fig. 11. Typical graph contributing to the perturbation expansion of $\Psi_o = U(0,-\infty)\Phi_o$. See Eq. (A.68) of the text for its explicit contribution.

Fig. 12. Graph used to illustrate the time integration. See Eq. (A.69) *et seq*.

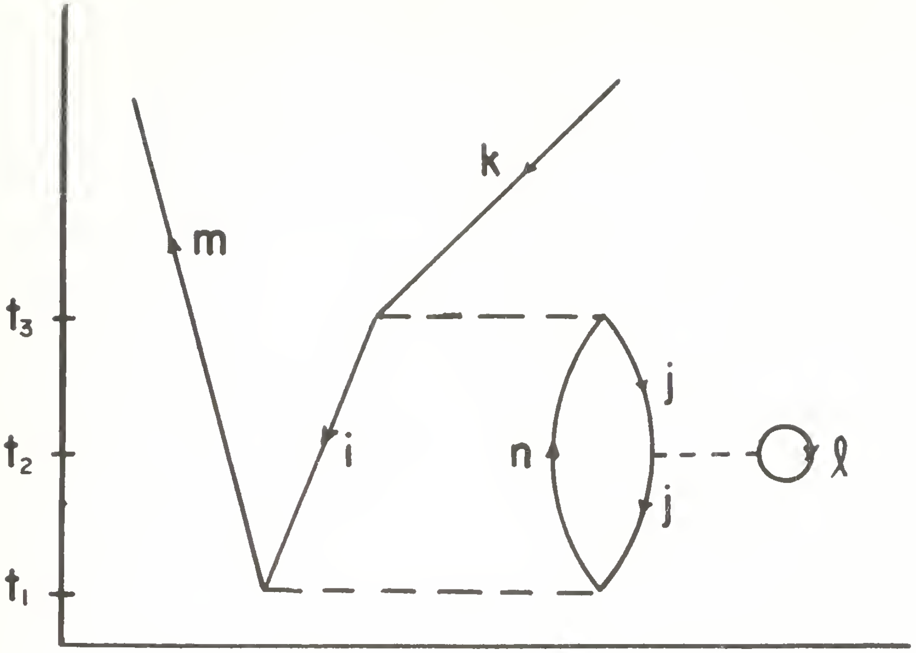

11

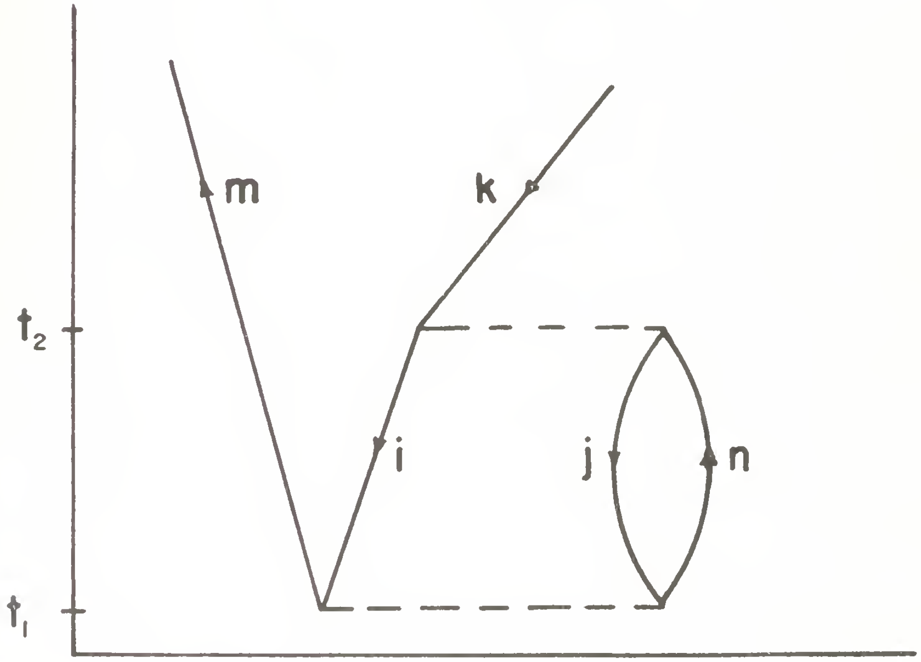

12

5. Proof of Linked Cluster Expansion

Let us now consider a graph having one or more unlinked parts, which are completely disconnected from the rest of the graph and which have no external lines. In the expression for $U_\alpha \Phi_o$ before the time integrations are preformed, the lines of a graph are labelled independently (this is the place at which it is necessary not to have to take the exclusion principle into account) and the factors attached to the interaction lines are independent. We now consider with our one graph with its unlinked parts all other graphs which differ only in having the group of unlinked parts in different positions relative to the rest of the graph, with the order of the interactions in the two parts separately kept fixed. The sum over all different relative positions of the two parts is obtained by carrying out the time integrations with the conditions $0>t_1>t_2\ldots>t_m$ and $0>t_{m+1}>t_{m+2}>\ldots>t_n$ instead of a single condition on the time integrations, with indices 1 through m referring to the unlinked parts and m + 1 through n to the rest of the graph. Thus the result is a product of the expressions obtained from the two parts separately. $U_\alpha \Phi_o$ then consists of a factor coming from the sum of linked graphs only (graphs containing no unlinked parts) multiplied by a factor coming from the sum of all possible combinations of unlinked parts. This latter factor is just $(\Phi_o, U_\alpha \Phi_o)$ (the sum of all possible graphs having no external lines -- i.e., beginning and ending at Φ_o), and is cancelled identically by the denominator in (A.38). Thus Ψ_o as defined by (A.38) is given by taking the

limit $\alpha \to 0$ in the sum of linked graphs only.

Let us now do the time integration for a simple example, Fig. 12. The contribution to $\Psi_o = \lim_{\alpha \to 0} U_\alpha \Phi_o$ from this figure is

$$\lim_{\alpha \to 0} (-1)^2 \int_{-\infty}^{o} dt_1 \int_{-\infty}^{t_1} dt_2 \; v_{ij;kn} \, e^{i(\epsilon_i+\epsilon_j-\epsilon_k-\epsilon_n-i\alpha)t_1}$$

$$v_{mn;ij} \, e^{i(\epsilon_m+\epsilon_n-\epsilon_i-\epsilon_j-i\alpha)t_2} n_i n_j (1-n_n) a_m^* a_k \Phi_o$$

$$= \lim_{\alpha \to 0} \int_{-\infty}^{o} dt_1 \; v_{ij;kn} \, e^{-i(\epsilon_k+\epsilon_n-\epsilon_i-\epsilon_j+i\alpha)t_1} \quad (A.69)$$

$$\left[\frac{-v_{mn;kj} \, e^{-i[\epsilon_i+\epsilon_j-\epsilon_m-\epsilon_n+i\alpha]t}}{-i[\epsilon_i+\epsilon_j-\epsilon_m-\epsilon_n+i\alpha]} \right]_{-\infty}^{t_1} n_i n_j (1-n_m) a_m^* a_k \Phi_o \; .$$

The convergence factor, αt, causes the term in brackets to vanish at the limit $-\infty$, and we have

$$\lim_{\alpha \to 0} (i) \int_{-\infty}^{o} dt \; v_{ij;kn} \, e^{-i(\epsilon_k-\epsilon_m+2i\alpha)t} \frac{1}{(\epsilon_m+\epsilon_n-\epsilon_i-\epsilon_n)+i\alpha}$$

$$v_{mn;ij} \, n_i n_j (1-n_n) a_m^* a_k \Phi_o \quad (A.70)$$

$$= \lim_{\alpha \to 0} \frac{1}{\epsilon_m-\epsilon_k+2i\alpha} v_{ij;kn} \frac{1}{\epsilon_m+\epsilon_n-\epsilon_i-\epsilon_j+i\alpha} v_{mn;ij} \, n_i n_j (1-n_n) a_m^* a_k \Phi_o \; .$$

The denominators above are just $E_o - H_o$ evaluated in the positions shown -- i.e., we have one of the possible terms in the expression

$$\lim_{\alpha \to 0} \frac{1}{E_o-H_o+2i\alpha} H_I \frac{1}{E_o-H_o+i\alpha} H_I \Phi_o \; . \quad (A.71)$$

In general, we have

$$\Psi_o = \lim_{\alpha \to 0} \sum_L \frac{1}{E_o - H_o + in\alpha} H_I \cdots H_I \frac{1}{E_o - H_o + 2i\alpha} H_I \frac{1}{E_o - H_o + i\alpha} H_I \Phi_o \ . \tag{A.72}$$

$\sum_L$ means that only linked graphs are to be summed. Φ_o cannot occur as an intermediate state in a linked graph as the part of the graph below that intermediate state would be an unlinked part. The interaction energy, ΔE, is given by (A.40), and is obviously

$$\Delta E = \lim_{\alpha \to 0} \sum_c (\Phi_o, H_I \frac{1}{E_o - H_o + in\alpha} H_I \cdots H_I \frac{1}{E_o - H_o + 2i\alpha} H_I \frac{1}{E_o - H_o + i\alpha} H_I \Phi_o) \ . \tag{A.73}$$

Here $\sum_c$ means summation over all connected graphs leading from Φ_o to Φ_o (i.e., linked graphs with no external lines). This equation is referred to throughout this paper as the Brueckner-Goldstone linked-cluster expansion (BG expansion). In the absence of a degenerate ground state or of an effective attractive interaction at the Fermi surface (which would lead to singularities in some of the above denominators), the restriction to intermediate states other than Φ_o means that all the intermediate state energies will be greater than E_o, and we can take the above limits by setting $\alpha = 0$ as no zero energy denominators can occur. Equations (A.72) and (A.73) can then be written

$$\Psi_o = \sum_L \left(\frac{1}{E_o - H_o} H_I \right)^n \Phi_o \tag{A.72'}$$

$$\Delta E = \sum_c (\Phi_o, H_I(\frac{1}{E_o - H_o} H_I)^n \Phi_o) . \qquad (A.73')$$

In Section 3 of this appendix, the rules are given for calculating the terms in the energy expansion, and the explicit series is indicated through third order.

6. Inclusion of Effective Single-Particle Potential

Goldstone,^{2} in his proof of the linked-cluster expansion, defined the unperturbed Hamiltonian as a sum of the kinetic energies and of an effective single-particle potential, V_i

$$H_o = \sum_i (\epsilon_i + V_i) = T + V \qquad (A.74)$$

so that the interaction Hamiltonian is

$$H_I = \sum_{i<j} v_{ij} - \sum_i V_i \quad . \qquad (A.75)$$

In second-quantized notation

$$H_o = \sum_n \epsilon_n a_n{}^* a_n \qquad (A.76)$$

where E_n is now the sum of the kinetic energy and the "effective potential," and

$$H_I = \frac{1}{2} \sum v_{rs;mn} \; a_r{}^* a_s{}^* a_n a_m - \sum V_{r;m} \; a_r{}^* a_m \; . \qquad (A.77)$$

The proof proceeds excatly as before, except that one now obtains a series of graphs with the V interaction and in the denominators of

every term one has the energies $\epsilon_k = \frac{k^2}{2m} + V_k$ instead of the kinetic energies, $k^2/2m$, alone. The matrix element $V_{r;m}$ is illustrated below:

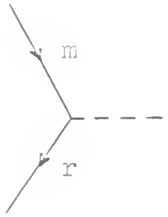

One then defines V_k in such a way that the graphs generated by the V-interaction cancel as many v-graphs as possible. For example, the Hartree-Fock approximation is obtained by choosing

$$V_{r;m} = \sum_n v_{rn;(rn)} \quad . \tag{A.78}$$

The sum is over all unperturbed states, Ψ_n . The states Ψ_n are determined by

$$(T+V)\ \Psi_n = E_n \Psi_n \quad . \tag{A.79}$$

(A.78) and (A.79) are the Hartree-Fock self-consistent equations. With this definition, to first order

$$\Delta E = \frac{1}{2} \Sigma\ v_{k\ell;(k\ell)}\ n_k n_\ell - \sum_k V_{k;k} n_k \quad . \tag{A.80}$$

Now

$$E_o = \sum_k \left(\frac{k^2}{2m} + V_{k;k}\right) n_k = \sum_k \epsilon_k n_k \tag{A.81}$$

so that to first order we have, using (A.78) and (A.80):

$$E = E_o + \Delta E = \sum_k \frac{k^2}{2m} + \frac{1}{2} \Sigma V_{k;k} n_k . \qquad (A.82)$$

We shall discuss later how this procedure is applied in the Brueckner theory.

C. COMMENTS ON THE BG EXPANSION

There have been several other derivations of the linked-cluster perturbation formula for many-fermion systems. Goldstone[2] has also derived it using time-independent perturbation theory. Hugenholtz[88] uses an expansion of the resolvent

$$R(z) = (H-z)^{-1} . \qquad (A.83)$$

The resolvent is related to the development operator used by Goldstone:

$$\begin{aligned} R(z) &= -i\int_{-\infty}^{0} U(t)\exp(izt)dt \qquad \text{for} \quad \text{Im } z < 0 \\ &= i\int_{0}^{\infty} U(t)\exp(izt)dt \qquad \text{for} \quad \text{Im } z > 0 , \end{aligned} \qquad (A.84)$$

and the methods used by the two authors are therefore closely related. As pointed out by Thouless,[20] the expansion of $U(t)$ is easier to manipulate, since we generally have to deal with products of functions rather than with the convolutions of functions which arise in the expansion of $R(z)$. The resolvent has more direct physical interpretation, since the poles of its matrix elements give

the eigenvalues of the Hamiltonian.

Bloch[89] has used a combination of time-dependent and time-independent theory, involving the use of both R(z) and U(t). Hubbard[90] has used a time-dependent procedure which is almost identical to Goldstone's, but indicates several intermediate steps that Goldstone leaves out.

Kohn and Luttinger[91] later examined the theory through fourth order with a finite temperature theory developed by Bloch and DeDominicis.[92] The Kohn-Luttinger investigation revealed that taking the limit $N \to \infty$ before taking the limit $T \to 0$ leads to certain "anomalous" terms in second and higher order for "non-spherical" systems. Using temperature-dependent Green's functions, Luttinger and Ward[93] have demonstrated that the anomalous terms are cancelled identically by the change in chemical potential from μ_o to μ to all orders for spin $\frac{1}{2}$ fermions under the conditions we have prescribed for our investigation, namely: a normal system interacting via an isotropic two-body interaction and characterized by a spherical unperturbed Fermi surface. In other words, the BG expansion (which, in their context, is an expansion in terms of μ_o) is valid for such a system. Kohn and Luttinger, who had reached the same conclusion for the first few orders of perturbation theory, have ascertained that the tensor force does not create an anomalous contribution in second order, and as pointed out by Bethe, Brandow and Petschek,[9] they probably do not produce anomalous contributions in any order, though the extension to higher order has not been proved.

Because we shall not be concerned with either finite-temperature theory or with systems for which the anomalous terms contribute, we refer the reader to the original papers for further details.

The Brueckner-Goldstone procedure leads to the lowest state which can be reached adiabatically from the chosen configuration. Until now we have assumed this configuration to be spherical, and for the "normal" system the BG expansion leads to the ground state. Suppose, however, that there was some other configuration of the "unperturbed" Fermi surface (where $H_o = \sum_k \epsilon_k V_k = \sum_k (\frac{k^2}{2m} + V_k)$ is the unperturbed Hamiltonian, V_k being the effective potential acting on the particle $\underset{\sim}{k}$). Then the BG expansion from the spherical Fermi surface would lead to some state other than the ground state. Our formalism can be trivially extended to a non-spherical starting configuration, however, if we know that configuration in advance. We merely utilize the definition of $\hat{n}_k$, and recognize that its expectation value must be

$$\begin{aligned} n_k &= 1 \quad \text{state } \underset{\sim}{k} \text{ occupied} \quad (\epsilon_k = \frac{k^2}{2m} + V_k \leq \epsilon_F) \\ &= 0 \quad \text{state } \underset{\sim}{k} \text{ unoccupied} \quad (\epsilon_k > \epsilon_F) \end{aligned} \tag{A.85}$$

If we do not know the shape of the unperturbed ground state, we should introduce a new equation which allows us to vary the shape of the unperturbed distribution until a minimum total system energy is obtained. This variation would not be too difficult to introduce formally, but in practice it would be very difficult to evaluate. In any situation in which the shape of the Fermi surface is the sole

cause of the non-cancellation of the "anomalous diagrams" of Kohn and Luttinger,[91] this procedure is all that is required to avoid them. Further, it may well be that this procedure is the easiest way to rigorously extend to higher orders the proof that tensor forces do not produce anomalous contributions. However, either the direct computation of the anomalous terms or the above variational calculation will be difficult.

A. Klein[94] has suggested just such a procedure as the above, with the surface being determined by the additional, self-consistent equation

$$\mu = \frac{p_F^{\,2}}{2m} + V(p_F) = \left(\frac{\partial E}{\partial N}\right)_\Omega = \frac{d}{d\rho}\left(\frac{E}{\Omega}\right)$$

$$= \frac{(2\pi)^3}{p_F^{\,2}(\omega)} \; \frac{\delta}{\delta p_F(\omega)} \left(\frac{E}{\Omega}\right) \qquad (A.86)$$

where μ is the chemical potential and the ω in $p_F(\omega)$ represents its dependence on angle.

One of the persistent myths about the Brueckner many-body theory is that there is something assumed or approximated when one uses the unperturbed Fermi distribution instead of the true momentum density. This is not the case for any system for which the power series in the interaction potential converges (which is another question again). As we have seen, the BG linked-cluster expansion is a rigorously correct perturbation theoretic expansion for the energy of the zero-temperature normal state which meets the symmetry

requirements outlined earlier. The occurrence of the n_k is a consequence of taking the expectation value $(\Phi_o, H\Psi)$ instead of $(\Psi, H\Psi)$. Either expectation value will yield the correct energy, but the potential and kinetic energy terms in the two will be quite different. The expectation value between the states Ψ has been shown to lead (see Eq. (A.59)) to the following expression for the interaction energy:

$$(\Psi, H_I\Psi) = \Delta E' = \lim_{\alpha \to 0} \frac{1}{2}\, i\alpha g\, \frac{\frac{\partial}{\partial g}(\Phi, U_\alpha(\infty, -\infty)\Phi)}{(\Phi, U_\alpha(\infty, -\infty)\Phi)} \tag{A.87}$$

which, to second order in v, is:

$$\Delta E' = \frac{1}{2} \sum_{k\ell} v_{k\ell;(k\ell)}\rho_k\rho_\ell + \lim_{\alpha \to 0} \sum_{k\ell mn} v_{k\ell;mn} \frac{(1-\rho_m)(1-\rho_n)}{\epsilon_k+\epsilon_\ell-\epsilon_m-\epsilon_n+i\alpha} v_{mn;(k\ell)}\rho_k\rho_\ell \, . \tag{A.88}$$

The kinetic energy expectation value is

$$(\Psi, E_o\Psi) = \sum_k \epsilon_k\, (\Psi, n_k\Psi) = \sum_k \epsilon_k\rho_k \, . \tag{A.89}$$

The above forms differ from the BG expansion

$$E_o + \Delta E = \sum_k \epsilon_k n_k + \frac{1}{2} \sum v_{k\ell;(k\ell)} + \frac{1}{2} \sum_{k\ell mn} v_{k\ell;mn} \frac{(1-n_m)(1-n_n)}{(\epsilon_k+\epsilon_\ell-\epsilon_m-\epsilon_n)} v_{mn;(k\ell)} n_k n_\ell \tag{A.90}$$

in second order, and higher. Further, from (A.87) it is apparent

that the difference in factors increases in the higher orders. Of course, the two expansions must give the same energy, and we need only expand the ρ_k in terms of n_k, using (2.22), to see that the sum of (A.89) and (A.90) reduces to the BG expansion in terms of n_k. However, any theory which obtains an expansion in which the kinetic energy is given by (A.90) must include an interaction energy term of the same structure as (A.89). The reason is obvious. The kinetic energy $\sum_k \epsilon_k \rho_k$ is larger than $\sum_k \epsilon_k n_k$ because ϵ_k is a quadratically increasing function of k; since $\sum_k \rho_k = \sum_k n_k$, the sum of ϵ_k times ρ_k weights the higher momenta more heavily than the sum with n_k. Consequently, the expectation value $(\Psi, H\Psi)$ is characterized by a higher "kinetic energy" than $(\Phi_0, H\Psi)$. Since the two expectation values are equal, the former must also yield a correspondingly more negative potential energy. The difference in coefficients in the potential energy expansion leads to precisely this cancellation.

We note as a matter of interest that (A.89) and (A.90) can be obtained directly from using the BG expansion for the wave function (A.72) in the expectation values of the kinetic and potential energies.

There are two other, related, problems in the BG theory which we shall discuss as they apply to infinite nuclear matter. One is the vanishing radius of convergence of the BG expansion as a power series expansion in the coupling constant, g, as the volume of the system becomes infinite. The other is the probable existence

of a superfluid ground state below the normal state.

The analytic structure of many-body perturbation theory has been studied by many authors, most of whom have concluded that it probably diverges.[95,96,97] However, Katz[98] has argued that the energy of every level of a large, but finite, many-body system can be obtained by analytic continuation of the BG expansion along properly chosen paths in the complex g plane (where g is the strength of the interaction). He shows for a simple problem that the Brueckner ladder approximation (see Appendix B) is an approximation to the analytic continuation along a path which always leads to the normal state (the state in which no binding occurs). He argues that this is true in general, but this has not yet been rigorously proved. The essence of his argument is that if one performs a partial summation of certain diagrams in every order of g, then much of the divergence of the expansion can be taken care of and the resulting expansion is effectively in terms of some other parameter (such as the density) and consequently may have a larger radius of convergence. Considerable further study is indicated, but the preliminary results are promising.

A related argument that perturbation theory might be invalid is that nuclear matter may exhibit a phenomenon similar to superconductivity. Bethe, Brandow and Petschek[9] review the experimental and theoretical grounds for this assertion, and point out that at most the energy gap associated with such a phenomenon is only 1 MeV, and its effect on the average energy per nucleon is likely to

be less than

$$\Delta E_{Av} = \frac{3}{8} \frac{(\Delta E)^2}{\omega_{p_F}} \simeq .008 \text{ MeV} \quad \text{for} \quad p_F = 1.5 \text{ F}^{-1} \qquad \text{(A.91)}$$

where ω_{p_F} is the Fermi energy, 47 MeV for $p_F = 1.5 \text{ F}^{-1}$ (chosen arbitrarily), and the factor 3/8 is the statistical probability of having a pair of nucleons in a state of even relative angular momentum. Thus we conclude that "superconductivity pairing," while of interest for the detailed level structure of even-even nuclei, has a negligible influence on the average binding energy.

D. THE ENERGY EXPANSION -- GRAPHICAL EVALUATION

The following rules for employing the graphical method apply to the ground state energy of an extended fermion system for which the unperturbed wave function is a determinant of those plane waves whose wave number is less than p_F and for which the Hamiltonian is given by (A.1).

To calculate the nth order contribution of H_I to energy in accordance with the Brueckner-Goldstone linked-cluster expansion (A.73), we draw n horizontal broken lines (called vertices, and representing two-body interactions) at different levels. The two ends of each line are called points. We connect the 2n points with every possible combination of particle and hole lines subject to the conditions that at every point one line "comes in" and one "goes out" and that there occur only "linked graphs" -- those in which there is no sub-graph which is not connected to the rest of the graph. A

particle line is a line directed upward and a hole line is directed downward; in our figures the direction of the line is indicated with an arrow when ambiguity is possible. Every line is then labelled in all possible ways (i.e., with all possible momenta). A line which closes on itself is a hole line (a consequence of Wick's theorem -- see Eq. (A.64)).

The contribution of a particular linked graph is the product of four factors:

1. One of these factors is $\frac{1}{2}v_{k\ell;mn}$ from each vertex, where $\underset{\sim}{m}$ and $\underset{\sim}{n}$ are lines entering the vertex on the left and right respectively and $\underset{\sim}{k}$ and $\underset{\sim}{\ell}$ are the lines leaving (on left and right respectively). Thus for

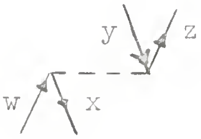

we have the contribution $\frac{1}{2}v_{xz;wy}$.

2. The second factor is the product of the "propagator" for each of the $\underline{n}$-1 intervals between successive vertices, each propagator being the reciprocal sum of the kinetic energies of the hole lines intersected by any horizontal section between the vertices minus the kinetic energies of the particle lines. Thus, for the propagator at a section of a graph which looks like this:

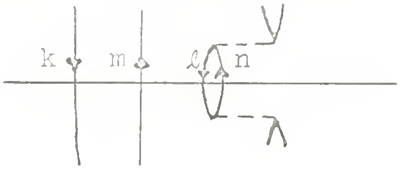

we have a factor $(\epsilon_k+\epsilon_\ell-\epsilon_m-\epsilon_n)^{-1}$, where $\epsilon_k = p_k^2/2m$.

3. The sign factor is $(-1)^{L+H}$ where L is the number of closed fermion lines and H is the number of hole lines in the graph. Thus, for

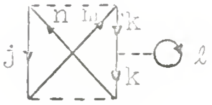

we have a factor $(-1)^{2+4} = +1$ (note that $\underset{\sim}{k}$ is counted twice since it is "broken" by the interaction with the hole $\underset{\sim}{\ell}$).

4. The final factor is a product of expectation values of the number operator, n_k, for every hole and $(1-n_m)$ for every particle, except that two or more particles or holes with identical momenta contribute only one term by virtue of the idempotency of the number operator (i.e., because $n_k^m = n_k$). This latter rule is necessary if the results are to be extended to finite temperatures, when the n_k are replaced by the temperature-dependent Fermi functions.

In labelling the lines, the exclusion principle is ignored in intermediate states. The Brueckner-Goldstone expansion is obtained only if this is done. This has two effects: (1) all intermediate sums are unrestricted except that they must be to states outside the Fermi sea; and, (2) diagrams such as the fourth order diagram (4e) of Fig. 1 (which explicitly violates the exclusion principle) must be included.

Through third order, the ground state energy is given by

the following terms (corresponding to the diagrams of Fig. 1, as indicated):

$$E = \sum_k \epsilon_k n_k$$

1(a) $$+ \frac{1}{2} \sum_{k\ell} v_{k\ell;(k\ell)} n_k n_\ell \qquad \left(= \frac{1}{2} \sum (v_{k\ell;k\ell} - v_{k\ell;\ell k}) n_k n_\ell\right)$$

2(a) $$+ \frac{1}{4} \sum_{k\ell mn} v_{k\ell;(mn)} \frac{n_k n_\ell (1-n_m)(1-n_n)}{\epsilon_k+\epsilon_\ell-\epsilon_m-\epsilon_n} v_{mn;(k\ell)}$$

$$\left(= \frac{1}{2} \sum_{k\ell mn} v_{k\ell;mn} \frac{n_k n_\ell (1-n_m)(1-n_n)}{\epsilon_k+\epsilon_\ell-\epsilon_m-\epsilon_n} v_{mn;(k\ell)}\right)$$

3(a) $$+ \frac{1}{8} \sum v_{k\ell;(m_2n_2)} \frac{(1-n_{m_2})(1-n_{n_2})}{\epsilon_k+\epsilon_\ell-\epsilon_{m_2}-\epsilon_{n_2}} v_{m_2n_2;(m_1n_1)}$$

$$\frac{(1-n_{m_1})(1-n_{n_1})}{\epsilon_k+\epsilon_\ell-\epsilon_{m_1}-\epsilon_{n_1}} v_{m_1n_1;(k\ell)} n_k n_\ell$$

3(b) $$- \frac{1}{4} \sum v_{k\ell;(mn)} \frac{n_k n_\ell (1-n_m)(1-n_n)}{\epsilon_k+\epsilon_\ell-\epsilon_m-\epsilon_n} v_{mn;(k\ell)}$$

$$\left\{\sum_j (v_{jk;(jk)}+v_{j\ell;(j\ell)}-v_{jm;(jm)}-v_{jn;(jn)})\, n_j\right\}$$

$$3(c) \quad + \frac{1}{8} \Sigma\, v_{k_2 \ell_2;(mn)} \frac{1}{\epsilon_{k_2}+\epsilon_{\ell_2}-\epsilon_m-\epsilon_n} v_{k_1 \ell_1;(k_2 \ell_2)}$$

$$\frac{(1-n_m)(1-n_n)}{\epsilon_{k_1}+\epsilon_{\ell_1}-\epsilon_m-\epsilon_n} v_{mn;(k_1 \ell_1)} n_{k_1} n_{k_2} n_{\ell_1} n_{\ell_2}$$

$$3(d) \quad + \frac{1}{8} v_{k_1 k_3;(m_1 m_3)} \frac{n_{k_1}(1-n_{m_1})(1-n_{m_3})}{(\epsilon_{k_1}+\epsilon_{k_3}-\epsilon_{m_1}-\epsilon_{m_3})} v_{m_3 k_2;(k_3 m_2)}$$

$$\frac{(1-n_{m_2}) n_{k_2} n_{k_2}}{(\epsilon_{k_1}+\epsilon_{k_2}-\epsilon_{m_1}-\epsilon_{m_2})} v_{m_1 n_1;(k_1 k_2)} \tag{A.92}$$

A "self-energy insert" as written above (in brackets) carries a factor one instead of $\frac{1}{2}$ because we must also include terms of the form $v_{kj;(kj)}$, etc., in the expansion. Since $v_{kj;(kj)}$ is equal to $v_{jk;(jk)}$, we can include it by using the above equation and the weight factor one.

APPENDIX B

THE BRUECKNER K-MATRIX APPROXIMATION

A. DERIVATION

In this Appendix the Brueckner K-matrix equations are derived and their application to nuclear matter discussed. Extensive references to early papers by Brueckner and his collaborators, as well as by several other authors who studied the theory in its early stages, can be found in the Brueckner-Gammel paper[3] (BG) in which are reported the first quantitative calculations of the properties of nuclear matter based only on the two-nucleon potential. The derivation given below is simpler than the original one because we have as our starting point the BG expansion. All that is necessary to obtain the K-matrix equations (in momentum space) is to perform selective summations of some of the terms in this expansion. A detailed discussion of the partial summation of the perturbation series with "reaction matrices" can be found in a paper by Tobocman.[99]

The first problem is to sum the series of "ladder diagrams" -- the two-body scattering diagrams, indicated through third order in Fig. 13. This series can be summed by using a reaction matrix, t , defined by

$$t_{ij;k\ell} = v_{ij;k\ell} + \sum_{mn} v_{ij;mn} \frac{(1-n_m)(1-n_n)}{\epsilon_k+\epsilon_\ell-\epsilon_m-\epsilon_n} v_{mn;k\ell} + \sum_{\substack{mn\\rs}} v_{ij;mn} \times$$

$$\times \quad \frac{(1-n_m)(1-n_n)}{\epsilon_k+\epsilon_\ell-\epsilon_m-\epsilon_n} v_{mn;rs} \frac{(1-n_r)(1-n_s)}{\epsilon_k+\epsilon_\ell-\epsilon_r-\epsilon_s} v_{rs;k\ell} + \cdot \cdot \cdot$$

$$= v_{ij;k\ell} + \sum_{mn} v_{ij;mn} \frac{(1-n_m)(1-n_n)}{\epsilon_k+\epsilon_\ell-\epsilon_m-\epsilon_n} t_{mn;k\ell} \quad . \qquad (B.1)$$

A very large class of diagrams can be summed by replacing every v which appears in the BG expansion by t, with the diagrams thus implicitly summed dropped from the explicit series. This procedure is particularly useful for hard core potentials (for which the matrix elements of v are infinite) because the matrix elements of t are finite.

In terms of the t-matrix, the BG expansion (A.92) is:

$$\Delta E(n,\epsilon) = \tfrac{1}{2}\sum_{k\ell} t_{k\ell;(k\ell)} n_k n_\ell - \tfrac{1}{2}\sum_{\substack{k\ell\\mn}} t_{mn;k\ell} \frac{n_k n_\ell (1-n_m)(1-n_n)}{(\epsilon_k+\epsilon_\ell-\epsilon_m-\epsilon_n)^2} t_{mn;(k\ell)} \quad \times$$

$$\times \quad \{ \sum_j (t'_{jk;(jk)} + t'_{j\ell;(j\ell)} - t'_{jm;(jm)} - t'_{jn;(jn)}) n_j \} +$$

$$+ \quad (\text{hole-hole and 3-body cluster of } O(t^3)) + O(t^4) \qquad (B.2)$$

where

$$t'_{jk;(jk)} = v_{jk;(jk)} + \sum_{mn} v_{jk;mn} \frac{(1-n_m)(1-n_n)}{\epsilon_j+\epsilon_k-\epsilon_m-\epsilon_n-\delta E} t'_{mn;(jk)}$$

$$= v_{jk;(jk)} + \sum_{mn} v_{jk;mn} \frac{(1-n_m)(1-n_n)}{\epsilon_j+\epsilon_k-\epsilon_m-\epsilon_n} v_{mn;(jk)} + \cdot \cdot \cdot +$$

$$+ \sum_{mn} v_{jk;mn} \frac{\delta E(1-n_m)(1-n_n)}{(\epsilon_j+\epsilon_k-\epsilon_m-\epsilon_n)^2} t'_{mn;(jk)} +$$

$$+ \sum_{\substack{rs\\mn}} v_{jk;rs} \frac{(1-n_r)(1-n_s)}{\epsilon_j+\epsilon_k-\epsilon_r-\epsilon_s} v_{rs;mn} \frac{\delta E(1-n_m)(1-n_n)}{(\epsilon_j+\epsilon_k-\epsilon_m-\epsilon_n)^2} \times$$

$$\times \; t'_{mn;(jk)} + \cdots$$

$$= t_{jk;(jk)} + \sum_{mn} t_{mn;jk} \frac{\delta E(1-n_m)(1-n_n)}{(\epsilon_j+\epsilon_k-\epsilon_m-\epsilon_n)^2} t'_{mn;(jk)} \qquad \text{(B.3)}$$

Eq. (B.2) is obtained as follows from the diagrams of the first few orders in the BG expansion. The first term is the sum of the simple ladder diagrams. The second term is derived from the lowest order self-energy insert, 3(b) of (A.92), by replacing each vertex v with the sum, t, of ladder diagrams. The replacement of the terms in the bracket by t' instead of t is a consequence of the shifted energy denominator for those terms due to the excitation energy of the other particles (so that, e.g., diagram 4(d) of Fig. 1 will be properly described). The energy shift, δE, is discussed in further detail later. The order of the indices of the t-matrix elements above should be noted. Such order is required of the left-hand term in the products above so that the energy denominators are properly specified in the diagrams summed by the t-matrices.

Another class of diagrams which can be summed is indicated in Fig. 14. We note that to every hole and particle line of every term in the BG expansion there can be attached, as a "self-energy

Fig. 13. "Ladder diagrams" contributing to the t-matrix.

Fig. 14. (a) "Self-energy" diagrams which are summed when the propogator includes the "self-consistent" single particle energies.

(b) Definition of the schematic notation of (a).

Fig. 15. Typical diagrams which are summed when the propogator of Fig. 14 and Eq. (B.4) occurs between two v interactions.

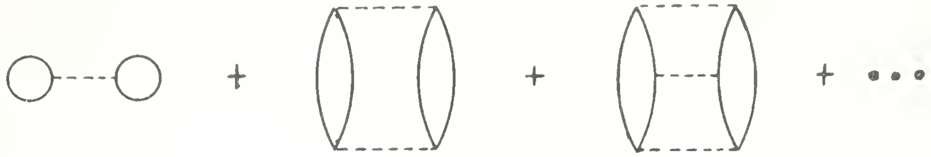

13

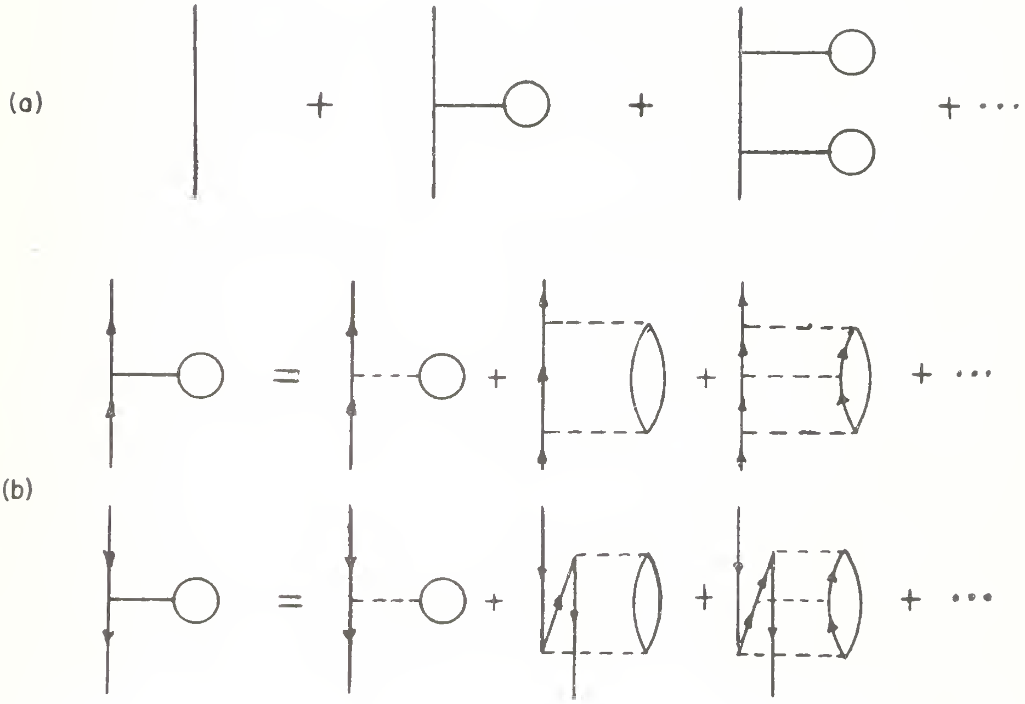

14

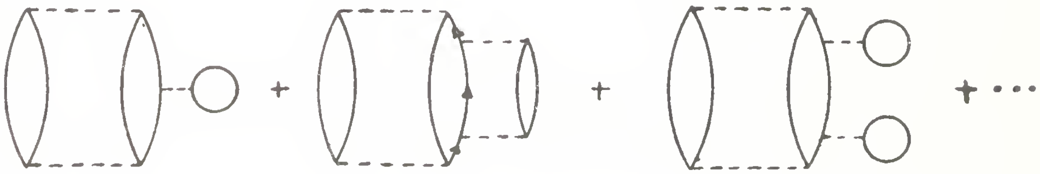

15

insert," an infinite set of diagrams, with each insertion leading to another diagram in the overall BG expansion. Furthermore, as we see in Fig. 14, self-energy diagrams can be inserted any number of times on any given line. The reason for defining the insert on the hole line as indicated in Fig. 14, violating the exclusion principle, will be seen later. Such terms do occur in the BG expansion, of course: the exclusion principle is to be neglected when labelling the lines. All possible terms of the sort indicated in Fig. 14 can be obtained by redefining the "propogator" as

$$\frac{1}{\epsilon_k+\epsilon_\ell-\epsilon_m-\epsilon_n} \rightarrow \frac{1}{\omega_k'+\omega_\ell'-\omega_m'-\omega_n'} \tag{B.4}$$

where

$$\omega_k' = \epsilon_k + \sum_\ell t_{k\ell;(k\ell)} n_k n_\ell \quad . \tag{B.5}$$

Note that ω_k' is analagous to ω_k of (2.34) without the rearrangement term. To see that this definition of the propogator reproduces the series indicated in Fig. 14, expand the denominator as

$$\frac{1}{1+x} = 1 - x + x^2 - \cdot \cdot \cdot \cdot \tag{B.6}$$

to obtain

$$\frac{1}{\omega_k'+\omega_\ell'-\omega_m'-\omega_n'} = \frac{1}{\epsilon_k+\epsilon_\ell-\epsilon_m-\epsilon_n} - \frac{1}{(\epsilon_k+\epsilon_\ell-\epsilon_m-\epsilon_n)^2} \Big\{ \sum_j (t_{jk;(jk)} + t_{j\ell;(j\ell)} - t_{jm;(jm)} - t_{jn;(jn)}) n_j \Big\} + \cdots \tag{B.7}$$

Thus, inserting the above propogator between two v interactions sums all terms such as those indicated in Fig. 15. There is a restriction which will be discussed shortly. Next, to continue the process, one defines a new reaction matrix, K, incorporating the modified propogators:

$$K_{ij;k\ell} = v_{ij;k\ell} + \sum_{mn} v_{ij;mn} \frac{(1-n_m)(1-n_n)}{\omega_k{}'+\omega_\ell{}'-\omega_m{}'-\omega_n{}'} K_{mn;k\ell} \quad , \qquad (B.8)$$

with

$$\omega_k{}' = \epsilon_k + \sum_j K_{jk;(jk)} n_j = \epsilon_k + V_k \quad . \qquad (B.9)$$

The BG expansion (A.92) or (B.2) then becomes

$$\Delta E = \tfrac{1}{2} \sum_{k\ell} K_{k\ell;(k\ell)} n_k n_\ell + O(K^3) \quad . \qquad (B.10)$$

The diagrams which this approximation sums are indicated through fourth order in Fig. 1 (along with two third order diagrams which it does not include, the hole-hole and three-body cluster diagrams).

The restriction mentioned above is concerned with the denominator of the terms occuring in the definition of the "self-consistent" V_k in (B.9). The problem involved is the proper treatment of terms such as 4(d) of Fig. 1, and is best illustrated by an example. The contribution of 4(d) to the interaction energy, ΔE, is

$$(B.11)$$

$$-\tfrac{1}{2} \sum_{\substack{k\ell \\ mn}} v_{k\ell;mn} \frac{n_k n_\ell (1-n_m)(1-n_n)}{(\epsilon_k+\epsilon_\ell-\epsilon_m-\epsilon_n)^2} v_{mn;(k\ell)} \left[\sum_{jrs} v_{jn;rs} \frac{n_j (1-n_r)(1-n_s)}{\epsilon_j+\epsilon_n-\epsilon_r-\epsilon_s-E} v_{rs;(jn)} \right]$$

where $-E'$ is obviously $\epsilon_k+\epsilon_\ell-\epsilon_m-\epsilon_n$. The term in parentheses is just one of the terms from the definition of V_n except for the occurrence of $-E'$ (which is the excitation energy of the remainder of the diagram at the point where the self-energy term is inserted). If we try to account for such terms by modifying the definition of the K-matrix to include the term $-E'$ in the denominator, we find that either we must compute the K-matrix for the full spectrum of possible excitation energies, or we must use some average $-E'$ in the denominator. The latter choice truncates an otherwise infinite series of equations by treating only approximately the fourth and higher order diagrams such as 4(d) in Fig. 1. The use of $-E'$ in the denominator violates energy conservation in the definition of the K-matrix in order that energy be conserved in the particular ground state term being described, and the K-matrix is then described as being computed "off the energy shell."

Another method for treating the energy denominators also exists. Eq. (B.11) can be written

$$-\frac{1}{2}\sum_{\substack{k\ell\\mn}} v_{k\ell;mn}\frac{n_k n_\ell(1-n_m)(1-n_n)}{(\epsilon_k+\epsilon_\ell-\epsilon_m-\epsilon_n)^2}v_{mn;(k\ell)}\left[\sum_{jrs} v_{jn;rs}\frac{n_j(1-n_r)(1-n_s)}{\epsilon_k+\epsilon_\ell-\epsilon_r-\epsilon_s-\delta E}v_{rs;(jn)}\right] \tag{B.12}$$

where $\delta E = \epsilon_m - \epsilon_j$. Thus, we can properly treat this diagram if we define the K-matrix for particles outside the Fermi sea by

$$K_{jn;jn} = v_{jn;jn} + \sum_{rs} v_{jn;rs}\frac{(1-n_r)(1-n_s)}{E-\omega_r'-\omega_s'-\delta E}v_{rs;jn} \tag{B.13}$$

and their self-consistent potential energy by

$$V_n(\Sigma) = \sum_j K_{jn;(jn)}(\Sigma)n_j \tag{B.14}$$

where Σ $(=\omega_k{}'+\omega_\ell{}')$ is a parameter in the equations which allows us to use as the particle energies in (B.8) quantities related to the energy of the holes coupled to the excitations (i.e., a quantity which represents the dependence of the particle's energy on the energy of the associated holes for the purposes of the above treatment of these complicated denominators). Eqs. (B.13) and (B.14), used in (B.10), will generate, among other terms, Eq. (B.12).

This latter formulation is advantageous if we are going to use an average value for the excitation energy instead of attempting to solve exactly. The reason is that the second method of treating the particle energies treats a larger portion of the energy denominators exactly; because of this, (B.13) and (B.14) are used as the definitions of the particle energies in the K-matrix calculations of Brueckner et. al. The average single particle excitation energy is usually taken to be

$$\overline{\delta E} = \overline{\omega_m{}'-\omega_j{}'} \equiv \Delta \simeq \omega_{p_F}{}' - \omega_{p=0} \,. \tag{B.15}$$

With the hole self-energy insert, such as 4(e) and 4(f) of Fig. 1, the situation is not the same. For either diagram alone, δE should again be the interaction energy of the original lines, but when we take the two diagrams indicated together, we have (looking only at the propogators):

$$\frac{1}{\epsilon_k+\epsilon_\ell-\epsilon_m-\epsilon_n}\,\frac{1}{\epsilon_j+\epsilon_k+2\epsilon_\ell-\epsilon_m-\epsilon_n-\epsilon_r-\epsilon_s}\,\frac{1}{\epsilon_k+\epsilon_\ell-\epsilon_m-\epsilon_n}\;+$$

$$+\;\frac{1}{\epsilon_k+\epsilon_\ell-\epsilon_m-\epsilon_n}\,\frac{1}{\epsilon_j+\epsilon_k+2\epsilon_\ell-\epsilon_m-\epsilon_n-\epsilon_r-\epsilon_s}\,\frac{1}{\epsilon_j+\epsilon_k-\epsilon_r-\epsilon_s}\;=$$

$$=\frac{1}{(\epsilon_k+\epsilon_\ell-\epsilon_m-\epsilon_n)^2}\,\frac{1}{\epsilon_j+\epsilon_k-\epsilon_r-\epsilon_s}\;. \qquad (B.16)$$

This is just the result we would obtain evaluating the insert "on the energy shell" (i.e., with $\delta E = 0$). This proof that hole energies should be computed on the energy shell has been extended to all orders of perturbation theory by Bethe, Brandow and Petschek.

Incidentally, the reason for including only the diagrams of Fig. 14 in the definition of the single particle energy should now be clear: their inclusion can be effected in a simple and natural way. One reason these terms are so easily included is because the only multiple scattering appearing in them is particle-particle scattering.

The "rearrangement energy" diagrams of Fig. 2, which correspond to the derivative terms in (2.34), have not been summed by the propogators defined above. They can be included, however, if the single particle energy (B.9) includes a derivative term such as the "rearrangement" term in (2.34):

$$\omega_p{}' = \epsilon_p + \sum_j K_{jp;(jp)} n_j + \sum_{jk} n_j n_k \frac{\delta}{\delta n_p} K_{jk;(jk)}\;. \qquad (B.17a)$$

As pointed out by Brueckner and Goldman,[21] the last term can be evaluated (in principle) during the numerical solution of the K-

matrix equations by making a definite shift in the population of the Fermi gas near the desired momentum and so determining $\delta K/\delta n_p$ from the finite shift in the K-matrix. The additional computational effort required would be considerable, however. The derivative term above corresponds to altering the definition of the "self-energy" inserts of Fig. 14 to include the second order Pauli-principle violating inserts on the particle lines and the "non-violating" hole inserts. The latter insertions would have to be computed "off-energy-shell" and the former "on-energy-shell" (following arguments identical to those of the previous paragraphs). To see how the terms in Fig. 2 are picked up by using (B.17a), expand the derivative term:

$$\frac{\delta}{\delta n_p} K_{jk;jk} = \frac{\delta}{\delta n_p} \sum_{mn} K_{mn;jk} \frac{(1-n_m)(1-n_n)}{\omega_j'+\omega_k'-\omega_m'-\omega_n'}$$

$$= -2 \sum_{n} \frac{(1-n_n)K_{pn;jk}^2}{\omega_j'+\omega_k'-\omega_p'-\omega_n'} + \sum_{mn} (1-n_n)(1-n_m)K_{mn;jk}^2 \frac{\delta}{\delta n_p} (\omega_j'+\omega_k'-$$

$$-\omega_m'-\omega_n')^{-1} \ . \quad \text{(B.17b)}$$

The first term on the right yields Fig. 2(a) (for $|\underset{\sim}{p}| \leq p_F$) and Fig. 2(b) (for $|\underset{\sim}{p}| > p_F$). This term would be obtained by a first order numerical evaluation of the derivative in (B.17a). The second term in (B.17b) would be obtained by iterating this procedure, and leads to terms corresponding to Fig. 2(c). However, there exist three other diagrams related to Fig. 2(c) in the same manner that 4(f) of Fig. 1 is related to 4(e). Brueckner, Gammel and Kubis[22] have shown that their total contribution to ΔE is only half of the

"on-energy-shell" third order insert involved in Fig. 2(c), and the numerical calculation would have to be modified accordingly.

Brueckner, Gammel and Kubis[22] have also shown that the rearrangement terms contribute only 1.5 Mev (repulsion) to the interaction energy, ΔE. Therefore, the additional complexity involved in computing them as indicated above is probably not justified by the slight improvement to be gained for most purposes. The derivative term in (B.17a) was not included in any of the calculations discussed in this dissertation.

One final feature of the K-matrix formulation must be mentioned. The single particle energies defined by (B.17a) are not identical to the true single particle energies defined by (2.34) because the former are calculated "off-energy-shell" in the two cases in which a singular denominator would be involved. This is the proper procedure for the K-matrix calculations because all the energies involved in the energy expansion are real (barring pairing leading to superfluidity). Therefore, the single particle energies appropriate to K-matrix calculations are not the true energies (which have imaginary terms if away from the Fermi surface because of finite lifetime effects), and the K-matrix energies will not, therefore, satisfy the Bethe-Hugenholtz-Van Hove theorem[8,30] that $E_{Av} = \omega(p_F)$. To check this theorem, it is therefore necessary to compute the single particle energies separately, and "on-energy-shell." This distinction between the K-matrix and the actual single particle energies must be borne in mind in the discussions of the nuclear matter and the finite nucleus calculations.

The final set of equations for the Brueckner approximation is given in Chapter II, (2.11) *et. seq.*

A more direct derivation of the K-matrix approximation is possible with the alternate linked-cluster expansion described in Appendix A in which the unperturbed Hamiltonian is the sum of the kinetic energy operator plus an effective single particle potential, V , and the interaction Hamiltonian is a difference of v and V interactions (A.77). The energy denominators in the BG expansion are then $(E_o - H_o)$, where E_o is now the sum of the kinetic energy and the effective potential. The set of graphs one obtains must then include all possible V interactions as well as v interactions, and V is chosen so that its graphs cancel as many v graphs as possible. Choosing $V_{r;m} = \sum_n v_{rn;(mn)}$ leads to the Hartree-Fock approximation^2 as we have mentioned earlier. Choosing V to be the "self-consistent" energy (2.13) or (2.17) as appropriate leads to Brueckner's K-matrix approximation.

B. BRUECKNER-GAMMEL APPROXIMATION

1. Reduction of the K-Matrix Equation

As pointed out in Chapter III, the nucleon-nucleon potential which is best justified on theoretical grounds is a Yukawa potential (with spin orbit and tensor components) with a repulsive core whose potential is very large (effectively infinite). This singular potential renders usual perturbation theory worthless (because the matrix elements of the potential are singular) and compli-

cates the problem in terms of the reaction matrix. In order to treat the core, it is best to transform the problem from momentum space to configuration space. As we shall see, one consequence of the added complications is that we will be unable to obtain the off-diagonal elements of the K-matrix. However, because the energy is defined in terms of the diagonal elements, this will not be too serious a defect. Its principal effect is to prevent exact calculations of higher order corrections.

The details of the reduction of the K-matrix equation are lucidly discussed by Brueckner and Gammel[3] (BG). We shall therefore present only the essential details.

2. Transformation to Coordinate Space

The reduction to coordinate space is done with plane wave basis states. Total momentum is conserved, so that in (2.19), for instance,

$$\mathbf{p}_k + \mathbf{p}_\ell = \mathbf{p}_m + \mathbf{p}_n = \mathbf{P} \quad , \tag{B.18}$$

where $\mathbf{P}$ is the total momentum. The relative momentum is defined as

$$\mathbf{k} = \tfrac{1}{2}(\mathbf{p}_k - \mathbf{p}_\ell) \quad . \tag{B.19}$$

Since the v's conserve total momentum, the K's do also, and the total momenta appear as parameters in the equations. For example, Eq. (2.12) becomes

$$K(P,\Sigma,\delta E)_{k';k} = v_{k';k} + \sum_{k''} \frac{v_{k';k''}\, K(P,\Sigma,\delta E)_{k'';k} f(P,k'')}{\Sigma - \omega_{P_+}(\Sigma) - \omega_{P_-}(\Sigma) - \delta E} \quad , \qquad (B.20)$$

where

$$\Sigma = \omega_k + \omega_\ell \qquad (B.21)$$

$$\omega_k = \epsilon_k + \sum_\ell K(P, \Sigma{=}\omega_k{+}\omega_\ell, \delta E{=}0)_{k;k} n_\ell \; ; \qquad \underset{\sim}{k} = \tfrac{1}{2}(\underset{\sim}{p}_k - \underset{\sim}{p}_\ell) \qquad (B.22)$$

$$\omega_m(\Sigma) = \epsilon_m + \sum_j K(P,\Sigma,\delta E{=}\Delta)_{k;k} n_j \; ; \qquad \underset{\sim}{k} = \tfrac{1}{2}(\underset{\sim}{p}_m - \underset{\sim}{p}_j) \qquad (B.23)$$

$$P_\pm = \tfrac{1}{2}\underset{\sim}{P} \pm \underset{\sim}{k}'' \quad , \qquad (B.24)$$

and the exclusion principle is enforced by the step function

$$f(P,k'') = 1 \quad \text{if} \quad P_+ > p_F \quad \text{and} \quad P_- > p_F$$
$$= 0 \quad \text{otherwise.} \qquad (B.25)$$

For the calculation of particle energies, Σ is merely a parameter, and is needed only for the range $2\omega_{p_k=0}$ to $2\omega_{p_k=p_F}$.

We now introduce a wave matrix Ω through the defining equation

$$K = V\Omega \quad . \qquad (B.26)$$

In matrix notation

$$K = v + v \frac{Q}{E-H} K \quad , \qquad (B.27)$$

and therefore

$$\Omega = 1 + \frac{Q}{E-H} V\Omega \quad . \qquad (B.28)$$

From (B.28) one obtains with a little manipulation the equation for the true wave function $\Psi_{P,k}(r)$ in terms of the plane-wave basis functions,

$$\psi_{P,k}(r) = (r|\Omega|k) = (r|k) + (r|\,\frac{Q}{E-H}\,V\Omega|k)$$

$$= \varphi_k(r) + \sum_{k''k'''} \int dr' \int dr'' (r|k'')(k''|\,\frac{Q}{E-H}\,|k''')(k'''|r'') \quad (B.29)$$

$$(r''|v|r')\,\psi_{P,k}(r') \;.$$

However, v is a local potential and Q/(E-H) is diagonal in momentum space, so that (B.29) reduces to

$$\psi_{P,k}(r) = \varphi_k(r) + \int dr' G_{P,k}(r,r')v(r')\psi_{P,k}(r') \;, \qquad (B.30)$$

where the Green's function is defined by

$$G_{P,k}(r,r') = \sum_{k''} \frac{\varphi_{k''}(r)\varphi_{k''}(r')f(P,k'')}{\Sigma-\omega_{P_+}(\Sigma)-\omega_{P_-}(\Sigma)-\delta E} \;. \qquad (B.31)$$

Thus, (B.26) gives

$$(k'|K|k) = \int dr \int dr' \sum_{k''} (k'|r')(r'|v|r')(r'|k'')(k''|r)(r|\Omega|k)$$

$$= \int dr\, \varphi_{k'}(r)\, v(r)\, \psi_k(r) \;. \qquad (B.32)$$

3. Partial Wave Expansion

The next step in the reduction of the K-matrix equations is the partial wave expansion. The employment of this technique is an approximation since the partial wave expansion is rigorously correct only when the energy denominators in e.g. (B.31) and the Pauli principle (B.25) do not depend on the angle between $\underset{\sim}{P}$ and $\underset{\sim}{k}''$. This is the case for two-body scattering, where $f(P,k'') \equiv 1$ and $\omega_{P_\pm}(\Sigma) = P_\pm^2/2M$, but it is not true in the many-body case for

$P \neq 0$. One then has two choices: (1) assume $P = 0$ and proceed rigorously from there, with that as the only additional approximation or, (2) treat the angular dependence of the total momentum in some average fashion. The dependence of the results on the total momentum has been found to be small,[3] and either approximation will introduce errors which are expected to be smaller than other uncertainties of the method (e.g., the higher order diagrams in the BG expansion which are neglected). The second procedure is expected to be the better approximation, and it is used in the BG and BM calculations. To decouple the dependence of the Green's function on $\underset{\sim}{P}$ and $\underset{\sim}{k}''$, we use the angular average of the quantities affected. Thus (B.25) becomes

$$\begin{aligned} f(P,k'') &= 0 && k''^2 + \tfrac{1}{4}P^2 \leq p_F^{\ 2} \\ &= 1 && k'' - \tfrac{1}{2}P > p_F \\ &= \frac{k''^2 + \frac{1}{2}P^2 - p_F^{\ 2}}{k''P} && \text{otherwise} \end{aligned} \qquad (B.33)$$

and, for use in calculating $P_{\pm}$ for the excitation energies in (B.31)

$$P_{\pm}^{\ 2} \to \tfrac{1}{2}P^2 + k''^2 \pm (1/\sqrt{3}) f^2(P,k'')Pk'' \ . \qquad (B.34)$$

The latter substitution removes the angular dependence between $\underset{\sim}{P}$ and $\underset{\sim}{k}''$ so that the summation over $\underset{\sim}{k}''$ reduces to an integral over the magnitudes of $\underset{\sim}{k}''$ alone.

The partial wave expansion then proceeds exactly as in the usual two-body scattering problem, and has been treated in considerable detail by Brueckner and Gammel.[3] The plane wave basis func-

tions, $\varphi_k(r) = \exp(i\underset{\sim}{k}\cdot\underset{\sim}{r})\,\chi_s^{m_s}$ ($\chi_s^{m_s}$ are the spin functions), are expanded in partial waves, $j_\ell(kr)$. In the presence of the tensor force, the orbital angular momentum ℓ is not a constant of the motion, but J , the total angular momentum, is. The expansion is recast (via Clebsch-Gordon coefficients) in terms of the total angular momentum, J , and the spin, s , and involves $j_\ell(kr)$ for $\ell = J$ and $\ell = J \pm 1$ and the corresponding eigenfunction of J , $F_\ell^{Jm_Js}$. A similar expansion for the coordinate space wave function ψ also involves the coupled states noted above. The two solutions which are generated from the orthogonal unperturbed solutions are defined so that under the action of the tensor force

$$j_{J-1}F_{J-1}^{Jm_Js} \rightarrow U_{J-1,J-1}^{Js}F_{J-1}^{Jm_Js} + U_{J-1,J+1}^{Js}F_{J+1}^{Jm_Js} ,$$

and (B.35)

$$j_{J+1}F_{J+1}^{Jm_Js} \rightarrow U_{J+1,J-1}^{Js}F_{J-1}^{Jm_Js} + U_{J+1,J+1}^{Js}F_{J+1}^{Jm_Js} .$$

The angular momentum expansion of the Green's function is

$$G(r,r') = \sum_\ell (2\ell+1)\, G^\ell(r,r')\, Y_\ell^0(\hat{r},\hat{r}')\,[4\pi/(2\ell+1)]^{\frac{1}{2}} ,$$

with

$$G^\ell_{P,k}(r,r') = \frac{1}{2\pi^2}\int_0^\infty \frac{k''^2dk''\; j_\ell(k''r)\; j_\ell(k''r')\; f(P,k'')}{\Sigma-\omega_{P_+}(\Sigma)-\omega_{P_-}(\Sigma)-\delta E} . \qquad \text{(B.36)}$$

We have used

$$\sum_{k''} \rightarrow (2\pi)^{-3}\int d\underset{\sim}{k}''$$

and have done the integration over angles of $\underset{\sim}{k}''$. Substituting the appropriate partial wave expansions and the Green's function expansion into (B.30) for $\psi_{P,k}(r)$, and then integrating over angles of $\underset{\sim}{r}$ and doing those summations which can be done immediately leads to the following equation for the $U_{\ell\ell'}{}^{Js}(P,k,r)$:

$$U_{\ell\ell'}{}^{Js}(P,k,r) = j_\ell(kr)\delta_{\ell\ell'} + 4\pi \sum_{\ell''} \int r'^2 dr' \, G_{P,k}^{\ell'}(r,r') V_{\ell'\ell''}{}^{Js}(r') \, U_{\ell\ell''}{}^{Js}(P,k,r') \; . \qquad (B.37)$$

The $V_{\ell'\ell''}{}^{Js}$ are defined in Chapter III, (3.17). For $s = 0$, only $\ell = \ell' = \ell'' = J$ is possible, and (B.37) has a very simple appearance. For $s = 1$, the only allowed values of the orbital quantum numbers are J or $J \pm 1$; the latter possibility leads to pairs of coupled equations for the $U(r)$ for $\ell \le 3$.

4. Treatment of the Hard Core

Because the procedure for handling the core, where $V(r')$ is infinitely repulsive, is similar for all ℓ , we suppressed the indices to obtain

$$U(r) = U_0(r) + 4\pi \int_0^\infty G(r,r')V(r')U(r')r'^2 dr' \; . \qquad (B.38)$$

We separate the integral into two parts, 0 to r_c (the radius of the hard core potential) and r_c to infinity. The latter integration causes no trouble. The first integral presents a problem because $U(r' \le r_c) = 0$ and therefore $V(r')U(r')$ is indeterminate within the core. In analogy with the treatment for the usual

scattering problem, we make the replacement

$$V(r')U(r') = \lambda\ \delta(r'-r_c) \qquad r'<r_c \tag{B.39}$$

where λ is chosen to make $U(r')$ vanish at the core. This substitution is exact for two-body scattering, but leads to a small error for the many-body problem (because it cannot be shown that the equation for $U(r)$ which we are about to derive vanishes inside the core). Bethe and Goldstone[100] and Brueckner and Gammel[3] have shown this error to be negligible for hole energies (less than 0.1% of the K-matrix). The error in particle energies is discussed further in Chapter IV. Putting (B.39) into (B.38), we find

$$U(r) = U_o(r) + 4\pi r_c^{\,2} G(r,r_c)\lambda + 4\pi \int_{r_c}^{\infty} G(r,r')V(r')U(r')r'^2dr' \ . \tag{B.40}$$

The condition $U(r_c) = 0$ then fixes λ. We set $r=r_c$ in (B.40) and solve for λ. Substituting this solution back into (B.40) yields

$$U(r) = s(r) + 4\pi \int_{r_c}^{\infty} F(r,r')V(r')U(r')r'^2dr' \ , \tag{B.41}$$

where

$$s(r) = U_o(r) - U_o(r_c)G(r,r_c)/G(r_c,r_c) \ , \text{ and}$$

$$F(r,r') = G(r,r') - G(r,r_c)G(r_c,r')/G(r_c,r_c) \ . \tag{B.42}$$

Restoring indices, we have

$$U_{\ell\ell'}^{Js}(P,k,r) = s^{\ell}_{P,k}(r)\delta_{\ell\ell'} + 4\pi \int_{r_c}^{\infty} F^{\ell'}_{P,k}(r,r')V_{\ell'\ell''}^{Js}(r')U_{\ell\ell''}^{Js}(P,k,r')\, r'^2dr' \tag{B.43}$$

with

$$s^{\ell}_{P,k}(r)=j_{\ell}(kr)-j_{\ell}(kr)\dot{G}^{\ell}_{P,k}(r,r_c)/G^{\ell}_{P,k}(r_c,r_c) \qquad (B.44)$$

$$F^{\ell}_{P,k}(r,r') = G^{\ell}_{P,k}(r,r') - G^{\ell}_{P,k}(r,r_c)G^{\ell}_{P,k}(r_c,r')/G^{\ell}_{P,k}(r_c,r_c). \qquad (B.45)$$

5. Determination of the K-Matrix Elements

We find the diagonal elements of the K-matrix by substituting our partial wave expansions into (B.32). We can perform the summation over projections of the spins explicitly, and after some algebra of Clebsch-Gordon coefficients and a treatment of the core similar to the treatment for the wave functions, we obtain

$$(k|K|k) = \sum_{Js}\sum_{\ell=J-1}^{J+1} C_{J\ell s}\Big\{\frac{-j_{\ell}^{2}(kr_c)}{G^{\ell}_{P,k}(r_c,r_c)} + 4\pi\int_{r_c}^{\infty} r^2 dr\, s^{\ell}_{P,k}(r) \sum_{\ell'=J-1}^{J+1}$$

$$V_{\ell\ell'}{}^{Js}U_{\ell\ell'}{}^{Js}(P,k,r) \; . \qquad (B.46)$$

The first term on the right is the (repulsive) core contribution (G is negative at the core). Note that the sum over m_s has been performed and yields the same factor (one) for both singlet and triplet states. The coefficient $C_{J\ell s}$ is the statistical weight of the state and s is the spin. In infinite nuclear matter we assume that the number of neutrons and protons are equal and that the Fermi momenta for neutrons and protons are equal. Further, we assume the nuclear potential to be charge-independent; K is therefore independent of T_z, the z-component of isotopic spin. Thus, for example, the energy of a proton with a given momentum must be equal

to the energy of a neutron with the same momentum. Finally, the only dependence of the K's on m_s was through certain Clebsch-Gordon coefficients, so the sum of m_s from -1 to 1 (for the triplet state) could be done. The product of spin, isotopic spin and space exchange is -1 (Pauli principle), so the exchange term contributes a factor 0 or 2 for like particles depending on the state. To assist us in assigning the proper statistical weights, we classify the possible states of two nucleons as indicated in Table IX.

Spin	Orbital State	Isotopic Spin	Possible Particle Pairs	Weight
Singlet	Even	Triplet	N-P, N-N, P-P	$\frac{3}{2}(2J+1)$
Triplet	Even	Singlet	N-P	$\frac{1}{2}(2J+1)$
Singlet	Odd	Singlet	N-P	$\frac{1}{2}(2J+1)$
Triplet	Odd	Triplet	N-P, N-N, P-P	$\frac{3}{2}(2J+1)$

Table IX. Possible states of 2 nucleons and their contributions to the statistical weights.

Contributing to the statistical weights noted above, there is a factor two for two particles per momentum state and the usual $(2J + 1)$ factor. To assign the proper weight, we need only look at the contributions for a given particle, say a proton:

$$K(\text{proton}) = \sum_J (2J+1) \Big\{ \frac{1}{4} \times 2 \times 2 \left(K_{\substack{\text{singlet} \\ \text{even}}}\right)_{\text{proton}} + \frac{1}{4} \times 2 \times 2$$

$$(K_{\substack{\text{triplet}\\ \text{odd}}})_{\text{proton}} + \frac{1}{4} \quad 2 \Big[(K_{\substack{\text{singlet}\\ \text{even}}}) + (K_{\substack{\text{singlet}\\ \text{odd}}}) \Big]_{\text{neutron}}$$

$$+ \frac{1}{4} \times 2 \Big[(K_{\substack{\text{triplet}\\ \text{even}}}) + (K_{\substack{\text{triplet}\\ \text{odd}}}) \Big]_{\text{neutron}} \Big\} . \qquad (B.47)$$

The factors are: $\frac{1}{4}$ (for the number of spin states), 2 (number of particles per momentum state), and 2 (exchange, for proton only). The sum over m_s was performed in (B.46) and yielded one for singlet and triplet states. Therefore, the "average" value of the sum over the triplet states was $1/3$, which multiplied by the triplet state probability, $3/4$, just gives the factor $\frac{1}{4}$ which is indicated above. The $C_{J\ell s}$ are thus

$$\begin{aligned} C_{J\ell s} &= \frac{3}{2}\,(2J+1) \quad \begin{array}{l}\text{singlet-even or}\\ \text{triplet-odd}\end{array} \\ &= \frac{1}{2}\,(2J+1) \quad \begin{array}{l}\text{singlet-odd or}\\ \text{triplet-even}\end{array} . \end{aligned} \qquad (B.48)$$

The $C_{J\ell s}$ in Eq. (2.7) of BM differ from the above by a factor of $3/2$: this factor has been included in the numerical factors in Eq. (2.8) of that paper.

6. Single Particle Energies

Equations (B.22) and (B.23) for the single particle energies now become

$$\omega_{\underset{\sim}{p}} = \frac{p^2}{2m} + V(p) \qquad (B.49)$$

where

$$V(p) = \sum_{\underset{\sim}{q}} K_{p,q;p,q}\, n_q \, , \qquad \text{(B.50)}$$

$K_{p,q;p,q}$ being computed on-energy shell ($\delta E = 0$) for $|p| \leq p_F$ and off-energy shell ($\delta E = \Delta$) for $|p| > p_F$. The average binding energy per particle, E_{Av}, is then given by

$$E_{Av} = \frac{\int_0^{p_F} p^2 dp \left[\frac{p^2}{2m} + \frac{1}{2} V(p) \right]}{\int_0^{p_F} p^2 dp} \; . \qquad \text{(B.51)}$$

The factor $\frac{1}{2}$ is simply a consequence of the fact that $V(p)$ is the potential between pairs of particles, and the integral sums over pairs twice.

7. Computational Procedure

The Brueckner-Gammel[3] computation solved these equations by iteration for S, P and D states as follows:

1) A table of $\omega_p (p < p_F)$ and $\omega_{p'}(\Sigma)(p' > p_F)$ was formed, with the initial guess of ω_p and $\omega_{p'}(\Sigma)$ just the kinetic energies $p^2/2M$ and $p'^2/2M$. Five p values were selected $(0.1(0.2)0.9\ p_F)$ and a three by five matrix of p' and Σ values $(p' = 1.1(0.5)2.1\ p_F$ and Σ varying between $\omega_{p=0}$ and $2\omega_{p_F})$. For $p' \geq 2.6\ p_F$, $\omega_{p'}(\Sigma)$ was always approximated by the kinetic energy alone, $p'^2/2M$, an approximation which was checked and found to introduce negligible error since, in this approximation,

$V(p') \xrightarrow[p' \geq 2.6 p_F]{} 0$.

2) The Green's functions (B.36) and (B.45) were computed by numerical integration to a very large value and an approximate analytical correction was used for the remainder of the integral. The Green's functions were required for every entry in the energy table, for every value of r and r' used in the numerical solutions, and for every magnitude and angle of $\underset{\sim}{q}$ in (B.50) with respect to $\underset{\sim}{p}$ (five each).

3) The wave functions (B.43) were computed by replacing the integral equations by sets of simultaneous linear equations and solving them by matrix inversion.

4) The K-matrix equation (B.46) was then integrated numerically.

5) Finally, the single particle energies (B.49) and the mean energy (B.50) were computed, and the energy table was updated for the next major iteration.

The next iteration began with step 2 above, and continued until the new energies agreed sufficiently well with the old ones. Five iterations, starting with the kinetic energies as a first guess, sufficed to make the new energy table agree with the old one to one part in 10^5. It must be emphasized that the most difficult part of the computation, and the most time consuming, was the computation of the many Green's functions.

We have discussed the above computational details to emphasize the magnitude of the computational problem for the very accurate solution of Brueckner's equations. The results of the computation

are discussed in Chapter IV.

APPENDIX C

TRANSFORMED BRUECKNER-GOLDSTONE EXPANSION

In the text it is shown that $\Delta E(\rho, w)_{BG}$ can be defined such that

$$\Delta E(\rho, w)_{BG} = \Delta E(n, \epsilon)_{BG} \tag{C.1}$$

where $\Delta E(n, \epsilon)_{BG}$ is the Brueckner-Goldstone linked-cluster expansion for the interaction energy of a system of interacting Fermions in their ground state. $\Delta E(\rho, w)_{BG}$ has the same functional form as $E(n, \epsilon)_{BG}$ with the true densities (given by (2.23) instead of the Fermi step functions, n, and the energy variables w in place of the free kinetic energies, ϵ. In this Appendix we prove that

$$w_k = \epsilon_k - \Delta\epsilon_k + O(v^2) \tag{C.2}$$

where $\Delta\epsilon_k$ is given by (2.31) and the correction by the last term of (2.75). Further, we shall prove that

$$\Delta E(\rho, \epsilon)_{\substack{\text{no self-energy}\\ \text{terms}}} = \Delta E(n, \epsilon)_{BG} + O(v^4) \ . \tag{C.3}$$

We shall actually show that the errors are $O(t^2)$ and $O(t^4)$ respectively, where t is the t-matrix defined by (B.1).

Now let us look at the correction term in (2.75). We will employ a Taylor series expansion about $\lambda = 0$. To expand

$$w_k = \epsilon_k - \Delta\epsilon_k - \Delta n_k \int_0^1 d\lambda' \left[\frac{\dfrac{\delta \Delta E(\rho(\lambda'),w(\lambda'))}{\delta \rho_k(\lambda')}}{\dfrac{\delta \Delta E(\rho(\lambda'),w(\lambda')}{\delta w_k(\lambda')}} - \frac{\Delta\epsilon_k}{\Delta n_k} \right] \qquad (C.4)$$

we need

$$\frac{d}{d\lambda} = \sum_j \left(\frac{d\rho_j(\lambda)}{d\lambda} \frac{\delta}{\delta \rho_j(\lambda)} + \frac{dw_j(\lambda)}{d\lambda} \frac{\delta}{\delta w_j(\lambda)} \right)$$

$$= \sum_j n_j \left(\frac{\delta}{\delta \rho_j(\lambda)} - \frac{\dfrac{\delta \Delta E(\rho(\lambda),w(\lambda))}{\delta \rho_j(\lambda)}}{\dfrac{\delta \Delta E(\rho(\lambda),w(\lambda))}{\delta w_j(\lambda)}} \frac{\delta}{\delta w_j(\lambda)} \right) \qquad (C.5)$$

from (2.73), (2.75) and (2.22). Thus, if we expand the integrand in (2.75) about $\lambda = 0$ and integrate, we obtain

$$w_k = \epsilon_k - \Delta\epsilon_k - \Delta n_k \sum_{\ell=1}^{\infty} \frac{1}{(\ell+1)!} \sum_{j_1} \cdots \sum_{j_\ell} \Delta n_{j_1} \cdots \Delta n_{j_\ell} \prod_{m=1}^{\ell} \left(\frac{\delta}{\delta n_{j_m}} - \frac{\dfrac{\delta \Delta E(n,\epsilon)}{\delta n_{j_m}}}{\dfrac{\delta \Delta E(n,\epsilon)}{\delta \epsilon_{j_m}}} \frac{\delta}{\delta \epsilon_{j_m}} \right) \frac{\Delta\epsilon_k}{\Delta n_k} . \qquad (C.6)$$

From (2.22) and (2.31)

$$\frac{\delta \Delta E(n,\epsilon)}{\delta \epsilon_j} = \Delta n_j \qquad \frac{\delta \Delta E(n,\epsilon)}{\delta n_j} = \Delta\epsilon_j . \qquad (C.7)$$

Thus, the $\ell = 1$ term in the above correction term is:

$$- \Delta n_k \frac{1}{2} \sum_j \Delta n_j \left(\frac{\delta}{\delta n_j} - \frac{\Delta\epsilon_j}{\Delta n_j} \frac{\delta}{\delta\epsilon_j} \right) \frac{\Delta\epsilon_k}{\Delta n_k} \tag{C.8}$$

$$= - \frac{1}{2} \sum \Big\{ \Delta n_j \frac{\delta}{\delta n_j} \Delta\epsilon_k - \frac{\Delta n_j \Delta\epsilon_k}{\Delta n_k} \frac{\delta}{\delta n_j} \Delta n_k -$$

$$- \Delta\epsilon_j \frac{\delta}{\delta\epsilon_j} \Delta\epsilon_k + \frac{\Delta\epsilon_j \Delta\epsilon_k}{\Delta n_k} \frac{\delta}{\delta\epsilon_j} \Delta n_k \Big\} . \tag{C.9}$$

To evaluate (C.9), we need the following expressions

$$\Delta\epsilon_k = \frac{\delta}{\delta n_k} \Delta E(n,\epsilon) = \sum_\ell t_{k\ell;(k\ell)} n_\ell + \ldots \tag{C.10}$$

$$\frac{\delta}{\delta\epsilon_q} t_{ij;k\ell} = \sum_{mn} t_{mn;ij} \frac{(1-n_m)(1-n_n)}{(\epsilon_k+\epsilon_\ell-\epsilon_m-\epsilon_n)^2} t_{mn;k\ell} \left(\delta_{mq}+\delta_{nq}-\delta_{kq}-\delta_{\ell q}\right) \tag{C.11}$$

(which is obtained from (C.10) by expanding the t-matrices and doing the differentiation), and

$$\Delta n_q = -n_q \sum_{\ell mn} t_{mn;q\ell} \frac{n_\ell(1-n_m)(1-n_n)}{(\epsilon_q+\epsilon_\ell-\epsilon_m-\epsilon_n)^2} t_{mn;(q\ell)} + \ldots$$

$$+ (1-n_q) \sum_{k\ell n} t_{qn;k\ell} \frac{n_k n_\ell (1-n_n)}{(\epsilon_k+\epsilon_\ell-\epsilon_q-\epsilon_n)^2} t_{qn;(k\ell)} + \ldots . \tag{C.12}$$

With the above equations, we can easily verify that all but the last term of (C.9) are of order t^3 and that the last term is $O(t^2)$,

proving (C.2).

In order to demonstrate (C.3), we note that the equation for $\Delta E(\rho,\epsilon)$ without self-energy terms is

$$\Delta E(\rho,\epsilon)_{\substack{\text{no self-energy}\\ \text{terms}}} = \frac{1}{2}\sum_{k\ell} t_{k\ell;(k\ell)}\, \rho_k \rho_\ell + \text{hole-hole term and 3-body cluster of } O(t^3) + O(t^4) \,. \qquad (C.13)$$

Since the zero order ρ_k is n_k (see (2.23)), the third order terms included in (C.13) are the same as the corresponding terms in $\Delta E(n,\epsilon)_{BG}$. The third order self-energy term must therefore be shown to come from the first term on the right in (C.13) if the equation is to be proved correct to fourth order. Using $\rho_k = n_k + \Delta n_k$ and (C.12) for Δn_k, we obtain

$$\frac{1}{2}\sum_{k\ell} t_{k\ell;(k\ell)}\, n_k n_\ell + \frac{1}{2}\sum_{k\ell} t_{k\ell;(k\ell)}\, n_k \Delta n_\ell + \frac{1}{2}\sum_{k\ell} t_{k\ell;(k\ell)}\, \Delta n_k n_\ell + O(t^4)$$

$$= \frac{1}{2}\sum_{k\ell} t_{k\ell;(k\ell)}\, n_k n_\ell - \frac{1}{2}\sum_{k\ell mn} t_{mn;k\ell}\, \frac{n_k n_\ell (1-n_m)(1-n_n)}{(\epsilon_k+\epsilon_\ell-\epsilon_m-\epsilon_n)^2}\, t_{mn;(k\ell)} \times$$

$$\times \sum_j (t_{jk;(jk)} + t_{j\ell;(j\ell)} - t_{jm;(jm)} - t_{jn;(jn)})n_j \,. \qquad (C.14)$$

A rearrangement of terms and a change of summation indices was required to obtain the last term. We have again used the fact that ρ_k is equal to n_k in lowest order. The last term above is just the third-order self-energy term in (C.7), so that $\Delta E(\rho,\epsilon)$ without

self-energy terms is indeed equal to $\overline{E}(n,$ [illegible] $)_{BG}$ through third order, proving (C.3). There is a difference in fourth order which would lead to an error in the mean energy of nuclear matter estimated to be of the order of 2 MeV.

APPENDIX D

COMPARISON OF PUFF EQUATIONS AND BG EXPANSION

In this appendix the second order difference between the Puff equations and the BG expansion are evaluated in the limit $\omega_k = \epsilon_k$. Using (6.46), this difference may be written (in the above limit) as

$$\delta\left(\frac{E}{N}\right)^2 = -4\rho^{-1}\left\{\frac{1}{2}\frac{\partial}{\partial\eta}\sum_{\substack{k\ell\le p_F\\ \text{all } mn}} v_{k\ell;mn}\,\frac{\partial\epsilon_{p_F}-\epsilon_m-\epsilon_n}{\eta+\epsilon_k+\epsilon_\ell-\epsilon_m-\epsilon_n}\,v_{mn;(k\ell)}\bigg|_{\eta=0}\right. +$$

$$\left. +\frac{1}{2}\sum_{\substack{k\ell\le p_F\\ mn>p_F}} v_{k\ell;mn}\,\frac{1}{\epsilon_k+\epsilon_\ell-\epsilon_m-\epsilon_n}\,v_{mn;(k\ell)}\right\} \tag{D.1}$$

where

$$\rho = 4\sum_{k\le p_F} 1 \ . \tag{D.2}$$

The Yamaguchi S-state separable potential[75] (see Appendix E) has been used to evaluate this difference. Taking the first integral first, we have

$$-4\rho^{-1}\,\frac{1}{2}\int v_{p;p'}\,\frac{M}{p^2-p'^2}\,v_{p';p}\,d\underset{\sim}{p}\,d\underset{\sim}{p}'\,d\underset{\sim}{P} = -\frac{4\lambda^2}{2M\rho}\int\frac{C^2(p)C^2(p')}{p^2-p'^2}\,d\underset{\sim}{p}\,d\underset{\sim}{p}'\,d\underset{\sim}{P}. \tag{D.3}$$

The integrals over angles can be done immediately. Choosing $\underset{\sim}{P}$ as the polar axis (and then doing the integral over angles of $\underset{\sim}{P}$) leads to

$$\int d\Omega_{\underset{\sim}{p}}\, d\Omega_{\underset{\sim}{p}} = 4\pi \qquad p < p_F - \frac{1}{2} P$$

$$= 0 \qquad p > \sqrt{p_F^{\,2} - \frac{1}{4}P^2} \qquad \text{(D.4)}$$

$$= \frac{4\pi(b^2-p^2)}{pP} \qquad \text{otherwise}$$

where $b = p_F + \frac{1}{2} P$. The integral over the angles of $\underset{\sim}{P}$ gave 4π . The p' integration is just $-J(p,P)$ of Appendix E (E.11)

$$- \int \frac{C^2(p')d\underset{\sim}{p}'}{p^2-p'^2} = - J(p,P) \ . \qquad \text{(D.5)}$$

The density, ρ , is given by (D.2) and is just $4(4\pi/3)p_F^{\,3}$. Therefore, the integral to be evaluated is

$$- \sum_s C_s \frac{12\pi\lambda^2}{2M_p p_F^{\,3}} \int_0^{p_F} C^2(p)p^2 dp \left[\int_0^{2(p_F-p)} P^2 dP J(p,P) + \right.$$

$$\left. + \int_{2(p_F-p)}^{2\sqrt{p_F^{\,2}-p^2}} P^2 dP \cos\alpha\, J(p,P) \right] \qquad \text{(D.6)}$$

where C_s is the appropriate statistical factor (3/2 for singlet and triplet states) and where $\cos\alpha$ is given by

$$\cos\alpha = \frac{p_F^{\,2}-p^2-\frac{1}{4}P^2}{pP} = \frac{a^2-p^2}{pP} \ . \qquad \text{(D.7)}$$

The first of the integrals in (D.1) is

$$\lim_{\eta \to 0} - \frac{4\lambda^2}{2M\rho} \frac{\partial}{\partial \eta} \int \frac{C^2(p)C^2(p')(a^2-p'^2)}{\eta + p^2 - p'^2} \, d\underset{\sim}{p} \, d\underset{\sim}{p}' \, d\underset{\sim}{P} = \frac{3\pi\lambda^2}{M p_F^3} \int_0^{p_F}$$

$$C^2(p)p^2dp \left[\int_0^{2(p_F-p)} P^2dP + \int_{2(p_F-p)}^{2\sqrt{p_F^2-p^2}} P^2dP \cos\alpha \right]$$

$$\times \left(\lim_{\eta \to 0} \frac{\partial}{\partial \eta} \int_0^{\infty} \frac{p'^2dp'(a^2-p'^2)}{(\eta+p^2-p'^2)(\beta^2+p'^2)^2} \right) . \qquad (D.8)$$

We do the p' integration, keeping only the principal part:

$$- \lim_{\eta \to 0} \frac{\partial}{\partial \eta} 4\pi \int_0^{\infty} \frac{(a^2-p'^2)p'^2dp'}{(\beta^2+p'^2)^2(\eta+p^2-p'^2)} =$$

$$= \lim_{\eta \to 0} \frac{\partial}{\partial \eta} \frac{\partial}{\partial \beta^2} \frac{4\pi}{2} \int_{-\infty}^{\infty} \frac{(a^2-p'^2)p'^2dp'}{(\beta^2+p'^2)(\eta+p^2-p'^2)} . \qquad (D.9)$$

This integral is easily evaluated by contour integration. Closing above, we obtain for the principal value

$$\lim_{\eta \to 0} 2\pi \frac{\partial}{\partial \eta} \frac{\partial}{\partial \beta^2} \frac{(a^2+\beta^2)\beta^2}{\beta(\beta^2+p^2+\eta)} - \frac{\pi^2}{\beta(\beta^2+p^2)^3} \left[a^2p^2 - 3\beta^2(a^2-p^2) - \beta^4 \right] . \qquad (D.10)$$

The remaining integrals in (D.8) are the same as those in (D.7). Thus, the integrands can be combined to yield the following kernel:

$$F(p,P) = \frac{\pi^2}{\beta(\beta^2+p^2)^3} \left[a^2p^2 - 3\beta^2(a^2-p^2) - \beta^4 \right] + J(p,P) \qquad (D.11)$$

where $J(p,P)$ is given by (E.19). The last two integrals were

performed numerically on the CDC-1604 computer at the University of California, San Diego:

$$\delta\left(\frac{E}{N}\right)^2 = \sum_s C_s \frac{6\pi\lambda^2}{M\,p_F^{\,3}} \int_o^{p_F} \frac{p^2 dp}{(\beta^2+p^2)^2} \left[\int_o^{2(p_F-p)} P^2 dP F(p,P) + \right.$$

$$\left. + \int_{2(p_F-p)}^{2\sqrt{p_F^{\,2}-p^2}} P^2 dP \cos\alpha \, F(p,P) \right] . \qquad \text{(D.12)}$$

The result was -59 MeV for $p_F = 1.48\ F^{-1}$. The value of the second Born approximation (the negative of the integral over $J(p,P)$ alone) was -8 MeV. However, it must be expected that the inclusion of higher order corrections (in particular, of the self-consistent denominators) will considerably reduce the above difference, and therefore this value is not quantitatively meaningful so far as the error-analysis of the Puff approximation is concerned. It does indicate that the second order differences do not vanish or cancel identically, however.

APPENDIX E

EVALUATION OF MOMENTUM DENSITY WITH SEPARABLE POTENTIAL

In this appendix we evaluate the momentum density

$$\rho_q = 1 - \sum_{\ell mn} t_{q\ell;mn} \frac{n_\ell(1-n_m)(1-n_n)}{(\epsilon_q+\epsilon_\ell-\epsilon_m-\epsilon_n)^2} t_{mn;(q\ell)} + \dots \qquad k_q \leq p_F$$

$$= \sum_{k\ell n} t_{k\ell;qn} \frac{n_k n_\ell(1-n_n)}{(\epsilon_k+\epsilon_\ell-\epsilon_q-\epsilon_n)^2} t_{qn;(k\ell)} + \dots \qquad k_q > p_F \tag{E.1}$$

to second order in the t-matrix defined in Appendix B (B.1). We use the Yamaguchi[75] two-body separable potential

$$(p'|v|p) = \frac{(-\lambda/M)}{(\beta^2+p^2)(\beta^2+p'^2)} = -\left(\frac{\lambda}{M}\right)C(p)C(p') \tag{E.2}$$

acting in singlet and triplet S-states only, with the following values of the parameters:

$$\lambda_S = 14.95\ \alpha^3 \qquad \lambda_T = 33.45\ \alpha^3$$

$$\beta_S = 5.4\ \alpha \qquad \beta_T = 6.26\ \alpha \tag{E.3}$$

$$\alpha = 0.2316\ F^{-1}$$

The above parameters were chosen to fit the appropriate equations in which sums are directly converted into integrals without the usual factor $(2\pi)^{-3}$. Therefore, we shall use the same convention throughout this Appendix, where appropriate.

Although (E.1) cannot be easily solved for local potentials because of the extreme difficulty of obtaining the off-diagonal elements of the t-matrix, it is not very difficult to solve with a separable potential. The integral equation to be solved to obtain the off-diagonal t-matrix elements is:

$$(p'|t|p) = (p'|v|p) + M \int\limits_{|p'' \pm \frac{1}{2} P| > p_F} d^3p'' \, \frac{(p'|v|p'')(p''|v|p)}{p^2 - p''^2} \quad . \tag{E.4}$$

It is easily shown that the integration over the angles of p'' leads to

$$\begin{aligned} \int d\Omega_{p''} &= 4\pi & & p'' > p_F + \frac{1}{2} P \\ &= 0 & & p'' < \sqrt{p_F^2 - \frac{1}{4} P^2} \\ &= 4\pi \, \frac{p'' + \frac{1}{4} P^2 - p_F^2}{p'' P} = 4\pi \cos \alpha & & \text{otherwise} \ . \end{aligned} \tag{E.5}$$

To solve for the t-matrix, we assume

$$(p'|t|p) = A(p'|v|p) \ . \tag{E.6}$$

Then, from (E.4)

$$A = 1 + (-\lambda) A \int\limits_{|p''| > p_F} \frac{C^2(p'') d^3p''}{p^2 - p''^2} = 1 + \lambda A J(p) \tag{E.7}$$

where

$$J(p) = \int_{|p''|>p_F} \frac{C^2(p'')\,d^3p''}{p''^2-p^2} \quad . \tag{E.8}$$

The solution of (E.7) is

$$A = \frac{1}{1-\lambda J(p^2)} \tag{E.9}$$

so that

$$(p'|t|p) = \frac{-(\lambda/M)C(p')C(p)}{1-\lambda J(p)} \quad . \tag{E.10}$$

Explicitly, we must evaluate

$$J(p) = J(p,P) = 4\pi \int_{\sqrt{p_F^2 - \frac{1}{4}P^2}}^{p_F+\frac{1}{2}P} \frac{\cos\alpha\, C^2(p'')}{p''^2 - p^2}$$

$$p''^2dp'' + 4\pi\int_{p_F+\frac{1}{2}P}^{\infty} \frac{C^2(p'')}{p''^2-p^2}\, p''^2dp'' \tag{E.11}$$

where

$$\cos\alpha = \frac{p''^2 + \frac{1}{4}P^2 - p_F^2}{p''P} \quad . \tag{E.12}$$

In the second integral, we note that p'' is never less than p in our calculations (this can be verified from our final equations and from the fact that we will extrapolate to the densities at momenta of zero and p_F). This being the case, the integrals involved are standard integrals, and we obtain

$$4\pi\int_b^\infty \frac{p''^2 dp''}{(\beta^2+p''^2)^2(p''^2-p^2)} = -4\pi\frac{\partial}{\partial\beta^2}\left\{\frac{1}{\beta^2+p^2}\left[\int_b^\infty \frac{p^2 dp''}{(p''^2-p^2)}\right.\right.$$

$$\left.\left.+\int_b^\infty \frac{\beta^2 dp''}{(\beta^2+p''^2)}\right]\right\}$$

$$= -4\pi\frac{\partial}{\partial\beta^2}\left\{\frac{1}{\beta^2+p^2}\left[\frac{p}{2}\ell n\frac{b+p}{b-p}+\right.\right.$$

$$\left.\left.+\frac{\pi\beta}{2}-\beta\tan^{-1}\frac{b}{\beta}\right]\right\}$$

$$= \frac{4\pi}{(\beta^2+p^2)^2}\left\{\frac{\beta^2-p^2}{2\beta}\left(\frac{\pi}{2}-\tan^{-1}\frac{b}{\beta}\right)-\right.$$

$$\left.-\frac{b(\beta^2+p^2)}{2(\beta^2+b^2)}\right\} \tag{E.13}$$

where

$$b = p_F + \frac{1}{2}P \; . \tag{E.14}$$

Similarly, defining

$$a = \sqrt{p_F{}^2 - \frac{1}{4}P^2} \tag{E.15}$$

we have for the first integral in (E.11)

$$\int_a^b \frac{(p''^2-a^2)C^2(p'')p''^2dp''}{p''P\,(p''^2-p^2)} = \frac{4\pi}{P}\int_a^b \frac{(p''^2-a^2)p''dp''}{(p''^2-p^2)(\beta^2-p''^2)^2} =$$

$$= -\frac{4\pi}{P}\frac{\partial}{\partial\beta^2}\int_a^b \frac{(p''^2-a^2)p''dp''}{(p''^2-p^2)(\beta^2-p''^2)} \ . \tag{E.16}$$

In our computations, p is always less than or equal to a so that none of the integrals are singular (for p = a, the above integral vanishes). Therefore, we may separate the above integral into two integrals. For the first we have

$$-\frac{4\pi}{P}\frac{\partial}{\partial\beta^2}\left\{\frac{1}{\beta^2+p^2}\int_a^b\left[\frac{p''\beta^2}{\beta^2+p''^2}+\frac{p^2p''}{(p''^2-p^2)}\right]dp''\right\} =$$

$$= -\frac{4\pi}{P}\frac{\partial}{\partial\beta^2}\left\{\frac{1}{\beta^2+p^2}\left[\frac{\beta^2}{2}\ \ell n\ \frac{\beta^2+b^2}{\beta^2+a^2}+\frac{p^2}{2}\ \ell n\ \frac{p^2-b^2}{p^2-a^2}\right]\right\}$$

$$= \frac{2\pi}{(\beta^2+p^2)P}\left\{\frac{1}{\beta^2+p^2}\left[\beta^2 \ell n\ \frac{\beta^2+b^2}{\beta^2+a^2}+p^2\ell n\ \frac{b^2-p^2}{a^2-p^2}\right] -\right.$$

$$\left. -\ \ell n\ \frac{\beta^2+b^2}{\beta^2+a^2}+\frac{\beta^2(b^2-a^2)}{(\beta^2+b^2)(\beta^2+a^2)}\right\} \tag{E.17}$$

and for the second

$$-\frac{4\pi}{P}\frac{\partial}{\partial\beta^2}\left\{\frac{-a^2}{\beta^2+p^2}\int_a^b\left[\frac{\beta^2}{\beta^2+p^2}+\frac{p^2}{p''^2-p^2}\right]\frac{dp''}{p''}\right\} =$$

$$= \frac{4\pi}{P}\frac{\partial}{\partial\beta^2}\left\{\frac{a^2}{\beta^2+p^2}\left[\frac{1}{2}\ \ell n\ \frac{p''^2}{\beta^2+p''^2}\bigg|_a^b-\frac{1}{2}\ \ell n\ \frac{p''^2}{p''^2-p^2}\bigg|_a^b\right]\right\}$$

$$= \frac{2\pi a^2}{P(\beta^2+p^2)}\left\{\frac{1}{\beta^2+p^2}\left[\ell n\ \frac{b^2-p^2}{a^2-p^2}-\ell n\ \frac{\beta^2+b^2}{\beta^2+a^2}\right]-\frac{b^2-a^2}{(\beta^2+b^2)(\beta^2+a^2)}\right\} . \tag{E.18}$$

Collecting terms (E.13), (E.17) and (E.18), we have

$$J(p,P) = \frac{4\pi}{(\beta^2+p^2)^2} \left\{ \frac{1}{2P} \left[(a^2-p^2) \left(\ell n \frac{\beta^2+b^2}{\beta^2+a^2} \ \ell n \frac{b^2-p^2}{a^2-p^2} \right) + \right. \right.$$

$$\left. + \frac{(\beta^2+p^2)(b^2-a^2)}{\beta^2+b^2} \right] + \frac{\beta^2-p^2}{2\beta} \left(\frac{\pi}{2} - \tan^{-1} \frac{b}{\beta} \right) +$$

$$\left. + \frac{p}{2} \ \ell n \frac{b+p}{b-p} - \frac{b}{2} \frac{(\beta^2+p^2)}{(\beta^2+b^2)} \right\}$$

$$= \frac{4\pi}{(\beta^2+p^2)^2} \left\{ \frac{\beta^2-p^2}{\partial\beta} \left(\frac{\pi}{2} - \tan^{-1} \frac{b}{\beta} \right) + \frac{p}{2} \ \ell n \frac{b+p}{b-p} + \frac{a^2-p^2}{\partial P} \right.$$

$$\left. \left(\ell n \frac{\beta^2+b^2}{\beta^2+a^2} - \ell n \frac{b^2-p^2}{a^2-p^2} \right) \right\} . \tag{E.19}$$

We have removed two terms by using the fact that

$$b^2 - a^2 - bP = 0 \tag{E.20}$$

from the definitions of b and a ((E.14) and (E.15)).

Let us now look at the equation for $\rho_q = \rho(k_q)$ for $|\underset{\sim}{k}_q| \le p_F$

$$\rho(k_q) = 1 - \Sigma \, C_s \int_{|k_\ell| \le p_F} d^3k_\ell \int_{\substack{|k_m| > p_F \\ |k_n| > p_F}} d^3k_m d^3k_n \ t^*_{qk;mn}$$

$$\frac{1}{(\epsilon_q+\epsilon_\ell-\epsilon_m-\epsilon_n)^2} \ t_{mn;q\ell} \tag{E.21}$$

C_s is the statistical factor (equal to 3/2 for both singlet and triplet states by the same arguments which led to (B.48) and the sum

is over the singlet and triplet states. We transform to center of mass and relative coordinates defined by

$$\underset{\sim}{P} = \underset{\sim}{k}_q + \underset{\sim}{k}_\ell = \underset{\sim}{k}_m + \underset{\sim}{k}_n$$

$$2\underset{\sim}{p} = \underset{\sim}{k}_q - \underset{\sim}{k}_\ell$$

$$2\underset{\sim}{p}' = \underset{\sim}{k}_m - \underset{\sim}{k}_n \; . \tag{E.22}$$

By this transformation

$$t_{mn;q\ell} = t_{p'p} = (p'|t|p) \tag{E.23}$$

and

$$\int\limits_{\substack{|k_\ell| \leq p_F \\ |k_m|,|k_n| > p_F}} d^3k_\ell \; d^3k_m \; d^3k_n \;=\; \int\limits_{\substack{|p' \pm \frac{1}{2} P| > p_F \\ |k_\ell| < p_F}} d^3p' \; d^3k_\ell \tag{E.24}$$

where we have used conservation of total momentum to remove one integral.

The integral over k_ℓ can be converted into an integral over p and P by the following transformation (see Fig. 16)

$$k_q^{\;2} \, dk_q \, \sin\theta \, d\,\theta \, d\varphi \to p^2 dp \, \sin\gamma \, d\,\gamma \, \alpha \, \lambda \; . \tag{E.25}$$

Now

$$k_q^{\;2} + p^2 - 2pk_q \cos\gamma = \frac{P^2}{4} \tag{E.26}$$

so that, for fixed $|p|$ and k_ℓ, we have

Fig. 16. Diagram illustrating the transformation (E.25) .

Fig. 17. Diagram used to obtain integration limits in Eq. (E.28).

Fig. 18. Diagram used to obtain integration limits in Eq. (E.30): (a) $P < p_F - k_q$; (b) $P > p_F - k_q$.

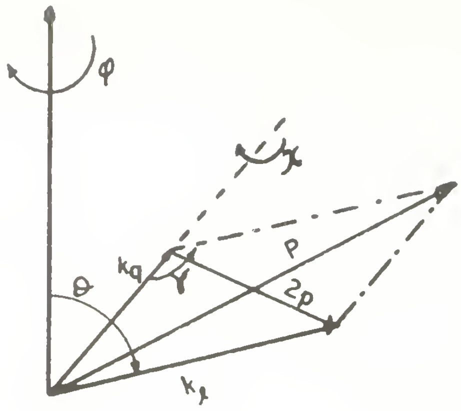

16

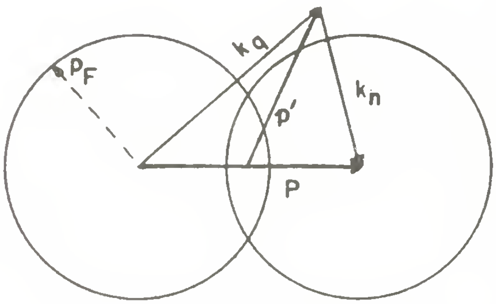

17

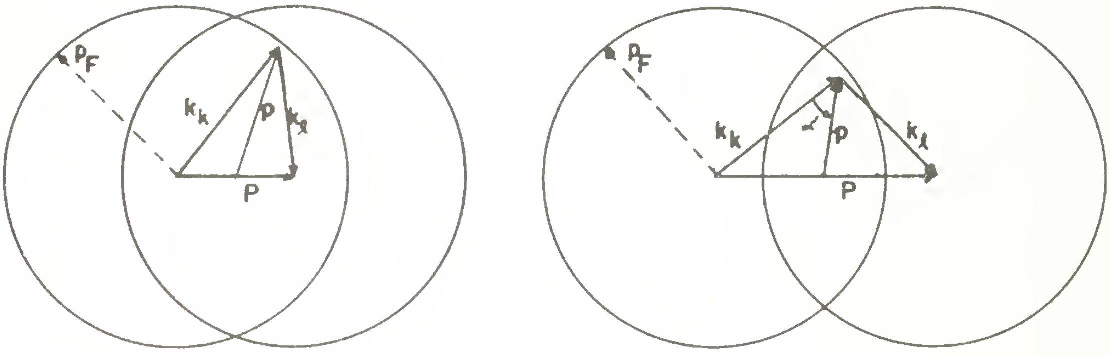

18

$$2pk_\ell \sin\gamma \, d\gamma = \frac{PdP}{2} . \tag{E.27}$$

Thus

$$p^2 dp \sin\gamma \, d\gamma \, d\chi = \frac{pdpPdPd\chi}{4k_q} . \tag{E.28}$$

Returning to (E.24) and doing the $d\chi$ integration, we have

$$\int\limits_{\substack{|k_\ell| \le p_F \\ |k_m|,|k_n| > p_F}} d^3k_\ell d^3k_m \, d^3k_n = \frac{\pi}{2k_q} \int\limits_{|p'\pm p| > p_F} d^3p' \int\limits_{|k_q - 2p| \le p_F} pdp \int PdP \quad . \tag{E.29}$$

Let us now look at the various limits of integration. From Fig. 17 we see that the angular part of the p' integration can be done immediately, leaving

$$\int d^3p' = 4\pi \int_{\sqrt{p_F^2 - \frac{p^2}{4}}}^{p_F + \frac{1}{2}P} \frac{p'^2 + \frac{p^2}{4} - k_F^2}{p'p} p'^2 dp' +$$

$$+ 4\pi \int_{p_F + \frac{1}{2}P}^{\infty} p'^2 dp' . \tag{E.30}$$

The p and P limits can be determined from Figures 18(a) and 18(b):

$$\int\limits_{|k_q - 2p| \le p_F} pdp \int PdP = \int_0^{p_F - k_q} PdP \int_{k_q - \frac{p}{2}}^{k_q + \frac{p}{2}} pdp + \int_{p_F - k_q}^{p_F + k_q} PdP$$

$$\int_{k_q - \frac{P}{2}}^{\frac{1}{\sqrt{2}}(k_F^2 + k_q^2 - \frac{1}{2}P^2)^{1/2}} pdp \quad . \tag{E.31}$$

We can now do the p' integration explicitly. From (E.19), (E.23) and (E.10) we have

$$H(p,P) = G(p,P)\left\{4\pi\int_a^b \frac{\cos\alpha\; C^2(p')p'^2dp'}{(p^2-p'^2)^2} + 4\pi\int_b^\infty \frac{C^2(p')p'^2dp'}{(p^2-p'^2)^2}\right\} \qquad (E.32)$$

where $\cos\alpha$ is defined by (E.5) and

$$G(p,P) = \frac{\lambda^2C^2(p)}{(1-\lambda J(p,P))^2} \quad . \qquad (E.33)$$

Thus

$$H(p,P) = G(p,P)\,\frac{\partial}{\partial p^2}\left\{4\pi\int_a^b \frac{\cos\alpha\; C^2(p')p'^2dp'}{(p'^2-p^2)} + \right.$$

$$\left. + 4\pi\int_b^\infty \frac{C^2(p')p'^2dp'}{(p'^2-p^2)}\right\} \quad . \qquad (E.34)$$

The term in brackets is just $J(p,P)$, (E.11). Using (E.19), we obtain

$$H(p,P) = G(p,P)\left\{-\frac{2F(p,P)}{(\beta^2+p^2)} + \frac{4\pi}{(\beta^2+p^2)^2}\left[-\frac{1}{2\beta}\left(\frac{\pi}{2} - \tan^{-1}\frac{b}{\beta}\right) + \right.\right.$$

$$\left.\left. + \frac{1}{4p}\,\ell n\,\frac{b+p}{b-p} - \frac{1}{2P}\left(\ell n\,\frac{\beta^2+b^2}{\beta^2+a^2} - \ell n\,\frac{b^2-p^2}{a^2-p^2}\right) - \frac{1}{2P(b^2-p^2)}(b^2-a^2-2bp)\right]\right\}$$

$$= G(p,P)\left\{\frac{4\pi}{(\beta^2+p^2)^2}\left[\frac{1}{2\beta}\left(\tan^{-1}\frac{b}{\beta} - \frac{\pi}{2}\right) + \frac{1}{4p}\ell n\,\frac{b+p}{b-p} + \frac{1}{2P}\right.\right.$$

$$\left.\left.\left(\ell n\,\frac{b^2-p^2}{a^2-p^2} - \ell n\,\frac{\beta^2+b^2}{\beta^2+a^2}\right)\right] - \frac{2F(p,P)}{(\beta^2+p^2)}\right\} \quad . \qquad (E.35)$$

We have again used (E.20). Thus we have the following equation for

the momentum density below the Fermi sea:

$$\rho(k_q) = 1 - \sum_s \frac{\pi C_s}{2k_q} \left\{ \int_0^{p_F - k_q} PdP \int_{|k_q - \frac{P}{2}|}^{k_q + \frac{P}{2}} pdp\ H(p,P) + \int_{p_F - k_q}^{p_F + k_q} PdP \int_{|k_q - \frac{P}{2}|}^{k_q + \frac{P}{2}} pdp\ H(p,P) \right\} . \qquad \text{(E.36)}$$

The lower limits on the p integrals have been changed to absolute values because the integrand is even in p and thus the integral from $(k_q - \frac{1}{2} P)$ to $|k_q - \frac{1}{2} P|$ vanishes.

For $k_q > p_F$, we have from (E.1)

$$\rho(k_q) = \sum_s C_s M^2 \int_{\substack{|k_k|,|k_\ell| \le p_F \\ |k_n| > p_F}} d^3k_k\ d^3k_\ell\ \frac{d^3k_n\ |t_{qn;k\ell}|^2}{(p^2 - p'^2)^2} =$$

$$= \sum_s C_s \frac{\pi}{2k_q} \int_{\substack{|p' \pm \frac{1}{2} P| > p_F \\ |p \pm \frac{1}{2} P| \le p_F}} d^3p\ PdPp'dp' \frac{G(p,P)C^2(p')}{(p-p'^2)^2} . \qquad \text{(E.37)}$$

With the aid of figures similar to Figures 17 and 18, we can see that the integration limits should be as follows:

$$\rho(k_q) = \sum C_s \frac{\pi}{2k_q} \left\{ \left(\int_0^{k_q - p_F} PdP \int_{k_q - \frac{1}{2} P}^{k_q + \frac{1}{2} P} p'dp' + \int_{k_q - p_F}^{2p_F} PdP \right. \right.$$

$$\int_{\sqrt{\frac{1}{2}\left(k_F^2+k_q^2-\frac{1}{2}P^2\right)}}^{k_q+\frac{1}{2}P} p'dp' \Bigg) \times$$

$$\times \Bigg(4\pi\int_0^{p_F-\frac{1}{2}P} \frac{p^2dp\,G(p,P)C^2(p')}{(p^2-p'^2)^2} + 4\pi\int_{p_F-\frac{1}{2}P}^{\sqrt{p_F^2-\frac{1}{4}P^2}} \frac{k_F^2-p^2-\frac{1}{4}P^2}{Pp'}$$

$$\cdot \frac{G(p,P)C^2(p')p^2dp}{(p^2-p'^2)^2} \Bigg) \Bigg\} . \qquad \text{(E.38)}$$

Again we can do the p' integrations. Defining

$$e_1 = k_q - \frac{1}{2}P$$

$$f = k_q + \frac{1}{2}P \qquad \text{(E.39)}$$

we obtain from the first p' integral:

$$H_1(p,P) = G(p,P)\frac{\partial}{\partial\beta^2}\frac{\partial}{\partial p^2}\left\{\frac{1}{\beta^2+p^2}\left(\int_{e_1}^{f}\frac{p'dp'}{p^2-p'^2} + \int_{e_1}^{f}\frac{p'dp'}{\beta^2+p'^2}\right)\right\}$$

$$= G(p,P)\frac{\partial}{\partial\beta^2}\frac{\partial}{\partial p^2}\left\{\frac{1}{\beta^2+p^2}\left[\frac{1}{2}\ln\left(\frac{p^2-e_1^2}{p^2-f^2}\right) + \right.\right.$$

$$\left.\left. + \frac{1}{2}\ln\left(\frac{\beta^2+f^2}{\beta^2+e_1^2}\right)\right]\right\}$$

$$= \frac{G(p,P)}{(\beta^2+p^2)^2}\left\{\frac{1}{\beta^2-p^2}\left[\ln\frac{\beta^2+f^2}{\beta^2+e_1^2} - \ln\frac{f^2-p^2}{e_1^2-p^2}\right] + \frac{(f^2-e_1^2)}{2}\right.$$

$$\left.\left[\frac{1}{(e_1^2-p^2)(f^2-p^2)} + \frac{1}{(\beta^2+e_1^2)(\beta^2+f^2)}\right]\right\} . \qquad \text{(E.40)}$$

The second p' integral is the same as the first except that e_1 is replaced by

$$e_2 = \frac{1}{\sqrt{2}} \sqrt{p_F^{\,2} + k_q^{\,2} - \frac{1}{2} P^2} \quad . \tag{E.41}$$

Therefore, we may write (for $k_q > k_F$):

$$\begin{aligned} \rho(k_q) = \sum_s C_s \frac{\pi}{2k_q} \Bigg\{ & \int_0^{k_q - p_F} PdP \left[\int_0^{p_F - \frac{1}{2} P} p^2 dp + \right. \\ & \left. + \int_{p_F - \frac{1}{2} P}^{\sqrt{p_F^{\,2} - \frac{1}{4} P^2}} \cos \alpha' \, p^2 dp \right] H_1(p,P) \\ & + \int_{k_q - p_F}^{2p_F} PdP \left[\int_0^{p_F - \frac{1}{2} P} p^2 dp + \int_{p_F - \frac{1}{2} P}^{\sqrt{p_F^{\,2} - \frac{1}{4} P^2}} \cos \alpha' \, p^2 dp \right] H_2(p,P) \Bigg\} \end{aligned} \tag{E.42}$$

where $H_2(p,P)$ is the same function as $H_1(p,P)$ with e_2 in place of e_1 and

$$\cos \alpha' = \frac{p_F^{\,2} - p^2 - \frac{1}{4} P^2}{pP} \quad . \tag{E.43}$$

The remaining integrals were evaluated numerically on the CDC-1604 computer at the University of California at San Diego with a standard integral routine which performed each integral by progressively doubling the number of points taken until agreement between next-to-last and last values of the integral were within prescribed limits (± 0.01% for the inner integral and ± .1% for the outer integral (i.e., the density itself)).

One problem does occur in the numerical integration. The function G(p,P), which is a factor in the kernel, is singular (the pole coming from the deuteron bound state). The principal value integral is easily taken, however, because the singularity has negligible effect on the overall result and the kernel can be replaced with a constant in the region of the singularity with negligible error, the constant being varied until the value of the integral changes negligibly with further variation. The resulting particle density is indicated in Chapter VII, Fig. 10.

APPENDIX F

BASIS FUNCTIONS AND RADIAL WAVE FUNCTIONS

Fig. 19. Basis functions $s_{\ell}(kr)$, Eq. (4.8):

a) $k = 0.1\ p_F$;

b) $k = 0.5\ p_F$;

c) $k = 0.9\ p_F$;

d) $k = 1.8\ p_F$.

Fig. 20. Radial wave functions $U_{\ell\ell'}^{Js}$, Eq. (4.10):

$k = 0.1\ p_F$: a) $\ell = 0$; b) $\ell = 1$; c) $\ell = 2$;

$k = 0.5\ p_F$: d) $\ell = 0$; e) $\ell = 1$; f) $\ell = 2$;

$k = 0.9\ p_F$: g) $\ell = 0$; h) $\ell = 1$; i) $\ell = 2$;

$k = 1.8\ p_F$: j) $\ell = 0$; k) $\ell = 1$; ℓ) $\ell = 2$.

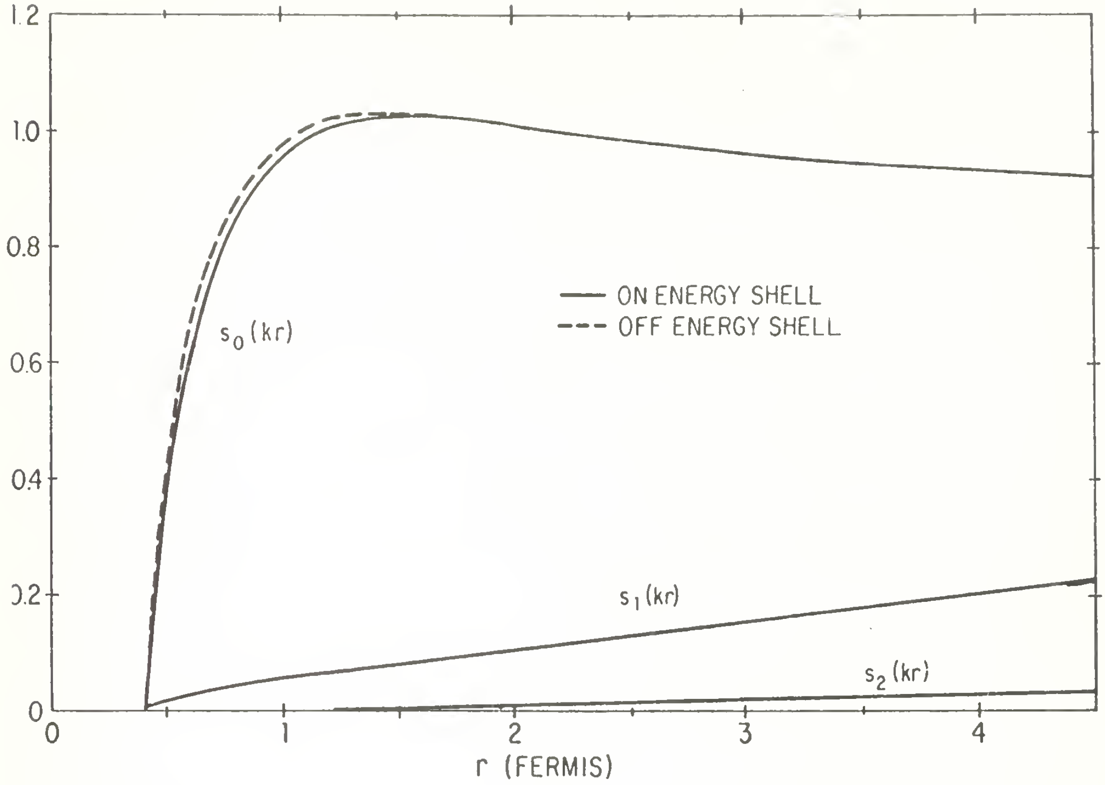
1.2
1.0
0.8
0.6
0.4
0.2
0
0
1
2
3
4
r (FERMIS)
ON ENERGY SHELL
OFF ENERGY SHELL
$s_0(kr)$
$s_1(kr)$
$s_2(kr)$

19a

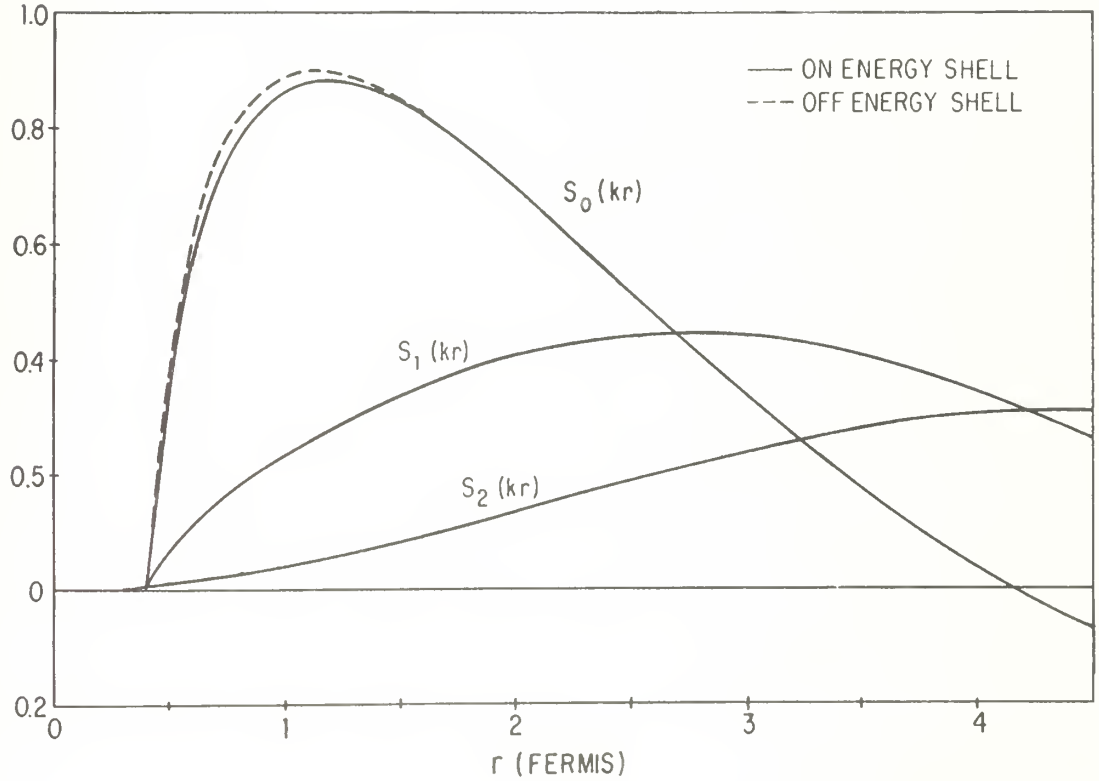
1.0
0.8
0.6
0.4
0.5
0
0.2
0
1
2
3
4
r (FERMIS)
ON ENERGY SHELL
OFF ENERGY SHELL
$S_0(kr)$
$S_1(kr)$
$S_2(kr)$

19b

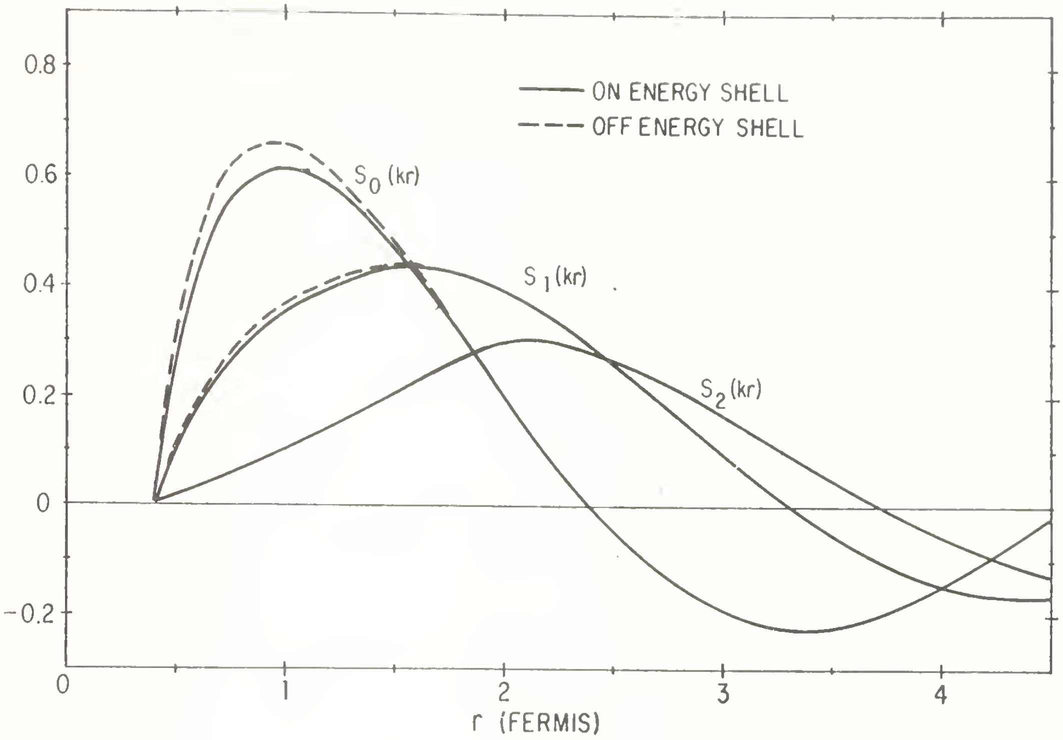

0.8
0.6
0.4
0.2
0
−0.2
0
1
2
3
4
r (FERMIS)
ON ENERGY SHELL
OFF ENERGY SHELL
$S_0(kr)$
$S_1(kr)$
$S_2(kr)$

19c

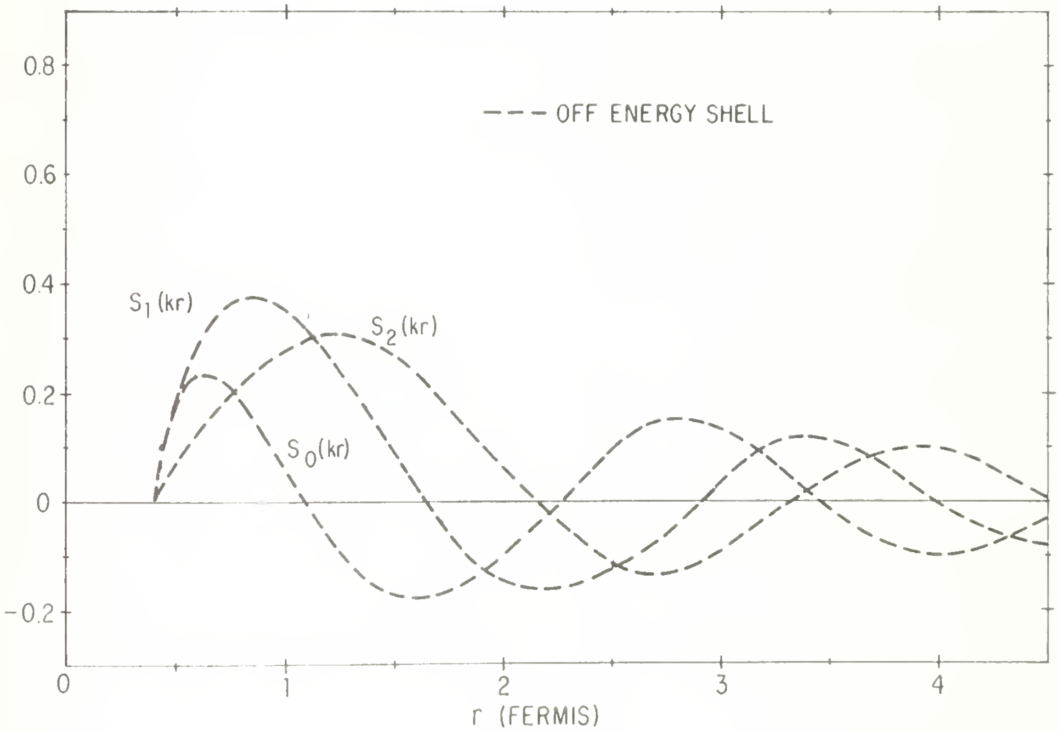

0.8
0.6
0.4
0.2
0
−0.2
0
1
2
3
4
r (FERMIS)
OFF ENERGY SHELL
$S_1(kr)$
$S_2(kr)$
$S_0(kr)$

19d

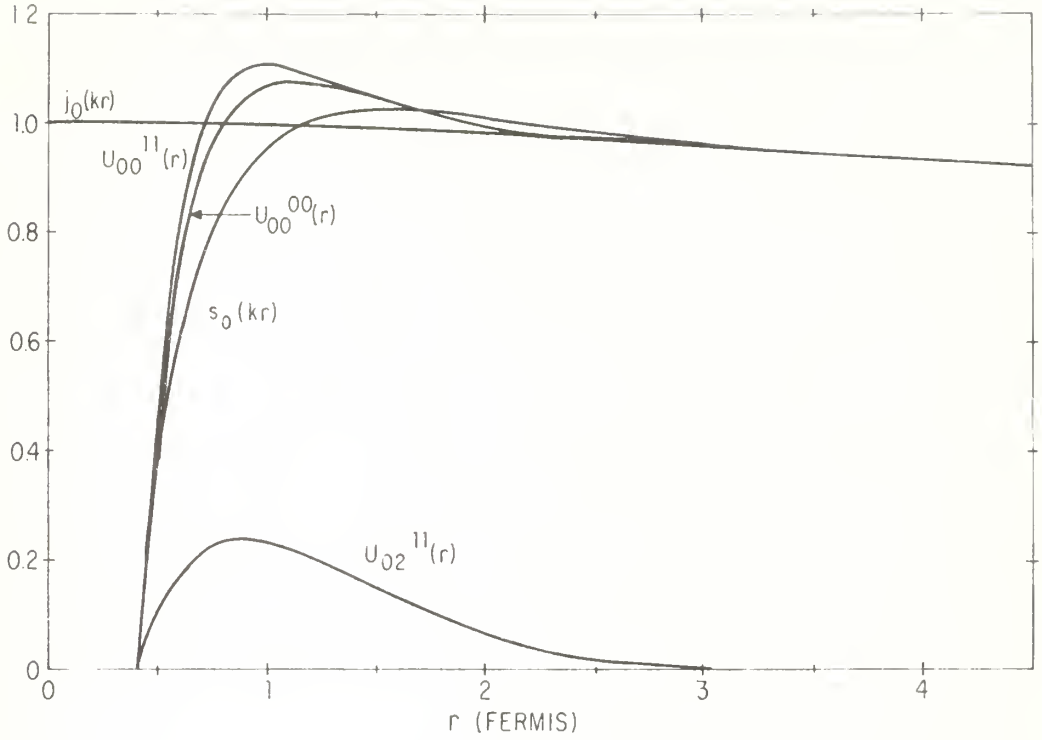
1.2
1.0
0.8
0.6
0.4
0.2
0
0
1
2
3
4
r (FERMIS)
$j_0(kr)$
$U_{00}^{11}(r)$
$U_{00}^{00}(r)$
$s_0(kr)$
$U_{02}^{11}(r)$

20a

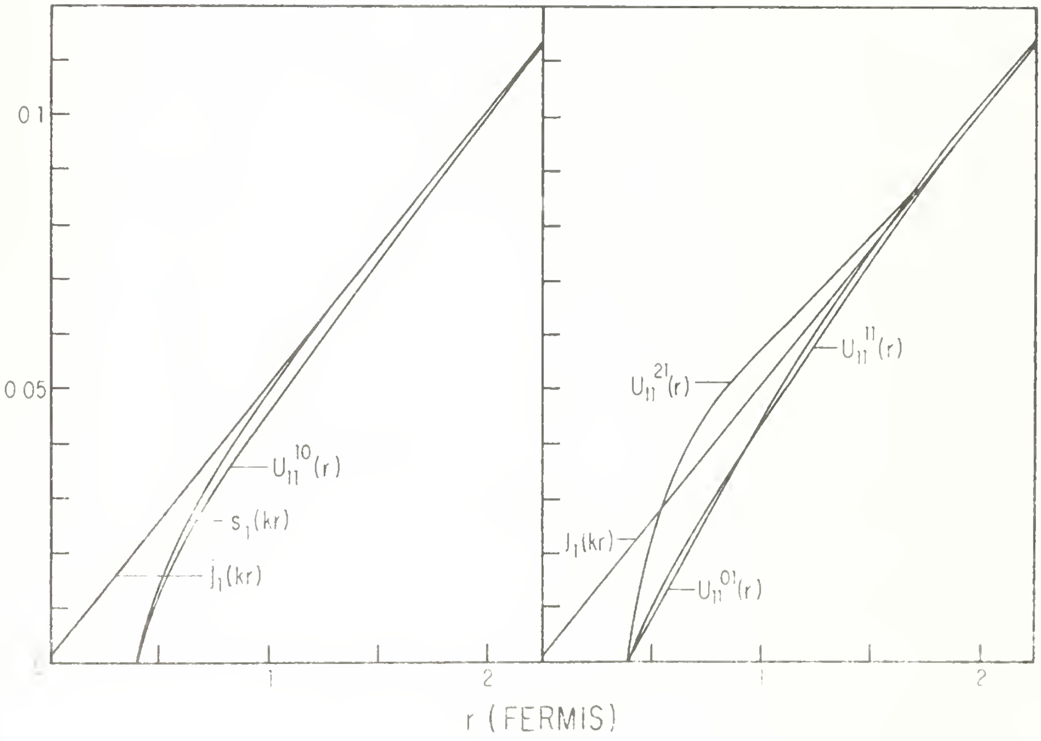
0.1
0.05
0
1
2
1
2
r (FERMIS)
$U_{11}^{10}(r)$
$s_1(kr)$
$j_1(kr)$
$U_{11}^{11}(r)$
$U_{11}^{21}(r)$
$j_1(kr)$
$U_{11}^{01}(r)$

20b

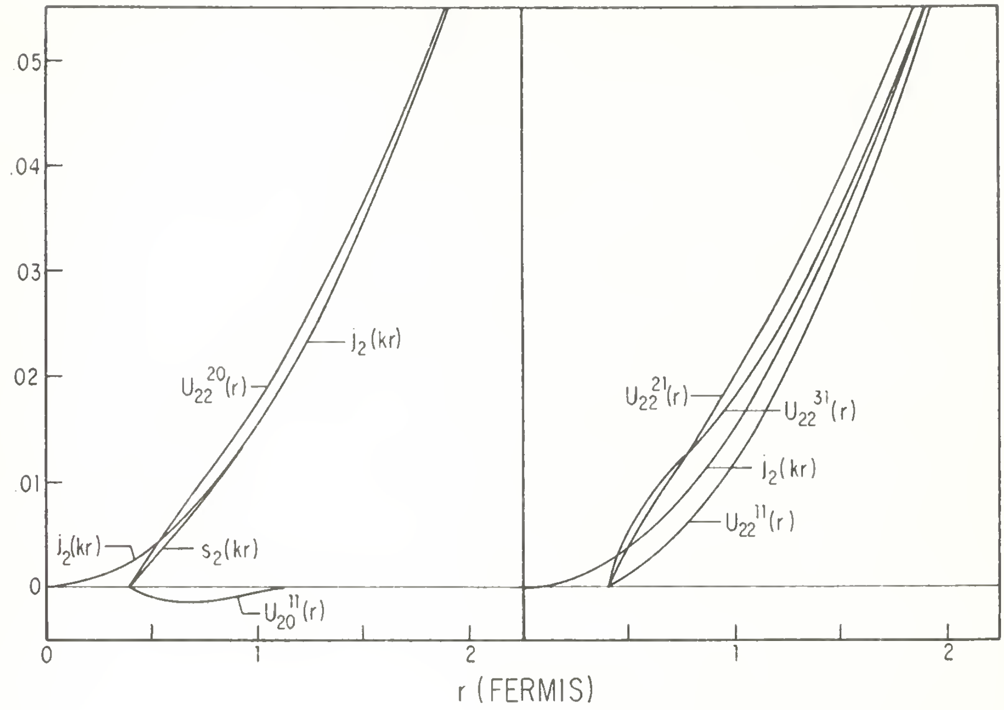
.05
.04
03
02
.01
0
$j_2(kr)$
$U_{22}{}^{20}(r)$
$j_2(kr)$
$s_2(kr)$
$U_{20}{}^{11}(r)$
$U_{22}{}^{21}(r)$
$U_{22}{}^{31}(r)$
$j_2(kr)$
$U_{22}{}^{11}(r)$
0
1
2
1
2
r (FERMIS)

20c

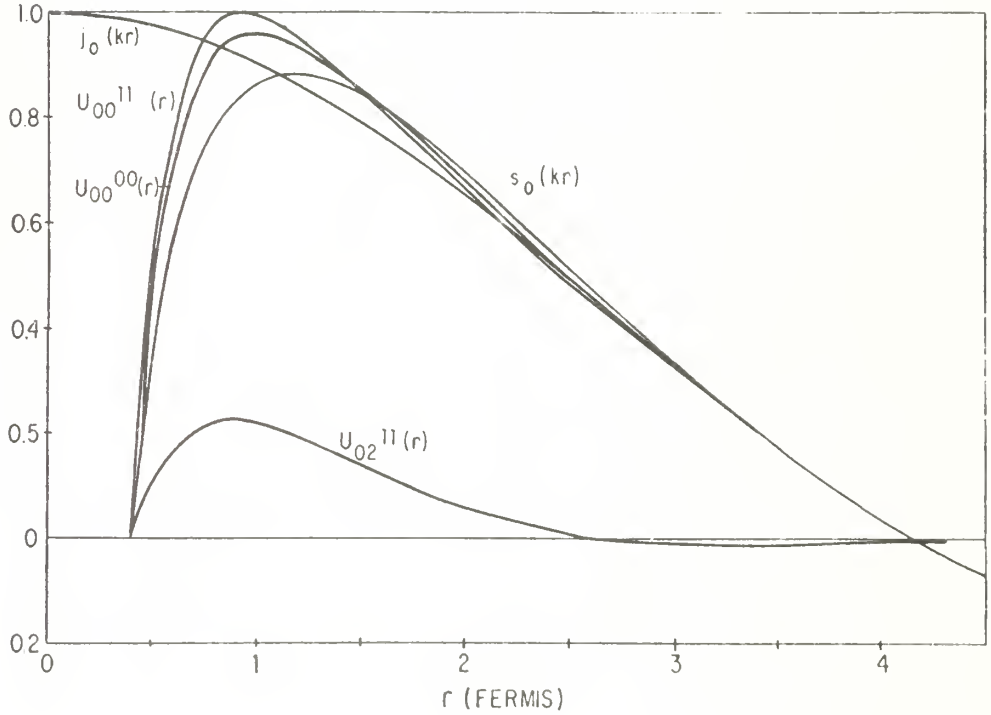
1.0
0.8
0.6
0.4
0.5
0
0.2
$j_0(kr)$
$U_{00}{}^{11}(r)$
$U_{00}{}^{00}(r)$
$s_0(kr)$
$U_{02}{}^{11}(r)$
0
1
2
3
4
r (FERMIS)

20d

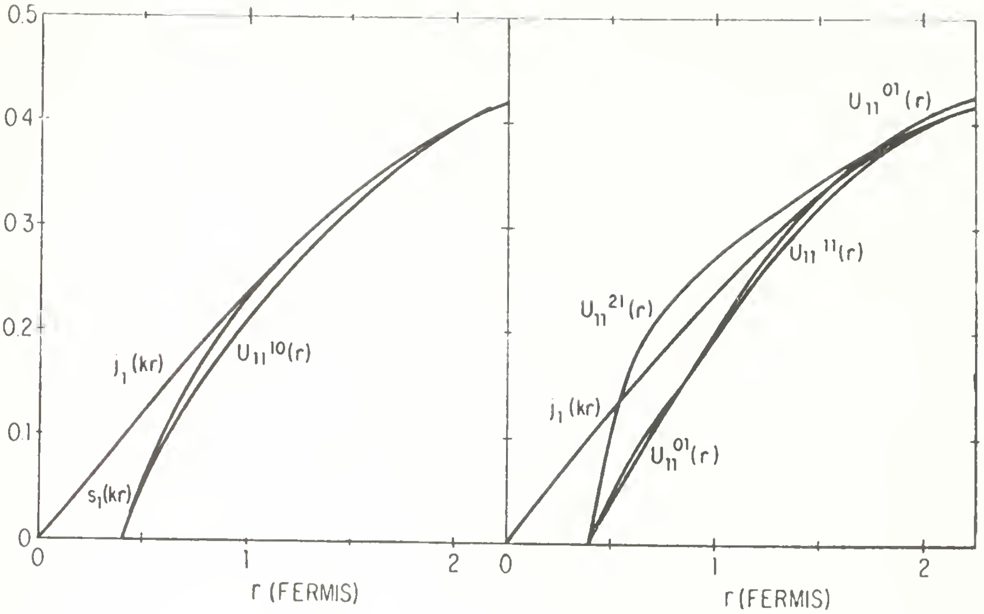
0.5
0.4
0.3
0.2
0.1
0
$j_1(kr)$
$U_{11}^{10}(r)$
$s_1(kr)$
0
1
2
r (FERMIS)
$U_{11}^{01}(r)$
$U_{11}^{11}(r)$
$U_{11}^{21}(r)$
$j_1(kr)$
$U_{11}^{01}(r)$
0
1
2
r (FERMIS)

20e

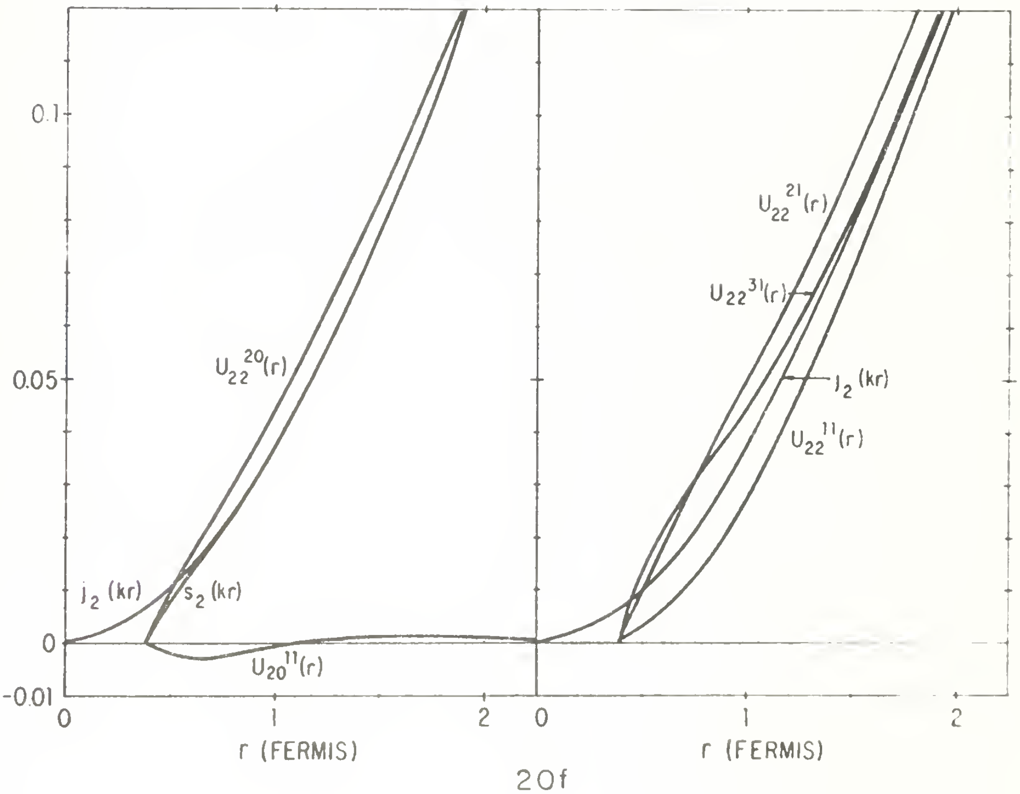
0.1
0.05
0
-0.01
$U_{22}^{20}(r)$
$j_2(kr)$
$s_2(kr)$
$U_{20}^{11}(r)$
0
1
2
r (FERMIS)
$U_{22}^{21}(r)$
$U_{22}^{31}(r)$
$j_2(kr)$
$U_{22}^{11}(r)$
0
1
2
r (FERMIS)

20f

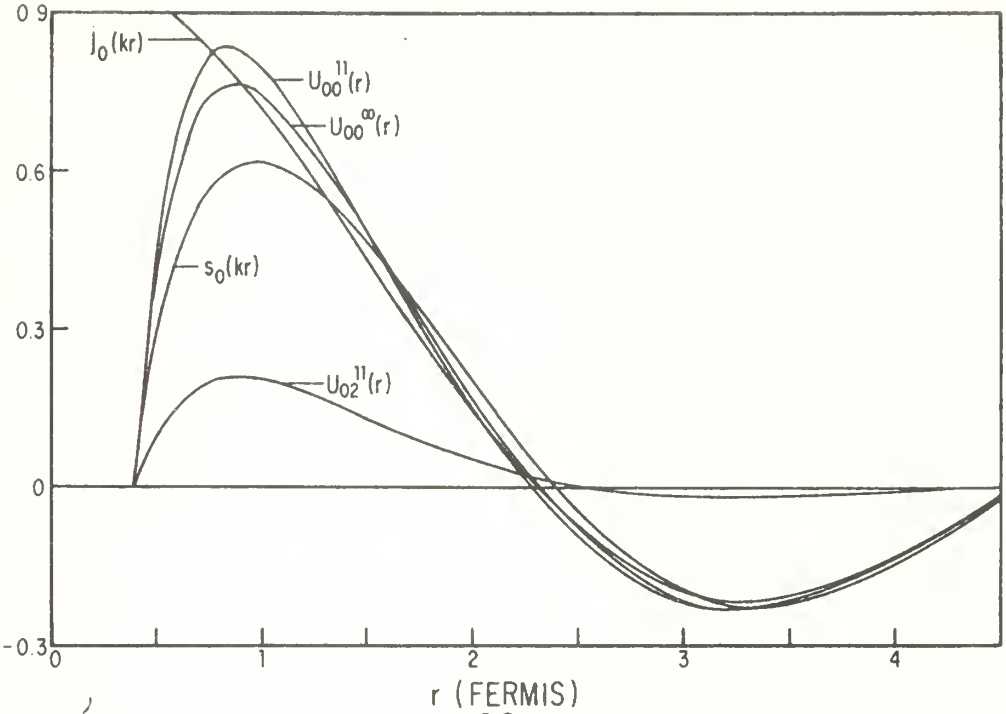
0.9
0.6
0.3
0
-0.3
0
1
2
3
4
r (FERMIS)
$j_0(kr)$
$U_{00}^{11}(r)$
$U_{00}^{\infty}(r)$
$s_0(kr)$
$U_{02}^{11}(r)$

20g

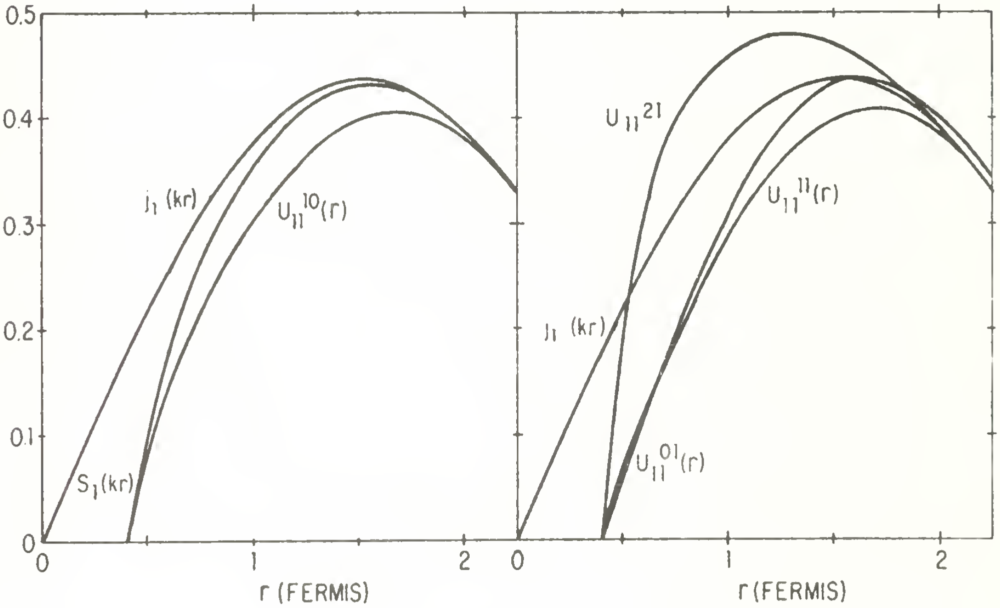
0.5
0.4
0.3
0.2
0.1
0
0
1
2
r (FERMIS)
$j_1(kr)$
$U_{11}^{10}(r)$
$S_1(kr)$
0
1
2
r (FERMIS)
U_{11}^{21}
$U_{11}^{11}(r)$
$j_1(kr)$
$U_{11}^{01}(r)$

20h

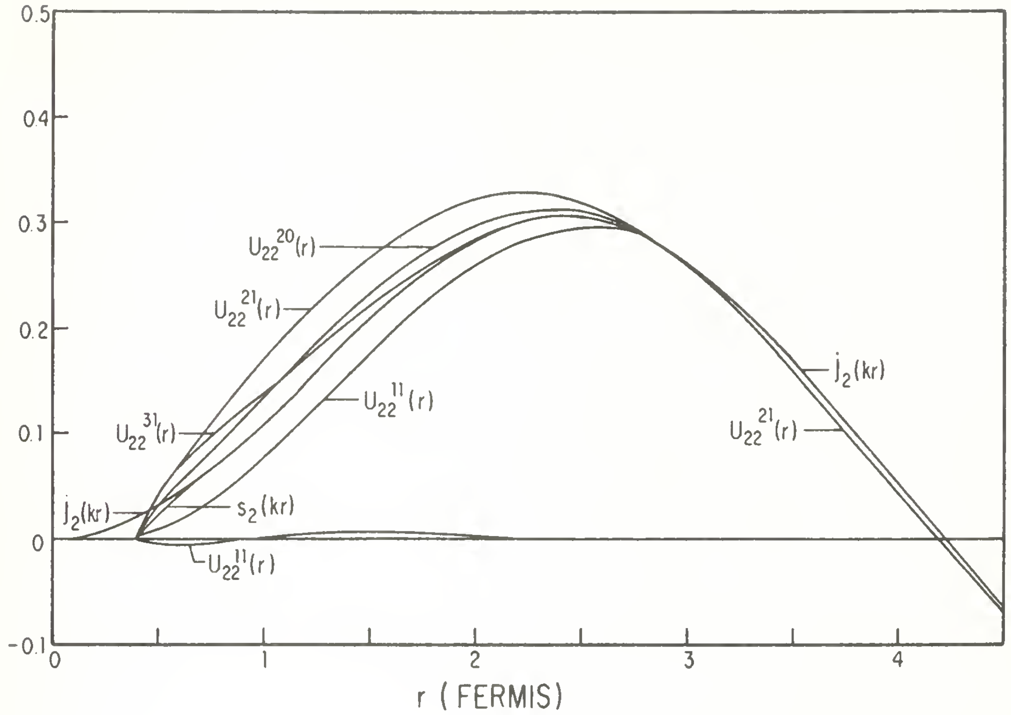
0.5
0.4
0.3
0.2
0.1
0
-0.1
$U_{22}^{20}(r)$
$U_{22}^{21}(r)$
$U_{22}^{11}(r)$
$U_{22}^{31}(r)$
$j_2(kr)$
$s_2(kr)$
$U_{22}^{11}(r)$
$j_2(kr)$
$U_{22}^{21}(r)$
0
1
2
3
4
r (FERMIS)

20i

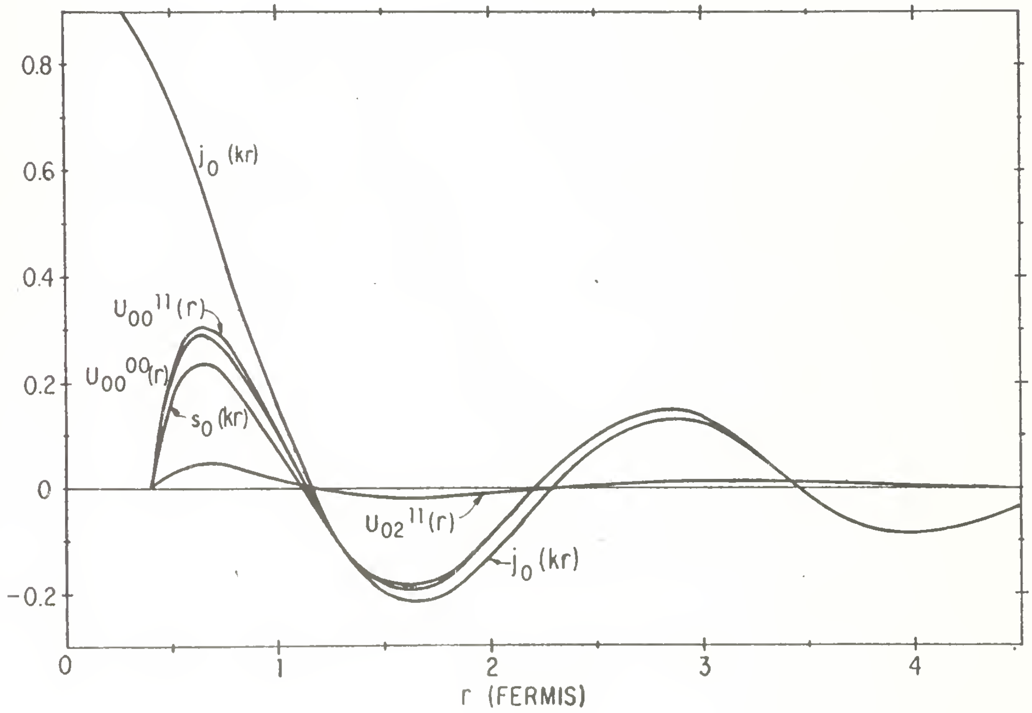
0.8
0.6
0.4
0.2
0
-0.2
j_0 (kr)
$U_{00}^{11}(r)$
$U_{00}^{00}(r)$
s_0 (kr)
$U_{02}^{11}(r)$
j_0 (kr)
0
1
2
3
4
r (FERMIS)

20j

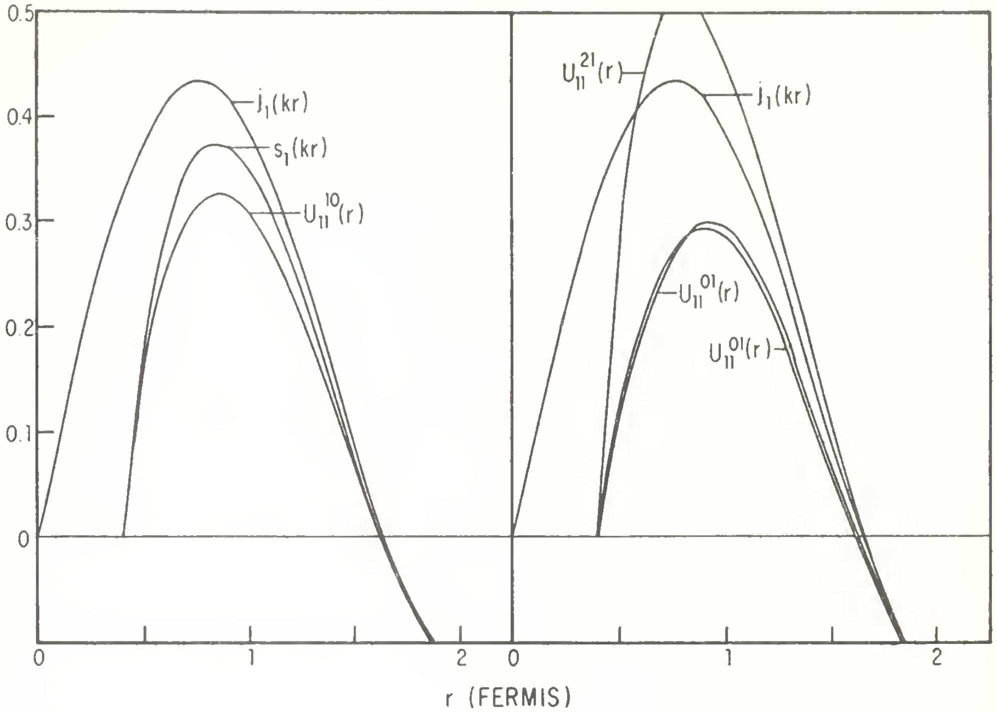
0.5
0.4
0.3
0.2
0.1
0
$j_1(kr)$
$s_1(kr)$
$U_{11}^{10}(r)$
$U_{11}^{21}(r)$
$j_1(kr)$
$U_{11}^{01}(r)$
$U_{11}^{01}(r)$
0
1
2
0
1
2
r (FERMIS)

20k

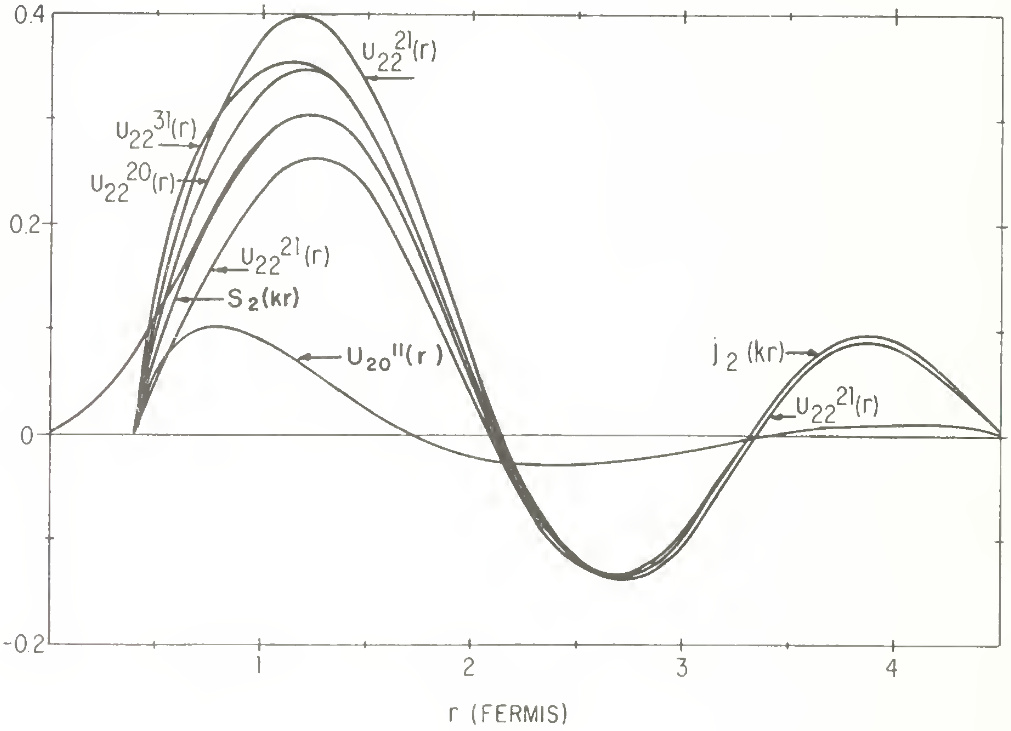
0.4
0.2
0
-0.2
$U_{22}^{21}(r)$
$U_{22}^{31}(r)$
$U_{22}^{20}(r)$
$U_{22}^{21}(r)$
$S_2(kr)$
$U_{20}^{11}(r)$
$j_2(kr)$
$U_{22}^{21}(r)$
1
2
3
4
r (FERMIS)

20l

APPENDIX G

Nuclear Matter Calculations and Phenomenological Potentials

K. A. Brueckner

and

K. S. Masterson, Jr.

(Physical Review, 128, 2267 (1962))

ABSTRACT

The properties of nuclear matter predicted for several different phenomenological potentials by the reaction matrix theory of Brueckner have been calculated. The calculations have shown that potentials which give supposedly equally good fit to scattering data do not necessarily lead to identical nuclear properties. Other approximation methods have been studied to determine their accuracy, with particular emphasis on the iterated Born approximation, and on comparison with the Moszkowski-Scott separation method and with the approximations of Mohling and of Puff.

I. INTRODUCTION

In a series of previous papers,[1] methods have been developed for the determination of the properties of nuclear matter. This theory has been applied by Brueckner and Gammel[1] (hereafter referred to as BG) to extended nuclear matter using both Gammel-Christian-Thaler potentials[2] and one of the sets of Gammel-Thaler potentials.[3,4] The latter were modified slightly to give correctly the low energy scattering parameters and deuteron properties. Accurate numerical solutions of the equations of the theory gave a mean binding energy of -15.2 Mev and equilibrium spacing of 1.02 fermi for the modified Gammel-Thaler potentials, in good agreement with semi-empirical values for the binding energy ranging from -15.83 Mev reported

by Green[5] to -17.04 Mev obtained by Cameron,[6] and with the equilibrium spacing, $r_o = (1.07 \pm 0.02)$ deduced from high-energy electron-nucleus scattering.

A detailed discussion of the K-matrix theory and the method of applying it to extended nuclear matter is contained in BG. Consequently, we shall indicate here only the basic equations, and in the next section introduce our additional approximations.

In BG, the K-matrix from which the energy is computed is defined by the equation

$$K_{ij,k\ell} = V_{ij,k\ell} + \sum_{\substack{m,n \\ p_m > p_F \\ p_n > p_F}} V_{ij,mn} \frac{1}{E_k + E_\ell - E_m^* - E_n^*} K_{mn,k\ell} \; . \qquad (1\text{-}1)$$

In this equation E_k and E_l are self-consistent energies for particles moving in the Fermi gas and E_m^* and E_n^* are energies appropriate to virtual excitations above the Fermi surface. The single particle potential is determined from the diagonal elements of the K-matrix by the relation

$$V(p_i) = \sum_j (K_{ij,ij} - K_{ij,ji}) \qquad (1\text{-}2)$$

with the sum over all filled states. Finally, the average binding energy per particle is

$$E_{av} = \frac{3}{{p_F}^3} \int_0^{p_F} p^2 dp \left[\frac{p^2}{2m} + \frac{1}{2} V(p) \right] \; . \qquad (1\text{-}3)$$

by Green[5] to -17.04 Mev obtained by Cameron,[6] and with the equilibrium spacing, $r_o = (1.07 \pm 0.02)$ deduced from high-energy electron-nucleus scattering.

A detailed discussion of the K-matrix theory and the method of applying it to extended nuclear matter is contained in BG. Consequently, we shall indicate here only the basic equations, and in the next section introduce our additional approximations.

In BG, the K-matrix from which the energy is computed is defined by the equation

$$K_{ij,k\ell} = V_{ij,k\ell} + \sum_{\substack{m,n \\ p_m > p_F \\ p_n > p_F}} V_{ij,mn} \frac{1}{E_k + E_\ell - E_m^* - E_n^*} K_{mn,k\ell} \; . \tag{1-1}$$

In this equation E_k and E_l are self-consistent energies for particles moving in the Fermi gas and E_m^* and E_n^* are energies appropriate to virtual excitations above the Fermi surface. The single particle potential is determined from the diagonal elements of the K-matrix by the relation

$$V(p_i) = \sum_j (K_{ij,ij} - K_{ij,ji}) \tag{1-2}$$

with the sum over all filled states. Finally, the average binding energy per particle is

$$E_{av} = \frac{3}{p_F^3} \int_0^{p_F} p^2 dp \left[\frac{p^2}{2m} + \tfrac{1}{2} V(p) \right] \; . \tag{1-3}$$

The normal density is assumed to be determined from the minimum of E_{av} as a function of density.

In the present paper we use an approximation of the Brueckner formalism which is simpler than that used in BG

1) to investigate the properties of nuclear matter predicted by the theory for various phenomenological potentials (six Gammel-Thaler potentials[7] and the Breit potential[8]);

2) to check the rapidity of convergence of successive Born approximations;

3) to obtain a comparison with the results of the separation method of Moszkowski and Scott;[9,10] and,

4) to check the accuracy of the approximation described by Bell[11] as the central element in the nuclear matter theories of Mohling[12] and of Puff and Martin.[13]

II. SOLUTION OF THE K-MATRIX EQUATIONS

In the investigations reported in this paper, we used the procedure of BG with one further approximation: we have assumed that the difference of energies in the denominator of Eq. (1-1) is independent of the total momentum. Thus, we make the replacement

$$E_k + E_\ell - E_m^* - E_n^* = 2\left[E(p_{k\ell}) - E^*(p_{mn}) \right] \tag{2-1}$$

with $p_{k\ell}$ and p_{mn} the relative momenta. This approximation is accurate if E_k has a quadratic dependence on p_k or if the relative momentum is

large compared with the total momentum. Consistent with the accuracy of this approximation, we replace the total momentum, which enters in the treatment of the exclusion principle, by its average value compatible with a given value of relative momentum, k . This is easily shown to be

$$\left(\frac{P^2}{4}\right)_{av} = \frac{3}{5}\, p_F^2 \left(1 - \frac{k}{p_F}\right) \frac{\left(1 + \frac{1}{2}\frac{k}{p_F} + \frac{1}{6}\frac{k^2}{p_F^2}\right)}{\left(1 + \frac{1}{2}\frac{k}{p_F}\right)} \, , \qquad k < k_F \, . \tag{2-2}$$

For $k \geq p_F$, we have set $P_{av} = 0$. These simplifications reduce considerably the problem of solving the BG equations and are not thought to introduce appreciable errors into the results, particularly since we are primarily interested in comparisons among various potentials and approximation methods.

We quote here the principal equations to be solved, as adapted from BG:

1) Green's functions:

$$G_\ell(r,r') = \frac{1}{2\pi^2} \int_0^\infty \frac{k''^2 dk'' \; j_\ell(k''r)\, j_\ell(k''r')\; f(P,k'')}{2\left[E(k) - E^*(k'')\right]} \tag{2-3}$$

for on-energy-shell propagation and with $(2[E(k) - E^*(k'')] - \Delta)$ in the denominator for off-energy-shell propagation. Δ is the mean excitation energy, assumed to be $E(p_F) - E(0)$. The Pauli step-function, $f(P,k'')$, is that given in BG Eq. (34) with the total momentum, P , replaced by P_{av} of Eq. (2-2); it excludes from the integrand values of k'' not

allowed by the exclusion principle.

2) Plane wave basis functions and Green's functions as modified by the hard core potential of radius r_c :

$$s_\ell(kr) = j_\ell(kr) - \frac{j_\ell(kr_c)\, G_\ell(r,r_c)}{G_\ell(r_c,r_c)} \ , \tag{2-4}$$

$$F_\ell(r,r') = G_\ell(r,r') - \frac{G_\ell(r,r_c)\, G_\ell(r_c,r')}{G_\ell(r_c,r_c)} \ . \tag{2-5}$$

As shown in BG, the above definitions result from requiring the wave functions (next equation) to vanish at the core.

3) Wave functions:

$$U_{\ell\ell'}{}^{Js}(k,r) = s_\ell(kr)\delta_{\ell\ell'} + 4\pi \sum_{\ell''} \int_{r_c}^{\infty} r'^2 dr' F_{\ell'}(r,r') V_{\ell'\ell''}{}^{Js}(r') U_{\ell\ell''}{}^{Js}(r') \ , \tag{2-6}$$

where the $V_{\ell'\ell''}{}^{Js}(r')$ are the phenomenological two-body potentials;

4) K-matrices:

$$(k|K|k) = \sum_{sJ} \sum_{\ell=J-1}^{J+1} C_{J\ell} \left\{ - \frac{j_\ell^2(kr_c)}{G_\ell(r_c,r_c)} + 4\pi \int_{r_c}^{\infty} r^2 dr\, s_\ell(kr) \sum_{\ell'=J-1}^{J+1} V_{\ell\ell'}{}^{Js}(r)\, U_{\ell\ell'}{}^{Js}(r) \right\} \ , \tag{2-7}$$

where $C_{J\ell}$ is the appropriate statistical weight(s being the spin); and,

5) Single particle potential:

$$V(p) = \frac{6}{\pi^2}\int_0^{\frac{p_F-p}{2}} k'^2dk'(k'|K|k') + \frac{3}{\pi^2}\int_{\frac{|p_F-p|}{2}}^{\frac{p_F+p}{2}} k'^2dk'(k'|K|k')\left(1+\frac{p_F^2-p^2-4k'^2}{4pk'}\right) \tag{2-8}$$

for $p < p_F$. For $p \geq p_F$, the first integral vanishes.

The above functions are graphed for various values of their parameters in Figures 1 through 4 respectively.

III. COMPUTATIONAL PROCEDURE

The computations were performed on the CDC-1604 solid-state digital computer. The compiler used was NELIAC,[14] and initial compilation and debugging was done on a Burroughs 220 at the U. S. Navy Electronics Laboratory, San Diego, California. Subsequently the problem was transferred to the computer at the University of California at San Diego, on which final debugging and production runs were made.

The computational procedure was straightforward. The Green's functions (Eq. (2-3) and (2-5)) were first computed. The first approximation for the energies appearing in the denominators was

$$E(k) = \frac{k^2}{2M} , \qquad k < p_F ;$$

$$= \frac{p_F^2}{2M} , \qquad k \geq p_F ;$$

$$E^*(k'') = \frac{k''^2}{2M} , \qquad \text{all } k'' . \tag{3-1}$$

The integration was done numerically to an intermediate value of k, k_{int}, and the integral from k_{int} to infinity was replaced by an analytical approximation to the following integral:

$$-\frac{M}{2\pi^2}\int_{k_{int}}^{\infty} j_\ell(k''r)\, j_\ell(k''r')\, dk'' \quad . \tag{3-2}$$

Here we have assumed that $E(k) << E^*(k'' \geq k_{int})$ and $E^*(k'' \geq k_{int}) = k''^2/2M$. On subsequent iterations, for $k \leq 2.6p_F$, values of $E(k)$ and $E^*(k'')$ from the previous iteration were used in place of Eq. (4-1) (with $E(k > p_F) = E(p_F)$) . For $k'' > 2.6\, p_F$ we use (as in BG)

$$E^*(k'' > 2.6p_F) = \frac{k''^2}{2M} \quad . \tag{3-3}$$

Each cycle leading to a new table of $E(k)$ and $E^*(k'')$ is called a major iteration.

The wave functions were then computed by iteration of Eq. (2-6). On the first iteration, the $s_\ell(kr)$ (Eq. (2-4)) were used as the first guess. On subsequent major iterations, the wave function from the previous iteration was used as the first guess. Each wave function iteration took about one second (for S, P and D waves).

The K-matrix elements (Eq. (2-7)) were computed by numerical integration from $r = r_{core}$ to $r = r_{max}$ where r_{max} was chosen such that contributions to the integral from higher terms were negligible (the exponential behavior of the $V_{\ell\ell'}^{Js}(r)$ made this possible).

The potential energies (Eq. (2-8)) were then computed by numerical integration and the new energy table was formed, with

$$E(k) = \frac{k^2}{2M} + V(p = k) \quad . \tag{3-4}$$

The binding energy was then computed from Eq. (1-3), completing the major iteration. Four minutes were required for a major iteration if the wave functions were iterated five times.

In the computations, all of the meshes used for the numerical integrations could be varied. In addition, in several cases both Weddle's rule and Simpson's rule could be employed for the first seven points. Simpson's rule was found to be adequate in all cases, and was employed in the calculations reported.

The following meshes (in fermis or inverse-fermis) yielded agreement of calculated binding energy to within 0.1 Mev of the most accurate results obtainable with our code:

1) Green's functions (Eq. (2-3)) and wave functions (Eq. (2-6)):

$$\begin{aligned} r,r' &= 0.4(0.05)\ 0.7(0.1)\ 1.5(0.2)\ 2.3(0.5)\ 4.3 \quad (f) \ ; \\ k'' &= 0(0.05)\ 10\ (f^{-1}) \text{ for } G_\ell(r_c,r_c) \\ &= 0(0.2)\ 10\ (f^{-1}) \text{ otherwise} \ . \end{aligned} \tag{3-5}$$

The additional precision for $G_\ell(r_c,r_c)$ was desired because of its importance in the modified Green's functions (Eq. 2-5)) and in the core term in the K-matrix equation (Eq. (2-7)).

2) K-matrix elements (Eq. (2-7)):

$$r,r' = 0.4(0.05)\ 0.7(0.1)\ 1.5(0.2)\ 2.3(0.5)\ 8.3 \quad (f) \tag{3-6}$$

with

$$U_{\ell\ell'}^{Js}(kr > 4.3\ k) = \delta_{\ell\ell'} j_{\ell}(kr) \tag{3-7}$$

for the following values of k:

$$\begin{aligned} k &= 0.1(0.2)\ 0.9\ p_F \text{ on- and off-energy shell} \\ &= 1.0(0.4)\ 1.8\ p_F \text{ off-energy shell} \quad . \end{aligned} \tag{3-8}$$

3) Potential Energies (Eq. (2-8)) and self-consistent total energies:

$$\begin{aligned} k' &= 0(0.05)\ 1.8\ p_F \quad , \\ p &= 0(0.2)\ 2.6\ p_F \quad . \end{aligned} \tag{3-9}$$

4) Mean binding energy (Eq. 1-3)):

$$p = 0(0.05)\ 1.0\ p_F \quad . \tag{3-10}$$

The K-matrix and energy tables were interpolated quadratically as necessary.

The normal computation procedure was to compute Green's functions, wave functions and K-matrix elements for each value of k , and to do the energy computations after all the K-matrix elements had been computed.

In order to investigate the rate of convergence of successive Born approximations and to evaluate the rate of convergence of the wave-function iteration procedure, the code was designed so that K-matrices could be calculated after each wave function iteration, and from these the binding energy was computed. Two procedures for integrating the wave functions

were employed. In order to obtain the successive Born approximations, two tables of wave functions were used. The "old" table was used on the right side of Eq. (2-6) to generate a "new" table (the left side of Eq. (2-6)). In order to increase the rate of convergence, the two wave-function tables were replaced for the remainder of the calculations by a single table, and the integration was performed with the same table used for both sides of Eq. (2-6). In addition, instead of starting each major iteration with

$$U_{\ell\ell'}^{Js}(r) = \delta_{\ell\ell'} s_{\ell}(kr) \tag{3-11}$$

as the initial value for the right side of Eq. (2-6), as was done for the Born approximations, we saved the wave functions from the previous major iteration as the "first guess" in the subsequent major iteration.

The above procedure was used for angular momentum states with $\ell = 0$, 1, and 2. The contribution from higher states has been previously shown to be negligible.[1]

IV. RESULTS

A. Application to the Gammel-Thaler and Breit Potentials

As a check on the method, we first determined the energy and equilibrium density of nuclear matter using the Brueckner-Gammel-Thaler (BGT) potential previously used by BG. The result was a binding energy of -16.9 Mev at $r_o = 1.00$ fermis, compared to the BG values of -15.2 Mev at $r_o = 1.02$ fermis. This difference gives a measure of the error introduced by the approximations of this paper. In figures 1 through 4 we present

some of the intermediate quantities computed (Green's functions, modified basis functions, wave functions, K-matrices, and self-consistent single-particle potential) for the BGT potential with $r_o = 1.00$ fermi ($p_F = 1.52\ f^{-1}$) .

To determine the variation of nuclear properties with various phenomenological potentials, we have calculated energy and equilibrium density for a set of Gammel-Thaler (GT) potentials and for the Breit potential. The Gammel-Thaler potentials differ from each other primarily in the central-tensor force ratio and the magnitude of spin-orbit force in the triplet even states. They give equally good fit to the binding energy and electric quadrupole moment of the deuteron and to the triplet neutron-proton scattering length, as well as good fits to scattering data up to about 90 Mev. Their parameters are given in Table I. Except where otherwise noted, the BGT odd state potentials were used in place of the GT odd state potentials because of a different core in the latter. This substitution was checked and was found to introduce negligible error.

The Breit potential is of the form

$$V = V^{(2)} + V_c + V_T S_{12} + V_{LS}(\underset{\sim}{L}\cdot\underset{\sim}{S}) + V_q[Q_{12} - (\underset{\sim}{L}\cdot\underset{\sim}{S})^2] \ . \tag{4-1}$$

The operator $[Q_{12} - (\underset{\sim}{L}\cdot\underset{\sim}{S})^2]$ has the value $-L(L + 1)$ for uncoupled states, $J = L$, and is zero otherwise. $V^{(2)}$ is the one-pion exchange potential,

$$V^{(2)} = \frac{1}{3}\mu_\pi\, \underset{\sim}{\tau}^{(1)} \cdot \underset{\sim}{\tau}^{(2)} \frac{f^2}{4\pi} \left\{ \left[\underset{\sim}{\sigma}^{(1)} \cdot \underset{\sim}{\sigma}^{(2)} + S_{12}\left(1 + \frac{3}{x} + \frac{3}{x^2}\right) \right] \frac{e^{-x}}{x} + \sigma^{(1)} \cdot \sigma^{(2)} \delta(x) \right\}, \tag{4-2}$$

where μ_π is the pion mass, and $x = \mu_\pi r$ (in units where $c = h = 1$) .

The delta-function term can be neglected in actual computations. The coupling constant, f^2, is given in terms of the related constant, g_0^2, by

$$\frac{1}{4\pi} f^2 = g_0^2 \left(\frac{\mu_\pi}{2M} \right)^2 \simeq \frac{g_0^2}{14^2} \quad , \tag{4-3}$$

where M is the nucleon mass. All the other potentials on the right side of Eq. (4-2) have the form

$$V = \sum_n a_n e^{-2x}/x^n \quad . \tag{4-4}$$

The values of a_n are listed in Table II. For singlet even states, $g_0^2 / 14 = 0.94$. It is unity otherwise. All potentials have a hard core corresponding to $x_c = 0.35$. For singlet-even and triplet-odd states the neutral pion mass is used, and for singlet-odd and triplet-even states a weighted mean of charged and neutral pion masses is used in the proportion of two to one. With $\mu_{\pi_0} = 135$ Mev and $\mu_{\pi_+} = 139.59$ Mev, this has the effect of requiring two core radii, 0.5116 fermi for the first and 0.5002 fermi for the second group of states.

Curves of binding energy vs. r_o for the Gammel-Thaler and the Breit potentials are given in Fig. 5. The binding energy and equilibrium spacing for these potentials are given in Table III. We also include in this table the binding energy for the various potentials at $r_o = 1.00$ fermis, including the effect of some modifications to the Breit potential and (for comparison) to the BGT potential.

These results for the Gammel-Thaler potentials show the considerable

sensitivity of the binding energy and density to the central-tensor force admixture of the Gammel-Thaler potentials, the energy varying from -14.1 to -22.3 Mev and the spacing from 0.90 to 1.08 fermis. The potentials with stronger central forces give greater binding at higher density. The results also indicate that the even-spin-orbit force has negligible effect.

The results obtained for the Breit potential show even more sensitivity to the potential form, since the binding energy -8.3 Mev at a spacing of 1.28 fermis is quite far from the empirical value. The considerable difference between the results of the Gammel-Thaler and Breit potentials appears to be due to these features of the Breit potential:

a) larger core radius,
b) strong odd-state repulsion,
c) quadratic spin-orbit terms, and
d) weaker even triplet central force.

These changes were introduced to give an improved fit to high energy scattering data and to match the one-meson exchange potential at large separation. Breit and his co-workers point out, however, that this potential is not unique, and that several features of the potential were to some extent arbitrary. It is also probable that the condition of matching the meson potential should not be literally interpreted for distances inside 2 or 3 fermis. If this condition is altered, a weaker even-state tensor force could be used, with a corresponding increase in the even triplet central force. The results of the calculations of the present paper point clearly to the need for further investigation with the goal of determining a truly unique potential.

B. Convergence of Successive Approximations

Eq. (1-1) for the K-matrix and Eq. (1-2) for the single-particle potential energy can be solved by successive approximation. It has been suggested that to a good approximation the energy can be obtained from first and second Born approximations applied to the long-ranged part of the interaction after the repulsive core has been separated and treated more exactly.

To study the accuracy of various approximations to Eqs. (1-1) and (1-2), we have first used the procedure of BG to treat the effects of the repulsive core, obtaining the equations quoted in Section II. A complete discussion of this treatment can be found in BG.

In solving these equations, we can determine the effects of two types of successive approximations. Since Eq. (2-6) for $U_{\ell\ell'}^{Js}(k,r)$ was first solved by iteration starting from $s_\ell(kr)$ as the first approximation, it was easy to evaluate the energy for various iterations of the wave function. This we term the first, second, etc., Born approximation, although this term is not strictly correct since we have treated the core exactly.

The second successive approximation is in the evaluation of the Green's function, $G_\ell(r,r')$, Eq. (2-3). We have started in our calculations with the first input for E_k simply

$$E(k) = \frac{k^2}{2M} .$$

This we call the first major iteration. In successive major iterations, we determine $V(k)$ from the previous major iteration for $(k|K|k)$.

A typical result for the binding energy as a function of successive Born approximations for the wave function is given in Table IV. The results of successive major iterations for the single particle energies is given in Table V. These results show that the K-matrix must be computed to at least third order in the interaction and that the self-consistent energy must be determined from K-matrices which themselves have the single particle energies accurate to at least first order in the K-matrices.

The importance of using energies which are self-consistent both as a function of phenomenological potential employed and as a function of r_o (e.g., of Fermi momentum) is illustrated by the self-consistent potential curves of Fig. 6(a) (in which we show the $V(k)$ appropriate to several different phenomenological potentials at $p_F = 1.52\ f^{-1}$ ($r_o = 1.00$ f)), and Fig. 6(b) (in which $V(k)$ is shown for several values of p_F). To test the dependence of the calculations on $V(k)$, we calculated at several densities the binding energy for the BGT potential using the $V(k)$ which was self-consistent at the energy minimum ($r_o = 1.00$ f). The result, shown in Fig. 7, clearly indicates the importance of the self-consistency requirement; there is no sign of saturation near normal density--the minimum is -23.2 Mev. at $r_o = 0.79$ f.

The slow convergence of the Born approximation sequence for the wave function is to a considerable extent due to the non-central forces. For the BGT potential, the binding energy at normal density ($k_F = 1.52\ f^{-1}$) in the absence of the even tensor force is -2.8 Mev compared with -16.9 Mev for the full potential. This contribution of -14.1 Mev from the tensor force is to be compared with -9.0 Mev determined in second Born approximation by Moszkowski and Scott.[10]

C. Comparison with the Separation Method of Moszkowski and Scott

Scott and Moszkowski have determined binding energy and density for the BGT potential and for potential 4305 of Gammel and Thaler (see Table I), using an approximation procedure based on the similarity of the wave function due to the core to that for free scattering. This method is described in detail in their papers,[9,10] and we only give the results here.

They found at normal density binding energies of -14.2 Mev and -23.6 Mev respectively for the potentials BGT and GT 4305 (modified to include the BGT triplet-odd parameters). They included contributions from all states with $\ell \leq 4$. Their results for just S , P , and D waves were -13.6 and -22.8 Mev respectively. The more accurately determined values obtained by the methods of this paper are -16.9 and -21.0 Mev for the same potentials. In addition, the same calculation fails to obtain saturation for the modified GT 4305 potential, in contrast to our minimum, -22.1 Mev at $r_0 = 0.91$ f. Their results, and ours, are shown in Fig. 8.

In Table VI we present a breakdown of the contributions to the binding energy for the BGT potential as computed with our code and as reported by Scott and Moszkowski.[10] The contributions of the D-states (and probably of higher states) are given with reasonable accuracy by the Moszkowski-Scott method (within 0.5 Mev). However, the S- and P-state contributions differ from our values by -5.2 and +2.3 Mev respectively. A major portion of the differences is probably a consequence of neglecting higher order terms. It should be mentioned that the Moszkowski-Scott method employs a relative momentum approximation for the energy dependence, as we have in this paper. Therefore, their results are more properly compared to our results than to those of BG.

The failure to obtain saturation for GT 4305 is to a considerable extent a consequence of using the Brueckner-Gammel self-consistent $V(k)$ for the BGT potential instead of a properly self-consistent $V(k)$. As we have already shown (Fig. 6 and Fig. 7), the dependence of the computed nuclear properties on the self-consistency of the single-particle potential, $V(k)$, is very marked.

Kohler[15] and Scott and Moszkowski[16] have reported a "new separation method" which converges more rapidly than the method used to obtain the results above. However, the new method gives less binding for the calculations reported, which would lead to even poorer agreement with our results.

D. Comparison with the Mohling-Puff Approximation

As emphasized by Bell, the central element of the nuclear matter theories of Mohling and of Puff is a scattering operator defined by Eq. (1) of reference 11, which differs from Eq. (1-1) as follows:

1) The excited state energies, E_i^* are replaced by $p_i^2/2M$.

2) The exclusion principle is ignored for scattering into intermediate states.

The energies E_i of particles in the Fermi sea are determined as in BG from Eq. (1-2). This approximation method is clearly a large departure from the BG method. Bethe has suggested that the Mohling-Puff approximation may nevertheless be quantitatively accurate, with the corrections arising from the two changes approximately cancelling.

In order to avoid in our calculations the difficulties of a vanishing denominator in Eq. (1-1) on the first major iteration (in which all energies are approximated by kinetic energies), the Pauli exclusion

principle was invoked for this iteration only. Because the initial convergence of successive major iterations was very poor (ten iterations for convergence to within ± 0.2 Mev), we averaged the single-particle potentials between iterations, and obtained the sequence indicated in Table V.

The results of this method are given in Fig. 9. The variation of energy with density is appreciably different for the two methods, with the Mohling-Puff approximation equilibrium values being -18.6 Mev at 0.90 fermis compared to our value of -16.9 Mev at 1.00 fermis for the BGT potential, and similar disagreement for the GT 4400 potential. In both cases, the value of r_o at the energy minimum is 10% less than our value.

V. CONCLUSIONS

Our results indicate a definite dependence of the predicted properties of nuclear matter on the choice of phenomenological potential. Although these calculations are not a sufficient criterion for selecting a "best" or "proper" potential, they do emphasize the desirability of further investigation in phenomenological potentials, with particular emphasis on a criterion for uniqueness. The uncertainty in the triplet-even potential does not appear to have been resolved satisfactorily by requiring assymptotic match to the one meson exchange potential. The choice of the radius of the core is also still somewhat arbitrary for those potentials employing a hard core. Determination of the optimum core size from experimental considerations would be very valuable. Gammel and Thaler considered their singlet-even potential to be a unique solution for a Yukawa potential, with $r_c = 0.4$ f , but were unable to differentiate in triplet-even states between

cores of 0.3, 0.4 and 0.5 f. Breit and his co-workers[8] state that the employment of hard cores was arbitrary.

Our calculations have shown that the integral equations of the Brueckner theory can be solved by successive approximation. The requirements are that the wave function iteration, which corresponds to successive Born approximations, be carried to at least the equivalent of the third Born approximation for reasonable accuracy (+0.5 Mev), and the self-consistent single-particle potentials determined to first order in the K-matrix. The sensitivity of results to the tensor-central force admixture demonstrates the requirement for accurate treatment of the tensor force.

The Moszkowski-Scott separation method does not account for the effects of the tensor potential or the S and P state contributions to sufficiently high order for accurate results, largely for the reasons stated above. However, the Moszkowski-Scott calculations do give good qualitative and semi-quantitative (to second order) results in a simple and intuitively pleasing calculation, presumably for any potential provided the self-consistency requirement is met.

The Mohling and Puff-Martin approximation, as we have employed it, also gives semi-quantitative results, leading to errors in binding energy and equilibrium spacing of about 10%. No appreciable reduction of the computational complexities results from this approximation, so that its utility is questionable.

ACKNOWLEDGEMENTS

We wish to acknowledge the cooperation and assistance of the computation facilities of the U. S. Navy Electronics Laboratory, San Diego, California (directed by Dr. M. H. Halstead) and of the University of California, San Diego (directed by Dr. C. L. Perry), and we particularly wish to thank Mr. and Mrs. S. W. Porter of NEL for assistance with NELIAC, the compiler used for these calculations. We are also indebted to Dr. John L. Gammel for suggesting a Padé approximant for Eq. (3-2), the Green's function correction.

FOOTNOTES

[*] This work was done in part under the auspices of the U. S. Atomic Energy Commission.

[+] Permanent address, University of California, San Diego, La Jolla, California.

[‡] Lieutenant, U. S. Navy, on duty under instruction at the University of California.

1. See K. A. Brueckner and J. L. Gammel, Phys. Rev. 109, 1023 (1958), for a list of references.
2. Gammel, Christian, and Thaler, Phys. Rev. 105, 311 (1957).
3. J. Gammel and R. M. Thaler, Phys. Rev. 107, 291 (1957).
4. J. Gammel and R. M. Thaler, Phys. Rev. 107, 1337 (1957).
5. A. E. S. Green, Revs. Modern Phys. 30, 569 (1958); Phys. Rev. 95, 1006 (1954).
6. A. G. W. Cameron, Can. J. Phys. 35, 1021 (1957).
7. J. S. Gammel and R. M. Thaler, in Progress in Elementary and Cosmic Ray Physics, J. G. Wilson and S. A. Wothuysen, eds., Vol. V, Chapter II. North Holland Publishing Co., Amsterdam, 1960.
8. K. E. Lassila, M. H. Hull, Jr., H. M. Ruppel, F. A. McDonald, and G. Breit, Phys. Rev. 126, 881 (1962).
9. S. A. Moszkowski and B. L. Scott, Annals of Phys. 11, 65 (1960).
10. B. L. Scott and S. A. Moszkowski, Annals of Phys. 14, 107 (1961).
11. J. S. Bell, Proceedings of the Rutherford Conference on Nuclear Structure, 1961 (to be published).
12. F. Mohling, Phys. Rev. 124, 583 (1961).

13. P. C. Martin and J. Schwinger, Phys. Rev. 115, 1342 (1959); R. D. Puff and P. C. Martin, Bull. Am. Phys. Soc. 5, 30 (1960); R. D. Puff, Annals of Phys. 13, 317 (1961).

14. H. Huskey, M. H. Halstead, R. McArthur, Comm. ACM 3, 463 (1960); K. S. Masterson, Jr., Comm. ACM 3, 608 (1960).

15. S. Kohler, Annals of Phys. 16, 375 (1962).

16. B. L. Scott and S. A. Moszkowski, Nuclear Physics 29, 665 (1962).

FIGURE CAPTIONS

Fig. 1. Green's functions for BGT potential at $r_o = 1.00$ f: (a) $G_0(r,r_c)$ for several values of k/p_F , both on- and off-energy shell; (b) $G_\ell(r,r_c)$ for $\ell = 0$, 1, and 2, and for $k/p_F = 0.1$ on-energy shell.

Fig. 2. Wave functions for BGT potential at $r_o = 1.00$ f: (a) for $k/p_F = 0.5$ and $\ell = 0$; (b) for $k/p_F = 0.5$ and $\ell = 1$; (c) for $k/p_F = 0.5$ and $\ell = 2$.

Fig. 3. Diagonal elements of the K-matrix for BGT potential at $r_o = 1.00$ f, (a) S-states; (b) P-states; (c) D-states; (d) total. Statistical weights are included.

Fig. 4. Self-consistent single-particle potential, V(k), for BGT potential at $r_o = 1.00$ f.

Fig. 5. Binding Energy vs. r_o for the phenomenological potentials of Tables 1 and 2.

Fig. 6. Variation of self-consistent single-particle potential, V(k), (a) with choice of Gammel-Thaler potentials,[7] at $r_o = 1.00$ f; (b) with Fermi momentum, p_F , using the BGT potential.

Fig. 7. Binding Energy vs. r_o for BGT potential using self-consistent single-particle potential, V(k), for $r_o = 1.00$ f. at all densities.

Fig. 8. Binding Energy vs. r_o for BGT and modified GT 4305 potentials as computed by Brueckner method (this paper) and by the Moszkowski-Scott method.[10]

Fig. 9. Binding Energy vs. r_o as computed by Brueckner method (this paper) and with the Mohling-Puff approximation (see text).

Potential	${}^3V_c^+$ Mev	${}^3\mu_c^+$ (fermi)$^{-1}$	${}^3V_T^+$ Mev	${}^3\mu_T^+$ (fermi)$^{-1}$	${}^3V_{LS}^+$ Mev	${}^3\mu_{LS}^+$ (fermi)$^{-1}$	${}^1V_c^+$ Mev	${}^1\mu_c^+$ (fermi)$^{-1}$
4100	-87.724	1.2183	-272.87	1.2183	0	---	-425.5	1.450
4200	-726.69	1.9554	-121.04	0.97772	0	---	-425.5	1.450
4205	-877.39	2.0909	-159.46	1.0454	-5,000	3.7	-425.5	1.450
BGT	-877.4	2.091	-159.4	1.045	-5,000	3.7	434	1.450
4305	-1964.4	2.4247	-67.106	0.80823	-5,000	3.7	-425.5	1.450
4400	-2019.9	2.3259	-22.719	0.58147	0	---	-425.5	1.450
	${}^3V_c^-$	${}^3\mu_c^-$	${}^3V_T^-$	${}^3\mu_r^-$	${}^3V_{LS}^-$	${}^3\mu_{LS}^-$	${}^1V_c^-$	${}^1\mu_c^-$
BGT	-14.0	1.00	22.0	0.80	-7,315	3.7	130.0	1.0
All others	0	---	22.0*	0.80	-7,317.5*	3.7	70	1.0
* $r_c = 0.4125$ f								

Table I. Parameters of the Gammel-Thaler potentials.[7] BGT is the potential used by Brueckner and Gammel.[1] $r_c = 0.40$ f except as indicated. Triplet and singlet states are designated by 3 and 1 respectively and parity by + and - . As explained in text, BGT odd-state potentials were used instead of the GT odd state potentials in all calculations where not otherwise indicated.

Potential	n=0	1	2	3	4	5	6	7
${}^1V_c{}^+$	21.925	-19.6303	-194.782	66.4334	-15.2873	-14.5395	1.115	0
${}^1V_q{}^+$	0.333	0.5	0.1	-2.0	-5.1083	-0.2333	0.2	0
${}^3V_c{}^-$	0	-14.28	18.72	-17.3	0	-5.3	-1.3	0
${}^3V_T{}^-$	1.5	50.8984	-83.3812	8.7693	-3.1988	1.6172	0.52	0
${}^3V_{LS}{}^-$	0	0	0	0	-2.9794	-76.4565	43.8285	-7.4186
${}^1V_c{}^-$	0	-96.0	-71.001	18.0	8.0	125.8	5.01	0
${}^3V_c{}^+$	0	-47.667	-18.47	-1.00	-3.55	0	0	0
${}^3V_T{}^+$	0	17.3933	7.775	13.535	3.0	-1.4971	0	0
${}^3V_{LS}{}^+$	0	0	0	0	14.35	7.4875	0	0
${}^3V_q{}^+$	0	0	5.3333	0	-13.5917	-7.4167	-1.6667	0

Table II. Parameters of the Breit Potential.[8] Values of coefficients a_n in Eq. (4-4) are in Mev.

Notation same as in Table I.

Potential	Minimum binding energy (Mev)	Equilibrium Spacing (fermi)	Binding energy at r_o=1.00 f (Mev)
GT 4100	-14.1	1.08	-13.6
GT 4200	-16.1	1.01	-16.1
GT 4205	-16.2	1.01	-16.2
BG			
a) full	-16.9	1.00	-16.9
b) without $^3V_T^+$			- 2.8
c) without P states			-18.1
d) without P state core			-23.1
GT 4305	-18.8	0.94	-18.4
GT 4400	-22.3	0.90	-20.8
Breit			
a) full	-8.3	1.28	-0.3
b) without P states			-9.2
c) without P states $^3V_q^+$ and $^1V_q^+$			-12.7
d) without P state core			-14.6
e) without P and D core			-15.2

Table III. Binding Energy and Equilibrium Spacing for potentials discussed in paper. Results indicated for modified potentials are calculated with a single-particle potential, V(k), self-consistent with respect to the modified potential.

Major Iteration	Born Approximation	Binding Energy
I	1	+1.304
	2	-19.590
	3	-25.974
	4	-26.824
II	1	+7.578
	2	-8.337
	3	-11.756
	4	-12.022
	5	-12.046
	6	-12.049

Table IV. Illustrative binding energy sequence for successive iterations of the wave function Eq. (2-6). Energies are in Mev.

Binding Energy in Mev		
Major Iteration	Brueckner Method	Mohling-Puff Approximation
1	-32.963	-2.110
2	-15.720	-15.338
3	-16.936	-17.554
4	-16.887	-17.990
5	-16.892	-18.045
6		-18.033
7		-18.017

Table V. Iteration sequences for Brueckner method and for Mohling-Puff approximation as implemented in this paper. Calculations are for BGT potential at $r_o = 1.00$ fermi. The self-consistent potential, V(k), was averaged between iterations for the Mohling-Puff approximation, improving the convergence of the binding energy sequence to that shown.

	Brueckner Method (this paper)	Moszkowski-Scott Method		
		1st order	2nd order	Total
S states	-38.7	-28.6	-4.9	-33.5
P states	+ 0.6	- 2.3	+0.6	- 1.7
D states	- 7.5	- 7.1	---	- 7.1
Total	-45.6	-38.0	-4.3	-42.3
Binding Energy	-16.9			-13.6
Tensor Contribution*				
a) self-consistent	-14.1			- 9.0
b) with V(k) above	-16.7			

Table VI. Analyses of contributions to binding energy as calculated in this paper and by Moszkowski and Scott.[10] The tensor contribution was calculated by setting ${}^3V_T^+ = 0$ and computing the binding energy (a) with a single particle potential V(k) that is self-consistent with respect to the modified phenomenological potential, and (b) with the single-particle potential V(k) with which the S, P, and D state contributions were computed. Moszkowski and Scott used a first-order approximation to a self-consistent V(k) to compute the tensor contribution.

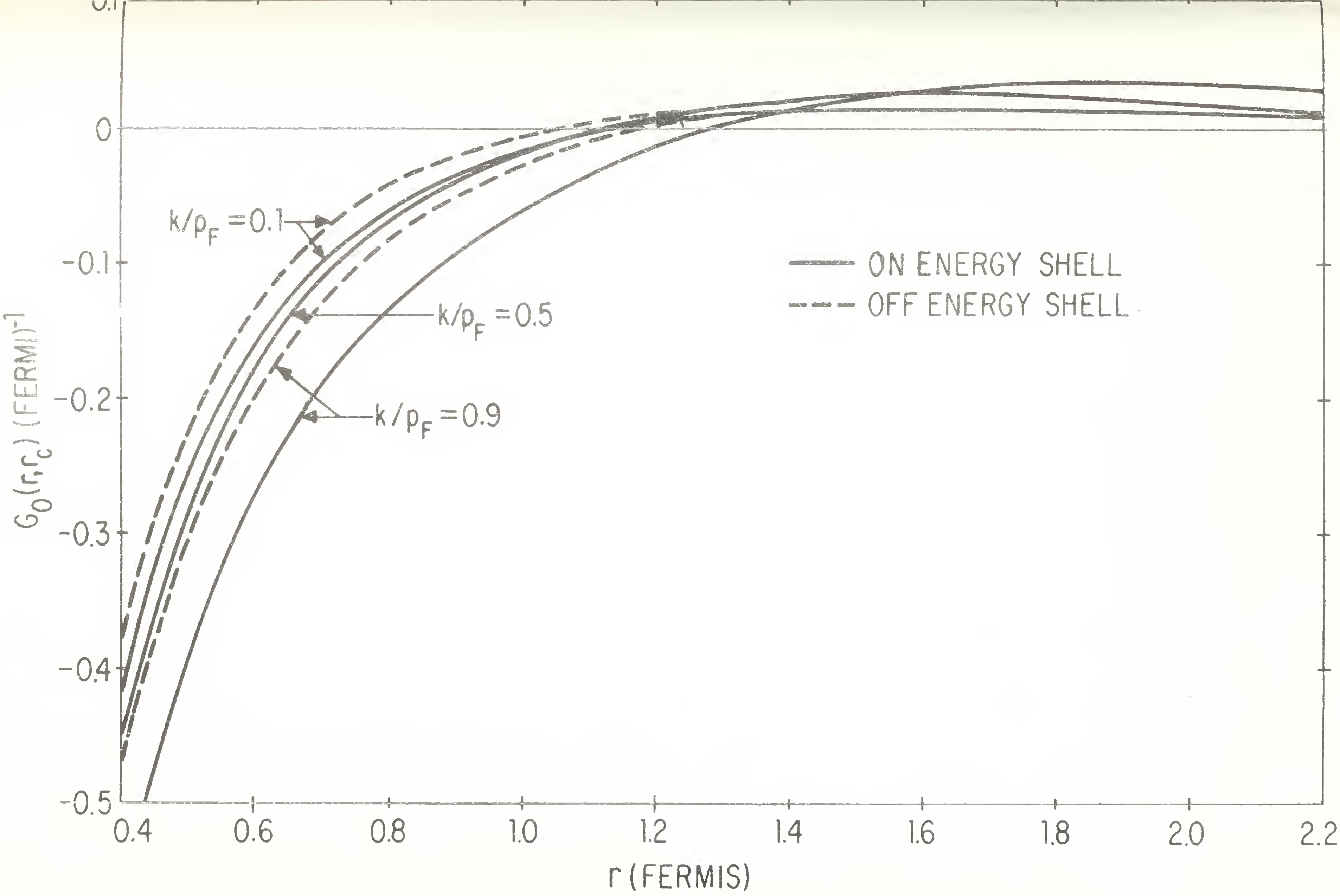
$G_0(r,r_c)$ (FERMI)$^{-1}$
0.1
0
-0.1
-0.2
-0.3
-0.4
-0.5
0.4
0.6
0.8
1.0
1.2
1.4
1.6
1.8
2.0
2.2
r (FERMIS)
$k/p_F = 0.1$
$k/p_F = 0.5$
$k/p_F = 0.9$
ON ENERGY SHELL
OFF ENERGY SHELL

Figure 1.a

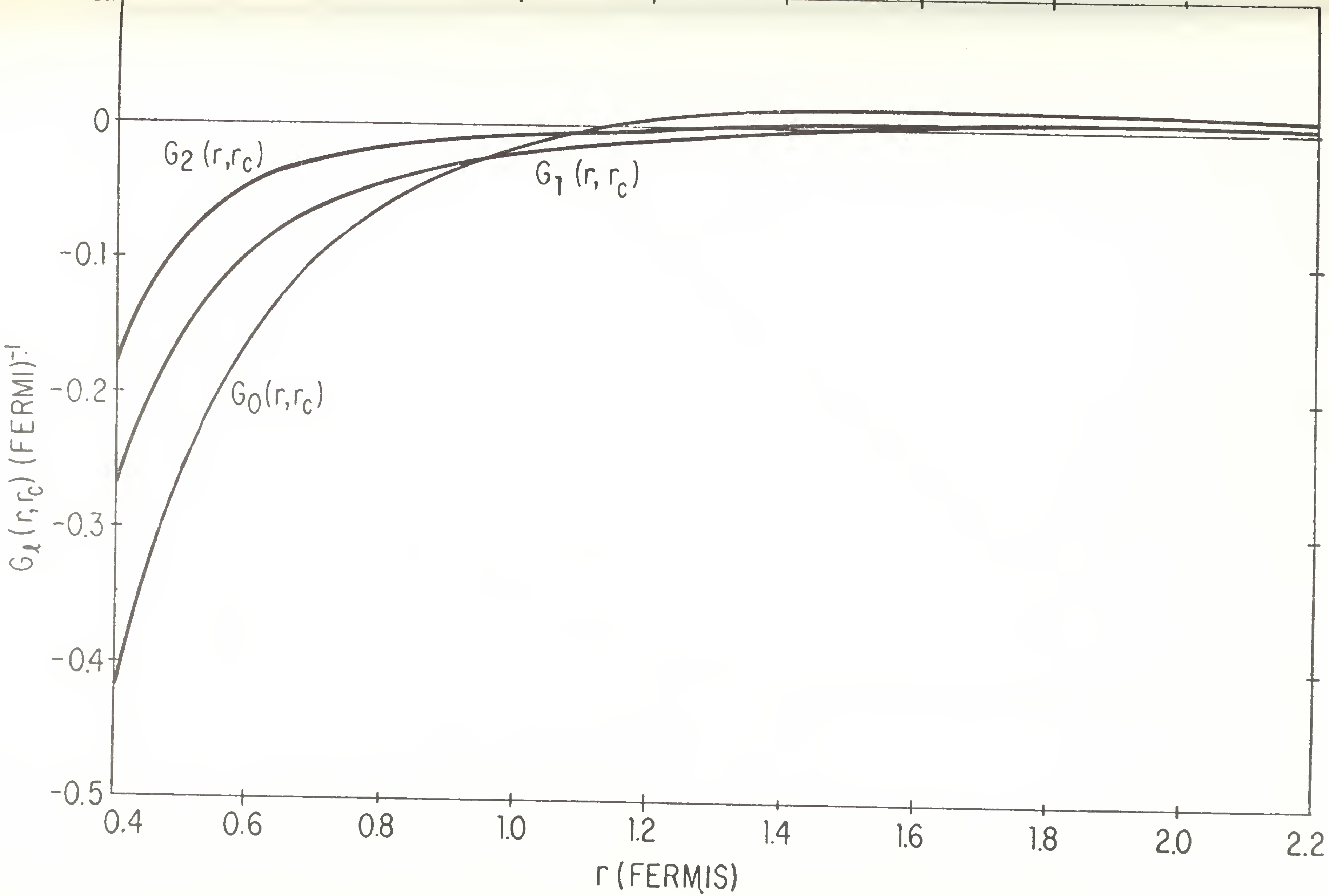
0
-0.1
-0.2
-0.3
-0.4
-0.5
$G_\ell(r,r_c)$ (FERMI)$^{-1}$
0.4
0.6
0.8
1.0
1.2
1.4
1.6
1.8
2.0
2.2
r (FERMIS)
$G_2(r,r_c)$
$G_1(r,r_c)$
$G_0(r,r_c)$

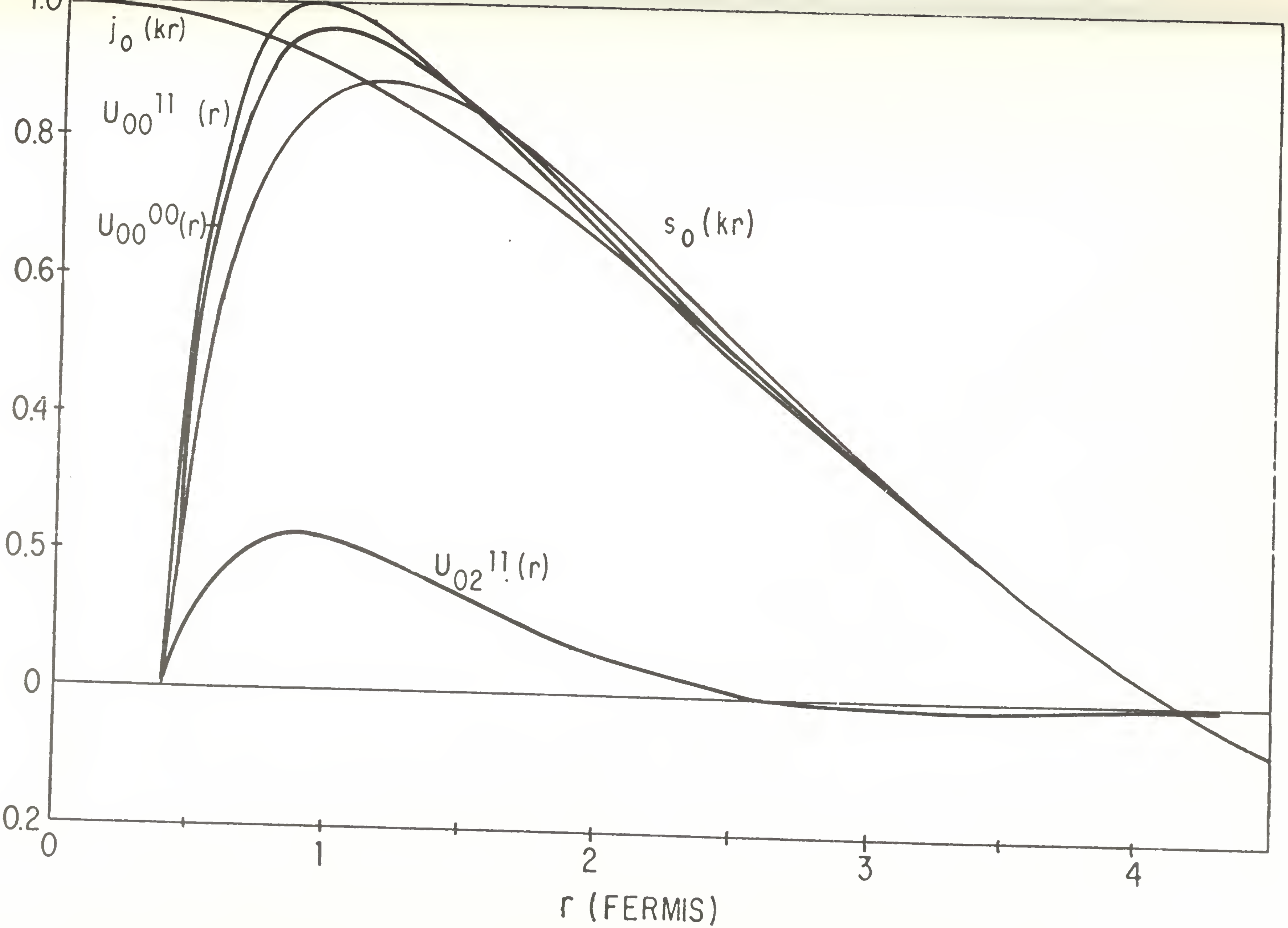
1.0
0.8
0.6
0.4
0.5
0
0.2
0
1
2
3
4
r (FERMIS)
$j_o(kr)$
$U_{00}^{11}(r)$
$U_{00}^{00}(r)$
$s_o(kr)$
$U_{02}^{11}(r)$

Figure 2(a)

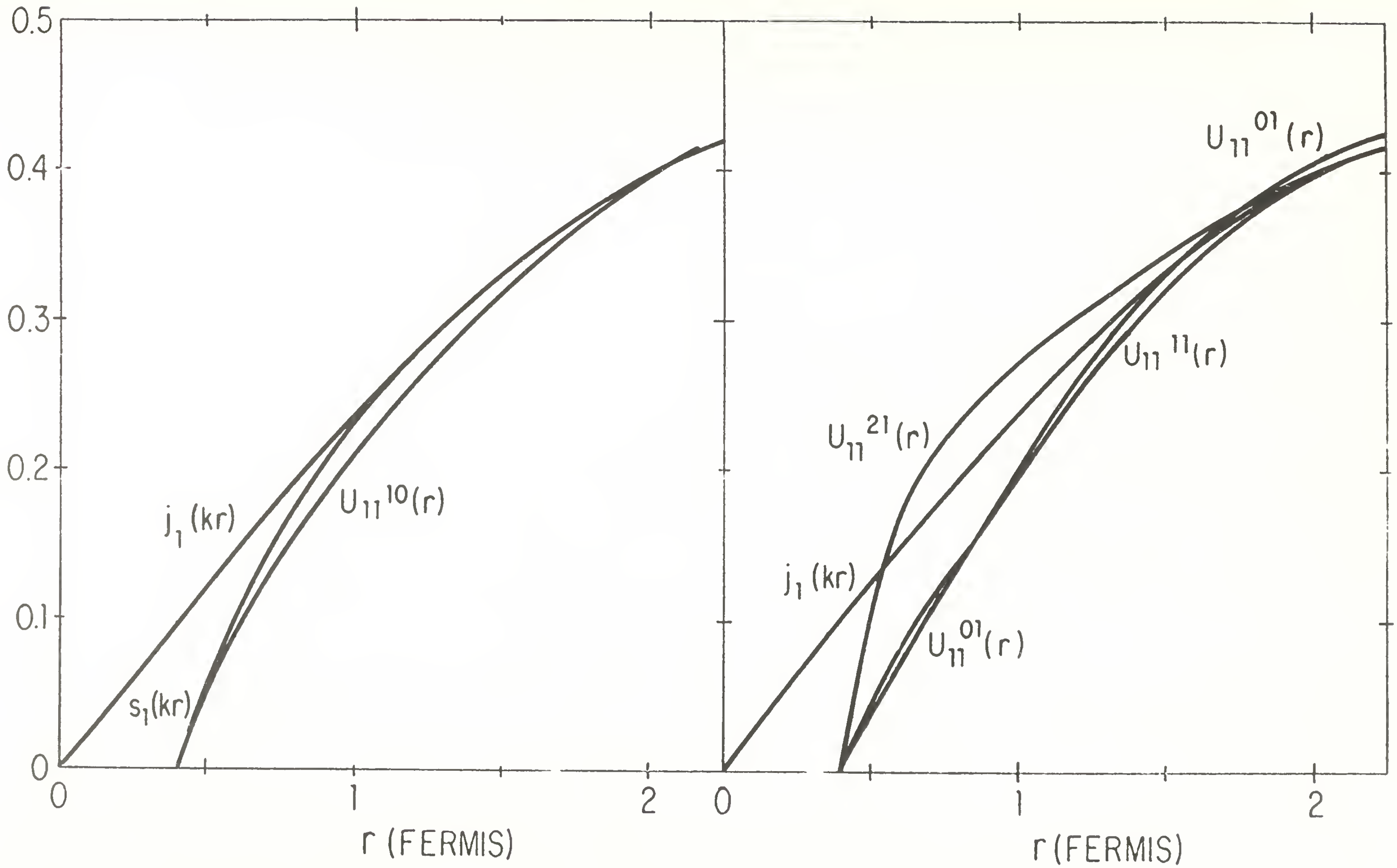
0.5
0.4
0.3
0.2
0.1
0
0
1
2
0
1
2
r (FERMIS)
r (FERMIS)
$j_1(kr)$
$s_1(kr)$
$U_{11}{}^{10}(r)$
$U_{11}{}^{01}(r)$
$U_{11}{}^{11}(r)$
$U_{11}{}^{21}(r)$
$j_1(kr)$
$U_{11}{}^{01}(r)$

Figure 2(b)

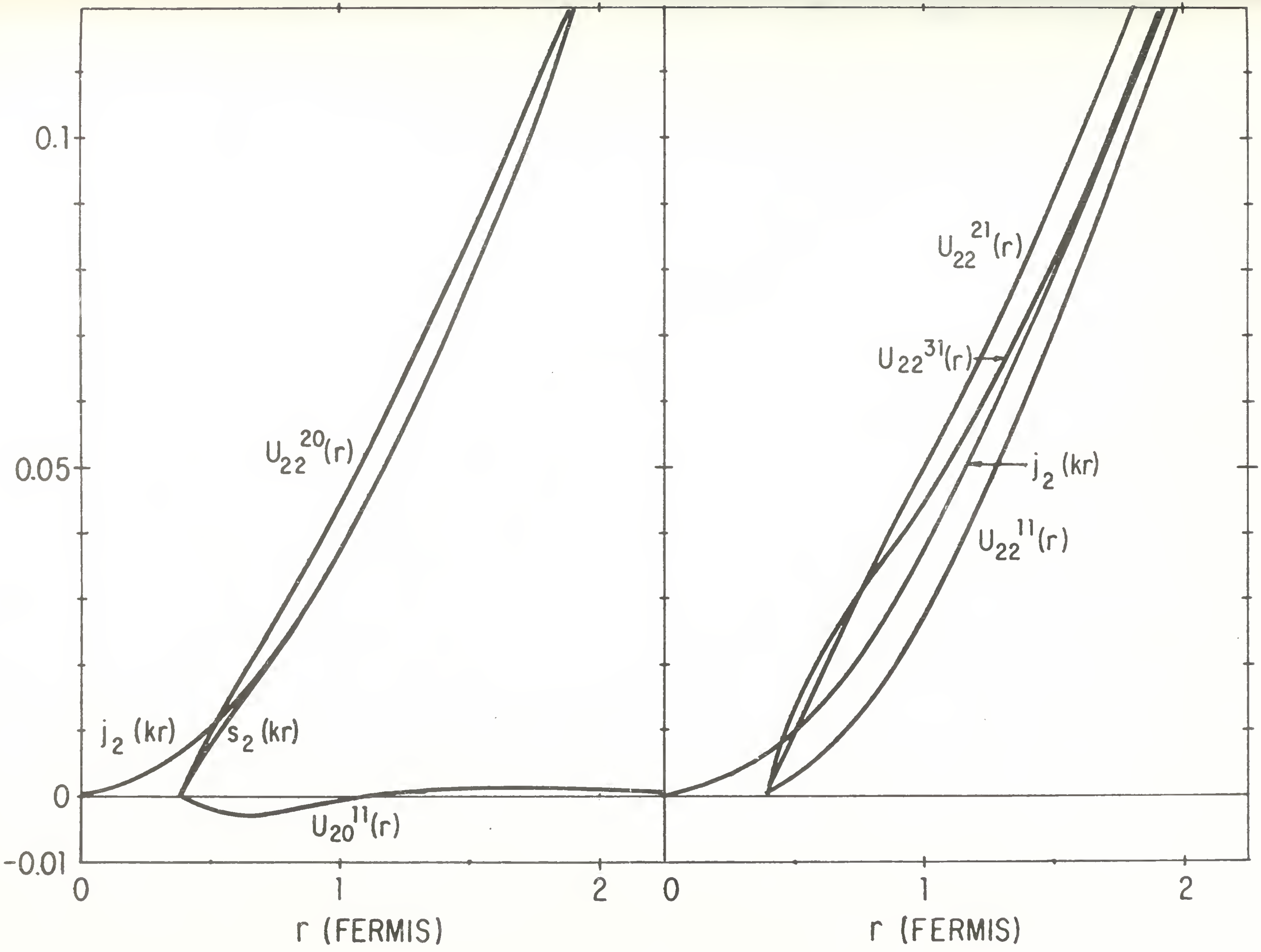
0.1
0.05
0
-0.01
0
1
2
r (FERMIS)
$U_{22}^{20}(r)$
j_2 (kr)
s_2 (kr)
$U_{20}^{11}(r)$
0
1
2
r (FERMIS)
$U_{22}^{21}(r)$
$U_{22}^{31}(r)$
j_2 (kr)
$U_{22}^{11}(r)$

Figure 2(c)

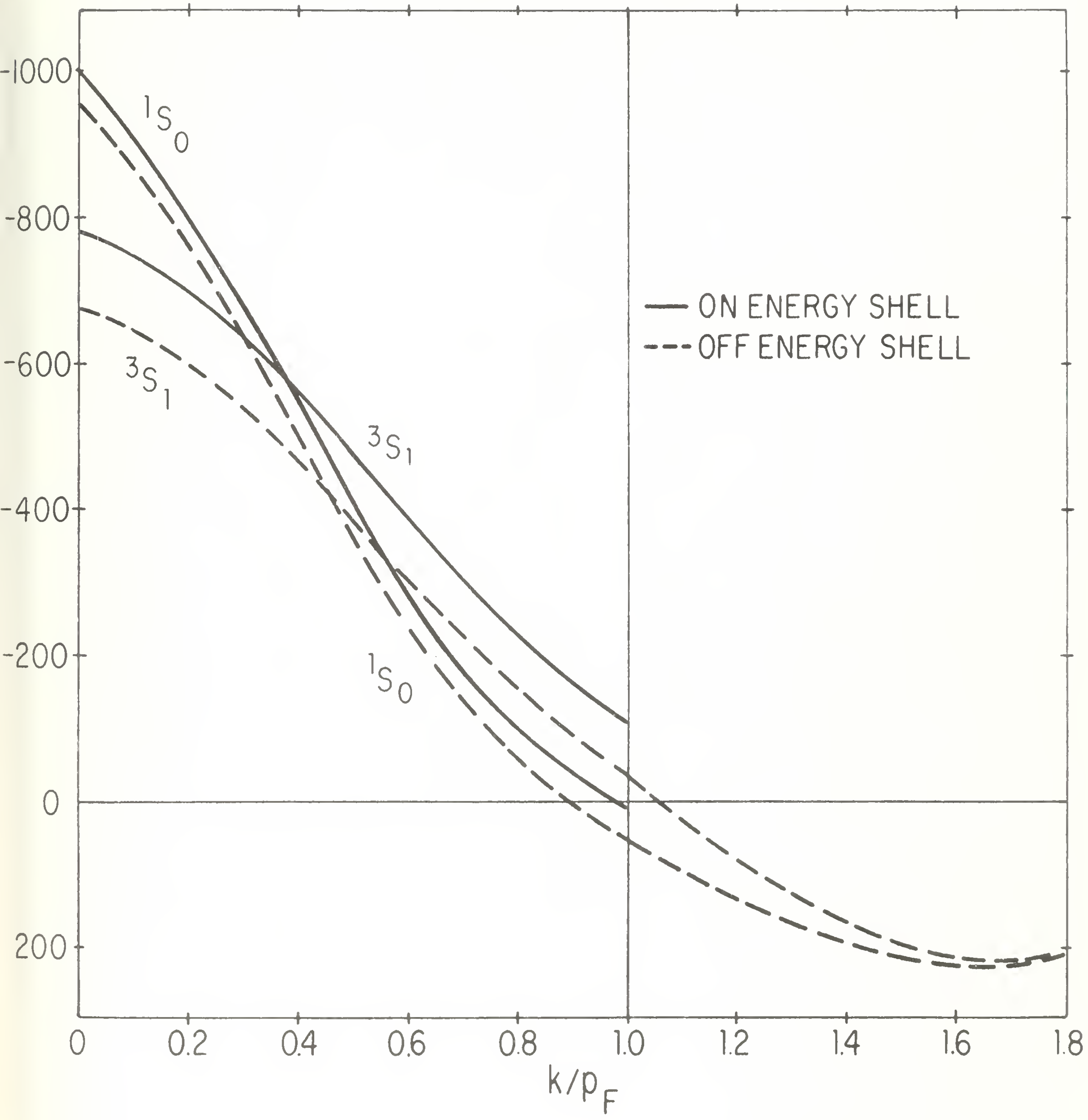
-1000
-800
-600
-400
-200
0
200
0
0.2
0.4
0.6
0.8
1.0
1.2
1.4
1.6
1.8
k/p_F
$^1S_0$
$^3S_1$
$^3S_1$
$^1S_0$
ON ENERGY SHELL
OFF ENERGY SHELL

igure 3(a`

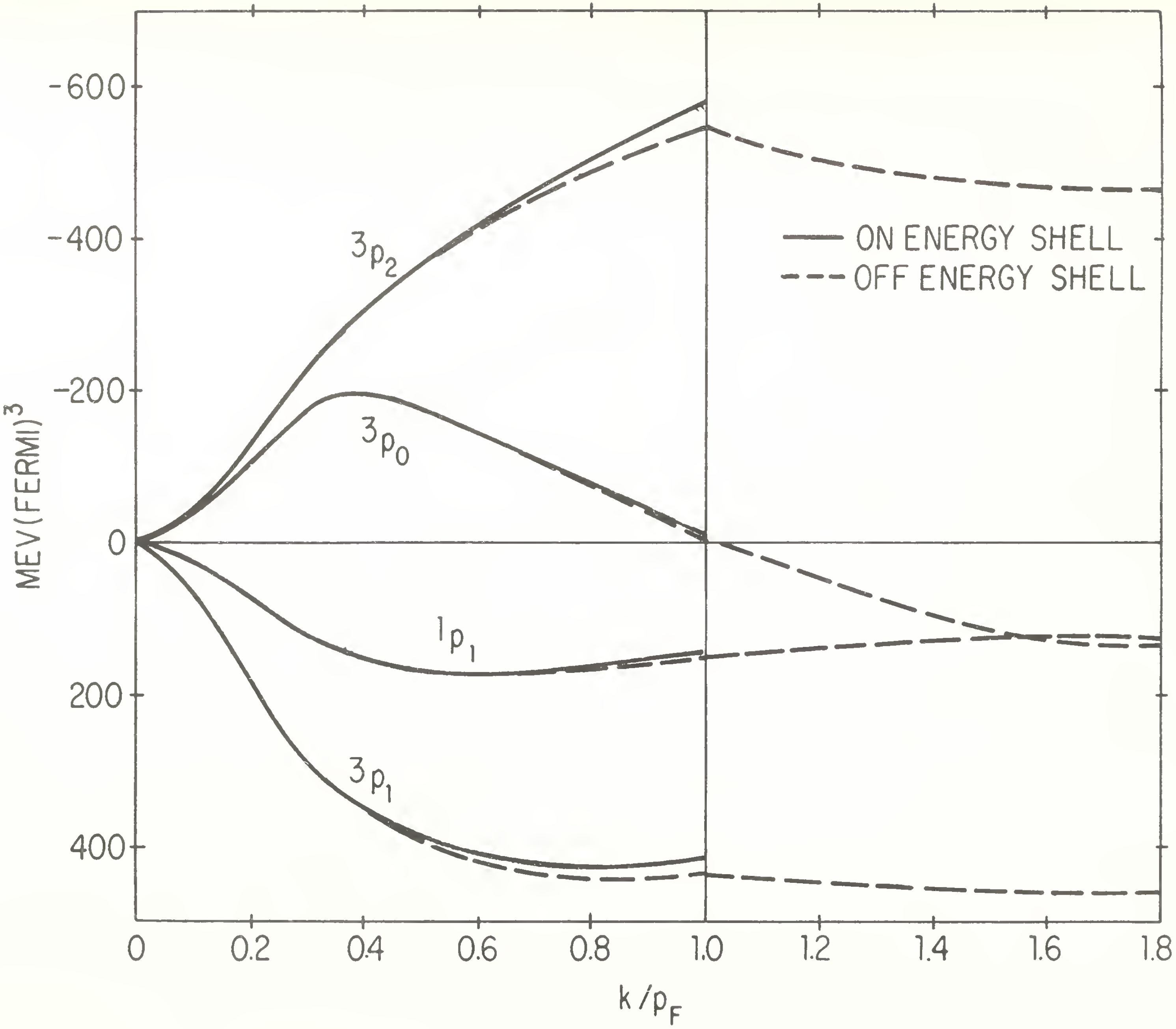
-600
-400
-200
0
200
400
MEV (FERMI)^3
$^3p_2$
$^3p_0$
$^1p_1$
$^3p_1$
ON ENERGY SHELL
OFF ENERGY SHELL
0
0.2
0.4
0.6
0.8
1.0
1.2
1.4
1.6
1.8
k/p_F

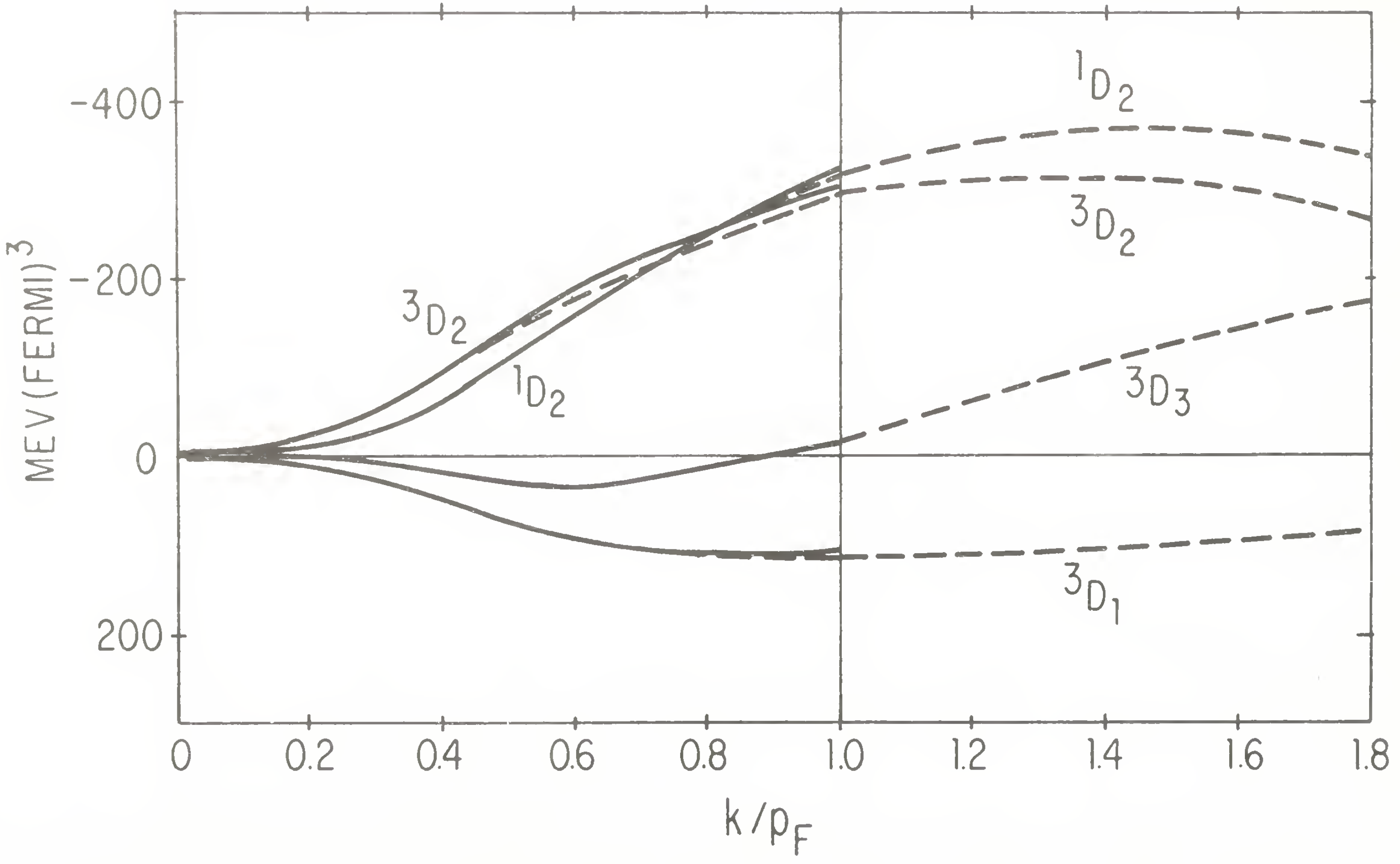
-400
-200
0
200
MEV (FERMI)^3
0
0.2
0.4
0.6
0.8
1.0
1.2
1.4
1.6
1.8
k/p_F
$^3D_2$
$^1D_2$
$^1D_2$
$^3D_2$
$^3D_3$
$^3D_1$

Figure 3(c)

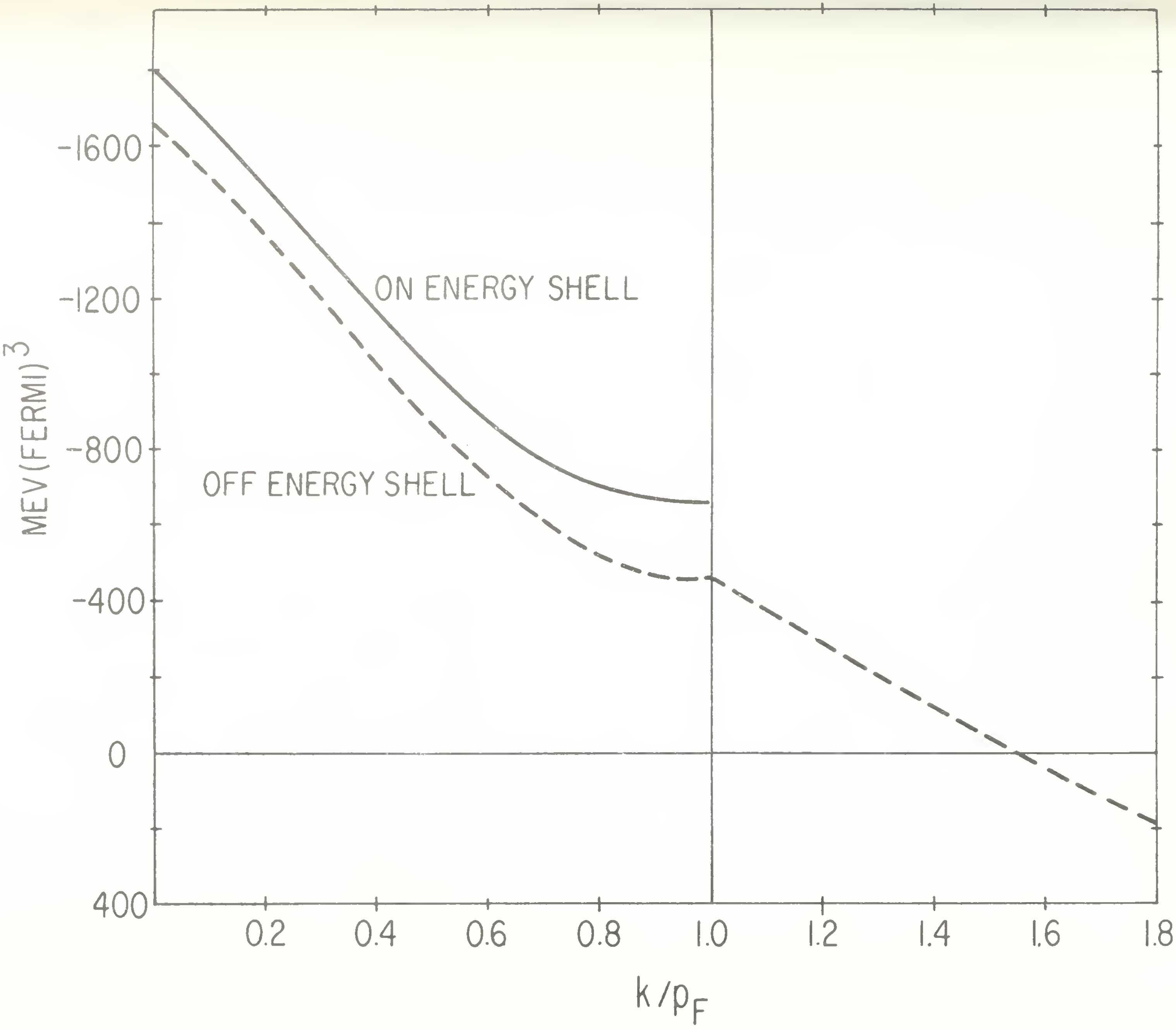
ON ENERGY SHELL
OFF ENERGY SHELL
-1600
-1200
-800
-400
0
400
MEV(FERMI)^3
0.2
0.4
0.6
0.8
1.0
1.2
1.4
1.6
1.8
k/p_F

Figure 3(d)

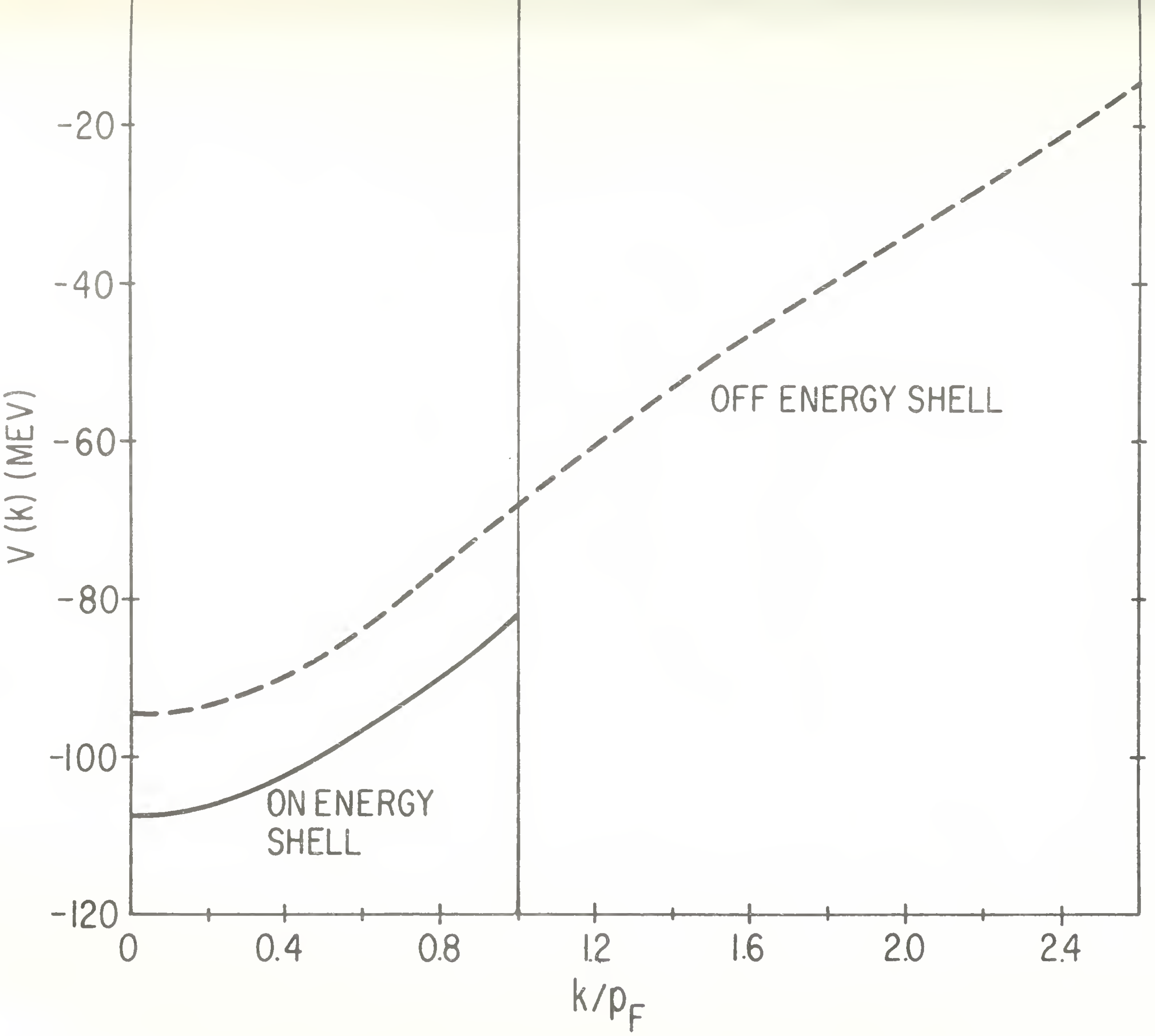
-20
-40
-60
-80
-100
-120
V (k) (MEV)
0
0.4
0.8
1.2
1.6
2.0
2.4
k/p$_F$
OFF ENERGY SHELL
ON ENERGY
SHELL

Figure 4

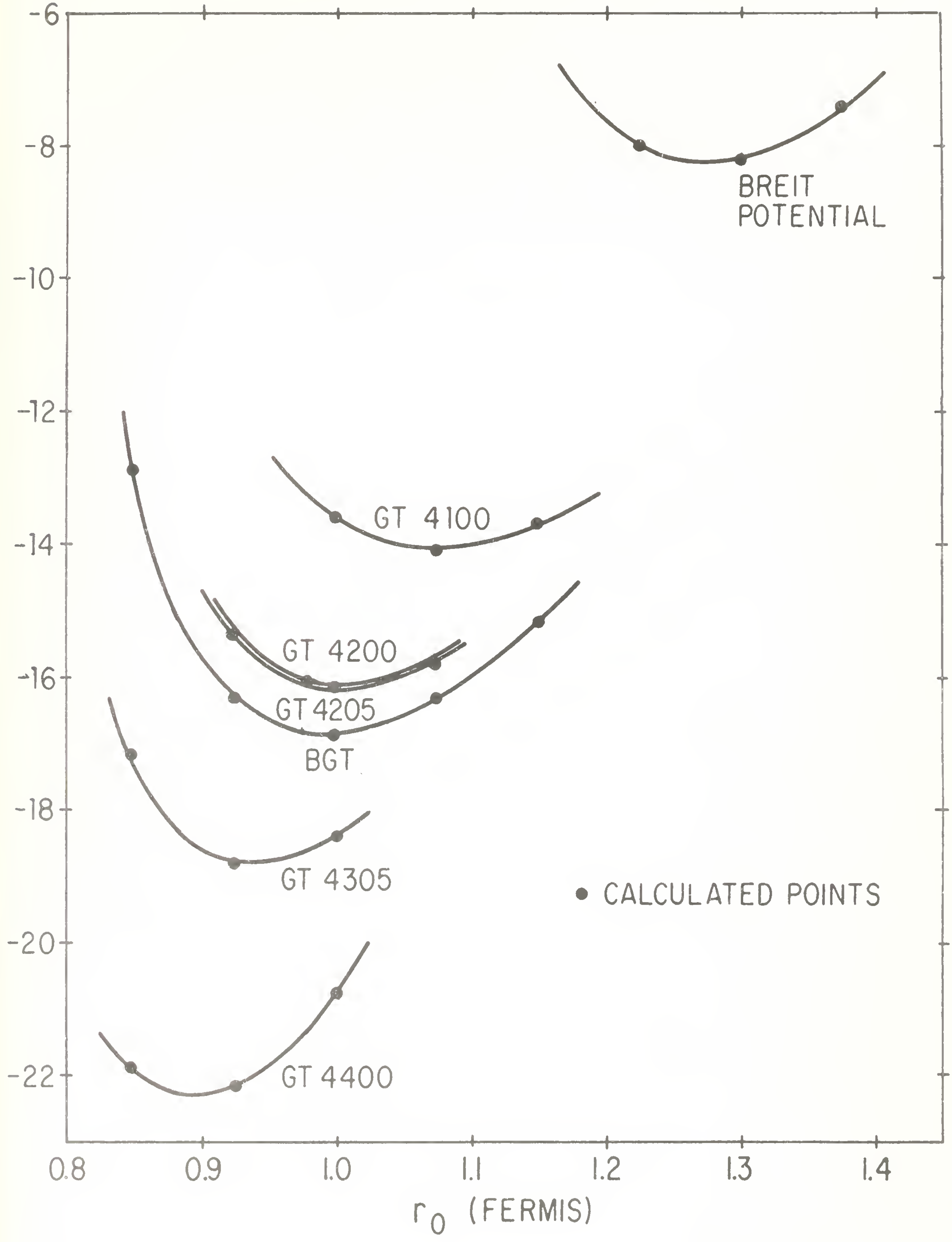
-6
-8
-10
-12
-14
-16
-18
-20
-22
0.8
0.9
1.0
1.1
1.2
1.3
1.4
r$_0$ (FERMIS)
BREIT POTENTIAL
GT 4100
GT 4200
GT 4205
BGT
GT 4305
GT 4400
● CALCULATED POINTS

Figure 5

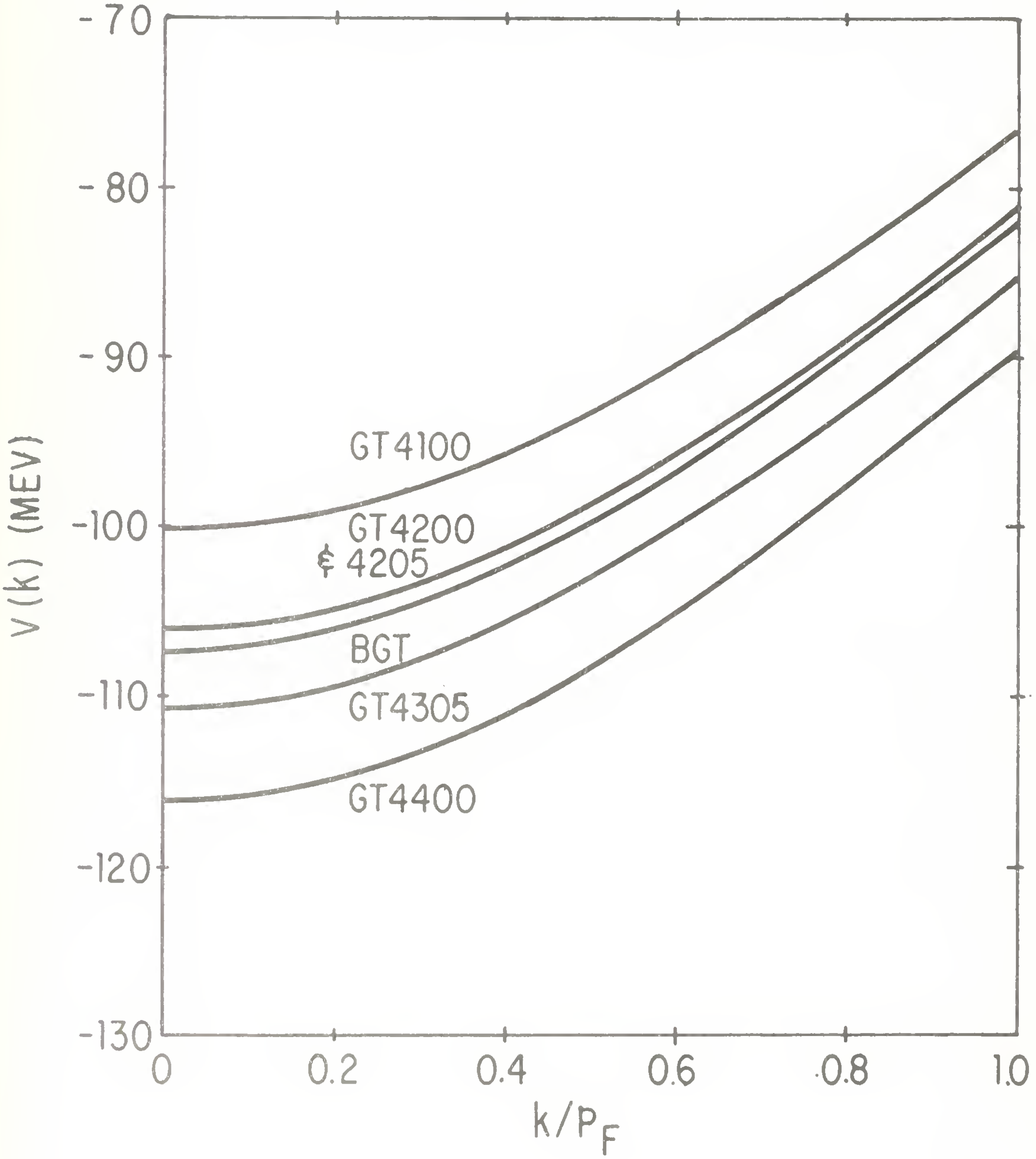
-70
-80
-90
-100
-110
-120
-130
V(k) (MEV)
0
0.2
0.4
0.6
0.8
1.0
k/P_F
GT4100
GT4200
& 4205
BGT
GT4305
GT4400

Figure 6(a)

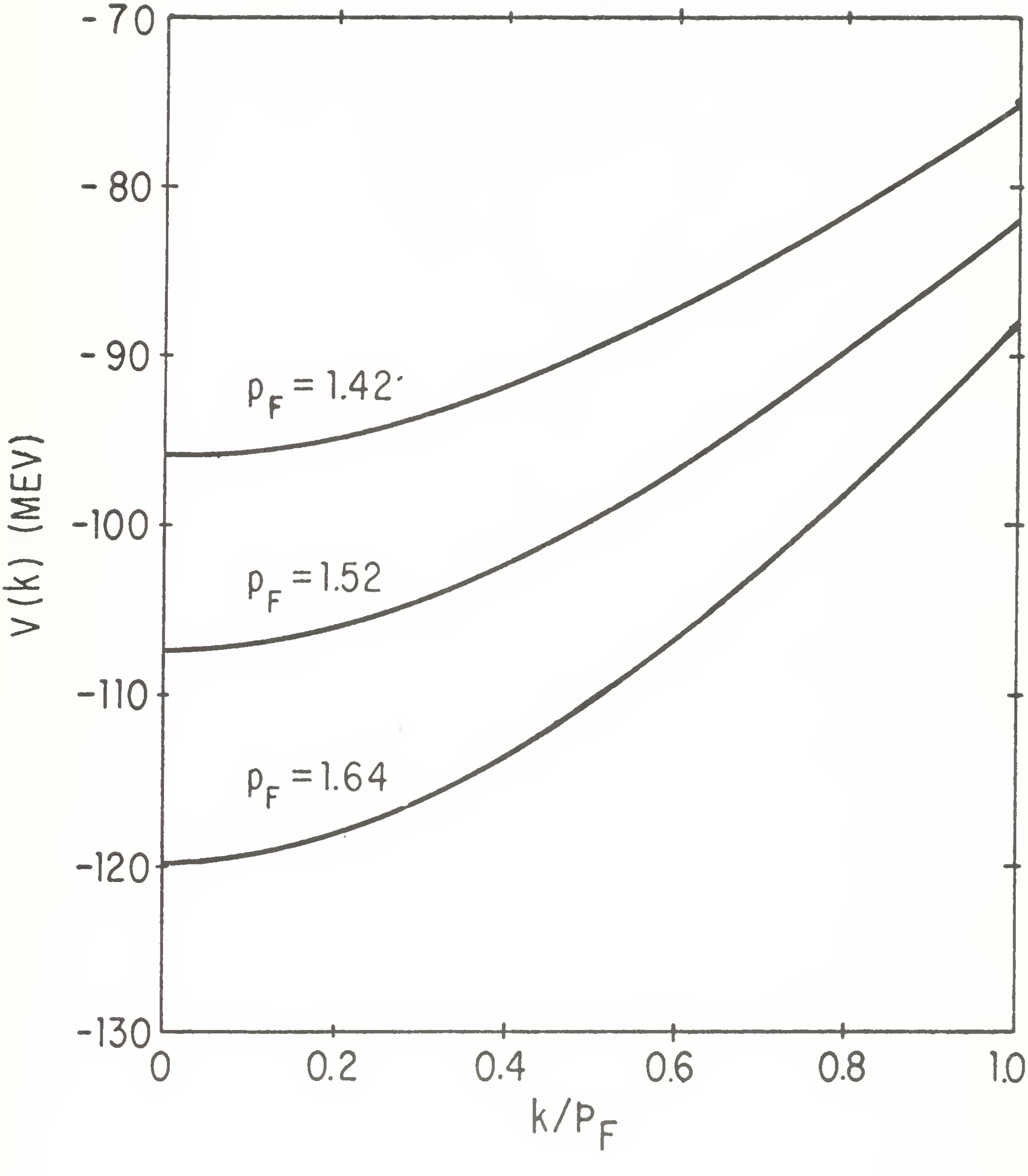

-70
-80
-90
-100
-110
-120
-130
V(k) (MEV)
$p_F = 1.42$
$p_F = 1.52$
$p_F = 1.64$
0
0.2
0.4
0.6
0.8
1.0
k/p_F

Figure 6(b)

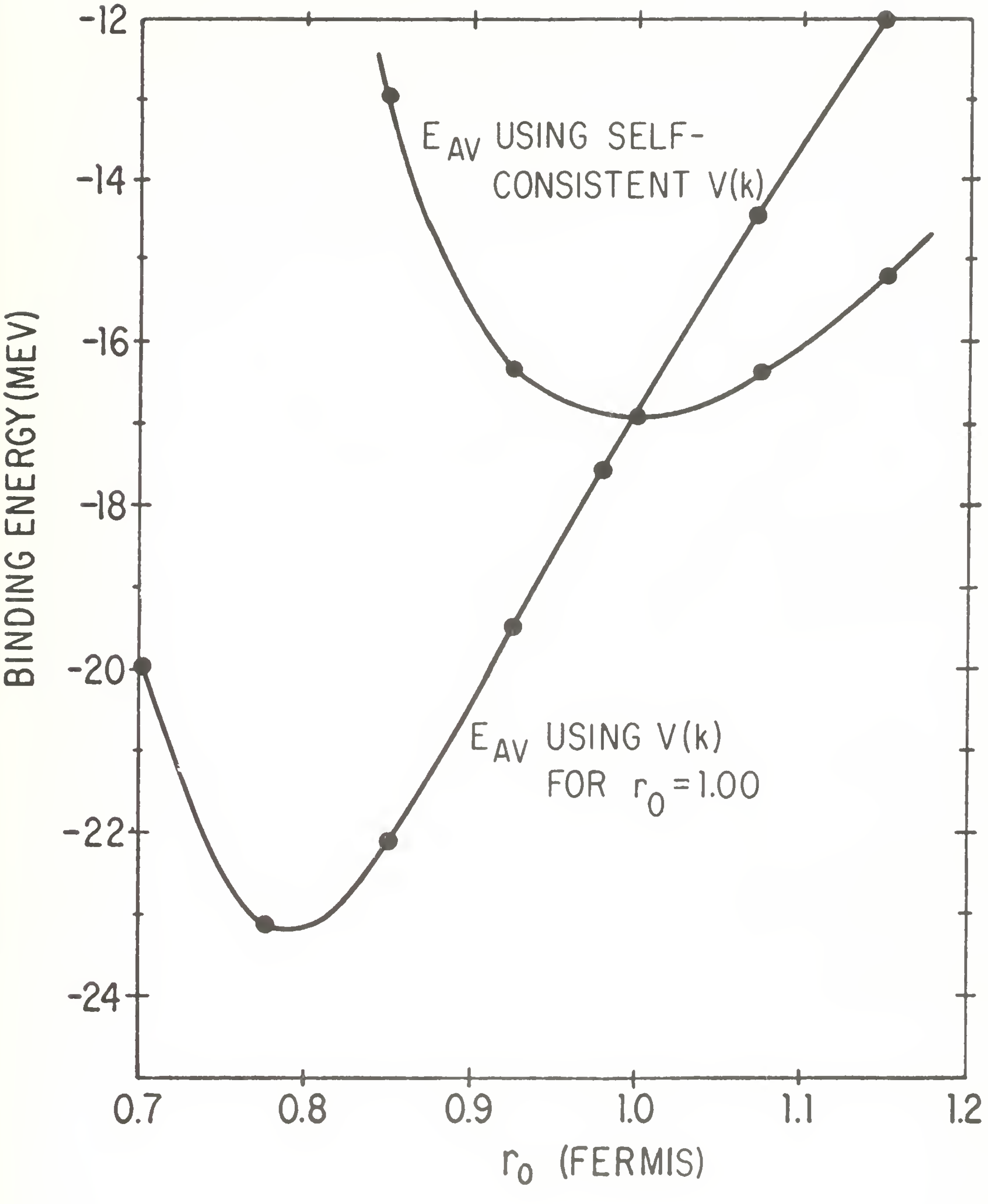

-12
-14
-16
-18
-20
-22
-24
BINDING ENERGY (MEV)
0.7
0.8
0.9
1.0
1.1
1.2
r_0 (FERMIS)
E_{AV} USING SELF-CONSISTENT V(k)
E_{AV} USING V(k) FOR $r_0 = 1.00$

Figure 7

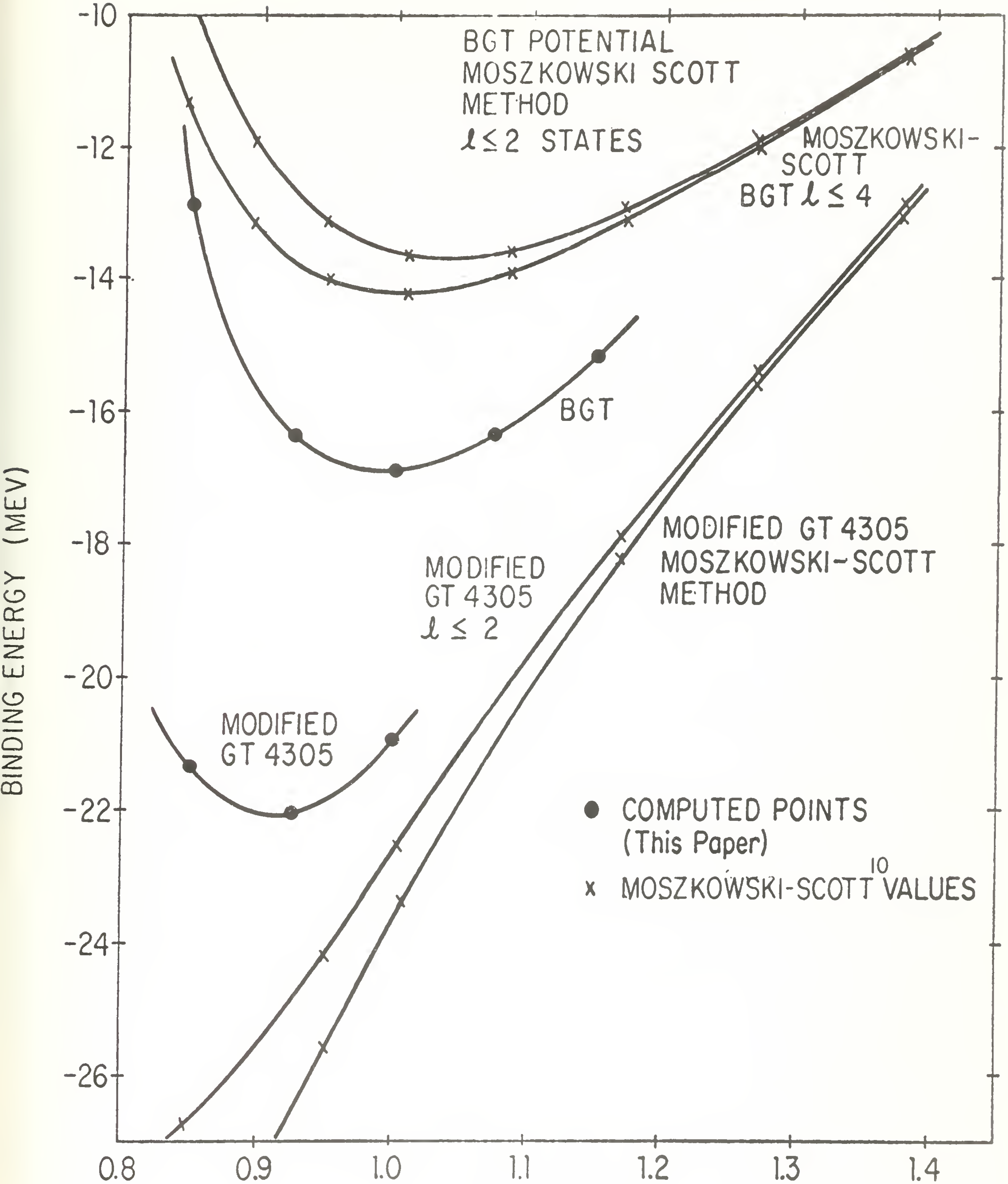
BGT POTENTIAL
MOSZKOWSKI SCOTT
METHOD
$l \leq 2$ STATES
MOSZKOWSKI-
SCOTT
BGT $l \leq 4$
BGT
MODIFIED GT 4305
MOSZKOWSKI-SCOTT
METHOD
MODIFIED
GT 4305
$l \leq 2$
MODIFIED
GT 4305
● COMPUTED POINTS
(This Paper)
x MOSZKOWSKI-SCOTT[10] VALUES
-10
-12
-14
-16
-18
-20
-22
-24
-26
BINDING ENERGY (MEV)
0.8
0.9
1.0
1.1
1.2
1.3
1.4
r_0 (FERMIS)

Figure 8

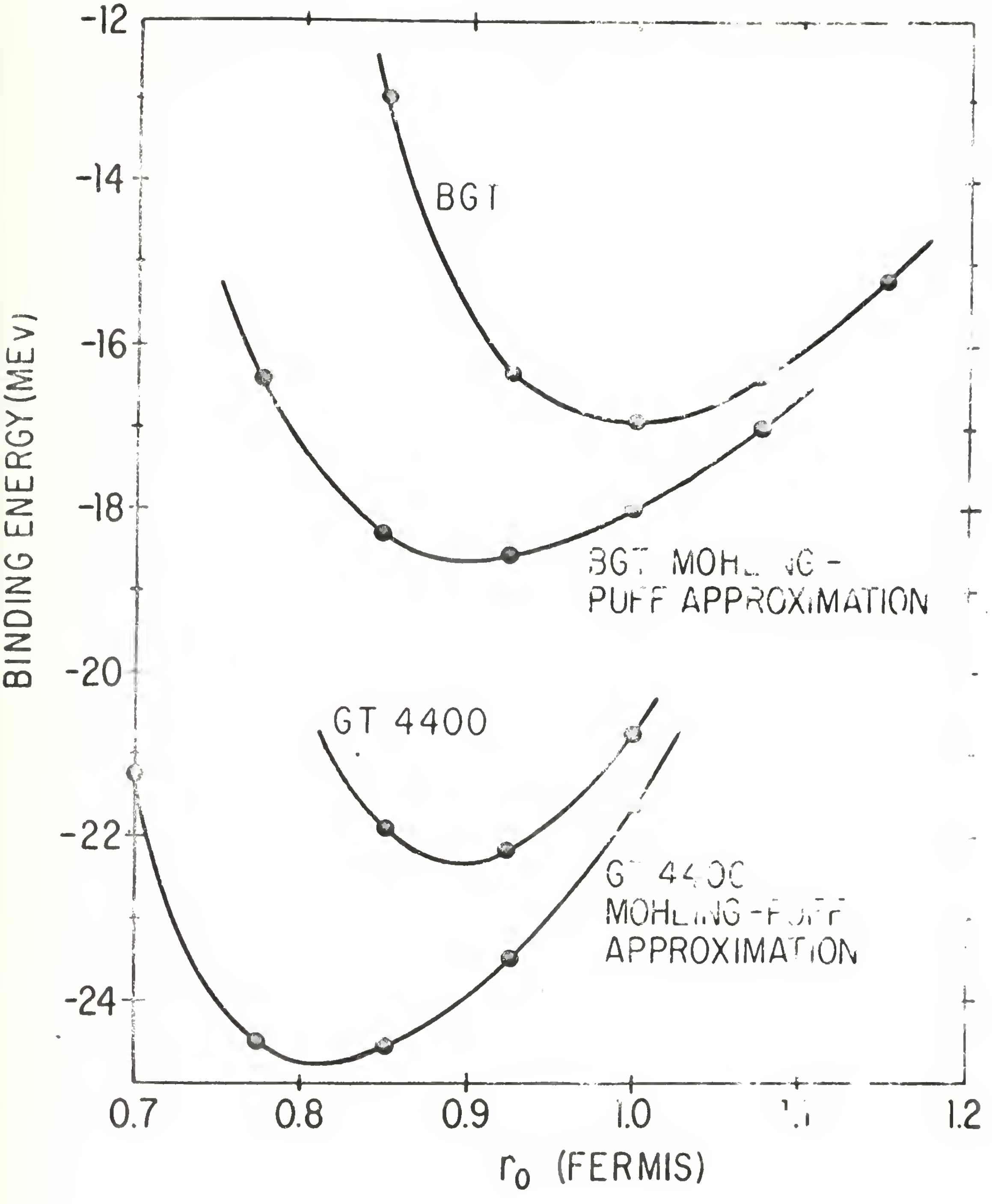
BINDING ENERGY (MEV)
-12
-14
-16
-18
-20
-22
-24
BGT
BGT MOHLING -
PUFF APPROXIMATION
GT 4400
GT 4400
MOHLING - PUFF
APPROXIMATION
0.7
0.8
0.9
1.0
1.1
1.2
r_0 (FERMIS)

Figure [illegible]

APPENDIX H

Properties of Finite Nuclei

K. S. Masterson, Jr.

and

A. M. Lockett

(Physical Review, (to be published))

ABSTRACT

The properties of Pb^{208} have been determined, using the Brueckner-Gammel-Weitzner theory of finite nuclei. Self-consistent solutions of the Hartree-Fock equations as modified by Brueckner and Goldman have been obtained. The properties computed include binding energy, mean proton and neutron radii, separation energies, spin-orbit splittings, nonlocal and state-dependent single-particle potentials, surface depth of density and potentials, and the potential-density relation. Semiquantitative agreement with experiment is obtained, the maximum difference between theory and experiment being of the order of 15%. Revised computations for Ca^{40} are reported to permit comparison between our results (with an improved treatment of the rearrangement energy) and those previously reported by Brueckner, Lockett and Rotenberg for O^{16}, Ca^{40}, and Zr^{90}.

I. INTRODUCTION

In a series of previous papers by K. A. Brueckner and co-workers,[1] methods have been developed for the study of many-fermion systems and have been applied in detail to the determination of the properties of nuclear matter. Approximate extensions of these methods to the study of finite nuclei were proposed by Brueckner, Gammel and Weitzner,[2] and the

properties of O^{16}, Ca^{40}, and Zr^{90} were calculated by Brueckner, Lockett and Rotenberg.[3] The IBM 704 at Los Alamos, on which these computations were done, did not have the capacity to do the Pb^{208} calculation, and the problem was transferred to the CDC-1604 at the University of California, San Diego. A better approximation of the rearrangement energy was used. This paper reports the results of the numerical study of the properties of Pb^{208} and revised computations of Ca^{40} (to permit comparison with the previous calculations by BLR).

II. COMPUTATIONAL PROCEDURE

BGW and BLR discuss the procedure for extending the nuclear matter calculations of Brueckner and Gammel[1] to finite nuclei and examine the approximations involved. Therefore, we shall confine ourselves to stating briefly the pertinent equations, several of which have not previously been stated explicitly.

The problem is essentially that of solving the eigenvalue equation:

$$E_i\varphi_i(\underset{\sim}{r}) = \frac{p^2}{2m}\,\varphi_i(\underset{\sim}{r}) + \int d\underset{\sim}{r}'V_i(\underset{\sim}{r},\underset{\sim}{r}')\varphi_i(\underset{\sim}{r}') + V_R(r)\varphi_i(\underset{\sim}{r}) \quad , \qquad (2.1)$$

where $V_i(\underset{\sim}{r},\underset{\sim}{r}')$ is a nonlocal potential derived from the K-matrices of the Brueckner theory and $V_R(r)$ is the rearrangement potential discussed and calculated by Brueckner and Goldman.[4]

The computational procedure consists of calculating a set of radial wave-functions $R_{n\ell j}(r)$ from a Saxon well with approximately correct radius and depth. These wave-functions are used to start the iteration

procedure which consists of two separate parts, HI and HII. HI takes the wave-functions and computes nonlocal potentials $V_{\ell j}(\underset{\sim}{r}, \underset{\sim}{r}')$. From these potentials and the wave-functions, $R_{n\ell j}(r)$, HII generates local equivalent potentials $F_{n\ell j}(r)$ and $G_{n\ell j}(r)$, and solves the Schroedinger equation for a new set of wave functions (using the iterative methods developed in BGW). The new wave functions are then used as input for the next iteration.

The nonlocal potential computed by HI is given by Eq. (94) of BGW:

$$V_{\ell j}(r_1,r_1') = V_\ell^{(c)}(r_1,r_1') + \tfrac{1}{2}\ell V_\ell^{(LS)}(r_1,r_1') \quad , \qquad j = \ell+\tfrac{1}{2} \ , \ \ell \geq 0$$

$$= V_\ell^{(c)}(r_1,r_1') - \tfrac{1}{2}(\ell+1)V_\ell^{(LS)}(r_1,r_1') \quad , \ j = \ell-\tfrac{1}{2} \ , \ \ell > 0 \quad , \tag{2.2}$$

where, by Eq. (4.17) of BLR

$$V_\ell^{(c)}(r_1,r_1') = \tfrac{1}{2}\int_{-1}^{1} d\mu \ P_\ell(\mu)(\underset{\sim}{r}_1|V^{(c)}|\underset{\sim}{r}_1')$$

$$= \tfrac{1}{2}\int_{|\underset{\sim}{r}_1 - \underset{\sim}{r}_1'|}^{\underset{\sim}{r}_1 + \underset{\sim}{r}_1'} \frac{x\,dx}{r_1 r_1'} \ P_\ell(\hat{\underset{\sim}{r}}_1 \cdot \hat{\underset{\sim}{r}}_1')(\underset{\sim}{r}_1|V^{(c)}|\underset{\sim}{r}_1') \quad , \tag{2.3}$$

with $\mu = \hat{\underset{\sim}{r}}_1 \cdot \hat{\underset{\sim}{r}}_1'$ and $\underset{\sim}{x} = \underset{\sim}{r}_1' - \underset{\sim}{r}_1$ (See Fig. 1). $V^{(LS)}(\underset{\sim}{r}_1, \underset{\sim}{r}_1')$ is given by a similar equation. $V_0(r, r')$ is graphed in Fig. 2 (a) for r = 1.0 fermi.

We trace the integral (2.3) back to the K-matrices tabulated in BGW or to an appropriate Born approximation as follows:

1. $(\mathbf{r}_1|V|\mathbf{r}_1')$ is expanded in Legendre polynomials, and the first two terms are retained (Eq. (4.9) of BLR):

$$(\mathbf{r}_1|V|\mathbf{r}_1') = (\mathbf{r}_1|V|\mathbf{r}_1 + \mathbf{x}) \simeq V_0(r_1,x) + V_1(r_1,x)\cos(\mathbf{r}_1,\mathbf{x}) \ , \qquad (2.4)$$

where V_0 and V_1 are obtained by evaluating $(\mathbf{r}_1|V|\mathbf{r}_1 + \mathbf{x})$ for $\mathbf{x}$ parallel and antiparallel to $\mathbf{r}_1$:

$$V_0(r_1,x) = \tfrac{1}{2}[(\mathbf{r}_1|V|\mathbf{r}_1 + x\hat{\mathbf{r}}_1) + (\mathbf{r}_1|V|\mathbf{r}_1 - x\hat{\mathbf{r}}_1)]$$

$$V_1(r_1,x) = \tfrac{1}{2}[(\mathbf{r}_1|V|\mathbf{r}_1 + x\mathbf{r}_1) - (\mathbf{r}_1|V|\mathbf{r}_1 - x\mathbf{r}_1)] \ . \qquad (2.5)$$

2. In general, $(\mathbf{r}_1|V|\mathbf{r}_1')$ is given by an equation of the form

$$(\mathbf{r}_1|V|\mathbf{r}_1') = \int d\mathbf{r}_2\, d\mathbf{r}_2'\, \varphi^*(\mathbf{r}_2)(\mathbf{r}_{12}|K|\mathbf{r}_{12}')\varphi(\mathbf{r}_2')\, \delta^3\left(\frac{\mathbf{r}_1+\mathbf{r}_2}{2} - \frac{\mathbf{r}_1'+\mathbf{r}_2'}{2}\right) \qquad (2.6)$$

(Eq. (77) and (78) of BGW). The $(\mathbf{r}_{12}|K|\mathbf{r}_{12}')$ are the matrix elements tabulated in BGW. The delta function expresses the conservation of center of mass implicit in the assumption (discussed in BGW) that the K-matrices have a negligible dependence on the total momentum. It is apparent that $\mathbf{r}_1$, $\mathbf{r}_1'$, $\mathbf{r}_2$ and $\mathbf{r}_2'$ must form a parallelogram (Fig. 1).

3. After performing the r_2' integration, one obtains for the terms on the right of Eq. (2.5)

$$\begin{aligned} V_N^{(c)}(\underset{\sim}{r}_1, \underset{\sim}{r}_1 \pm x\hat{\underset{\sim}{r}}_1) = 16\pi \int_0^\infty r_{12}^2 \, dr_{12} \int_{|r_{12} - 2x|}^{r_{12} + 2x} \frac{r'_{12} dr'_{12}}{2xr_{12}} \Big\{ \tfrac{1}{2} H_N(\underset{\sim}{r}_2, \underset{\sim}{r}'_2)_\pm \times \\ \times \; [(r_{12}|K|r'_{12})_{s,e} + 3(r_{12}|K|r'_{12})_{t,o,\text{central}}] + \tfrac{1}{4} H_P(\underset{\sim}{r}_2, \underset{\sim}{r}'_2)_\pm \times \\ \times \; [(r_{12}|K|r'_{12})_{s,e} + 3(r_{12}|K|r'_{12})_{t,o,\text{central}} + (r_{12}|K|r'_{12})_{s,o} + \\ + 3(r_{12}|K|r'_{12})_{t,o,\text{central}}] \Big\} \, , \end{aligned} \qquad (2.7)$$

and

$$\begin{aligned} V_N^{(LS)}(\underset{\sim}{r}_1, \underset{\sim}{r}_1 \pm x\hat{\underset{\sim}{r}}_1) = 16\pi \int_0^\infty r_{12}^2 dr_{12} \int_{|r_{12} - 2x|}^{r_{12} + 2x} \frac{r'_{12} dr'_{12}}{2xr_{12}} \Big(1 - \frac{\underset{\sim}{r}_1 \cdot \underset{\sim}{r}_2}{r_1^2}\Big) \times \\ \times \Big\{ \frac{3}{2} H_N(\underset{\sim}{r}_2, \underset{\sim}{r}'_2)_\pm \; (r_{12}|K|r'_{12})_{t,o,LS} + \frac{3}{4} H_P(\underset{\sim}{r}_2, \underset{\sim}{r}'_2)_\pm \times \\ \times [(r_{12}|K|r'_{12})_{t,e,LS} + (r_{12}|K|r'_{12})_{t,o,LS}] \Big\} \; . \end{aligned} \qquad (2.8)$$

The proton potentials are given by similar equations with H_N and H_P (the density matrix elements) interchanged. These equations are derived in BGW (Eq. (89) and (90)) and in BLR (Eq. (4.15)). The factor 16π comes from the Φ integration and the delta function in Eq. (2.6). Note that $\underset{\sim}{r}_2$ and $\underset{\sim}{r}'_2$ appearing above are determined by $\underset{\sim}{r}_1$, $\underset{\sim}{r}'_1$ and the variables of integration, including x and the sign with which it appears in the terms on the left. We have appended the subscript "±" on H_N and H_P to

indicate this dependence. The density matrix elements are defined by Eq. (85), (86) and (87) of BGW:

$$H_N(\underset{\sim}{r}_2,\underset{\sim}{r}_2') = \sum_{n\ell j} \frac{R_{n\ell j}(r_2)\, R_{n\ell j}(r_2')\, N_{n\ell j}}{4\pi r_2 r_2'} P_\ell^0\,(\underset{\sim}{r}_2,\underset{\sim}{r}_2') \quad , \tag{2.9}$$

with a similar equation for H_P. $N_{n\ell j}$ is the occupation number for the state (2j + 1 for full shells).

4. In the computations, the even state K-matrix elements were used for the S and D states in the following combination:

$$(r_{12}|K|r_{12}')_{s,e} = \sum_{\ell+0,2} (2\ell+1)(r_{12}|K_\ell|r_{12}')_{s,e} P_\ell(\underset{\sim}{r}_{12},\underset{\sim}{r}_{12}') \quad , \tag{2.10}$$

with a similar equation for $(r_{12}|K|r_{12}')_{t,e}$. For the D states, a local equivalent potential was calculated by hand from the BGW K-matrix elements (see BLR for the reason and justification for this). The odd state central and tensor potentials were not included: they cancel each other almost completely. As discussed in BLR, the even spin-orbit term in Eq. (2.8) was also dropped (its experimental justification being questionable). For the odd state spin-orbit contribution in Eq. (2.8), and for the even state terms outside the nonlocal region (e.g., outside the range of the tables in BGW), the Born approximation was used. The Born terms were calculated from the potentials in Table I, and for S and D states they are

$$(r_{12}|K|r_{12}') = V(r_{12}') \frac{\delta(r_{12}' - r_{12})}{4\pi r_{12} r_{12}'} \quad , \tag{2.11}$$

where, in terms of the parameters of Table I, V(r) is of the form

$$V(r) = V\,\frac{e^{-\mu r}}{\mu r} \quad . \tag{2.12}$$

For the spin orbit term, we obtain (using only the P state contribution):

$$V_N^{(LS)}(\underset{\sim}{r}_1, \underset{\sim}{r}_1 \pm x\hat{\underset{\sim}{r}}_1) = 16\pi \int_0^\infty r_{12}^2\,dr_{12} \int_{|r_{12}-2x|}^{r_{12}+2x} (\pm g)\,\frac{r'_{12}\,dr'_{12}}{2x r_{12}} \times$$

$$\times \left[\frac{3}{2} H_N(\underset{\sim}{r}_2, \underset{\sim}{r}'_2)_\pm + \frac{3}{4} H_p(\underset{\sim}{r}_2, \underset{\sim}{r}'_2)_\pm\right] 3P_1(\underset{\sim}{r}_{12}, \underset{\sim}{r}'_{12}) \times$$

$$\times \frac{\delta(r_{12}-r'_{12})}{4\pi r_{12}^2}\; V_{t,o}^{(LS)}\; \frac{e^{-\mu_{t,o}^{(LS)} r'_{12}}}{\mu_{t,o}^{(LS)} r'_{12}} \quad . \tag{2.13}$$

The factor g is an approximation to the $(1 - \underset{\sim}{r}_1 \cdot \underset{\sim}{r}_2 \,/\, r_1^2)$ term in Eq. (2.8). The appropriate expression is obtained by expanding $H(\underset{\sim}{r}_2, \underset{\sim}{r}'_2)$ about $\underset{\sim}{r}_1$ and ignoring derivatives higher than the first (which is justified by the near locality of the spin-orbit K-matrix), and then by averaging over the angles which occur in the subsequent integrations. This procedure leads to

$$g = \frac{1}{3}\,\frac{r_{12}}{r_1}\cos\,(\underset{\sim}{x}, \underset{\sim}{r}_{12})\left(1 - \frac{2r_{12}^2}{x}\right) \quad . \tag{2.14}$$

This approximation reduces to the Thomas expression if $V^{(LS)}$ is independent of ℓ . The corresponding proton potential (~~Eq.~~ 2.13) is obtained

by interchanging H_N and H_P in Eq. (2.13).

5. The core contribution, as computed from Eq. (54) and (56) of BGW, is

$$(r_c|K|r_c) = A \frac{\delta(r_{12}-r_c)\ \delta(r'_{12}-r_c)}{4\pi r_c^2} \frac{(1 - b/1.07)}{(1 - b/r_o)} , \qquad (2.15)$$

with A = 215 or 257 Mev-fermi and b = 0.488 or 0.459 fermi for singlet or triplet states respectively, and

$$r_o = \left(\frac{3}{4\pi\rho(r)} \right)^{\frac{1}{3}} . \qquad (2.16)$$

The density, $\rho(r)$, is the diagonal element of the total density matrix, e.g., $H_N(\underset{\sim}{r},\underset{\sim}{r}) + H_P(\underset{\sim}{r},\underset{\sim}{r})$.

Because of the magnitude of the problem of computing the nonlocal potential for Pb^{208}, some modification of the order of integration from that of BLR was necessary. For a given value of all the variables of integration, the appropriate terms were calculated for $r'_1 = r_1 + x$ and $r'_1 = r_1 - x$. Then the r'_{12} and r_{12} integrations were performed, the r'_{12} integration being inside the r_{12} integration. The x integration was then done for all values of r'_1 simultaneously; e.g., for each point in the x integral, the terms were computed for every value of r'_1 . This sequence was repeated for each of the 50 r_{12} points. The total time for this phase of the computation was 70 minutes. The meshes were (in fermis):

r_1	50 points	0.2 (0.2) 10.0
r_1'	125 points	-1.55 (0.025) 1.55
x	43 points	0.0 (0.05) 2.1
r_{12}	13 points	0.4 (0.1) 1.0 (0.3) 1.6 (0.5) 3.6
r_{12}'	17 points	$(r_{12} - 0.60)$ (0.05) $(r_{12} + 0.20)$.

An intermediate step between HI and HII was required for the lead calculation. The nonlocal potentials were generated by HI and stored on magnetic tape as four matrices (neutron and protons, $j = \ell \pm \frac{1}{2}$) of dimension 7 × 125 (ℓ, r') for each of the 50 values of r (here we change notation from r_1 to r and r_1' to r'). The intermediate code reordered these records on magnetic tape to 22 sets of $V_{\ell j}(r,r')$ in the order in which HII treated each state. (Of the 38 states involved in this calculation, 16 differ from some other proton or neutron state only in the principal quantum number, n, and thus have the same $V_{\ell j}(r,r')$.) This intermediate operation took 15 minutes.

Two calculations were performed by HII. The first calculation was of the potential functions F and G (Eq. (4.24) and (4.25) of BLR):

$$F_{n\ell j}(r) = 4\pi r\int r'dr' \, \frac{V_{\ell j}(r,r')}{D_{n\ell j}(r)} \left[R_{n\ell j}(r')R_{n\ell j}(r) + a^2 \, \frac{dR_{n\ell j}(r')}{dr'} \, \frac{dR_{n\ell j}(r)}{dr} \right]$$

$$+ V_c(r) \quad , \tag{2.17}$$

and

$$G_{n\ell j}(r) = 4\pi a^2 r\int r'dr' \, \frac{V_{\ell j}(r,r')}{D_{n\ell j}(r)} \left[R_{n\ell j}(r') \, \frac{dR_{n\ell j}(r)}{dr} - R_{n\ell j}(r) \, \frac{dR_{n\ell j}(r')}{dr'} \right] , \tag{2.18}$$

where

$$D_{n\ell j}(r) = [R_{n\ell j}(r)]^2 + a^2 \left[\frac{dR_{n\ell j}(r)}{dr} \right]^2 , \qquad (2.19)$$

and $V_c(r)$ is the coulomb potential. The constant a was chosen to be one fermi (the order of the range of the nonlocality of $V(r,r')$), as in BLR. Representative potential functions $F(r)$ and $G(r)$ and radial wave functions, $R(r)$, are plotted in Fig. 2.

A simple iterative method for solving the radial eigenvalue equation derived from Eq. (2.1) is described by BGW. It leads to an equation for the (n+1)st iterate of the radial wave function $R_{n\ell j}(r)$ in terms of the n-th iterate values of the $F(r)$ and $G(r)$ given by Eq. (2.17) and (2.18):

$$(E_i - H_o) \frac{R^{n+1}(r)}{r} = [F^n(r) + V_R(r)] \frac{R^{n+1}(r)}{r} + \frac{G^n(r)}{r} \frac{dR^{n+1}(r)}{dr} . \qquad (2.20)$$

We have used an improved approximation to the rearrangement potential, $V_R(r)$, which is suggested by the analysis of Brueckner and Goldman,[4] who determined the dependence of the rearrangement potential on the single particle momentum (as a fraction of p_F). In BLR, $V_R(r)$ was approximated as a constant factor times $[\rho(r)]^2$. Our new approximation is

$$V_R(r) = \left\{ 26 - 14 \left[\frac{E^{N \text{ or } P}_{n\ell j} - E_{\text{bottom}}}{E_{\text{top}} - E_{\text{bottom}}} \right] \right\} \left(\frac{\rho(r)}{\rho(r_o = 1.07)} \right)^2 . \qquad (2.21)$$

$\rho(r_o = 1.07) = 0.19488$ particles/fermi^3 . This equation interpolates in

terms of the energy eigenvalues between the rearrangement energy corresponding to the approximate mean momentum of the deepest state and the energy appropriate to the top state (e.g., between 26 and 12 Mev respectively at normal density). This improved treatment of the rearrangement energy is the only essential difference between our calculation and that of BLR.

The solution of Eq. (2.20) is discussed in detail in BLR. The procedure starts with choosing an appropriate trial eigenvalue and doing a Runga-Kutta integration out from the origin to an intermediate radius, R_{test}, and in from a very large radius to R_{test}. The latter integration starts with the logarithmic derivative of $R_{n\ell j}(r)$ set equal to that of the appropriate asymptotic solution of the Schroedinger equation. This integration is done with successively better estimates of the eigenvalues until the logarithmic derivatives of the wave functions match at R_{test}. The wave functions are then normalized to unity. The entire HII calculation had to be repeated three or four times per iteration to obtain satisfactory convergence. This minor iteration procedure took about 25 minutes, ten of which were required for calculating the F and G .

The total energy per particle quoted in the next section (and in BLR) is given by

$$E_{\substack{\text{total per}\\ \text{particle}}} = E_{\text{total}} \,/\, \text{number of particles} , \tag{2.22}$$

where

$$E_{\text{total}} = \sum_{\substack{i\\ \text{all}\\ \text{particles}}} \left\{ E_i - \int dr \left[R_i^2(r)\left(\tfrac{1}{2}F_i(r) + V_R(r)\right) + \tfrac{1}{2}R_i(r)G_i(r)\,\frac{dR_i(r)}{dr} \right] \right\} , \tag{2.23}$$

a result which is easily derived

III. RESULTS

A. Comparison with previous rearrangement energy approximation.

In order to check our revised code and to ascertain the effects of the new treatment of the rearrangement energy, we calculated the properties of Ca^{40} and compared our results with the original code used by BLR at Los Alamos, both with and without the new energy treatment. The agreement between the BLR code and our code was good: -6.87 vs. -6.55 MeV mean energy per particle, 3.00 vs. 2.99 Fermi rms radii, and 0.7 MeV or less difference in the eigenvalues. The differences are entirely attributable to a few minor coding errors in the original program. Table II compares the new results with those reported in BLR. The net effect of our improved rearrangement energy approximation is slightly better agreement with experiment for almost every property tabulated: separation energies, total energy per particle, and rms radii. In addition, the spin-orbit splittings are more nearly proportional to the $(2\ell + 1)$ separations generally expected. However, the magnitude of the total energy per particle is still not large enough (-6.55 MeV vs. the experimental -8.55 MeV[5]), the proton rms radius is too small (although it is increased by 3% to a new value which is 83% of the experimental value[6]), and there is slightly too much difference between the separation energy of the last particle and the total energy per particle (1.1 MeV compared to the previous 1.2 MeV and the experimental 0.2 MeV). Comparative potential energies and eigenvalues are given in Table III for every state of Ca^{40} with the old and new approximations. The range of eigenvalues has been reduced from -70.1 through -4.9 MeV to -48.7 through -5.5 MeV. This reduction in spread of energies indicates that the previous approximation reproduced the absolute magnitudes of the energy spectrum quite poorly except

near the top levels; the otherwise close agreement between the two calculations indicates that the approximation employed in BLR was adequate for the computation of the average properties of the nuclei (such as mean energies, rms radii, etc.), and that further improvement in this direction would not be likely to change such properties appreciably.

B. General properties of Pb^{208}.

In Table IV we tabulate the principal properties of Pb^{208} as calculated by the theory for hard core strengths equal to 90% and 100% of the normal strength. The 100% core data is the result of a single full iteration from the 90% data. Experience with the rapid convergence of these computations indicates that the properties tabulated are very near the values we would obtain with further iteration (e.g., probably within 0.1 Mev for the mean energy and 0.01 fermi for the rms radii). Since the individual energy level predictions (next section) are subject to slight fluctuations on the first iterations, they are not quoted for the full core. The 90% core was chosen to permit comparison with the calculations in BLR. In those calculations, the reduced core contributions were arbitrarily employed as a means of improving the binding energies. As we see in Table V, too little binding was obtained for the smaller nuclei even with the reduced core strength. However, for lead with the 90% core the binding energies of the last particles are a fraction of an Mev too great (-8.8 vs. -8.4 Mev for the top neutron and -8.9 vs. -8.0 Mev for the proton), and the magnitude of the total energy per particle (10.0 Mev) is 2.1 Mev greater than that calculated from the masses. The energy of the top nucleon differs by 1.2

Mev from the total energy per particle, compared with the experimental value of 0.5 Mev. For the 100% core, the magnitude of the total energy per particle is several Mev less than the energy with the 90% core, and is one Mev less than the experimental value.

The rms proton radii are 16% and 15% too small (for the 90% and 100% cores respectively). Similar errors were reported for Ca^{40} and Zr^{90}. The surface depths are 1.8 and 1.9 fermis for the proton distributions and 1.9 and 2.1 fermis for the total distributions. (We have taken the surface depth to be the distance over which the density falls from 90% to 10% of its maximum value in the vicinity of the center of the nucleus.) The computed depths are slightly smaller than the experimentally deduced (2.2 ± 0.3) fermis for the charge distribution[6] and $(2.45 \begin{smallmatrix} +\ 0.45 \\ -\ 0.15 \end{smallmatrix})$ fermis for the nuclear distribution.[7] The small discrepancies might vanish with the correction of the error in the rms radii.

C. Energy spectrum.

Table VI gives the energy spectrum for the reduced (90%) hard core strength. The ordering of states is generally in accord with that deduced from experiment for the shell model.[8] Up through the $1g_{9/2}$ state, the Pb^{208} level assignment is the same as that calculated for Zr^{90} (and differs from the Ca^{40} order in the $1d_{3/2}$ and $2s_{1/2}$ states). With the new rearrangement energy treatment, the spread in energy levels and the coarse level spacing are probably the most accurate calculated to date. Thus we compare our spread in eigenvalues of about 70 Mev with those determined in the shell-model calculations with central potentials and spin-orbit coupling of (for example)

Malenka[9] (about 30 Mev) and of Ross, Mark and Lawson[10] (less than 40 Mev). In general, their relative spacing of low-lying levels is in good agreement with ours. However, both authors obtain a level sequence at the surface which differs from ours: for instance, for neutrons, Ross et al have $3p_{1/2}$, $3p_{3/2}$, $2f_{5/2}$, $1i_{13/2}$, ... compared to our $3p_{1/2}$, $1i_{13/2}$, $2f_{5/2}$, $3p_{3/2}$, ...; and, for protons, they have $3s_{1/2}$, $2d_{3/2}$, $1h_{11/2}$, ... compared to our $1h_{11/2}$, $3s_{1/2}$, $2d_{3/2}$, ... In both cases, the spread of energies is less than 2 Mev. The above differences can be traced to the spin-orbit potential, which is imperfectly known and which is treated as a parameter in the shell-model calculations to improve agreement with experiment.

The spin-orbit splittings for the various states are tabulated in Table VII. They are of the right order of magnitude and follow in a reasonable manner the expected $(2\ell + 1)$ graduation in magnitude. In Fig. 2(g) and 2(h) we have indicated the dependence of the local equivalent potential, F(r), and of the wave functions on this splitting. In particular, we note an appreciable spatial splitting of levels with the same orbital angular momentum but with opposite spin.

D. Neutron-proton density relations.

The neutron, proton and total density distributions are indicated in Fig. 3 for the two core strengths. We note the remarkably uniform total density, and the moderate non-uniformity of the neutron and proton contributions. We also see that the neutron and proton wave functions (Fig. 2(d) and 2(f) are almost identical for corresponding states, with the exception of a very slight shift towards the center of the nucleus in the low angular

momentum states. Thus, much of the difference in the density distributions is due to the "extra" neutrons in the outer energy shell (which are distributed throughout the nucleus as well as at the surface). We find that the neutron-proton radii differ by about 0.2 fermi, extending to the larger nuclei the tendency noted in BLR for the proton and neutron distributions to have nearly equal radii. The origin of this effect lies in the symmetry energy and in the insensitivity of the wave functions to differences in potential. The absence of an appreciable neutron-proton difference for the light nuclei (BLR) and the slight difference noted for lead are compatible with experimental results.[11] Quantitatively, for lead we conclude from pion and nucleon scattering calculations[7] that $R_N - R_p = (0.2 \pm 0.2)$ fermi, where R is the half-density radius, in agreement with our calculation. This figure does not include that part of the difference which results from the finite extension of the nuclear potential beyond the matter distribution when the radii are determined from separate nuclear and charge-dependent interactions. We discuss this difference next.

E. Density-potential relations.

In Fig. 4 we have plotted the potential function $F(r)$ for the two top neutron states against the density distribution. The top proton potential is not shown because it lies inside the neutron potentials, a consequence of the smaller proton distribution. The separation between total density and potential (0.5 fermi) is slightly less than that of Ca^{40} and Zr^{90} (0.75 fermi); the difference between the proton half-density point and the nuclear potential half-maximum is 0.7 fermi. These results agree within

the limits of experimental error with the differences between $R_P = (1.18 \pm 0.02)\ A^{1/3} = (7.00 \pm 0.14)$ fermis from electron scattering[6,12] and from μ mesonic atoms,[13] and $R_V = (1.25 \pm 0.05)\ A^{1/3} = (7.41 \pm 0.30)$ fermis from low and high energy neutron scattering.[14] Wilets[15] has concluded from neutron and proton scattering that the difference between the nuclear potential radius and the matter radius is independent of A and is (1.0 ± 0.3) fermi. This difference in radii is largely due to three effects previously discussed,[16] namely: (a) finite range of interaction; (b) nonlinear variation of potential energy with density (Wilets effect);[17] and (c) nonlocality of the effective interaction.

F. Comparison with surface predictions of other theories.

It is interesting to compare the character of the nuclear surface as predicted by previous semi-empirical theories with our results (which are essentially from "first principles" if the concept of a two-body nuclear potential is valid). We will mention only two previous calculations to indicate the degree of precision obtainable. One is the pure Hartree-Fock calculation by Rotenberg[18] with $N = Z = 92$. It yielded surface thicknesses of 2.7 and 3.1 fermis for Gaussian and Yukawa wells respectively, and predicted a marked dip in the proton distribution near the origin (which is absent in our more exact calculation). The calculated separation between the rms radii of the particle density and of the self-consistent collective potential in this model was less than 0.2 fermi. An intermediate step between the pure Hartree-Fock calculation and the BGW theory is the semi-empirical model of Berg and Wilets.[15,17] This model yields $R_N - R_P = 0.2$ fermi (in agreement with our result) and R(potential) - R(nucleon) = 0.7 fermi (compared to our 0.5 fermi).

G. Summary of results for the four nuclei studied to date.

The following is a summary of the general features of the results for full-shell nuclei (O^{16}, Ca^{40}, Zr^{90} and Pb^{208}) studied in this paper and in BLR.

1. The magnitudes of the total energy per particle and of the separation energies are smaller than their experimental counterparts.

2. The difference between observed and calculated energies decreases with increasing nuclear size.

3. The energy spectrum is in general agreement with experiment, and the computation of the coarse spacing, with the new rearrangement energy approximation, is probably the most accurate to date. However, the detailed spacing between close levels, particularly when widely different angular momenta are involved, may not be correct in every instance.

4. The energy spectrum is quite sensitive to any changes in the calculation (as, for example, the changes in the treatment of the rearrangement energy and in the core strength). This is to be expected, because the single particle energies are to be compared with potential wells of the order of 70 Mev. Thus an Mev change in particle energy is less than a 2% change in potential energy.

5. The radii of the nucleon distributions are in good agreement with experiment for O^{16}, with full core, but are about 15% too small for the other nuclei studied.

6. These radii are relatively insensitive to changes in the calculation, a "stiffness" which has been observed in the calculations of BLR and of this paper.

The theory predicts t[illegible] deta[illegible] he [illegible] distribution, and the calculations hav[illegible] broug[illegible] rer[illegible] rat[illegible] neutron and proton densities in the lighter nuclei with [illegible] nor va[illegible] in Pb^{208}. To date it has not been possible to verify the de[illegible] inte[illegible] distributions of these nuclei experimentally, although th[illegible] ar[illegible] of [illegible] and Hill[12] indicates that the charge distribution for lead is probably [illegible]sonably uniform (and especially that there is no dip in the center as de[illegible]ed for gold),[6] in agreement with our results.

8. The calculated surface properties are compatible with present experimental evidence. In particular, the surface depth, neutron-proton radius differences, and the matter-potential relations at the surface are quantitatively predicted.

IV. CONCLUSIONS

The surface depth of the nucleus is now known experimentally to within about 10%.[6] Our results are compatible with experiment and form a theoretical explanation of its shape from first principles. Indeed, there is a need for further refinement of the experiment to verify the internal structure of each nucleus and to ascertain the surface shape consistent with it. There is also a need for further refinement of the BGW theory to obtain better rms radii, with the result that the surface depths predicted might be more accurate. In addition, our theoretical knowledge of the neutron and proton density ratios and of the potential-density relation at the surface is compatible with, and at present more definitive than, experiment. A feature

of the surface which this theory does not describe is possible existence (discussed by Wilkinson)[19] of nucleon clusters, possibly "alpha" particles, in the nuclear surface. Superfluidity in the low density region, if present, is also not treated, but it is believed to have negligible effect on a gross property such as surface depth.

For the remaining properties (binding energy, mean proton and neutron radii, separation energies, and spin-orbit splittings), the theory is in semiquantitative agreement with experiment, the maximum errors being of the order of 15%. The sources of these errors can be grouped into three categories: 1) the numerical procedures, 2) the input (i.e., the phenomenological potentials), and 3) the theory itself (both the Brueckner theory of infinite nuclear matter and the BGW theory of finite nuclei). The first of these (the numerical procedures) is rejected as a source of major error on the basis of the thorough tests by BLR of the meshes employed and the improvement of the results with nuclear size in spite of the fact that any errors from the numerical procedures probably increased also.

However, some of the error may arise in the choice of the phenomenological two-body nuclear potential. Recent calculations[20] of the properties of nuclear matter show that different phenomenological potentials which apparently give "equally good" fit to scattering data do not necessarily lead to identical nuclear properties for the many-body system. It is possible that a better potential would resolve some of the discrepancies between our calculations and experiment. It should be noted that of the seven potentials employed in the calculations of reference,[20] the potential of Table I gives the best agreement between the calculated and semi-empirical

properties of infinite nuclear matter. This, however, does not mean that this potential is the "correct" one, and more work in phenomenological potentials is indicated. Further, in the more accurate calculations of Brueckner and Gammel [1] this potential yielded for nuclear matter a slightly smaller binding energy (-15.2 Mev) than the semi-empirical value (best value -15.8 Mev, but values from -15.5 to -17.0 are also quoted)[21] and an equilibrium spacing that was 5% too small (1.02 vs 1.07 F). These effects undoubtedly influence the computations of BLR and of this paper. In addition, there is some question whether the hard core should be nearer 0.4 F (as in the Gammel-Thaler potential we use) or 0.5 F (as suggested by more recent determinations of phenomenological potentials).[22] A potential with a larger core might give lower density saturation and larger nuclear radii.

The improvement with increasing mass number of the computed binding energy strongly suggests that the principal source of error is in the treatment of the "surface" energy, which is considerably too large. It should be emphasized that the "surface" energy, in our calculations, does not arise solely from the classical effect related to the density variation in the surface. The rearrangement energy, which is essential in the finite system in the determination of the wave function and density, and hence indirectly in the determination of the total energy, does not appear in the uniform system. Thus its effect in the finite nucleus is in fact a "surface" effect. The methods of BLR and of this paper are at best a treatment of the rearrangement problem based on plausibility; they are not rigorously proved. Further investigations of this many-body problem peculiar to the finite system are clearly needed.

In conclusion, we have ascertained that the BGW theory of finite nuclei is in semiquantitative agreement with experiment, the agreement improving with nuclear size. Further, we have seen that our state-dependent approximation to the rearrangement energy correction gives appreciably better results than those obtained in the previous calculations. Finally, it appears probable that much of the residual error in the results can be removed by improvements in the phenomenological two-body potential upon which the calculations are based, and by improvement of the "surface" energy.

ACKNOWLEDGEMENTS

We wish to acknowledge the cooperation and assistance of the computation facility of the University of California, San Diego (directed by Dr. C. L. Perry). We also wish to thank Dr. K. A. Brueckner for his support and many helpful discussions during the progress of the calculations.

FOOTNOTES

* This work was done in part under the auspices of the U. S. Atomic Energy Commission.

† Lieutenant, U. S. Navy, on duty under instruction at the University of California.

1. See K. A. Brueckner and J. L. Gammel, Phys. Rev. 109, 1023 (1958), for a list of references.
2. Brueckner, Gammel and Weitzner, Phys. Rev. 110, 431 (1958), hereafter referred to as BGW.
3. Brueckner, Lockett and Rotenberg, Phys. Rev. 121, 255 (1961), hereafter referred to as BLR.
4. K. A. Brueckner and D. T. Goldman, Phys. Rev. 116, 424 (1959), and Phys. Rev. 117, 207 (1960).
5. The experimental energies quoted in this paper are calculated from experimental masses tabulated by König, Mattauch and Wapstra, Nuc. Phys. 31, 18 (1962).
6. The proton radii and surface depths quoted in this paper are the electron scattering values summarized by R. Hofstadter, Revs. Modern Phys. 28, 214 (1956), and by D. G. Ravenhall, Revs. Modern Phys. 30, 430 (1958).
7. L. R. B. Elton, Revs. Modern Phys. 30, 557 (1958).
8. M. G. Mayer and J. H. D. Jensen, Elementary Theory of Nuclear Shell Structure (John Wiley & Sons, Inc., New York, 1956).
9. B. J. Malenka, Phys. Rev. 86, 68 (1952).
10. Ross, Mark and Lawson, Phys. Rev. 102, 1613 (1956).

11. W. N. Hess and B. J. Moyer, Phys. Rev. 101, 337 (1955); R. W. Williams, Phys. Rev. 98, 1387 (1955).
12. K. W. Ford and D. L. Hill, Ann. Rev. Nuclear Sci. 5, 25 (1955).
13. E. M. Henly, Revs. Modern Phys. 30, 438 (1958).
14. S. Fernbach, Revs. Modern Phys. 30, 414 (1958); Atkinson, Hess, Perez-Mendez and Wallace, Phys. Rev. 123, 1850 (1961).
15. L. Wilets, Revs. Modern Phys. 30, 542 (1958).
16. K. A. Brueckner, Phys. Rev. 103, 1121 (1956); Revs. Modern Phys. 30, 561 (1958).
17. R. A. Berg and L. Wilets, Phys. Rev. 101, 201 (1956); L. Wilets, Phys. Rev. 101, 1805 (1956).
18. M. Rotenberg, Phys. Rev. 100, 439 (1955).
19. D. H. Wilkinson, Proceedings of the International Conference on Nuclear Structure, Kingston, Canada, University of Toronto Press, Toronto (1960), p. 20.
20. K. A. Brueckner and K. S. Masterson, Jr., Phys. Rev. (to be published).
21. A. E. S. Green, Revs. Modern Phys. 30, 569 (1958); A. G. W. Cameron, Can. J. Phys. 35, 1021 (1957).
22. Lassila, Hull, Ruppel, McDonald and Breit, Phys. Rev. 126, 881 (1962).

Table I Parameters of the Gammel-Thaler potential. The potentials have the Yukawa form outside of the repulsive core.

State	Strength V (MeV)	μ
Triplet central even	- 877.39	2.0900
Tensor even	- 159.40	1.0491
Spin-orbit even	-5000	3.70
Singlet even	- 434.0	1.45
Triplet central odd	- 14.0	1.00
Tensor odd	22.0	0.80
Spin-orbit odd	-7315	3.70
Singlet odd	130.0	1.00

Table II. Properties of Ca^{40} calculated with the new rearrangement energy approximation (this paper) compared to the previous calculations of BLR and to experiment. Energies are in Mev, distances in fermis.

Property	Calculated value This paper	Previous (BLR)	Experimental value
Separation energy			
neutron	-12.6	-13.5	-15.63
proton	- 5.5	- 4.9	- 8.34
difference	- 7.1	- 8.6	- 7.29
Total energy per particle	- 6.55	- 6.12	- 8.55
Rms radii			
Total	2.99	2.88	
neutron	2.98	2.84	
proton	3.00	2.91	3.52 ± 0.07
Spin-orbit splitting			
$1p_{1/2} - 1p_{3/2}$			
neutron	3.6	6.1	
proton	3.5	5.9	
$1d_{3/2} - 1d_{5/2}$			
neutron	4.9	7.1	
proton	4.8	6.7	

Table III. Calculated potential energies and eigenvalues for Ca^{40} with the new approximation to the rearrangement energy (this paper) and with the previous approximation (BLR). The core strength was 90% of the normal value. All energies are in Mev.

	This Paper				Previous Calculation (BLR)			
	Potential Energy		Eigenvalue		Potential Energy		Eigenvalue	
State	Neutron	Proton	Neutron	Proton	Neutron	Proton	Neutron	Proton
$1s_{1/2}$	-58.4	-51.1	-48.7	-41.4	-82.4	-72.1	-70.1	-60.0
$1p_{3/2}$	-51.4	-44.1	-34.0	-26.7	-65.2	-55.1	-44.7	-35.1
$1p_{1/2}$	-48.5	-41.1	-30.4	-23.2	-59.3	-49.3	-38.6	-29.2
$1d_{5/2}$	-43.0	-35.5	-17.5	-10.3	-48.3	-38.2	-20.6	-11.6
$2s_{1/2}$	-38.1	-30.2	-14.8	- 7.6	-40.5	-30.0	-16.0	- 7.3
$1d_{3/2}$	-37.9	-30.3	-12.6	- 5.5	-39.6	-29.6	-13.5	- 4.9

Table IV. Properties of Pb^{208} calculated for core repulsion strengths 90% and 100% of normal values. Energies are in Mev and distances in fermis.

	Calculated		Experimental
	90% core	100% core	
Separation energy or			
top eigenvalue			
neutron	-8.8		-7.38
proton	-8.9		-8.04
difference	+0.1		+0.66
Total energy			
per particle	-10.00	-6.86	-7.87
Total rms radius	4.67	4.75	
neutron radius	4.74	4.84	
proton radius	4.56	4.62	5.42 ± 0.11
Surface depth			
total	1.9	2.1	$2.45 {+0.45 \atop -0.15}$
neutron	1.9	2.3	
proton	1.8	1.9	2.2 ± 0.3

Table V. Recapitulation of results for O^{16}, Ca^{40} and Zr^{90} with the old arrangement energy (V_R) approximation and results of this paper for Ca^{40} and Pb^{208} with the new rearrangement energy approximation, Eq. (2.21).

Element	Core Strength	V_R	E_{av}		R_{rms}	
			Calc.	Exp.	Calc.	Exp.
O^{16}	1.00	old	- 2.02	-7.98	2.58	2.57 ± 0.05
	0.825	old	- 4.41		2.41	
Ca^{40}	1.00	old	- 3.89	-8.55	3.07	3.52 ± 0.07
	0.90	old	- 6.12		2.91	
	0.90	new	- 6.55		3.00	
Zr^{90}	1.00	old	unbound	-8.71	--	~4.24
	0.90	old	- 5.80		3.56	
Pb^{208}	1.00	new	- 6.86	-7.87	4.62	5.42 ± 0.11
	0.90	new	-10.00		4.56	

Table VI. Calculated potential energies and eigenvalues for Pb^{208} for core strength 90% of the normal value. All energies are in Mev.

	Potential Energy		Eigenvalue	
State	Neutron	Proton	Neutron	Proton
$1s_{1/2}$	-70.3	-58.4	-65.9	-54.1
$1p_{3/2}$	-68.6	-56.7	-59.7	-48.0
$1p_{1/2}$	-67.9	-56.1	-58.4	-47.0
$1d_{5/2}$	-65.9	-54.1	-51.7	-40.1
$1d_{3/2}$	-65.2	-53.3	-49.7	-38.3
$2s_{1/2}$	-64.1	-51.5	-47.5	-35.2
$1f_{7/2}$	-62.6	-50.8	-42.5	-30.8
$1f_{5/2}$	-62.0	-49.9	-39.5	-28.1
$2p_{3/2}$	-59.4	-47.0	-36.8	-24.4
$2p_{1/2}$	-59.7	-47.1	-34.7	-22.7
$1g_{9/2}$	-59.0	-47.0	-32.2	-20.3
$1g_{7/2}$	-58.3	-46.0	-28.0	-16.5
$2d_{5/2}$	-53.3	-41.2	-25.2	-12.7
$2d_{3/2}$	-55.5	-42.6	-22.6	-10.4
$3s_{1/2}$	-52.4	-39.8	-22.5	- 9.7
$1h_{11/2}$	-54.8	-42.9	-21.1	- 8.9
$1h_{9/2}$	-54.0		-15.6	
$2f_{7/2}$	-45.5		-13.5	
$3p_{3/2}$	-41.9		-10.9	
$2f_{5/2}$	-49.9		-10.3	
$1i_{13/2}$	-50.2		- 9.2	
$3p_{1/2}$	-45.0		- 8.8	

Table VII. Spin-orbit splitting for Pb^{208} in Mev. The core strength was 90% of its normal value.

	neutron	proton
$1p_{1/2} - 1p_{3/2}$	1.3	1.0
$2p_{1/2} - 2p_{3/2}$	2.1	1.7
$3p_{1/2} - 3p_{3/2}$	2.1	
$1d_{3/2} - 1d_{5/2}$	2.0	1.8
$2d_{3/2} - 2d_{5/2}$	2.6	2.3
$1f_{5/2} - 1f_{7/2}$	3.0	2.7
$2f_{5/2} - 2f_{7/2}$	3.2	
$1g_{7/2} - 1g_{9/2}$	4.2	3.8
$1h_{9/2} - 1h_{11/2}$	5.5	

FIGURE CAPTIONS

Fig. 1. Relationships between variables in the theory of finite nuclei.

Fig. 2. Representative potential and wave functions for Pb^{208}. (a) Nonlocal potential, $4\pi rr'V(r,r')$ for $r = 1.00$ fermi, illustrating variation with strength of hard core potential (90% and 100% of normal) and differences between neutron and proton potentials; (b) Potential function $F(r)$ for s states, indicating the variation with principal quantum number and differences between neutron and proton functions; (c) Potential function $G(r)$ for s state neutrons, indicating dependence on principal quantum number; (d) Radial wave functions, $R(r)$, for the s state protons and neutrons; (e) Potential function $F(r)$ for neutrons and protons for two representative states; (f) Radial wave functions, $R(r)$, for neutrons and protons for selected states illustrating the variation with orbital quantum number; (g) Potential function $F(r)$ for both core strengths for selected states illustrating the spin-orbit splitting; (h) Radial wave functions corresponding to the potential functions of 2(g). Unless otherwise indicated, all data are for core strength 90% of normal.

Fig. 3. Proton, neutron and total densities for repulsive core strengths equal to 90% and 100% of normal values.

Fig. 4. $F(r)$ for the highest two neutron states of Pb^{208} and the total density as a function of radius. The core strength was 90% of normal.

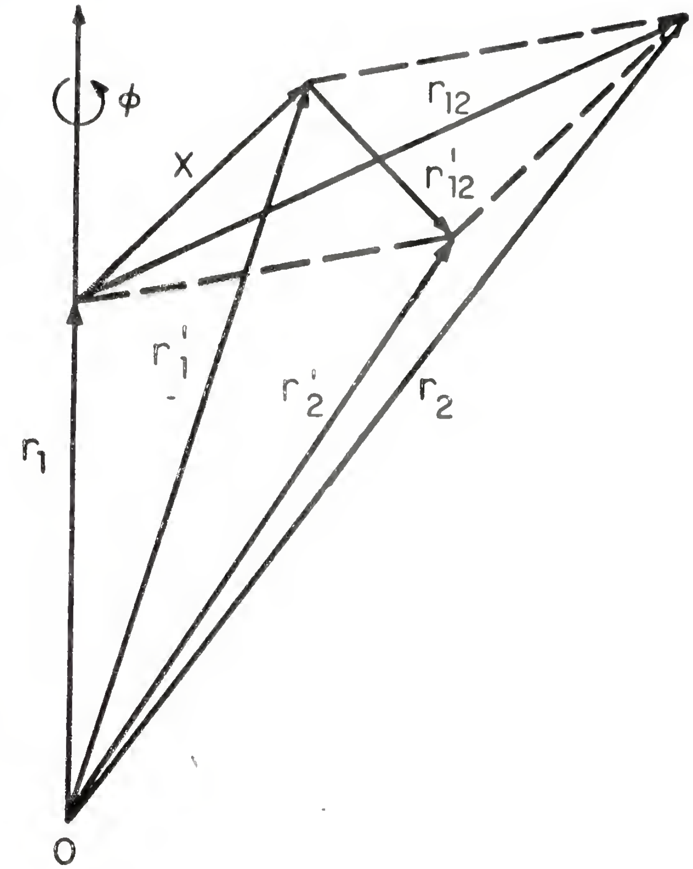

Figure 1

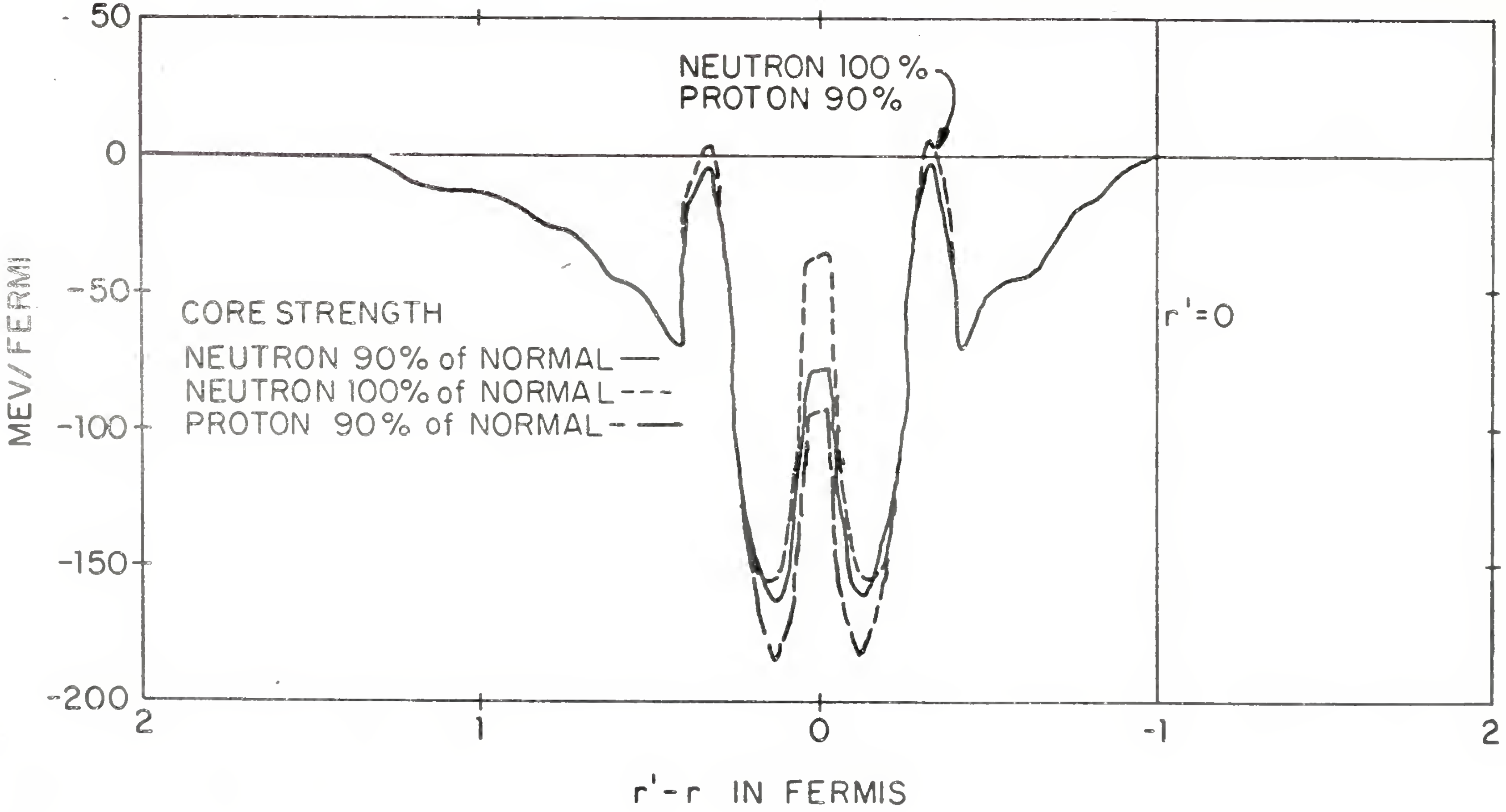
NEUTRON 100 %
PROTON 90%
CORE STRENGTH
NEUTRON 90% of NORMAL —
NEUTRON 100% of NORMAL ---
PROTON 90% of NORMAL - —
r'=0
MEV/ FERMI
50
0
-50
-100
-150
-200
2
1
0
-1
2
r'-r IN FERMIS

Figure 2(a)

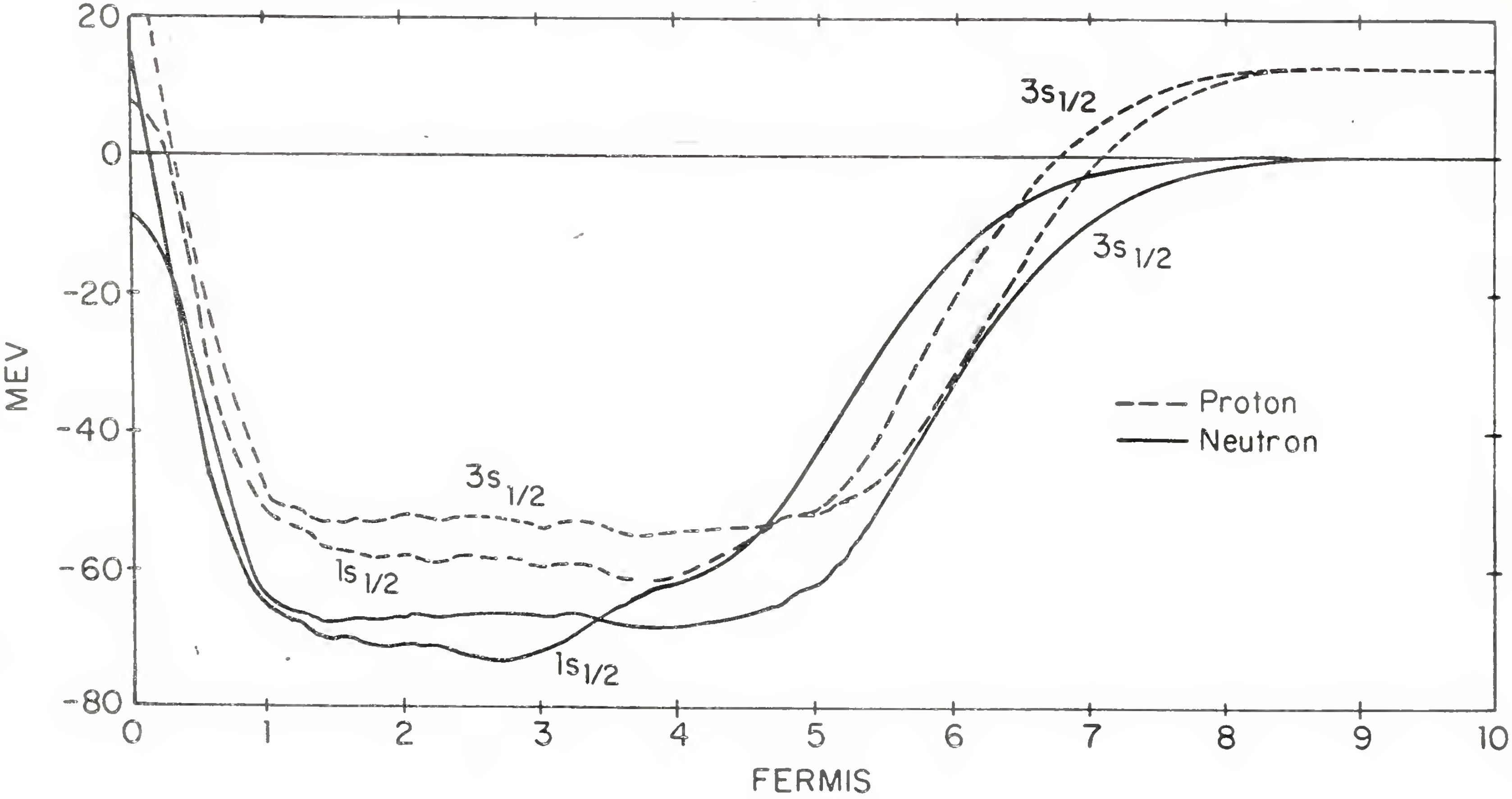
20
0
-20
-40
-60
-80
MEV
0
1
2
3
4
5
6
7
8
9
10
FERMIS
$3s_{1/2}$
$3s_{1/2}$
$3s_{1/2}$
$1s_{1/2}$
$1s_{1/2}$
Proton
Neutron

Figure 2(b)

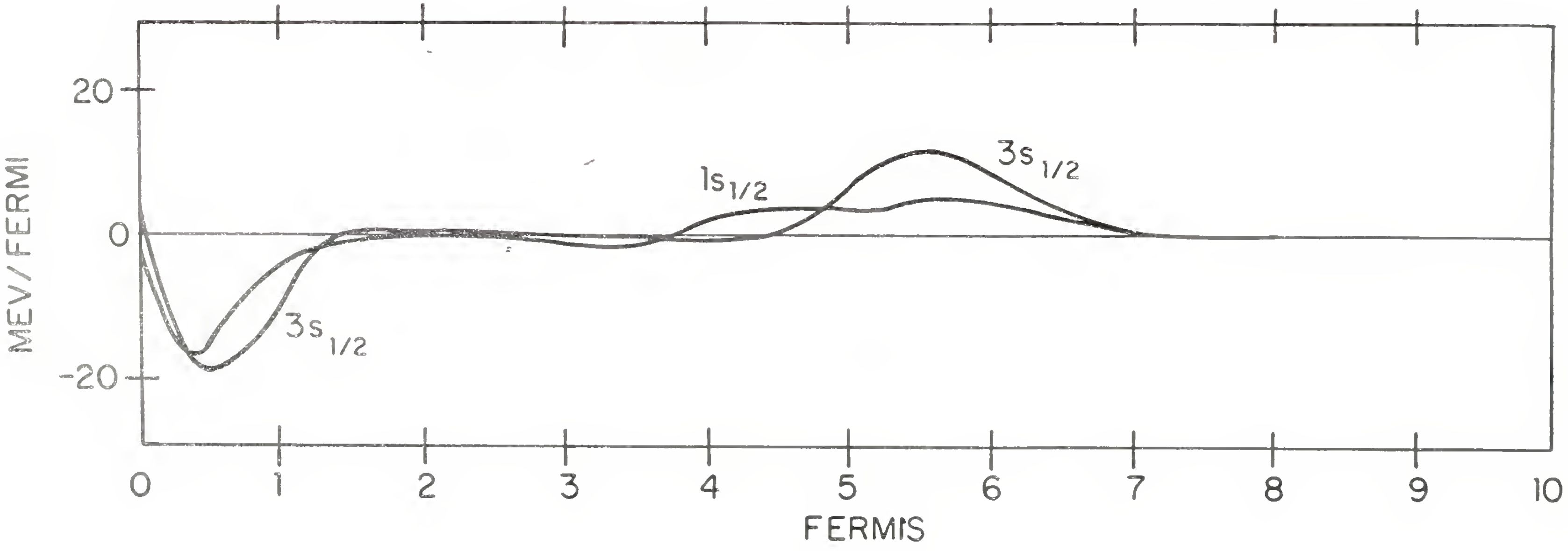

Figure 2(c)

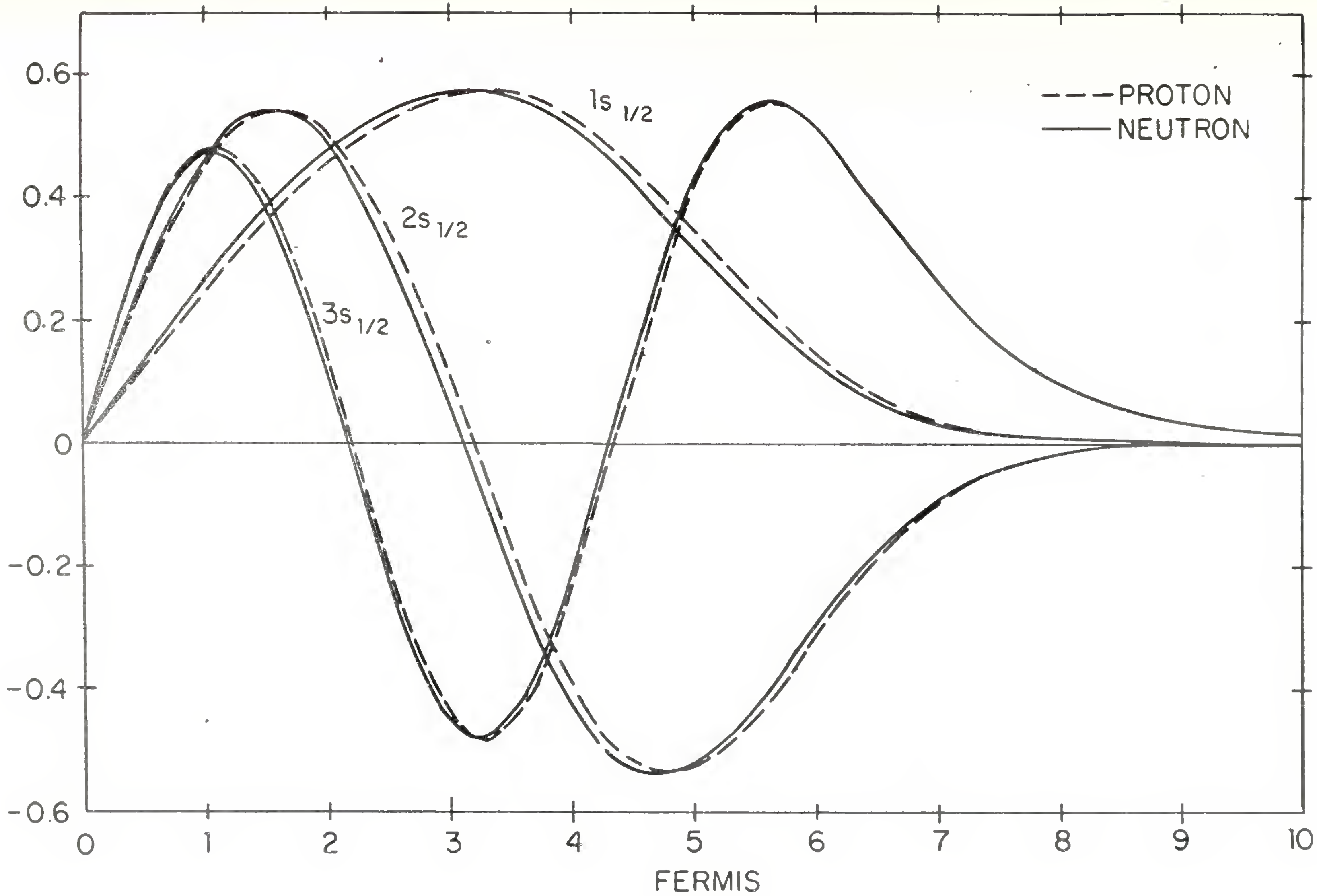
0.6
0.4
0.2
0
-0.2
-0.4
-0.6
0
1
2
3
4
5
6
7
8
9
10
FERMIS
---PROTON
—NEUTRON
$1s_{1/2}$
$2s_{1/2}$
$3s_{1/2}$

Figure 2(d)

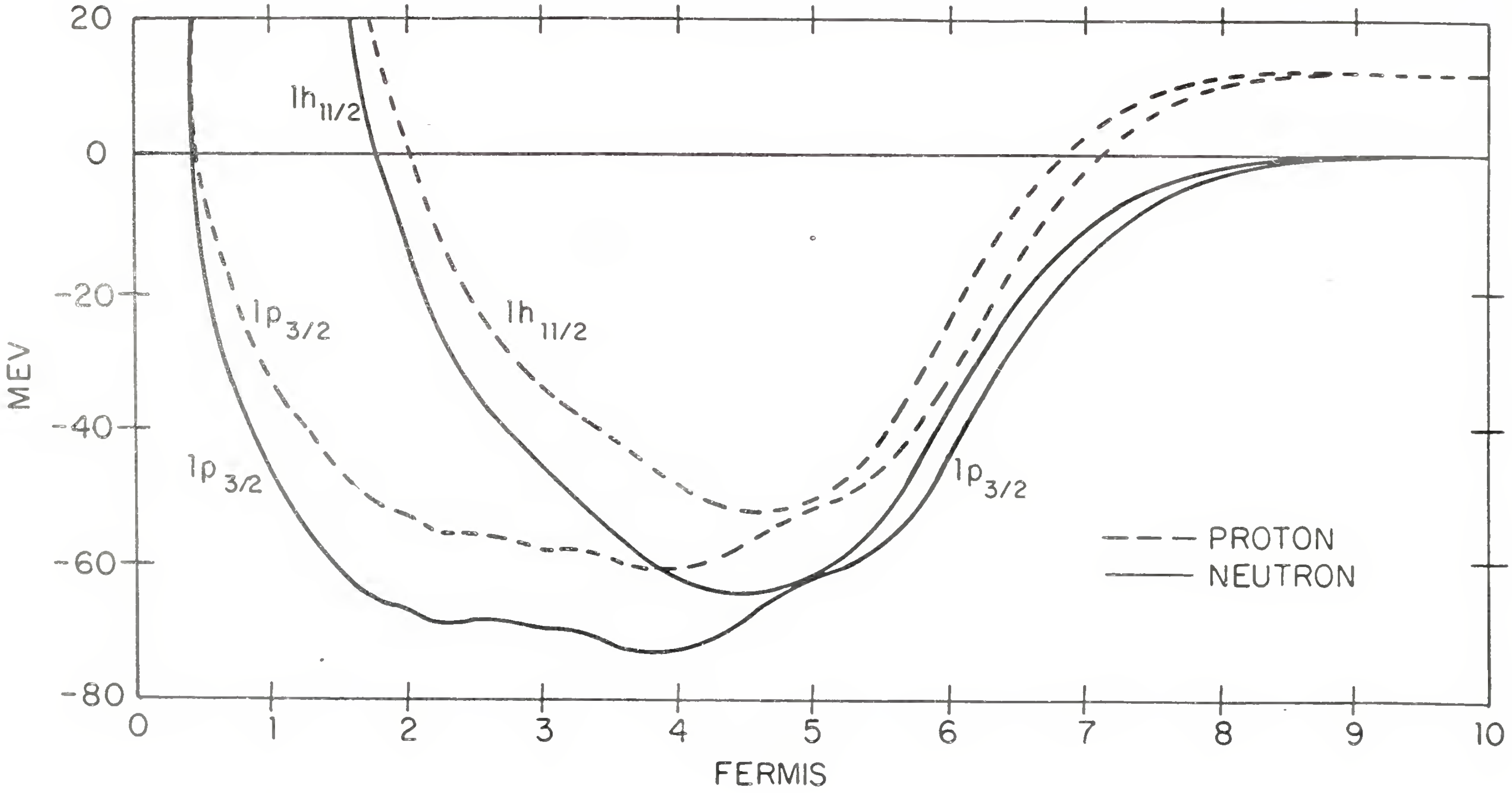
20
0
-20
-40
-60
-80
MEV
0
1
2
3
4
5
6
7
8
9
10
FERMIS
$1h_{11/2}$
$1p_{3/2}$
$1h_{11/2}$
$1p_{3/2}$
$1p_{3/2}$
PROTON
NEUTRON

Figure 2(e)

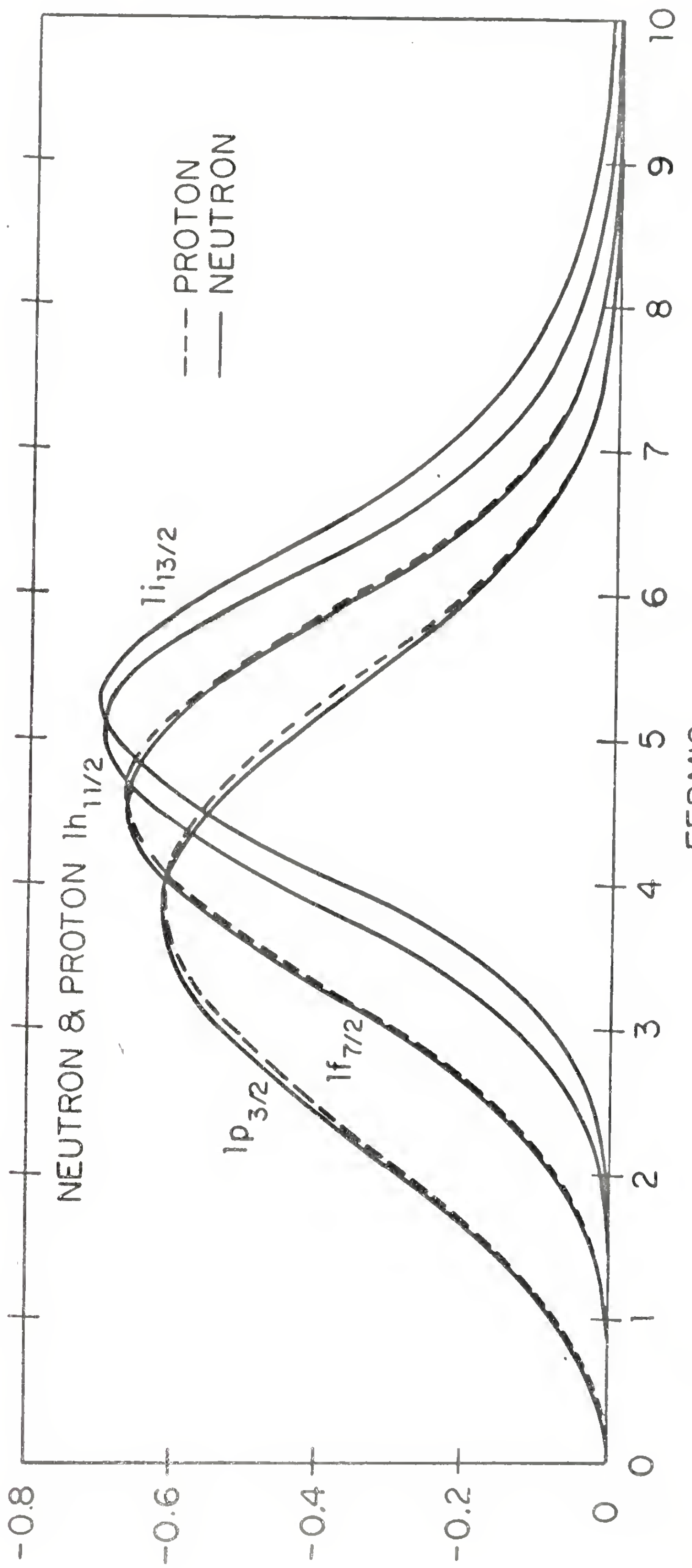
NEUTRON & PROTON 1h11/2
1p3/2
1f7/2
1i13/2
--- PROTON
— NEUTRON
FERMIS
0
1
2
3
4
5
6
7
8
9
10
0
-0.2
-0.4
-0.6
-0.8

Figure 2(f)

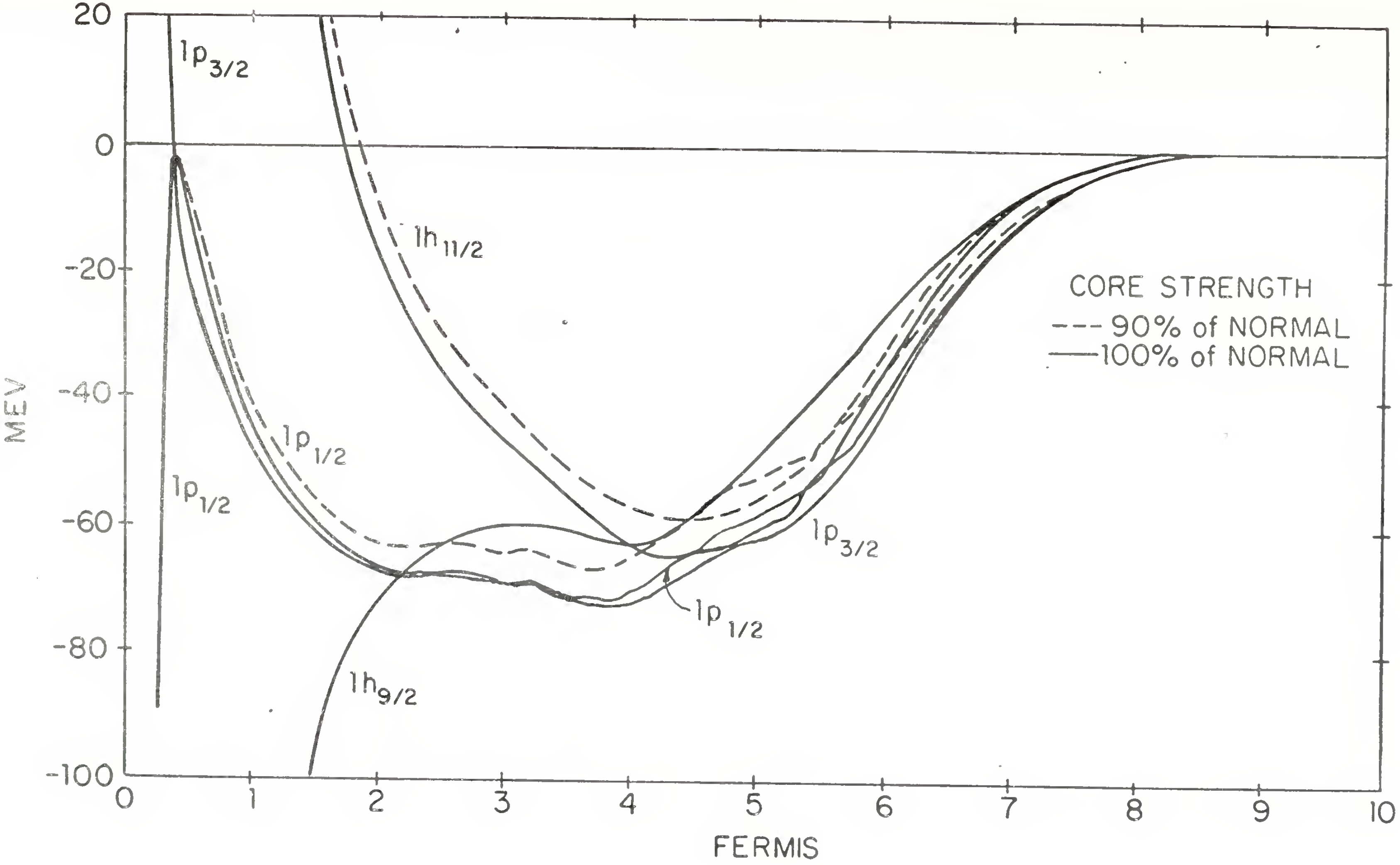
20
0
-20
-40
-60
-80
-100
MEV
0
1
2
3
4
5
6
7
8
9
10
FERMIS
$1p_{3/2}$
$1p_{1/2}$
$1p_{1/2}$
$1h_{11/2}$
$1h_{9/2}$
$1p_{3/2}$
$1p_{1/2}$
CORE STRENGTH
--- 90% of NORMAL
— 100% of NORMAL

Figure 2(g)

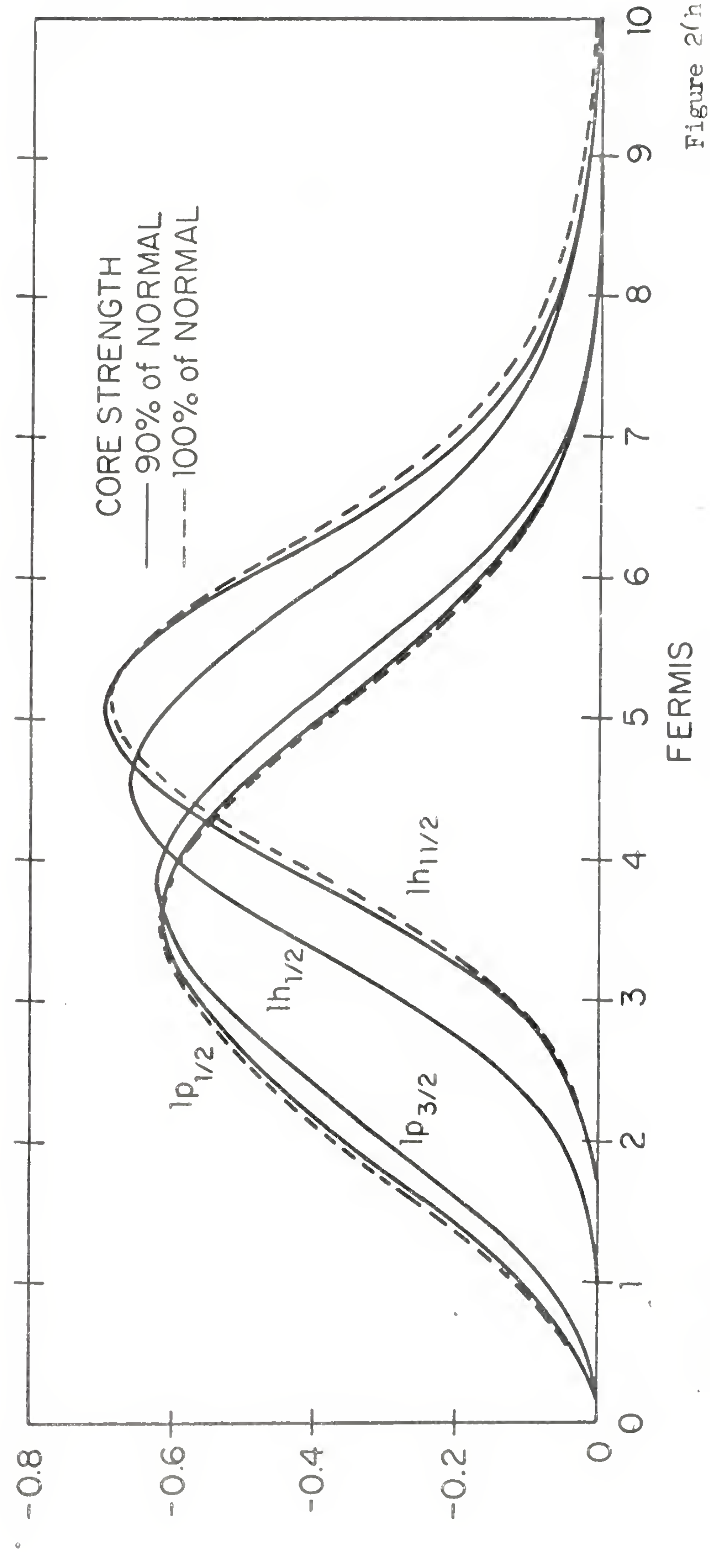
-0.8
-0.6
-0.4
-0.2
0
0
1
2
3
4
5
6
7
8
9
10
FERMIS
CORE STRENGTH
90% of NORMAL
100% of NORMAL
$1p_{1/2}$
$1p_{3/2}$
$1h_{1/2}$
$1h_{11/2}$

Figure 2(h)

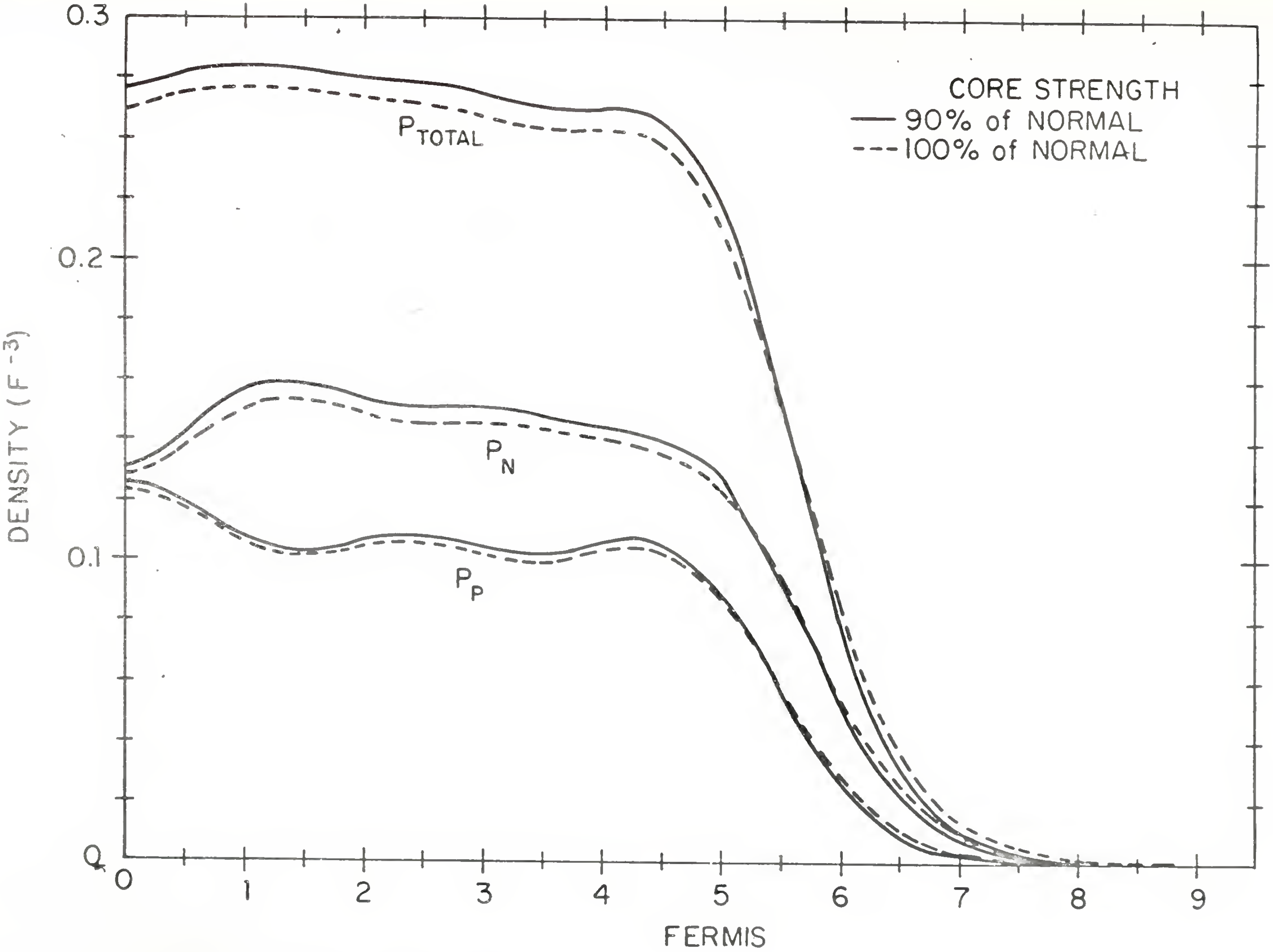
CORE STRENGTH
90% of NORMAL
100% of NORMAL
P_{TOTAL}
P_N
P_P
DENSITY (F -3)
0.3
0.2
0.1
0
0
1
2
3
4
5
6
7
8
9
FERMIS

Figure 3

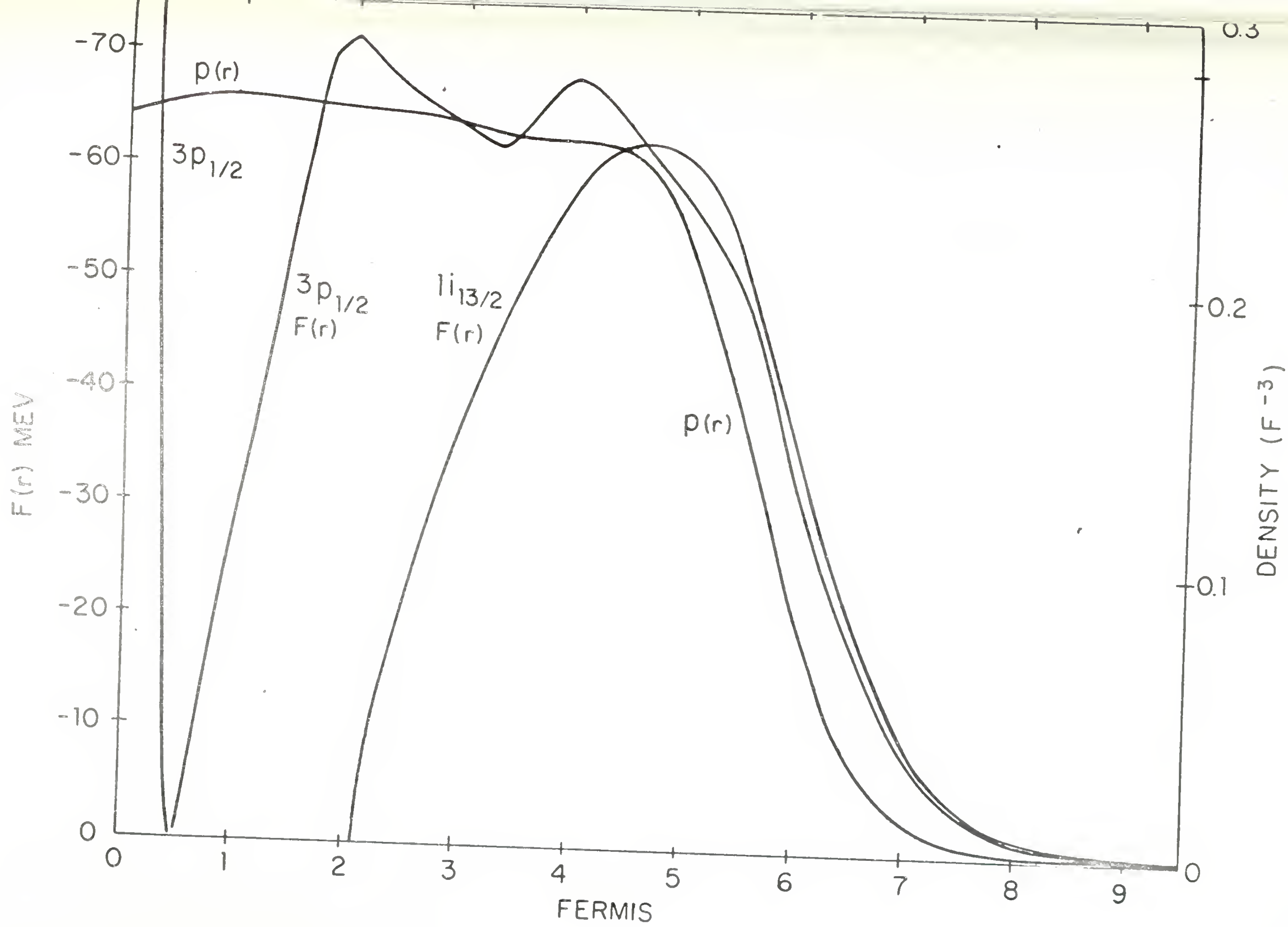
F(r) MEV
-70
-60
-50
-40
-30
-20
-10
0
DENSITY (F -3)
0.3
0.2
0.1
0
FERMIS
0
1
2
3
4
5
6
7
8
9
p(r)
$3p_{1/2}$
$3p_{1/2}$ F(r)
$1i_{13/2}$ F(r)
p(r)

Figure 4

FOOTNOTES

1. K. A. Brueckner, Phys. Rev. 100, 36 (1955).

2. J. Goldstone, Proc. Roy. Soc. (London) A239, 267 (1957).

3. K. A. Brueckner and J. L. Gammel, Phys. Rev. 109, 1023 (1958). Referred to as BG. This paper gives extensive references to previous work.

4. J. L. Gammel and R. M. Thaler, Progress in Elementary Particle and Cosmic Ray Physics, Vol. V (North Holland Publishing Co., Amsterdam, 1960), p. 98; R. J. N. Phillips, Repts. Progr. in Physics 22, 562 (1959). Extensive references can be found in both works. The Gammel-Thaler paper lists several apparently "equally good" phenomenological potentials which are referred to in the text as the GT potentials.

5. K. A. Brueckner, J. L. Gammel and H. Weitzner, Phys. Rev. 110, 431 (1958). Referred to as BGW.

6. K. A. Brueckner, A. M. Lockett and M. Rotenberg, Phys. Rev. 121, 255 (1961). Referred to as BLR.

7. K. E. Lassila, M. H. Hull, Jr., H. M. Ruppel, J. A. McDonald and G. Breit, Phys. Rev. 126, 881 (1962).

8. H. A. Bethe, Phys. Rev. 103, 1353 (1956).

9. H. A. Bethe, B. H. Brandow and A. G. Petschek, Phys. Rev. (to be published).

10. R. Rajaraman, Phys. Rev. (to be published).

11. S. A. Moszkowski and B. L. Scott, Bull. Am. Phys. Soc. 5, 31 (1960); Ann. Phys. (New York) 11, 65 (1960).

12. P. C. Martin and J. Schwinger, Phys. Rev. 115, 1342 (1959).

13. R. D. Puff and P. C. Martin, Bull. Am. Phys. Soc. 5, 30 (1960).

14. R. D. Puff, Ann. Phys. (New York) 13, 317 (1961).

15. F. Mohling, Phys. Rev. 122, 1043 (1961); ibid. 122, 1062 (1961); ibid. 124, 583 (1961).

16. F. Mohling, Phys. Rev. **[illegible]**, [illegible] ([illegible]).

17. B. L. Scott and S. A. Moszkowski, Ann. Phys. (New York) **14**, 107 (1961).

18. H. S. Köhler, Ann. Phys. (New York) **16**, 375 (1961).

19. J. S. Bell, *Proceedings of the Rutherford Jubilee International Conference* (Heywood & Co., London, 1961), p. 373.

20. D. J. Thouless, *The Quantum Mechanics of Many-Body Systems* (Academic Press, New York, 1961).

21. K. A. Brueckner and D. T. Goldman, Phys. Rev. **117**, 207 (1960).

22. K. A. Brueckner, J. L. Gammel and J. T. Kubis, Phys. Rev. **118**, 1438 (1960).

23. K. Sawada, L. Bruch and K. S. Masterson, Jr., (to be submitted for publication). Referred to as SBM.

24. A. Klein and R. E. Prange, Phys. Rev. **112**, 994 (1958).

25. P. Nozières and J. M. Luttinger, Phys. Rev. **127**, 1423 (1962); J. M. Luttinger and P. Nozières, Phys. Rev. **127**, 1431 (1962).

25a. This identity is valid because all terms except the zero order term (n_p) cancel upon summation over p. This can be seen in second order by using (2.23) for ρ_p.

25b. The structure of this equation differs radically from (2.23) in third and higher orders; however, only the second order expansion is required for subsequent discussions.

25c. This technique is used without further comment in the remainder of this Chapter.

25d. The other "culprit," and the reason for the inapplicability of the Bethe-Hugenholtz-Van Hove theorem to reaction matrix calculations is that the single-particle energies which should be used in such calculations must be computed "off-energy-shell" when singular denominators are involved. Therefore, they are not the energies defined in this section (e.g., for $p = p_F$, the separation energy), and need not satisfy the theorem. Appendix B contains further discussion of these energies.

26. E. Daniel and S. H. Vosko, Phys. Rev. **120**, 2041 (1960).

27. K. A. Brueckner, Phys. Rev. 110, 597 (1958).

28. K. A. Brueckner and D. T. Goldman, Phys. Rev. 116, 424 (1959).

29. D. J. Thouless, Phys. Rev. 112. 906 (1958).

30. N. M. Hugenholtz and L. Van Hove, Physica 24, 363 (1958).

31. A. B. Migdal, JETP 32, 399 (1957); Soviet Phys. 5, 333 (1957).

32. J. M. Luttinger, Phys. Rev. 119, 1153 (1960).

33. D. S. Falk and L. Wilets, Phys. Rev. 124, 1887 (1961).

34. J. S. Langer, Phys. Rev. 120, 714 (1960).

34a. This equation may not define a unique w. However, the procedure we employ to solve for w leads to the physically reasonable solution.

35. K. A. Brueckner (private communication).

36. K. A. Brueckner and K. S. Masterson, Jr., Phys. Rev. 128, 2267 (1962). Referred to as BM and included with this dissertation as Appendix G.

37. R. Balian, C. Bloch and C. de Dominicis, Nuclear Phys. 25, 529 (1961).

38. H. Suhl and N. R. Werthamer, Phys. Rev. 122, 359 (1961); N. R. Werthamer and H. Suhl, Phys. Rev. 125, 1402 (1962).

39. A. E. S. Green, Revs. Modern Phys. 30, 569 (1958); Phys. Rev. 95, 1006 (1956).

40. A. G. W. Cameron, Can. J. Phys. 35, 1021 (1957).

41. R. Ayres, W. F. Hornyak, L. Chan and H. Fann, Nuclear Phys. 29, 212 (1962).

42. M. A. Preston, *Physics of the Nucleus* (Addison-Wesley Publishing Company, Inc., Reading, Massachusetts, 1962).

43. Reviews and further references are given by R. Hofstadter, Revs. Modern Phys. 28, 214 (1956) and Annual Reviews of Nuclear Science 7, 231 (1957) and by D. C. Ravenhall, Revs. Modern Phys. 30, 430 (1958).

44. G. Breit, Revs. Modern Phys. [illegible], [illegible] ([illegible]).

45. G. F. Chew and S. C. Frautschi, Phys. Rev. [illegible], [illegible] ([illegible]).

46. J. M. Charap and S. P. Fubini, Nuovo cimento [illegible], [illegible] ([illegible]); ibid. 15, 73 (1960); J. M. Charap and M. J. Tausner, Nuovo cimento 18, 316 (1960).

47. R. E. Peierls, Proceedings of the International Conference on Nuclear Structure, Kingston (University of Toronto Press, Toronto, 1960); p. 7; J. S. Levinger and L. M. Simmons, Phys. Rev. 124, 916 (1961); M. Razavy, G. Field and J. S. Levinger, Phys. Rev. 125, 269 (1962); O. Rojo and L. M. Simmons, Phys. Rev. 125, 273 (1962).

48. J. S. Bell, The Many-Body Problem, Lecture Notes from the First Bergin International School of Physics, 1961 (W. A. Benjamin, Inc., New York, 1962; Editor: C. Fronsdal), p. 214.

49. G. A. Baker, Jr., Phys. Rev. 128, 1485 (1962).

50. A. M. Green, Physics Letters 1, 136 (1962).

51. A. N. Mitra, Phys. Rev. 123, 1892 (1961).

52. A. N. Mitra and V. L. Narasimham, Nuclear Phys. 14, 407 (1960).

53. A. N. Mitra and S. P. Pandya, Nuclear Phys. 20, 455 (1960).

54. D. A. Giltinan and R. M. Thaler, Bull. Am. Phys. Soc. 7, 540 (1962).

54a. J. L. Gammel, R. S. Christian and R. M. Thaler, Phys. Rev. 105, 311 (1957).

55. H. S. Wall, Continued Fractions (Van Nostrand, New York, 1948), Chapter XX.

55a. See Appendix B for a more complete discussion.

56. S. A. Moszkowski and A. M. Sessler, Nuclear Phys. [illegible], [illegible] (1960).

57. K. A. Brueckner, The Many-Body Problem, edited by C. DeWitt and P. Nozières (Wiley and Sons, New York, 1959), p. 47.

58. K. A. Brueckner, Quantum Theory, edited by D. R. Bates (Academic Press, Inc., New York, 1962), p. 260.

59. H. S. Köhler, Ann. Phys. (New York) 16, [illegible] (19[illegible]).

60. The experimental energies quoted in this Chapter are calculated from experimental masses tabulated by König, Mattauch and Wapstra, Nuc. Phys. 31, 18 (1962).

61. The proton radii and surface depths quoted in this Chapter are the electron scattering values summarized by references cited in Footnote 43.

62. L. R. B. Elton, Revs. Modern Phys. 30, 557 (1958).

63. M. G. Mayer and J. H. D. Jensen, Elementary Theory of Nuclear Shell Structure (John Wiley & Sons, Inc., New York, 1955).

64. B. J. Malenka, Phys. Rev. 86, 68 (1952).

65. A. A. Ross, H. Mark and R. D. Lawson, Phys. Rev. 102, 1613 (1956).

66. B. R. Mottelson and S. G. Nilsson, Kgl. Danske Videnskab. Selskab, Mat.-fys. Mead. 1, No. 8 (1959).

67. W. N. Hess and B. J. Moyer, Phys. Rev. 101, 337 (1955); R. W. Williams, Phys. Rev. 98, 1387 (1955).

68. K. W. Ford and D. L. Hill, Ann. Rev. Nuclear Sci. 5, 25 (1955).

69. E. M. Henly, Revs. Modern Phys. 30, 438 (1958).

70. S. Fernbach, Revs. Modern Phys. 30, 414 (1958); Atkinson, Hess, Perez-Mendez and Wallace, Phys. Rev. 123, 1850 (1961).

71. L. Wilets, Revs. Modern Phys. 30, 542 (1958).

72. K. A. Brueckner, Phys. Rev. 103, 1121 (1956); Revs. Modern Phys. 30, 561 (1958).

73. R. A. Berg and L. Wilets, Phys. Rev. 101, 201 (1956); L. Wilets, Phys. Rev. 101, 1805 (1956).

74. M. Rotenberg, Phys. Rev. 100, 439 (1955). However, Rotenberg uses Gaussian and Yukawa effective potentials instead of the actual nucleon-nucleon potential.

74a. D. H. Wilkinson, Proceedings of the International Conference on Nuclear Structure, Kingston, Canada (University of Toronto Press, Toronto, 1960). p. 20.

75. Y. Yamaguchi, Phys. Rev. [illegible], 16[illegible] (195[illegible]).

76. B. L. Scott and S. A. Moszkowski, Nuclear Phys. 29, 665 (1962).

77. L. C. Gomes, J. D. Walecka and V. F. Weisskopf, Ann. Phys. (New York) 3, 241 (1958).

78. K. M. Watson, Phys. Rev. 88, 1163 (1952).

79. M. Gell-Mann and M. Goldberger, Phys. Rev. 91, 398 (1953).

80. R. L. Becker, Phys. Rev. 127, 1328 (1962).

81. E. Montroll and J. Ward, Phys. Fluids 1, 55 (1958).

82. N. Fukuda and R. G. Newton, Phys. Rev. 103, 1558 (1956).

83. K. A. Brueckner, Phys. Rev. 103, 172 (1956).

84. S. S. Schweber, An Introduction to Relativistic Quantum Field Theory (Row, Peterson & Co., Evanston, Illinois, 1961).

85. F. J. Dyson, Phys. Rev. 75, 486 (1949).

86. M. Gell-Mann and F. Low, Phys. Rev. 84, 350 (1951).

87. G. C. Wick, Phys. Rev. 80, 268 (1950).

88. N. M. Hugenholtz, Physica 23, 481 (1957).

89. C. Bloch, Nuclear Phys. 7, 451 (1958).

90. J. Hubbard, Proc. Roy. Soc. (London) A240, 539 (1957).

91. W. Kohn and J. M. Luttinger, Phys. Rev. 118, 41 (1960).

92. C. Bloch and C. de Dominicis, Nuclear Phys. 7, 459 (1958).

93. J. M. Luttinger and J. C. Ward, Phys. Rev. 118, 1417 (1960).

94. A. Klein, Phys. Rev. 121, 950 (1961).

95. N. M. Hugenholtz, Physica 23, 533 (1957).

96. L. Van Hove, Physica 25, 849 (1959).

97. L. N. Cooper, Bull. Am. Phys. Soc., [illegible], 16 (1961).

98. A. Katz, *The Many-Body Problem--Lecture Notes from the First Bergen International School of Physics*, 1961 (W. A. Benjamin, Inc., New York; 1962, Editor: C. Fronsdal), p. 223; Nuc. Phys. *18*, 177 (1960); *ibid.* *20*, 663 (1960).

99. W. Tobocman, Phys. Rev. *107*, 203 (1957).

100. H. A. Bethe and J. Goldstone, Proc. Royal Soc. (London) *A238*, 551 (1957).

thesM368
Perturbation theory of nuclear matter an
3 2768 002 12501 5
DUDLEY KNOX LIBRARY